University of Bath

PHD

Intracellular compartmentalisation of GLUT4 in insulin-sensitive tissues

Gillingham, Alison K.

Award date:
1999

Awarding institution:
University of Bath

Link to publication

Alternative formats
If you require this document in an alternative format, please contact:
openaccess@bath.ac.uk

Copyright of this thesis rests with the author. Access is subject to the above licence, if given. If no licence is specified above, original content in this thesis is licensed under the terms of the Creative Commons Attribution-NonCommercial 4.0 International (CC BY-NC-ND 4.0) Licence (https://creativecommons.org/licenses/by-nc-nd/4.0/). Any third-party copyright material present remains the property of its respective owner(s) and is licensed under its existing terms.

Take down policy
If you consider content within Bath's Research Portal to be in breach of UK law, please contact: openaccess@bath.ac.uk with the details. Your claim will be investigated and, where appropriate, the item will be removed from public view as soon as possible.

Download date: 05. May. 2023

Intracellular Compartmentalisation of GLUT4 in Insulin-Sensitive Tissues

submitted by Alison K. Gillingham

for the degree of Doctor of Philosophy
of the University of Bath
1999

Attention is drawn to the fact that copyright of this thesis rests with its author. This copy of the thesis has been supplied on condition that anyone who consults it is understood to recognise that its copyright rests with its author and that no quotation from the thesis and no information derived from it may be published without the prior written consent of the author.

This thesis may be made available for consultation within the University Library and may be photocopied or lent to other libraries for the purpose of consultation.

UMI Number: U118005

All rights reserved

INFORMATION TO ALL USERS
The quality of this reproduction is dependent upon the quality of the copy submitted.

In the unlikely event that the author did not send a complete manuscript
and there are missing pages, these will be noted. Also, if material had to be removed,
a note will indicate the deletion.

UMI U118005
Published by ProQuest LLC 2013. Copyright in the Dissertation held by the Author.
Microform Edition © ProQuest LLC.
All rights reserved. This work is protected against
unauthorized copying under Title 17, United States Code.

ProQuest LLC
789 East Eisenhower Parkway
P.O. Box 1346
Ann Arbor, MI 48106-1346

UNIVERSITY OF BATH
LIBRARY
55 - 7 FEB 2000
PHD

Contents

Abstract

The potential involvement of intracellular pH and adaptor proteins in GLUT4 trafficking has been investigated in insulin-sensitive tissues. To this end, a cardiomyocyte isolation protocol was established and characterised. Glucose transport in cardiomyocytes prepared by a modified isolation procedure was increased 4-15-fold depending on cell batch. Photoaffinity labelling of cardiomyocytes using both ATB-[^{3}H]-BMPA and Bio-lc-ATB-BMPA revealed that insulin increased the level of GLUT4 at the plasma membrane by 3.5 to 5.2-fold, whereas GLUT1 was increased by approximately 2-fold. Immunocytochemical analysis of GLUT4 in these cells demonstrated that under basal conditions, GLUT4 is predominantly intracellular and particularly abundant just under the cell surface and in the perinuclear region. Upon insulin stimulation GLUT4 was translocated to the sarcolemma, as expected.

Intracellular pH was perturbed by the addition of the sodium-proton inhibitor HOE-642 prior to insulin stimulation. Under these conditions insulin-stimulated hexose transport into adipocytes and cardiomyocytes was partially inhibited. Furthermore the level of fully functional GLUT4 at the plasma membrane was reduced by approximately 35% as judged by photoaffinity labelling with Bio-lc-ATB-BMPA. However confocal analysis of GLUT4 in cardiomyocytes and subfractionation and Western blotting of GLUT4 in adipocytes showed no change in the cell surface content of GLUT4. Similar results were obtained when v-ATPases were inhibited by the addition of bafilomycin A_1, however the inhibition of insulin stimulated glucose transport was more potent, being approximately 60%. These results demonstrate that glucose transport and GLUT4 translocation can be partly dissociated from one another and may imply that glucose transporters at the plasma membrane exist in occluded or fusion incompetent states. The exact mode of action of pH in regulating protein trafficking is unknown but may be as a result of modulating interactions between receptor tails containing targeting motifs and adaptor proteins.

Using Nycodenz and glycerol gradients the association of adaptor complexes with GLUT4 vesicles was examined. Both AP1 and AP3 co-migrate with GLUT4 on Nycodenz gradients. On addition of GTPγS, GLUT4 fractionates as a heavier population of vesicles. Under these conditions there is an increase in the co-sedimentation of GLUT4 with AP1, but not with AP3. On glycerol gradients only AP3

migrates with the GLUT4 fraction. However upon addition of GTPγS AP1 is also found in fractions containing GLUT4, whereas the levels of AP3 are unchanged.

Western blotting of proteins associated with immunoadsorbed GLUT4 vesicles from adipocytes shows the presence of high levels of AP1 and AP3 but not AP2. Cell free, *in vitro*, association of AP1 is increased approximately 4-fold by the addition of GTPγS and an ATP regenerating system. Following GTPγS treatment ARF is also recruited to isolated GLUT4 vesicles. Both AP1 and ARF exhibit temperature dependent GTPγS-stimulated recruitment. AP1 and ARF association with GLUT4 vesicles is inhibited by incubation with brefeldin A. These data demonstrate that the coating of GLUT4 vesicles can be studied in isolated cell-free fractions. Furthermore at least two distinct adaptor complexes are recruited to GLUT4 vesicles, where they are likely to be responsible for directing the trafficking of GLUT4 through the labyrinth of intracellular compartments.

Acknowledgements

I am grateful to Geoff Holman for supervising my PhD and for the critical reading of this thesis. I would also like to thank the British Diabetic Association and Moose International for funding my PhD studentship.

Thanks go to all past and present members of the Holman lab. Thanks to Jing who taught me everything there is to know (and a lot more!) about adipocytes. Thanks to Lee who helped me to settle in in my first year and carried Sorvall rotors around for me! Thanks to Francoise for the awesome pancake parties held at her house and for helping me with the glycerol gradients and cross-linking experiments. Thanks to Alison and Jazz for helping Jing and I establish an era of 'girl power'!? in the lab. Thanks to Darren for the word 'concomitant', (*Chapter 4, Section 4.2.4*), (*Chapter 5, Section 5.1*)!!! And thanks to Paul and Celia who took on the arduous task of reading the first draft of this thesis.

I would also like to thank my mum and dad, who spurred my interest in science by buying me a chemistry set for Christmas, and then taking it away because they thought I would be too dangerous. Finally big thanks go to my husband, Alan, who has resisted the urge to tidy away the big piles of papers which have cluttered up our tiny bedsit, has calmed me down when I was having one of my 'computer tantrums' and without whose love and support I would never had got this far.

Abbreviations

ABABA	N,N'-bis-[(ethylamino)tartaryl]-ethylenediamine
AEBSF	[4-(2-Aminoethyl)benzenesulfonylflouride, HCl]
AP	Adaptor Protein
APS	Ammonium Persulphate
ARF	ADP Ribosylation Factor
ATB-BMPA	2-*N*-4-(1-azi-2,2,2-trifluroethyl)benzoyl-1,3-bis(D-mannos-4-yloxy-propylamine
ATP	Adenosine Trisphosphate
BDM	2,3-butanedione monoxime
BFA	Brefeldin A
Bio-Ic-ATB-BMPA	Biotinylated ATB-BMPA
BSA	Bovine Serum Albumin
CHO	Chinese Hamster Ovary Cells
CYT	Cytosol
DAB	3, 3'-Diaminobenzidine
DNAse	Deoxyribonuclease
DPM	Disintergrations Per Minute
DTT	DL-Dithiothreitol
ECL	Enhanced Chemiluminescence
EDTA	Diaminoethanetetra-acetic acid disodium salt
EEA1	Early Endosome Antigen 1
EGF	Epidermal Growth Factor
FCS	Foetal Calf Serum
GLUT	Glucose Transporter
GLUT1	Erythrocyte Glucose Transporter
GLUT4	Insulin-Regulated Glucose Transporter
GSVs	GLUT 4 Storage Vesicles/ Compartment
GTPγS	Guanosine 5'-O-(3-thiotriphosphate)
HDM	High Density Microsomes
HEPES	(N-[2-Hydroxyethyl]piperazine-N'-[2-ethenesulfonic acid])
HES	HEPES-EDTA-Sucrose
HOE 642	((4-isopropyl-3-methanesulphonyl-benzoyl)guanidine methanesulphonate)
HOE-694	((3-methylsulphonyl-4-piperidino-benzoyl)guanidine methanesulphonate)
HRP	Horseradish peroxidase
IR	Insulin Receptor
IRS1/2/3/4	Insulin Receptor Substrate-1/2/3/4
k_{en}	Rate of endocytosis
k_{ex}	Rate of exocytosis
KRH	Krebs-Ringer-HEPES
LDM	Low Density Microsomes

M6PR	Mannose 6-phospate Protein Receptor
NEM	N-ethylmaleimide
NHE1/2/3/4	Sodium-Hydrogen Exchanger-1/2/3/4
NIDDM	Non-insulin Dependent Diabetes Mellitus
NSF	N-ethylmaleimide Sensitive Fusion
Nycodenz	5-(N-2,3-dihydroxypropylacetamido)-2,4,6-triiodo-N,N'-bis(2,3-dihydroxypropyl)isophthalamide
PBS	Phosphate-buffered Saline
PDGF	Platelet-derived Growth Factor
PH	Pleckstrin Homology Domain
PI	Phosphatidylinositol
PI 3-Kinase	Phosphoinositide 3-kinase
PI 3-P	Phosphatidylinositol 3-phosphate
PI 4-P	Phosphatidylinositol 4-phosphate
PI 3,4-P_2	Phosphatidylinositol 3,4-bisphosphate
PI 4,5-P_2	Phosphatidylinositol 4,5-bisphosphate
PIP_3	Phosphatidylinositol 3,4,5-trisphosphate
PKA	Protein Kinase A
PKB	Protein Kinase B
PKC	Protein Kinase C
PLC	Phospholipase C
PLD	Phospholipase D
PM	Plasma Membrane
PMA	Phorbol 12-myristate 13-acetate
PP2A	Protein Phosphatase 2A
PTB	Phosphotyrosine-binding Domain
rATP	Regenerating ATP System
s-ABABA-s	N,N'-bis[(N-succinyl ethylamino)tartaryl]-ethylenediamine
SDS-PAGE	Sodium Dodecyl Sulphate- Polyacrylamide GeElectrophoresis
SH2 Domain	Src Homology 2 Domain
SH3 Domain	Src Homology 3 Domain
SNAP	Soluble NSF Attachment Protein
SNARE	Soluble NSF Attachment Protein Receptor
TBS	Tris-buffered Saline
TBS-T	Tris-buffered Saline with Tween 20
TEMED	N, N, N', N'-tetramethylethylenediamine
TES	Tris-EDTA Sucrose
Tf	Transferrin
TfR	Transferrin Receptor
TGN	*trans*-Golgi Network
TGN38	*trans*-Golgi Network Marker 38
TGR	*trans*-Golgi Reticulum

Thesit	Nonaethyleneglycol dodecyl ether
Tris	Tris(hydroxymethyl)methylamine
t-SNARE	target SNAP Receptor
Tween-20	Polyoxyethylene sorbitan monolaureate
VAMP	Vesicle Attachment Membrane Protein
v-ATPase	vacuolar ATPase
v-SNARE	vesicle SNAP Receptor

1.0 Introduction

1.1 Glucose Transporters

Glucose is the major metabolic substrate utilised by eukaryotic cells. Its catabolism via glycolysis, the citric acid cycle and oxidative phosphorylation provides cellular energy in the form of ATP. Polymerisation of glucose to form the readily mobilised storage molecule glycogen is used by higher organisms to protect against times of fuel shortage. Glucose homeostasis is maintained, despite the varied metabolic demands of the animal, by the relative concentrations of two hormones, insulin and glucagon, in the blood. Insulin stimulates glucose uptake by gluconeogenesis; while glucagon promotes glucose release via the glycogenolysis pathway. The major organ involved in the maintenance of blood glucose levels is the liver, however a number of other cell types are concerned with post-prandial, insulin-responsive glucose disposal.

Under normal physiological conditions uptake of glucose is the rate-limiting step in glucose utilisation. Since glucose is a polar molecule and therefore cannot cross the lipid membrane, specific carriers are required to mediate its transport into cells. These glucose transporters allow passive facilitated diffusion, an energy independent process in which the creation of a glucose concentration gradient across the membrane provides the driving force for glucose to enter or exit the cell (reviewed in Gould and Holman, 1993). Cloning and sequencing of the first glucose transporter was reported in 1985, (Mueckler *et al.*, 1985). Since then a number of glucose transporter (GLUTs) isoforms have been identified (Gould and Holman, 1993). These transporters are variably expressed in tissues (Bell *et al.*, 1993), enabling them to perform a variety of distinct functions to maintain cellular homeostasis.

1.1.1 GLUT1

GLUT1 is a ubiquitous glucose transporter. It is present at high concentrations in erythrocytes, comprising 3-5% of the membrane protein. In the late 1970s, GLUT1 was purified from erythrocyte membranes (Baldwin *et al.*, 1979). The kinetics were then studied in defined lipid vesicles and this led to the production of anti-sera against the transporter. These antibodies enabled Mueckler and co-workers to screen a cDNA library prepared from the HepG2 cell line, and to clone the cDNA for GLUT1

(Mueckler *et al.*, 1985). The open reading frame of the GLUT1 cDNA is 1476 bases and codes for a 492-residue polypeptide with a predicted molecular weight of 54,117 daltons. Hydropathy plots in conjunction with chemical and proteolytic digestion experiments predict 12-membrane spanning domains, comprising of α-helical segments each containing around 21 amino acids. These amphipathic helices are arranged so that both the N- and C- termini of the protein, along with a large hydrophilic loop situated between putative transmembrane helices 6 and 7, are cytoplasmic.

Tissues which respond to insulin have a unique glucose transport system. This transport system is capable of increasing glucose uptake 20 to 40-fold in a timescale of minutes. Although GLUT1 is expressed in insulin-responsive cells, namely adipocytes and muscle (Flier *et al.*, 1987), it is unlikely to mediate this massive change in glucose transport in response to insulin, for a number of reasons. Firstly immunocytochemical evidence has shown that GLUT1 is particularly abundant in cells which comprise the blood-brain barrier and is only expressed at low levels in fat and muscle (Flier *et al.*, 1987). Secondly under basal conditions a large proportion of GLUT1 is localised to the plasma membrane in insulin-sensitive cells. Therefore following insulin treatment there is only a relatively small increase in GLUT1 at the cell surface (2 to 3-fold). Thus the concentration of GLUT1 in fat and muscle, the amount of transporter in the plasma membrane under basal conditions and the low level of stimulation (2-3 fold) cannot account for the large change in glucose transport observed upon insulin stimulation.

GLUT1 has been extensively characterised with respect to its kinetic properties. The transporter is unusual in that it exhibits asymmetrical transport of sugar. This mechanistic feature of GLUT1 was demonstrated in intact human erythrocytes by the measurement of the net flux of D-[^{14}C]-glucose into or out of a sugar-free compartment using a quenched-flow apparatus and automated syringe, (Lowe and Walmsley, 1986). Transport data from these experiments revealed that the K_m for the efflux of glucose was far greater that that for its influx. The asymmetrical nature of GLUT1 kinetics has led to the suggestion (Gould and Holman, 1993) that it may operate under conditions of glucose starvation, where it could effectively function in a predominantly influx mode.

1.1.2 GLUT4

Immunoblotting with a monoclonal antibody against the fat cell glucose transporter resulted in the identification of GLUT4 in 1988 (James *et al.*, 1988). One year later, five independent laboratories isolated cDNA clones for GLUT4 from a variety of tissues and cell lines (James *et al.*, 1989; Birnbaum, 1989; Fukumoto *et al.*, 1989; Charron *et al.*, 1989; Kaestner *et al.*, 1989). The polypeptide sequence of GLUT4 is 509 amino acids long in rats and humans (James *et al.*, 1989; Birnbaum, 1989; Charron *et al.*, 1989), and 510 amino acids long in mice (Kaestner *et al.*, 1989). The human and rat GLUT4 proteins share 65% sequence identity with GLUT1 isoforms from the same species, mainly differing in the N- and C-termini and in the hydrophilic intracellular loop *(Figure 1.1)*.

The kinetic properties of GLUT4 differ substantially from GLUT1, appearing to function as a simple, symmetrical carrier. In order to identify whether the differences in the kinetic properties of GLUT1 and GLUT4 were due to their expression in distinct environments or due to inherent properties of the respective transporters, GLUT1 and GLUT4 mRNAs were injected into *Xenopus* oocytes. Transport assays using the *Xenopus* oocyte expression system revealed that the half saturation constants (K_ms) for 3-*O*-methyl-D-glucose transport under equilibrium exchange conditions were 21 mM for GLUT1 and 1.8 mM for GLUT4 (Keller *et al.*, 1989). The K_m values obtained in *Xenopus* oocytes agree well with values obtained in erythrocytes for GLUT1 and adipocytes for GLUT4 (reviewed in Baldwin, 1993) and suggest that the differences in the kinetic properties are intrinsic to each transporter. The relatively low K_m for GLUT4 ensures that the transporter operates close to its V_{max} over the normal range of blood glucose concentrations.

In fat and muscle, the massive insulin-induced increase in glucose transport is attributed to GLUT4. This effect is mediated by an increase in the V_{max} of the transporter with very little change in K_m (Taylor and Holman, 1981). In 1980, two groups independently demonstrated, by cytochalasin B binding and subcellular fractionation, that insulin increases the V_{max} of transport by mobilising a population of transporters, now known to be GLUT4, from an intracellular compartment to the plasma membrane (Suzuki and Kono, 1980; Cushman and Wardzala, 1980). Thus in the absence of insulin, GLUT4 is localised primarily to an internal compartment. Upon insulin stimulation, GLUT4 is

Figure 1.1 Hypothetical Model of GLUT4. The protein is predicted to contain 12 transmembrane helices with both the N- and C-termini situated intracellularly. Ligand binding and labelling studies have shown separation of the external and internal glucose binding sites, with putative helices 7-9 making up the exofacial site and 10-11 comprising the endofacial site. Both the N- and C-termini contain signal sequences and an N-linked glycosylation site is predicted in the exofacial loop between helices 1 and 2.

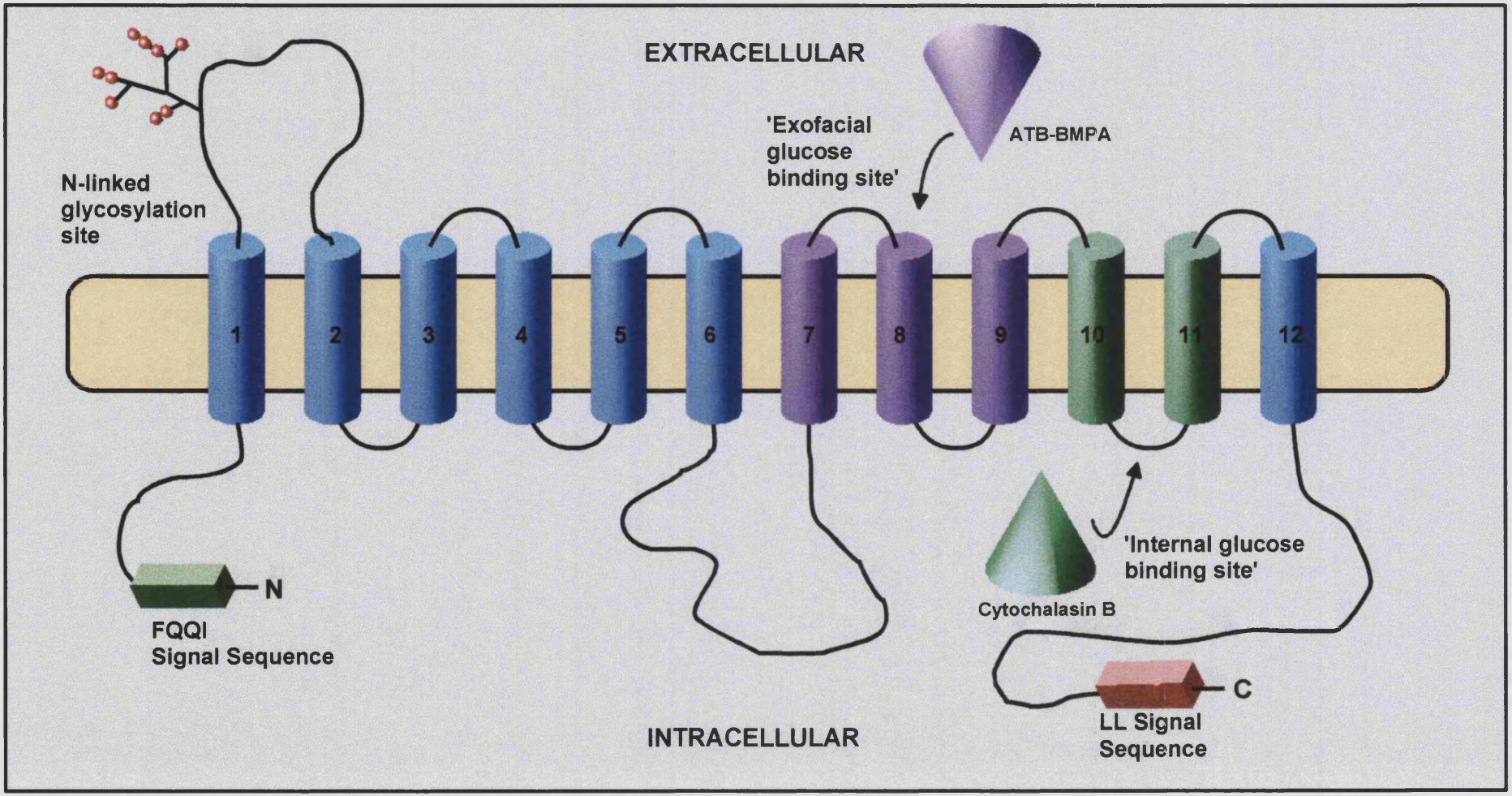

quickly translocated from this compartment to the plasma membrane, where its presence results in a substantial increase in glucose transport. When the stimulus is removed, GLUT4 re-enters the cells and returns to the storage compartment. This major property of GLUT4 distinguishes it from all other glucose transporters and makes it crucial in the hormonal regulation of glucose homeostasis. Since patients with pathophysiological disorders such as morbid obesity and type 2 diabetes have unaltered levels of total GLUT4 in their muscle (Kahn, 1992), defects in the signalling to GLUT4 and/or the translocation of GLUT4 from the intracellular storage site to the plasma membrane have been implicated in these diseases.

1.2 The Insulin Signalling Pathway

Insulin stimulation of glucose transport into muscle and adipose cells is a multi-step process. In order to fully understand the processes of GLUT4 trafficking and translocation, a knowledge of the mechanisms by which receipt of a hormone signal is translated in to movement of vesicles from a storage pool to the plasma membrane, is required. Thus a brief overview of the insulin-signalling cascade has been included here *(Figure 1.2)*.

1.2.1 The Insulin Receptor

The insulin receptor (IR) is a heteromeric protein consisting of two α and two β subunits ($\alpha_2\beta_2$). Binding of insulin to its receptor results in autophosphorylation of tyrosine residues in the β-subunits which in turn leads to the association and phosphorylation of downstream proteins. The intrinsic kinase activity of the insulin receptor is an important step in the signal-transduction process since tyrosine kinase deficient receptors transfected into rat adipocytes are incapable of transmitting the signal for increased hexose uptake (Roth *et al.*, 1994). Target proteins for the insulin receptor include a family of multi-functional docking proteins known as insulin-receptor substrates (IRS). Four members of the IRS family have been described so far: IRS-1, (Sun *et al.*, 1991), -2, (Sun *et al.*, 1995), -3 (Lavan *et al.*, 1997a) and -4 (Lavan *et al.*, 1997b). Phosphorylation of IRS proteins triggers the activation of a number of signalling cascades, one of which includes activation of phosphatidylinositol 3-kinase (PI 3-kinase) and protein kinase B (PKB). This signal transduction pathway ultimately

results in the exocytic translocation of GLUT4 vesicles from an intracellular pool to the plasma membrane.

1.2.2 Insulin Receptor Substrates

IRS-1 and IRS-2 are ubiquitously expressed while IRS-3 is found in adipocytes, fibroblast and liver cells, and IRS-4 has only been detected in embryonic kidney cells in culture (reviewed in Shepherd *et al.*, 1998). All the IRS proteins display remarkably similar architecture, sharing homologous N-terminal pleckstrin homology domains (PH domains) and phosphotyrosine binding domains (PTB domain). The PTB domain binds directly to the insulin receptor at an NPEY motif (He *et al.*, 1995), whereas the PH domain (although also implicated in receptor binding) seems to interact with phosphoinositides, and may play a modulatory role in IRS function (Rameh *et al.*, 1997). IRS molecules also contain many potential sites for tyrosine phosphorylation, the majority of which resemble the YMXM or YXXM motifs (Shoelson *et al.*, 1992). Phosphorylation of specific tyrosine residues within IRS-1 allows the protein to recruit a number of signalling molecules through interactions with their *src*-homology domains. These include Grb2, the small adaptor protein, Nck and PI 3-kinase (reviewed in Shepherd *et al.*, 1996).

One of the difficulties in studying the role of the IRS proteins in signalling cascades is their ability to compensate for one another. This was demonstrated in studies using IRS-1 knockout mice (Araki *et al.*, 1994). In the skeletal muscle of these mice, where the concentration of IRS-2 is low, insulin-stimulated PI 3-kinase activity was diminished. However in hepatocytes, where the levels of IRS-2 are comparable with IRS-1, PI 3-kinase activity was near normal. Furthermore, in adipocytes, it was IRS-3 and not IRS-2 which compensated for the loss of IRS-1, although IRS-3 was unable to completely activate PI 3-kinase (Smith-Hall *et al.*, 1997). Thus there appears to be some partial redundancy between the IRS proteins.

The relationship between PI 3-kinase and the IRS proteins has been most extensively studied for IRS-1. During insulin stimulation, IRS-1 becomes hyper-phosphorylated on tyrosine residues and this enables it to bind to the *src* homology 2 domains (SH2 domains) on the p85 regulatory subunit of PI 3-kinase (reviewed in Shepherd *et al.*, 1998). This binding results in the activation of the p110 catalytic subunit of PI 3-

kinase, and the production of phosphatidylinositol 3,4,5-trisphosphate (PIP_3) from phosphatidylinositol 4,5 bisphosphate (PI 4,5-P_2).

1.2.3 PI 3-Kinase

PI 3-kinase was originally identified as the protein responsible for the phosphorylation of the D-3 position of the inositol head group of phosphoinositides (Stephens *et al.*, 1993). It is now known to play a pivotal role in many cellular processes. These include cell growth and differentiation (Toker and Cantley, 1997), synthesis and degradation of carbohydrates, lipids and proteins (Holman and Kasuga, 1997), cytoskeletal rearrangement (Toker and Cantley, 1997) and membrane trafficking (Holman and Kasuga, 1997).

PI 3-kinases form a large family of enzymes, with some homology both to PI 4-kinases and even to enzymes with no identifiable lipid kinase activity (Vanhaesebroeck *et al.*, 1997). The PI 3-kinase superfamily can be sub-divided into 3 classes based on their substrate specificity. Class 1 PI 3-kinases can be further subdivided into Class 1A and 1B. Activation of the insulin-receptor tyrosine kinase results in the immediate targeting of class 1A PI 3-kinase into signalling complexes. As well as class 1A, class 2 PI 3-kinases are also stimulated by insulin (Shepherd *et al.*, 1998). Class 2 PI 3-kinases are, however, unlikely to play an important role in insulin signalling to GLUT4 for two reasons. Firstly they are unable to produce PIP_3 as a product (thought to be an important intermediate in the insulin pathway), (Domin *et al.*, 1996; Virbasius *et al.*, 1996; Rameh and Cantley, 1999), and secondly they are not susceptible to certain cell-permeable inhibitors (Domin *et al.*, 1996; Virbasius *et al.*, 1996), to which many insulin-induced events are intimately sensitive. Such inhibitors include the fungal metabolite wortmannin and the structurally independent LY29002 compound, both of which have been widely used to inhibit GLUT4 translocation (Clarke *et al.*, 1994). Although wortmannin acts to varying degrees on all classes of PI 3-kinases, class 1A is most sensitive exhibiting an IC_{50} in the low nanomolar range. In addition, dominant negative forms of class 1A PI 3-kinase (Hara *et al.*, 1994), and experiments using antisense RNA to p85 (Yin *et al.*, 1998), have shown the absolute requirement for this class of lipid kinase in the insulin signalling cascade.

Stimulation of PI 3-kinase by insulin results in the translocation of GLUT4 from an intracellular compartment to the plasma membrane. This insulin-stimulated recruitment of GLUT4 is completely abolished by incubation with nanomolar concentrations of wortmannin. Conversely insulin recruits PI 3-kinase to the internal pool, where it interacts with tyrosyl-phosphorylated IRS-1. Analysis of microsomal membranes by sucrose gradient centrifugation (Clark *et al.*, 1998), has shown that GLUT4 sediments at 30/50% sucrose while cytoskeletal markers, PI 3-kinase and IRS-1 are resolved in a separate fraction (at 60% sucrose). This differential localisation suggests that GLUT4 and PI 3-kinase/IRS-1 are derived from different vesicles, the latter being strongly tethered to the actin cytoskeleton, (although there is one report of a direct recruitment of PI 3-kinase to GLUT4 vesicles (Heller-Harrison *et al.*, 1996)).

How does PI 3-kinase activity lead to downstream activation? Mounting evidence suggests that PIP_3, the major product of PI 3-kinase, acts as a second messenger, relaying information concerning agonist stimulation, to other components of the signalling pathway(s). Firstly, the rise in PIP_3 concentration occurs rapidly after insulin binding, and is thought to precede the activation of signalling molecules downstream of PI 3-kinase (Shepherd *et al.*, 1998). Secondly, increases in PIP_3 concentration are transient, being precisely regulated both at the level of synthesis and at the level of degradation (Stephens *et al.*, 1991; Cross *et al.*, 1997). Finally, experiments using membrane permeant forms of PIP_3 have shown that this lipid is capable of directly modulating downstream events (Jiang *et al.*, 1998). The mode of action of PIP_3 is unclear but two mechanisms have been proposed. The first is that PIP_3 could insert into membranes, transiently altering their composition and resulting in membrane curvature, which may facilitate vesicle budding, (Schu *et al.*, 1993). The second is that PIP_3 specifically interacts with proteins downstream in the trafficking pathway, perhaps acting as an allosteric modulator, or inducing a change in the conformation of the target protein such that it is now capable of interacting with other downstream molecules (Shepherd *et al.*, 1997). Indeed a number of proteins have been shown to bind PIP_3 *in vitro*. These include protein kinase B (PKB) (*Section 1.2.4*), PI 3-kinase dependent protein 1 (PDK-1) (*Section 1.2.4*), the atypical protein kinase C-ζ (PKC-ζ) (*Section 1.2.4*), the G-protein Dynamin (*Section 1.5.2*), the ARF-GEFs GRP1 and cytohesin-1 *(Section 1.5.5)*, the ARF-GAP, centaurin-α *(Section 1.5.6)* and the adaptor protein complexes, AP1-4 *(Section 1.6.6)*.

1.2.4 Downstream Targets of PI 3-kinase

The involvement of a serine/threonine kinase downstream of PI 3-kinase in the signalling cascade has been suggested by the finding that stimulation of GLUT4 translocation by serine phosphatase inhibitors is not blocked by PI 3-kinase inhibitors (Kanai *et al.*, 1993a). The exact serine/threonine kinase is not known but may include PKBβ, which has been shown to be targeted to GLUT4 vesicles (Calera *et al.*, 1998) or PKCλ, which can cause GLUT4 translocation in response to insulin (Kotani *et al.*, 1998).

1.2.4.1 Protein Kinase B

Protein kinase B is a serine/threonine kinase (Coffer and Woodgett, 1991). Three isoforms of PKB have been identified to date, namely PKBα (Coffer and Woodgett, 1991), PKBβ (Cheng *et al.*, 1992) and PKBγ (Konishi *et al.*, 1993). All three are activated by insulin to varying degrees in a cell specific manner. An absolute requirement for PI 3-kinase in the activation of PKB has been demonstrated both by the use of inhibitors of PI 3-kinase, such as wortmannin (Franke *et al.*, 1995), and by the expression of dominant negative forms of p85, the PI 3-kinase adaptor subunit (Burgering and Coffer, 1995). PKB contains one pleckstrin homology (PH) domain, which is capable of binding PIP_3, and it was initially thought that this in some way attenuated PKB activation (Burgering and Coffer, 1995). However, activation of PKB results from phosphorylation by a serine/threonine kinase (on Thr^{308} and Ser^{73}). So where is the requirement for a lipid? In fact the kinase which phosphorylates PKB has now been characterised and cloned, and named PDK-1 (PI 3-kinase dependent protein 1) (Walker *et al.*, 1998). This protein binds PIP_3 avidly, however this does not increase the intrinsic activity of the enzyme (Alessi *et al.*, 1998). Thus it is proposed that binding of PIP_3 to PKB, somehow results in a conformational change, which places Thr^{308} and possibly Ser^{73} into more accessible positions for phosphorylation by PDK-1 (Shepherd *et al.*, 1998). Since both PKB and PDK-1 are capable of binding PIP_3, this may constitute a mechanism by which the two proteins are brought into close proximity with one another (for review see Shepherd *et al.*, 1998).

Figure 1.2 The Insulin Signalling Pathway. Binding of insulin to its receptor in the plasma membrane leads to autophosphorylation of the β-subunits. This in turn leads to the association of the receptor with insulin receptor substrates (for example IRS1), which also become phosphorylated. PI 3-kinase interacts with tyrosyl phosphorylated IRS1 via the p85 regulatory subunit. Activation of PI 3-kinase leads to the generation of PIP_3, which ultimately signals to GLUT4 possibly via Protein Kinase B (PKB) or an atypical Protein Kinase C (PKC).

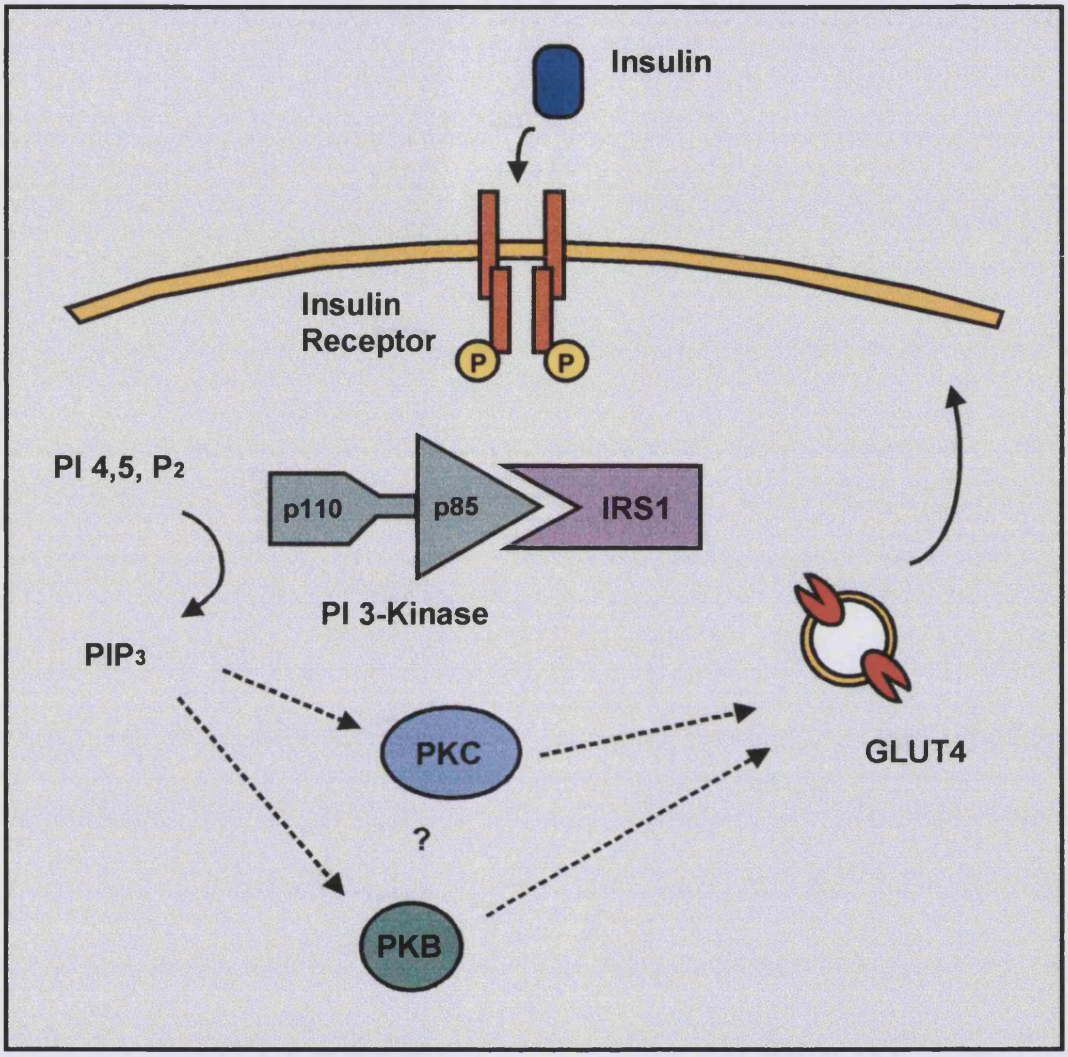

Doubts are raised over the involvement of PKB, by a recent study, (Kitamura *et al.*, 1998), in which the expression of a dominant negative form of PKB in 3T3-L1 adipocytes resulted in the inhibition of protein synthesis but had no effect on glucose transport. In contrast to this, a study of PKB activity in L6 myotubes showed that transfection of a constitutively active haemoglutinin tagged PKB into these cells, results in an increase in cell surface GLUT4 (Wang *et al.*, 1999). Furthermore this GLUT4 translocation could be reduced by co-transfecting the haemoglutinin tagged PKB with a kinase inactive, phosphorylation deficient PKB mutant. Thus the use of dominant negative PKB constructs has provided mixed results as to the importance of PKB in GLUT4 translocation. Specific inhibitors could more definitively ascribe a role for PKB, but as yet none have been described.

1.2.4.2 Protein Kinase C

A role for PI 3-kinase in the stimulation of protein kinase C (PKC) activity has recently been established by the observation that introduction of constitutively active PI 3-kinases into cells, results in the activation of atypical PKC isoforms (PKC-ζ and -λ)(Standaert *et al.*, 1997; Kotani *et al.*, 1998). Although these proteins do not contain PH domains, they do seem to bind PIP_3 with reasonable affinity, (Palmer *et al.*, 1995). Thus it is possible that PIP_3 acts on atypical PKC isoforms in an analogous manner to its action on PKB; altering the conformation of the protein to expose serine/threonine residues for phosphorylation, and attenuating the co-localisation of PKC with its serine/threonine kinase (possibly PDK-1).

Thus a complex signalling pathway exists between the insulin receptor and the glucose transporter. Evidence to date conclusively demonstrates a role for the insulin receptor substrates and for PI 3-kinase. However more data is required to decisively place PKB or PKC in this signal transduction cascade.

1.3 Insulin-stimulated Translocation of Glucose Transporters

1.3.1 Kinetics of GLUT4 Trafficking

In order to examine the movement of GLUT4 (and GLUT1) between the plasma membrane and the intracellular storage site(s), a method for accurately quantitating cell

surface glucose carriers is required. Initially a subfractionation and Western blotting protocol was employed to address this issue. Adipocytes were fractionated into 4 fractions: the plasma membrane (PM), the low density microsomes (LDM), containing endosomes, Golgi and TGN membranes, the high density microsomes (HDM), containing endoplasmic reticulum, and the cytosolic pool. The amount of GLUT4 in each of these fractions was then analysed by immunoblotting. Results obtained using this method revealed a translocation of GLUT4 from the LDM fraction to the plasma membrane. However the relatively small insulin-induced increase in GLUT4 concentration at the plasma membrane did not correlate well with the impressive augmentation of hexose transport activity observed (Gould and Holman, 1993).

Originally it was thought that the discrepancy between transporter number and glucose uptake was due to an insulin-induced increase in the 'intrinsic activity' of the transporter (Czech *et al.*, 1992). However it soon became clear that part of the inconsistency was due to contamination of the plasma membrane fraction with microsomal membranes (LDM), a substantial problem, which needed to be circumvented. To this end, the bis-mannose photolabel ATB-BMPA (Clark and Holman, 1990) and its biotinylated derivative Bio-lc-ATB-BMPA (Koumanov *et al.*, 1998) were developed. Due to their bulky hydrophilic nature, these compounds are membrane impermeable, allowing only those transporters exposed at the cell surface to be tagged. Upon UV irradiation, the diazirine group on the label produces a carbene, which can directly insert into the target protein. Using this approach in rat adipose cells, researchers (Holman *et al.*, 1990) have shown that cell surface levels of GLUT4 increase markedly (15-20 fold) upon insulin stimulation, while the levels of cell surface GLUT1 increase only moderately (3-5 fold). The photolabelling technique can also be used to monitor the distribution of glucose transporters among subcellular pools. Since only plasma membrane proteins are labelled, a pulse-chase approach can be utilised, i.e. transporters can be labelled with ATB-BMPA and the time-course of cell surface tagged GLUT4 equilibration with internal microsomes analysed. ATB-BMPA tagged transporters monitored in cells from both basal and insulin-stimulated states show that the rate constant for the internalisation of transporters is unaffected (or slightly decreased) by the presence of insulin. Conversely the rate of exocytosis is markedly stimulated by insulin (Satoh *et al.*, 1993). Studies with ATB-BMPA have also shown that, even under basal conditions, a small proportion of the glucose transporters

continually recycle between the plasma membrane and the internal microsomes (Yang and Holman, 1993).

Stimulation of glucose transport in rat adipose tissue is rapid, occurring with a half-time of approximately 3 min at 37°C (Clark *et al.*, 1991). However Western blotting of subcellular fractions and photolabelling have demonstrated that the appearance of GLUT1 and GLUT4 at the cell surface pre-empts transport activity, occurring with a half-time of ≈ 2 min (Clark *et al.*, 1991). The lag period between precipitation of transporters at the cell surface and the increase in carrier activity may be due to a population of glucose transporters in occluded precursor/fusion-incompetent states or bound to regulatory proteins which prevent the full exposure of the transporter to the extracellular environment (Holman and Cushman, 1994). This lag phenomenon has been observed in both rat adipocytes (Clark *et al.*, 1991) and 3T3-L1 adipocytes (Yang *et al.*, 1992).

The kinetic data obtained from photolabelling experiments of GLUT4 (Clark *et al.*, 1991; Yang *et al.*, 1992) has enabled a mathematical analysis of its trafficking behaviour *(Figure 1.3)*. Mathematically, insulin can increase the number of transporters on the cell surface either by increasing the rate of exocytosis, decreasing the rate of endocytosis, or both. The "2-pool model" (Holman *et al.*, 1994) consists of an intracellular pool (the endosomes) and the plasma membrane, which are governed by two rate constants, one for endocytosis (k_{en}) and one for exocytosis (k_{ex}). Under basal conditions the number of transporters at the plasma membrane is small. Thus following insulin stimulation a marked decrease in the rate of endocytosis of GLUT4 would be required in order to allow for the necessary increase in steady-state glucose transporters (Holman *et al.*, 1994). In addition, the rate of appearance of GLUT4 at the cell surface and its endocytosis should be the same as both are dependent on the same values for k_{ex} and k_{en}. Neither of these criteria are mathematically feasible, nor does the biochemical evidence support them. For example, in rat adipose tissue, the half-times ($t_{1/2} = In_2/k$) for exocytosis and endocytosis of GLUT4 are 2.7 min and 10.6 min respectively (Satoh *et al.*, 1993).

In the "3-pool model" (Holman *et al.*, 1994), a second intracellular pool, the tubulovesicular pool is predicted. The involvement of the tubulovesicular pool allows insulin to stimulate a rapid initial translocation of GLUT4 from this pool without a

Figure 1.3 GLUT4 Recycling Models. In the 'two-pool' model the functional GLUT4 at the plasma membrane (T_p) is in equilibrium with one intracellular early endosomal pool (T_{ee}). In the 'three pool' model a second distinct intracellular pool, the tubulovesicular pool (T_{tv}) is evoked. Figure adapted from Holman *et al.*, 1994.

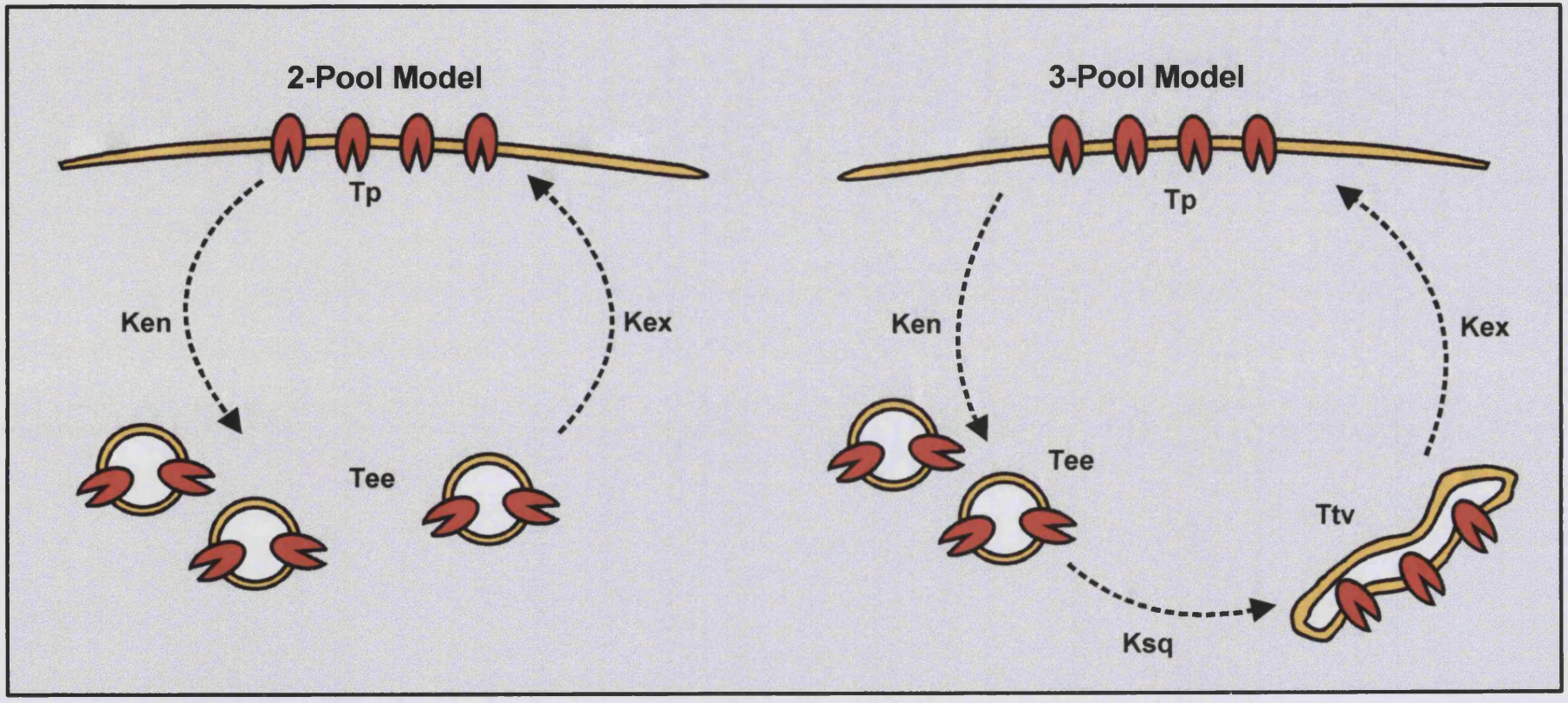

significant effect on the rate of endocytosis (k_{en}). Thus the tubulovesicular pool acts as a reservoir responsible for the initial translocation of GLUT4 to the plasma membrane, which may later re-fill via the endosomal system. In this model, in addition to the GLUT4 in the tubulovesicular pool, GLUT4 present in the endosomal system can also translocate to the plasma membrane by constitutive recycling. The biochemical data for GLUT4 trafficking is more consistent with the "3-pool model" than with the "2-pool model". GLUT4 trafficking data can also be fitted to more complex 4- and 5- pool models in which the formation of occluded populations of vesicles at the plasma membrane are considered (Holman *et al.*, 1994).

1.3.2 GLUT4 Vesicles

GLUT4 vesicles comprise 2-3% of the light microsomes (James *et al.*, 1987; Kandror *et al.*, 1995). These vesicles are homogeneous, round-shaped, 50-70 nm particles with a sedimentation co-efficient of ≈120 *S* in sucrose (Kandror and Pilch, 1996). Upon insulin stimulation the sedimentation co-efficient of the vesicles increases by 20 *S* and consequently the buoyant density decreases, although no major changes in their protein composition are observed (Kandror and Pilch, 1998). One important question to address is whether GLUT4 vesicles obtained by subcellular fractionation are a true representation of the storage compartment *in vivo*, or an artefact of the homogenisation procedure. A plethora of observations suggest that GLUT4 vesicles isolated *in vitro* are not damaged by the subfractionation procedure. Firstly, vesicles isolated by a number of differing protocols from both fat and muscle are essentially the same (Kandror *et al.*, 1995). Secondly, if the vesicles were fragments of the intracellular membranes then they would exhibit similar protein compositions, however this is not the case. Silver staining profiles of GLUT4 vesicles and LDM protein show that they are very different (Kandror and Pilch, 1996). Finally a change in the density of isolated GLUT4 vesicles can be evoked by the addition of insulin to intact cells, which cannot be mimicked *in vitro* (Kandror and Pilch, 1996).

Using subcellular fractionation in combination with a number of other approaches, a timpani of proteins have been found to reside on GLUT4 vesicles. One technique that has provided some interesting data is cell surface biotinylation. Using this method several proteins have been shown to translocate to the cell surface in response to insulin. These included the mannose-6-phosphate receptor (M6PR) and the TfR. However this

procedure has flaws, since small proteins, and those with inaccessible domains such as GLUT4, have low specific biotinylation and may be overlooked (Kandror and Pilch, 1996).

At the time of writing, vp165 (also known as gp160 and IRAP) is the only protein that has been identified, which has a distribution and translocation pattern superimposable with that of GLUT4. Unlike GLUT1, the TfR, and the M6PR, which show only a small 2 to 3-fold insulin-dependent increase in cell surface levels, vp165 is upregulated 10 to 40-fold (comparable with GLUT4), with a half-time of $\approx$ 2 min (Ross *et al.*, 1997). Furthermore a small proportion of vp165 continually recycles between the LDM and the plasma membrane in the basal state (Ross *et al.*, 1997).

Vp165 is a member of the family of zinc-dependent membrane aminopeptidases and has homology to aminopeptidase N. It also exhibits aminopeptidase activity *in vitro* (Kandror *et al.*, 1994). It consists of a large extracellular catalytic domain, a single transmembrane domain and a unique extended cytoplasmic region which contains 2 di-leucine motifs (*Section 1.3.5).* Unlike aminopeptidase N, which is targeted to the plasma membrane with its catalytic domain exposed, vp165 is sequestered intracellularly in the absence of insulin, with the catalytic domain buried within the vesicle. One interesting point to note is that a number of aminopeptidases have been identified in other secretory vesicles, for example on the secretory granules of mast cells and on water channel vesicles from renal epithelia, the latter of which exhibits hormone-induced translocation of vesicles from the microsomes to the plasma membrane (Serafin *et al.*, 1991; Harris *et al.*, 1994). This raises the possibility that vp165 may act to regulate or organise the GLUT4 secretory machinery in an insulin-responsive manner, perhaps behaving as a hormone sensor. Conversely, insulin may act on GLUT4 and vp165 independently but they share the same carrier vesicle. The tissue distribution of vp165 is less restrictive than that of GLUT4, raising the prospect that vp165 regulates distinct specialised secretory vesicles in other cell types independent of insulin action (Keller *et al.*, 1995).

Other proteins including sortilin (Lin *et al.*, 1997), acyl CoA synthase (Sleeman *et al.*, 1998), VAMPs (Tamori *et al.*, 1996), SCAMPS (Laurie *et al.*, 1993), small GTP-binding proteins (Cormont *et al.*, 1993) and components of the insulin-signalling pathway, (Heller-Harrison *et al.*, 1996; Calera *et al.*, 1998) (*Section 1.2)* have all been

detected in the membrane of GLUT4 vesicles. However it is not known whether GLUT4 vesicles carry specific cargo in their lumen. One possible cargo protein is the secreted proteinase adipsin (Kitagawa *et al.*, 1989). However in these studies, GLUT1 was used to adsorb vesicles from 3T3-L1 adipocytes, which probably led to the isolation of a heterogeneous population of both GLUT1 and GLUT4 vesicles. Thus as yet no results have been obtained in insulin-responsive fat or muscle. One intriguing possibility is the recently discovered protein, leptin, the gene-product of the *ob* gene, thought to be involved in the control of appetite (MacDougald *et al.*, 1995).

1.3.3 Compartmentalisation of GLUT4

Established studies on endocytosis have characterised two fates for the endocytosed protein: degradation and/or re-exocytosis to the plasma membrane (Mellman, 1987). However, more recently it has become clear that many cells sequester proteins in specialised pools from which they can be mobilised upon receipt of a viable signal (Mellman, 1996). GLUT4 is a classic example of such a protein, as are the proteins of the small synaptic vesicles (SSVs) of neuroendocrine cells (Rothman and Warren, 1994).

Immunochemical studies (Slot *et al.*, 1991a) have localised GLUT4 to many separate cellular locations, some of which demonstrate elements of the recycling pathway. In the basal state, a small proportion of GLUT4 is found associated with the plasma membrane, with clathrin-coated vesicles and the TGN, and with early endosomes. However a sizeable fraction of GLUT4 ($\approx$ 60%) is found in a dynamic array of tubules and vesicles distributed throughout the peripheral and perinuclear region, which are thought to represent a specialised secretory compartment, and have been referred to as the GLUT4 storage compartment (GSVs) (James and Rea, 1997).

According to the evidence from electron microscopy, at any particular moment approximately 1% of GLUT4 at the plasma membrane is associated with clathrin coated pits (Slot *et al.*, 1991a). Furthermore biochemical data from two groups suggest an interaction between GLUT4 and clathrin-coated vesicles at both the plasma membrane and the TGN (Robinson *et al.*, 1992; Chakrabarti *et al.*, 1994). Thus it is likely that at least some of the GLUT4 at the cell surface is internalised via a coated pit mechanism and enters an early endocytic pathway. From here GLUT4 may be sequestered into the

tubular vesicular storage compartment (GSVs) where it remains in the basal state. Administration of insulin would therefore 'release' GLUT4 from this reservoir, enabling it to traverse the intracellular membranes and traffic to the plasma membrane (Slot *et al.*, 1991a).

This basic representation of GLUT4 trafficking can be derived from a number of possible scenarios, which can be illustrated by four (or a combination of four) more sophisticated models (*Figure 1.4*). However a word of caution is necessary - a number of problems face the researcher when analysing data concerning the endocytosis/exocytosis of a target protein. Firstly, segregation between compartments is not easy to define due to their complex, 3-dimentional structure. Secondly, the choice of markers to delimit an internal compartment is not unequivocal – most internalised markers do not move synchronously through the intracellular membrane maze. Lastly, the membrane compartments are highly dynamic, with continuously evolving morphology. All of these factors complicate the analysis of static morphological data. That said, a wealth of data has been collected concerning the GLUT4 trafficking itinerary, which can be interpreted as follows:

In the first model (*Figure 1.4A*) the GLUT4 storage compartment buds directly from the endosomes. This theory is supported by the observation that there is a partial overlap between some endosomal markers and GLUT4 (Martin *et al.*, 1996a), and by electron micrographs which show GLUT4 in tubular structures adjacent to sorting endosomes, (Slot *et al.*, 1991a). However, in many cells the recycling endosomes are located in the peri-Golgi region, juxtaposed to the Golgi stack and to the TGN, making them difficult to distinguish. Nevertheless, immunoprecipitation of GLUT4 vesicles from skeletal muscle has revealed the existence of two populations of vesicles with differential responses to insulin (Sevilla *et al.*, 1997). One population of vesicles, the 'insulin-insensitive' pool is rich in GLUT4, secretory carrier membrane proteins (SCAMPs) and vesicle associated membrane proteins-2 and -3 (VAMPs 2 and 3); the other, the 'insulin-sensitive' pool is populated by GLUT4 and VAMP2 alone. The precise nature of these GLUT4 populations is unknown, however the pattern of proteins in each pool suggests that the 'insulin-insensitive' pool is an inherent component of the endosomal locus, while the 'insulin-sensitive' pool is derived from it.

The second model (*Figure 1.4B*) suggests that GLUT4 is internalised via clathrin coated vesicles into an endosome which is distinct from other recycling proteins, such as the transferrin receptor (TfR). Data to support this model comes from experiments in PC-12 cells, following the reformation of synaptic vesicle-like membranes (Schmidt *et al.*, 1997). Since there are many parallels between mechanisms initially reported for synaptic vesicle exo- and endocytosis, and for GLUT4 translocation, it would not be impossible for the GLUT4 storage compartment to be reminiscent of the specialised synaptic endosomal sorting station that has been described (Schmidt *et al.*, 1997). Indeed one of the features of this specialised compartment is that traffic out of the compartment is blocked at low temperature. In rat adipocytes, prolonged incubation at 18°C can inhibit insulin-stimulated GLUT4 translocation. In addition, experiments comparing the internalisation of GLUT4 and the TfR show that GLUT4 accumulates within peripheral compartments, which exclude the TfR, at both 15°C and 37°C. GSV formation is blocked at 15°C but reappears when cells are returned to 37°C (Wei *et al.*, 1998). Thus this study suggests that GLUT4 and the TfR are sorted primarily at the plasma membrane into distinct endosomes, (Wei *et al.*, 1998). One problem with this model is that it fails to address the partial co-localisation of GLUT4 with endosomal markers described by a number of laboratories, (Martin et al., 1996a; Malide and Cushman, 1997) unless it is assumed that after its' formation endosomal 'mixing' can occur. Possible evidence for this comes from electron microscopy studies of TfR recycling in polarised MDCK cells. In these studies TfR labelled with gold and internalised apically was shown to mix with TfR tracers endocytosed basolaterally in a common compartment (reviewed in Robinson *et al.*, 1996). These experiments demonstrate that mixing of the contents of some endosomes does occur.

Another major obstacle with this model of GLUT4 trafficking is that in studies where GLUT4 has been expressed in the neuroendocrine cell line PC12, it does not behave like the SSVs (on which the model is based). PC12 cells are known to contain two populations of vesicles, SSVs and secretory granules. However glycerol gradient centrifugation of homogenates from PC12 cells transfected with GLUT4, revealed that the transporter is targeted to neither population of known vesicles but rather forms another storage organelle that can sediment twice as rapidly, and that excludes endosomal markers such as the TfR and synaptobrevin, (Herman *et al.*, 1994). This population of GLUT4 vesicles was also observed in transfected fibroblast cell lines and

Figure 1.4 Models for GLUT4 Trafficking. A. GSVs bud directly from the endosomes. B. GLUT4 is internalised into an endosome which is distinct from the recycling endosomes. C. The GSVs are an integral component of the TGN. D. GLUT4 traffics back to the TGN from the plasma membrane from where it buds to form the GSVs. Adapted from Rea and James, 1997.

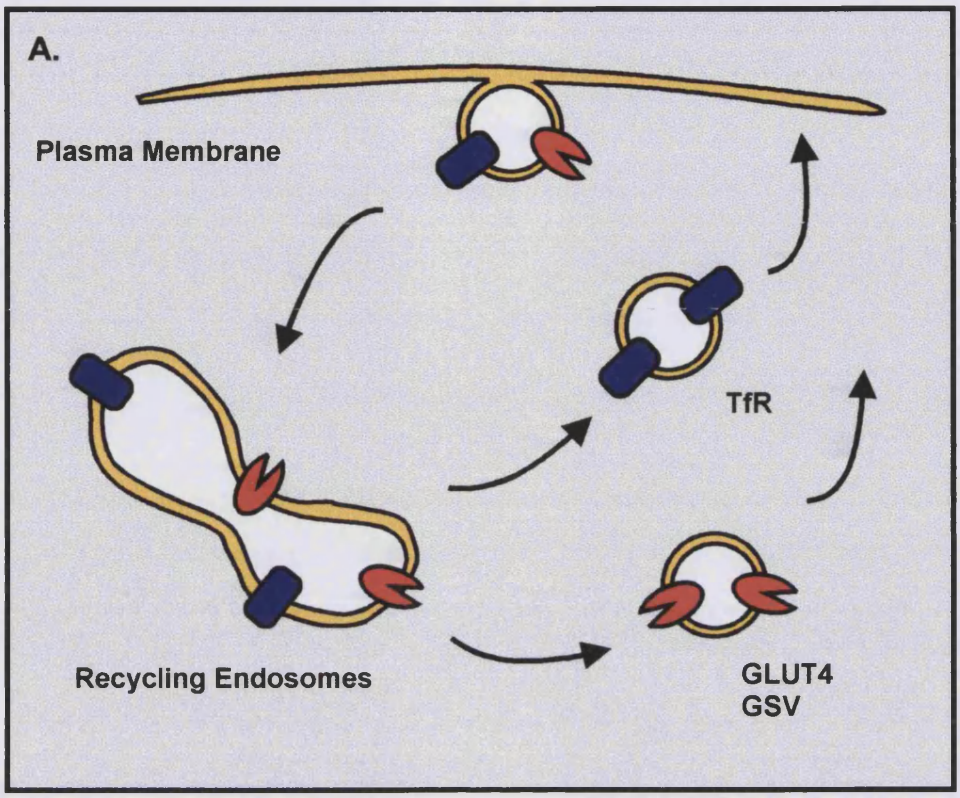

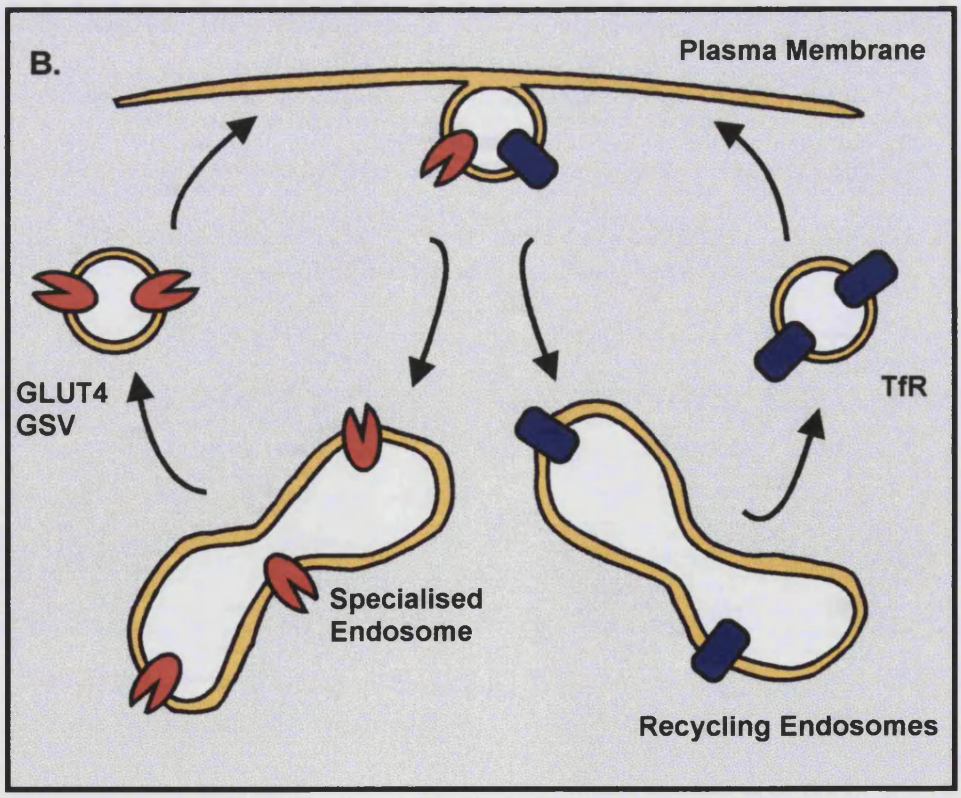

Figure 1.4 (continued). Models for GLUT4 Trafficking.

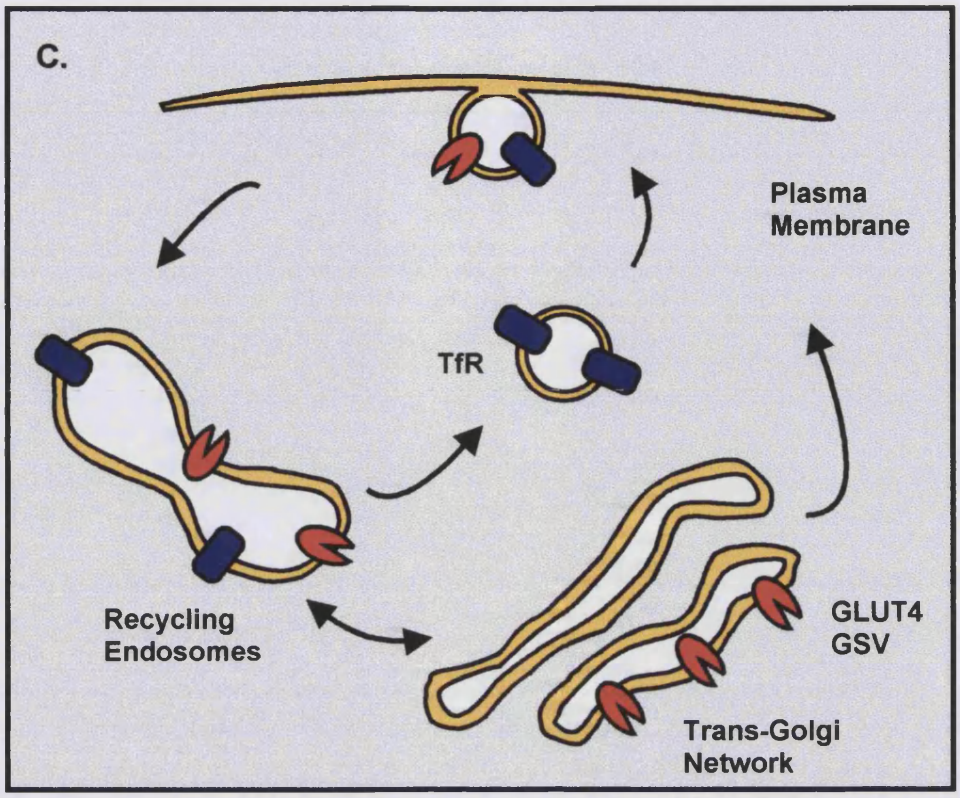

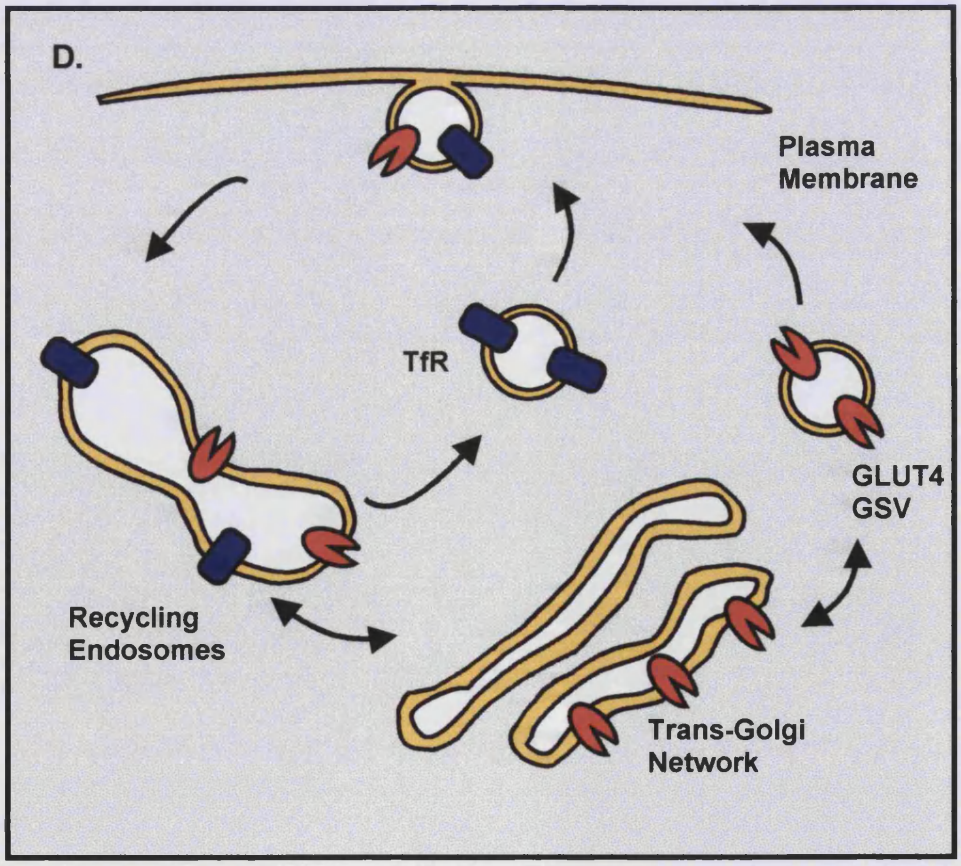

rat adipocytes. Excitingly, insulin provoked a redistribution of GLUT4 from this storage organelle to a population of even faster-sedimenting vesicles.

The third model *(Figure 1.4C)* anticipates that part of the TGN represents the specialised storage locus. This model is supported by EM studies which indicate that at least 13% of the total GLUT4 is enriched in the TGN (Slot *et al.*, 1991a), and by confocal microscopy which reveals partial co-localisation of GLUT4 with γ-adaptin, a subunit of the TGN-specific adaptor complex, AP1 (Malide *et al.*, 1997). In addition an elegant microscopical analysis of GLUT4 in C2 skeletal myotubes has shown that in this tissue the transporter is predominantly located in the *trans*-most cisternae of the Golgi complex and in vesicles just beyond (presumably representing the TGN) (Ralston and Ploug, 1996). GLUT4 in these membranes partially co-localises with the Golgi marker, Giantin. Treatment of these myotubes with brefeldin A results in the fusion of the GLUT4 containing compartment with neighbouring endosomes, and this in turn leads to a loss of co-localisation of GLUT4 with markers of the Golgi and an increase in its association with TfR containing compartments. The authors therefore conclude that GLUT4 is localised to the TGN, but has a 'functional and dynamic connection' with TfR containing endosomes. An uncertainty with this model is the observation that TGN38, a marker of the *trans*-Golgi reticulum, does not co-immunoprecipitate with the GSVs (Martin *et al.*, 1994). One theory is that the TGN comprises of a number of microenvironments in which proteins may be segregated from one another (Millar *et al.*, 1997). Thus TGN38 may inhabit a sub-domain of the TGN which is distinct from that enriched in GLUT4.

The final model (*Figure 1.4D*) suggests (like model 3) that GLUT4 may traffic back to the TGN from the plasma membrane, but from here it buds to create the GSVs. This model is supported by studies which showed, using the selective action of the fungal metabolite, brefeldin A *(Section 1.6.6.2)*, that GLUT4 interacts with clathrin-coated vesicles budding from the TGN (Chakrabarti *et al.*, 1994). Furthermore a recent study in atrial cardiomyocytes (Slot *et al.*, 1997) demonstrated that a large proportion of GLUT4 (50-60%) enters ANF-containing secretory granules, apparently at the level of the TGN. This GLUT4 does not appear to be newly synthesised since incubation with the protein synthesis inhibitor cycloheximide, does not block its localisation. This data suggests that a sizeable portion of GLUT4 must recycle via the TGN, (the principal sorting station in the secretory pathway of mammalian cells).

Corroborating evidence for this model comes from studies using the technique of compartmental 'ablation' (Millar *et al.*, 1997). This technique utilises the recycling properties of the TfR. Transferrin conjugated to horseradish peroxidase (HRP) is internalised by the TfR with normal kinetics, and enters the endosomal system. Addition of 3, 3'-diaminobenzidine (DAB) and H_2O_2 allows HRP to transfer electrons from DAB to H_2O_2, and leads to cross-linking of the conjugate within its sequestered compartment. This, in turn, results in the formation of a high-molecular-mass complex and the compartment is designated 'ablated'. Using this approach it has been shown that while almost all of the TfR, GLUT1 and mannose-6-phosphate receptor (M6PR) is lost, only 40% of the total cellular GLUT4 is ablated (Livingstone *et al.*, 1996). This indicates that the remaining GLUT4 must reside in a post-endosomal compartment.

1.3.4 The Role of the Endosomal GLUT4 Pool in Insulin-Stimulated Glucose Uptake

It clear both from immunocytochemical evidence (Slot *et al.*, 1991a) and from biochemical approaches such as ablation (Livingstone *et al.*, 1996) that GLUT4 and GLUT1 partially overlap, presumably within the endosome. Ablation experiments have also shown that if the endosomal compartment is made inaccessible by cross-linking, insulin is still able to initiate enhanced exocytosis of GLUT4, albeit with a lag period (Martin *et al.*, 1998). Two possible explanations for this observation have been surmised. The first is that GLUT4 recycles from the GSV via the endosome to the plasma membrane (Martin *et al.*, 1998). In this model the lag period can be explained as the time it takes to reconstruct the endosomal apparatus. The second hypothesis assumes that GLUT4 bypasses the endosomes moving directly from the GSVs to the plasma membrane (Martin *et al.*, 1998). If insulin recruits GLUT4 back to the endosomes more quickly than the movement of GLUT4 from the endosome to the GSVs then the lag would be due to the lost endosomal GLUT4. Either way, these models show the importance not only of the GSVs but also of the endosomal pool.

In addition to GLUT4, a host of other proteins including GLUT1, the TfR and the M6PR are trafficked to the plasma membrane as a direct response to insulin (reviewed in Kandror and Pilch, 1996). The magnitude of the insulin effect on each of these proteins is far less than that observed on GLUT4. How can this be reconciled with the proposed existence of a specialised GLUT4 locus and with the observation that many of

these proteins can be immunoprecipitated with GLUT4 vesicles? One hypothesis is that insulin acts differentially on vesicles in the GSVs and the endosomes, both of which contain some GLUT4. It is conceivable that proteins within these compartments or within the insulin-stimulated signalling cascades to these compartments act as molecular modulators, regulating the action of vesicle populations in response to insulin. Indeed heterogeneity of signalling to the endosomal pool of glucose transporters has been observed. For example this pool of transporters is not only regulated by insulin but also by phorbol esters (Holman *et al.*, 1990) and by the protein phosphatase inhibitor okadaic acid (Lawrence, Jr. *et al.*, 1990). The effects of phorbol esters partially mimic those of insulin. Stimulation of rat adipose cells with phorbol 12-myristate 13-acetate (PMA) causes the translocation of both GLUT1 and GLUT4 to the plasma membrane to similar extents (3-fold). However the translocation of GLUT4 in response to PMA is much lower than that induced by insulin (Gibbs *et al.*, 1991). This observation has led to speculation that PMA acts discretely on the population of GLUT4/GLUT1 vesicles present in the endosome. Downregulation of protein kinase C (PKC) by phorbol 12,13-dibutyrate pre-treatment inhibits PMA-stimulated glucose transport, but has no effect on insulin-stimulated glucose transport (Todaka *et al.*, 1996). By contrast, inhibition of PI 3-kinase by wortmannin inhibits insulin-stimulated GLUT4 translocation, but is without effect on PMA action (Todaka *et al.*, 1996). Thus heterogeneity of signalling to glucose transport can be partially dissected.

Preliminary data from the laboratory of Tavare and colleagues (Biochemical Society meeting lecture) revealed that the GLUT4 storage pool is regulated by protein kinase B (*Section 1.2.4*) and is sensitive to botulinum toxins, while the endosomal pool is not. These researchers argue that inhibition of GLUT4 vesicle exocytosis from the GSV pool, results in shunting of GLUT4 vesicles to the endosomal pool, from where insulin can recruit them to the plasma membrane.

1.3.5 Sorting Signals in GLUT4

The identification of multiple intracellular compartments for GLUT4 has important implications in terms of GLUT4 trafficking. It insinuates that the transporter must be recognised by subcellular trafficking proteins in several sorting depots. For many proteins the major determinant in establishing their steady state distribution is the rate of internalisation. This is controlled by a particular amino acid motif (Collawn *et al.*,

1990). Sorting signals can be divided essentially into three classes; the tyrosine based sequences generally YXXØ, the leucine/di-leucine based sequences consisting of ZXXXLØ, and the acidic-based clusters, (single amino acid code, where Z is negatively charged, Ø is hydrophobic and X is any amino acid). The tyrosine and di-leucine based sequences share structural similarities and usually form β-turns.

GLUT1 and GLUT4 are very similar in terms of their primary sequence and their predicted secondary structure, however under basal conditions they are targeted to distinct subcellular locations, GLUT4 being predominantly intracellular whereas GLUT1 is present at high levels in the plasma membrane (Birnbaum, 1992). When expressed in non-insulin responsive cells such as HepG2 or 3T3 fibroblasts via DNA-mediated gene transfer, the unique pattern of targeting for GLUT1 and GLUT4 is recapitulated (Haney *et al.*, 1991). This suggests that the information to sequester GLUT4 in an intracellular compartment is contained within the protein itself (Haney *et al.*, 1991). Small intrinsic differences between GLUT1 and GLUT4 must therefore be recognised by trafficking and/or protein sorting machinery.

1.3.5.1 The Amino Terminus of GLUT4

In a search for targeting information, many laboratories have analysed small regions of sequence diversity, which exist between GLUT1 and GLUT4. In 1992, Piper and colleagues constructed chimeras of GLUT1 and GLUT4 which they transiently expressed in CHO cells (Piper *et al.*, 1992). Using these chimeras they showed that the N-terminus of GLUT4 (and not the C-terminus) is required for intracellular sequestration in the absence of insulin. In addition they reported that the sequence which confers this segregation selectivity is contained within the first 19 amino acids at the cytoplasmic side of the membrane. In this region at position 5 is an aromatic amino acid (phenylalanine), which may take the place of tyrosine in the formation of a GLUT4 'tyrosine-like' internalisation motif. The sequence FQQI bears some resemblance to internalisation motifs found in other proteins such as the TfR and the M6PR (Collawn *et al.*, 1990; Canfield *et al.*, 1991). These amino acids may enable GLUT4 to interact with clathrin coated pits via adaptor proteins causing efficient endocytosis *(Section 1.6.5)* (Pearse and Robinson, 1990). Other studies have shown that aromatic residues may have pleiotropic effects on protein targeting. For example, the tyrosine residue in the

cytoplasmic tail of lgp120, is responsible not only for internalisation but also for directing the protein from the TGN to the lysosomes (Harter and Mellman, 1992).

Confirming their earlier work and expanding upon it, Piper and co-workers expressed GLUT4 constructs containing deletions or alanine substitutions in the N-terminus (Piper *et al.*, 1993). Use of these engineered transporters revealed that the loss of the first 8 amino acids or substitution of F for A at position +5, resulted in a marked accumulation of the transporter at the cell surface. Furthermore co-localisation of GLUT4 with clathrin lattices at the plasma membrane is abolished by deleting the first 13 amino acids or by the $F^5 \rightarrow A$ substitution. In order to test whether the N-terminus could act as an internalisation motif independent of the remainder of the glucose transporter the first 23 amino acids of GLUT4 were grafted onto the H1 subunit of the asialoglycoprotein receptor. This chimera exhibited an increase in its intracellular sequestration when compared with the wild-type H1 protein, which clearly demonstrates that the N-terminus of GLUT4 can function as an autonomous sorting domain (Piper *et al.*, 1993). However, not only did the N-terminal domain increase the internalisation rate of the asialoglycoprotein but it also targeted the protein to the peri-nuclear region, a subcellular location normally inhabited by GLUT4 but not by the H1 protein.

One interesting study addressed the importance of the N-terminus of GLUT4 as an internalisation signal using chimeras of GLUT4 and the TfR (Garippa *et al.*, 1994). The N-terminus of the TfR was substituted with the corresponding region of GLUT4 and the endocytic behaviour of the chimera was characterised in CHO cells, using radioactive transferrin as a tracer. The GLUT4-TfR chimera trafficked back to the plasma membrane at the same rate as the wild-type TfR, indicating that the N-terminus does not promote intracellular retention, however the internalisation of the chimera was reduced by $\approx$ 50%. Substitution of F^5 for A slowed the rate of endocytosis even further to a level approximately equivalent to the rate of bulk membrane flow. Conversely substitution of F^5 for Y resulted in an increase in internalisation equivalent to the endogenous TfR. None of these substitutions affected the rate of recycling back to the cell surface (Garippa *et al.*, 1994).

As already discussed the N-terminal GLUT4 motif FQQI fulfils the presumed requirements for a functional clathrin-coated pit internalisation motif i.e. an aromatic residue separated by 2 residues from a bulky hydrophobic amino acid (Collawn *et al.*,

1990). In addition nuclear magnetic resonance has indicated that the N-terminus of GLUT4 folds into the predicted β-turn (of such motifs) in solution, and that this conformation is lost by the $F^5 \rightarrow A$ substitution. Thus an important question to ask is whether there is a physiological significance for the use of phenylalanine (an intermediate internalisation motif) over tyrosine (a strong internalisation motif) in GLUT4? One observation is that the presence of phenylalanine in the GLUT4 motif results in the transporter remaining at the cell surface approximately twice as long as tyrosine motif-containing proteins (Garippa *et al.*, 1994). It is therefore possible that this may be of some benefit during times of insulin stimulation.

1.3.5.2 The Carboxyl Terminus of GLUT4

In addition to the N-terminal sequence, GLUT4 also contains a potential sorting motif in the C-terminal cytoplasmic tail. This region was analysed in two studies using similar chimeras expressed in COS-7 cells (Czech *et al.*, 1993) or NIH 3T3 and PC12 cells (Verhey *et al.*, 1993). In both cases the GLUT1/GLUT4 transporters were epitope tagged in a region of the protein that would not interfere with targeting motifs, thus enabling the chimeras to be distinguished from endogenous GLUTs. The results from these groups were near identical and illustrated the importance of the last 30 amino acids at the C-terminus in the sequestration of GLUT4 and to a lesser extent the first ≈150 amino acids of the N-terminus. This was in contrast to Piper and colleagues who saw no effect of the C-terminus under their experimental conditions (Piper *et al.*, 1992). Thus Czech *et al.* (Czech *et al.*, 1993) speculated that at physiological concentrations of transporter the major structural determinant for GLUT4 sequestration is at the C-terminus. However when transporters are expressed at high levels (as in the study by Piper *et al.*, 1992) this determinant becomes saturated and the intracellular sequestration information is now switched to motifs in the N-terminus and intracellular loops.

When the C-terminal domain was analysed in more detail a sequence around amino acids 489-490 was identified, which is consistent with di-leucine based internalisation motifs described in other recycling proteins (Verhey and Birnbaum, 1994). Using GLUT1/GLUT4 chimeras in NIH 3T3 cells researchers demonstrated that L^{489} and L^{490} are important residues for intracellular sequestration since mutating them to A^{489} and S^{490} causes the movement of the chimera from the perinuclear region to the cell periphery. Thus the di-leucine motif is likely to regulate endocytosis but may also play

a role at the TGN to sort proteins away from a default pathway to the cell surface. The authors also suggest that upon removal of insulin both the phenylalanine and the di-leucine motif are important in the return of GLUT4 from plasma membrane.

The results obtained in the studies described thus far have provided many clues as to the important targeting information contained within GLUT4. However some of the earlier reports were plagued with contradiction. A number of possible explanations can be surmised to explain the varied results. Firstly the choice of expression system used in the study is of importance since vectors which induce high levels of expression, surpassing endogenous protein concentrations, may saturate sorting machinery, as has been described for other systems (Reaves and Banting, 1994). Indeed in studies using transgenic mice overexpressing GLUT4, the basal level of the transporter at the plasma membrane is substantially increased, indicating either saturation of a cytoplasmic compartment or of the machinery responsible for endocytosis (Liu *et al.*, 1993). Secondly, it is possible that two or more regions of the transporter, although discontinuous in the primary structure, may be juxtaposed in the native transporter to form a single sorting motif. These motifs would be difficult to analyse using the chimera approach. Thirdly, there is a risk when using chimeras in which large domain are swapped, that they will not fold correctly. Fourthly chimeras may exhibit the phenomenon of "piggy-backing" where by virtue of their ability to oligomerise, engineered transporters may couple with and be targeted by endogenous protein. Finally, and of utmost importance, all of these studies have been performed in non-insulin regulated systems. These cell lines may lack the unique insulin sensitive sorting machinery responsible for targeting GLUT4 in fat and muscle.

Some of these problems were addressed in a study analysing the targeting of GLUT4 in bona-fide insulin responsive cells (Marsh *et al.*, 1995). Three constructs were expressed in 3T3-L1 adipocytes: TAG, (epitope-tagged wild-type GLUT4), FAG (GLUT4 containing an $F^{5}\rightarrow A$ mutation in the N-terminal FQQI motif) and LAG (GLUT4 in which $L^{489}L^{490}$ were mutated to AA in the C-terminal di-leucine motif). All three mutants were expressed to the same level and the TAG construct was targeted to the same compartment as endogenous transporters. FAG accumulated at the plasma membrane, whereas LAG was only trapped at the cell surface if it was expressed at levels four-fold greater than the endogenous transporter. Thus one can speculate that the F-based motif is important in plasma membrane to endosomal trafficking. Under

these experimental conditions, both FAG and LAG were stimulated to the plasma membrane by insulin, suggesting that the N- and C-terminal targeting motifs are not important for insulin-regulated movement.

A more extensive characterisation of the motifs was performed in an ablation study using the same TAG, FAG and LAG GLUT4 mutants (Melvin *et al.*, 1999). Analysing the intracellular locations of the mutants using the DAB/H_2O_2 technique showed that the internal pool of FAG transporters was substantially ablated. This pool of mutant GLUT4 (FAG) was therefore either confined to the recycling endosomes with TfRs or does not accumulate in the non-ablated compartment. Conversely the LAG mutant escaped ablation even more effectively than the wild-type transporter (TAG). While the authors could not show conclusively that the failure to ablate the LAG mutant was not due to inappropriate targeting, the observation that the LAG mutant co-fractionates with vp165 *(Section 1.3.2)* provides compelling circumstantial evidence that LAG is targeted to the same pool as the wild-type GLUT4. The authors suggest a model to explain their results in which GLUT4 is internalised into the recycling endosomal compartment and from here traffics to the TGN from which the GSVs bud. They also suggests that internalisation into the endosomal compartment requires both the FQQI and LL motifs and that transfer to the TGN may be dependent upon the FQQI motif, explaining the reduced levels of FAG in the non-ablated compartment. Similarly, the LL motif may be required for the translocation of GLUT4 from the TGN to the GSVs. Thus in the LAG mutant, GLUT4 accumulates in the TGN resulting in a bottle-neck in its constitutive recycling and hence a greater proportion of it is protected from ablation, compared with the wild-type transporter (Melvin *et al.*, 1999). One important observation is that the LL motif is adjacent to a site of phosphorylation on GLUT4 and as such it would be interesting to examine whether the AA mutation abrogates phosphorylation, and whether this effects trafficking. Indeed studies in other systems have suggested that post-translational modifications such as phosphorylation can modulate intracellular sorting (Trowbridge *et al.*, 1993).

Recently a series of experiments have analysed the involvement of the C-terminus of GLUT4 in rat adipose cells (Lee and Jung, 1997). Rat epididymal adipocytes were fused with erythrocyte ghosts preloaded with GLUT4 C-terminal peptide via polyethylene glycol-induced cell-cell fusion. The C-terminal GLUT4 peptide caused an increase in glucose transport and GLUT4 translocation in basal cells but not in insulin

treated cells. This implies that information contained within the C-terminus of GLUT4 is important for retaining GLUT4 in an intracellular compartment or is involved in GLUT4 endocytosis at the plasma membrane. The authors suggest that auxiliary proteins interact with the C-terminus of GLUT4 under basal conditions, tethering it to an internal locus, and that these proteins are released by the actions of insulin. Addition of exogenous C-terminal GLUT4 peptide may therefore saturate the intracellular binding site for GLUT4, and enable endogenous transporter to be released and traffic to the plasma membrane. The C-terminal peptide used in this study was 43 amino acids long and contained the di-leucine motif. Whether it is the LL motif or another sequence contained within the C-terminal peptide which confers this 'docking' ability remains to be established.

Like GLUT4, the di-leucine motifs in the aminopeptidase vp165 are also important for the control of its intracellular trafficking. Indeed use of chimeras of vp165 and the TfR have shown that the di-leucine motifs within vp165 are responsible for the maintenance of a slow endocytic recycling mechanism in response to insulin (Johnson *et al.*, 1998).

Many proteins exhibit complex recycling patterns, which must be governed by a number of intrinsic sorting sequences. For example, the M6PR contains 2 motifs both in its cytoplasmic tail, which are involved in regulating its intracellular repertoire. One of these motifs is a tyrosine based sequence that is required for efficient internalisation, the other is a di-leucine based motif which is responsible for regulating the recycling between the Golgi and the late endosomes (Johnson and Kornfeld, 1992). Identification of a number of potential targeting domains in GLUT4 is therefore not surprising, when considered in the context of the labyrinth of intracellular compartments in which it is known to reside. Clearly both components of the N- and C-termini are instrumental in defining the trafficking and the compartmentalisation of GLUT4 under basal conditions. Presumably the C-terminus and potential additional signals are also required to elicit or further regulate entry into the specialised GLUT4 compartment *(Section 1.3.3)*. These targeting motifs may not be as well conserved as the di-leucine or tyrosine based signals but could include a short sequence found at the extreme C-terminus of GLUT4 which shows some homology to a sequence found in the cytoplasmic tail of vp165 (Rea and James, 1997).

1.4 Exercise and Contraction Induced GLUT4 Pools

As well as insulin, a host of other stimuli (e.g. catecholamines, hypoxia, and growth factors) can alter glucose transport, however the only other major regulator of transport is exercise/contraction. Contraction-induced changes in glucose uptake occur in the heart and in slow and fast twitch muscles (Hayashi *et al.*, 1997). Like insulin, contraction can increase glucose transport through an increase in the V_{max} of the transporter with little change in K_m (Holloszy and Narahara, 1967). Initial experiments using a motorised rodent treadmill to exercise rats and a subfractionation protocol to separate skeletal membrane fractions demonstrated that, like insulin, muscle contraction stimulates glucose transport by the translocation of glucose carriers from an internal storage site to the plasma membrane (Douen *et al.*, 1989). Subsequently, using a modified subfractionation procedure, exercise was shown to induce not only a substantial translocation of GLUT4 to the plasma membrane, but also to the transverse tubules (t-tubules) (Marette *et al.*, 1992). This exercise-induced redistribution of GLUT4 to the t-tubules may serve to deliver glucose to sites deep within the muscle (Hayashi *et al.*, 1997).

The combinatorial effect of insulin and contraction on glucose transport is greater than the individual actions of these stimuli (Wallberg-Henriksson and Holloszy, 1985). The 'additive' nature of the contraction and insulin stimuli implies that they act independently. In support of this view, a recent study, using discontinuous sucrose gradients, demonstrated the existence of two pools of glucose transporters (Coderre *et al.*, 1995). These pools, which were found to fractionate at 32 and 36% sucrose, responded independently to insulin and exercise. Stimulation with both insulin and contraction caused the depletion of GLUT4 from both pools. Furthermore, vp165, an inherent component of GLUT4 vesicles was found to subfractionate with both pools (Coderre *et al.*, 1995). In a corroborating study using EM microscopy, GLUT4 was observed at the TGN in two compartments: large depots, and small tubulovesicular elements (Ploug *et al.*, 1998). The small pools could be further subdivided into TfR-positive and TfR-negative pools. Insulin increased the co-localisation of GLUT4 and TfR, while contraction/exercise reduced this association. Thus contraction and insulin may act upon different populations of GLUT4 vesicles in whole muscle fibres.

Unlike insulin, exercise stimulated GLUT4 translocation in skeletal muscle does not result in autophosphorylation of the insulin receptor nor is it mediated by PI 3-kinase, as indicated by the lack of effect of the PI 3-kinase inhibitor, wortmannin (Lund *et al.*, 1995). A caveat to this is that wortmannin does inhibit contraction stimulated glucose transport in cardiac myocytes (Till *et al.*, 1997). Protein kinase B shown to be a down stream target of PI 3-kinase in the insulin signalling pathway (*Section 1.2.4*), is also unaffected by skeletal muscle contraction (Lund *et al.*, 1998).

So how does contraction stimulate glucose transport? Calcium which is released from the sarcoplasmic reticulum in response to depolarisation of the plasma membrane may play a role in exercise-induced glucose uptake, since agents which increase intracellular calcium concentrations also stimulate glucose transport (for review see Hayashi *et al.*, 1997). This calcium-mediated effect may be due to activation of PKC-dependent pathways. Some studies have also suggested that exercise can cause the local release of bradykinin, a nonapeptide hormone, which may be involved in glucose transport. Indeed addition of exogenous bradykinin to L6 myotubes expressing G_q-coupled bradykinin receptors stimulates GLUT4 translocation to the plasma membrane in a PI 3-kinase-independent manner (Kishi *et al.*, 1998). Aside from these examples, little definitive information is available as to how exercise increases glucose transport. Clearly much work is required to elucidate the contraction-signalling pathway to GLUT4.

1.5 Role of GTP binding Proteins in Vesicle Trafficking

1.5.1 GTPγS-stimulated Glucose Transport

Baldini and co-workers first demonstrated that guanosine 5'-*O*-(3-thiotriphosphate) (GTPγS) can display insulinomimetic effects in 1991 (Baldini *et al.*, 1991). Using alpha-toxin permeabilised rat adipocytes, these researchers showed that GTPγS-induced a 3 to 6-fold increase in GLUT4 translocation, while GTP had no effect. The stimulatory effects of GTPγS can be mimicked by treatment with AlF_4^-, implicating the involvement of heterotrimeric G-proteins (Kanai *et al.*, 1993b). Indeed in Chinese Hamster Ovary cells (CHO) and 3T3-L1 adipocytes, activation of receptors coupled to G_q can stimulate glucose transport (Kishi *et al.*, 1996). More recently, the GTPγS responsive glucose transport pathway has been shown to be independent of insulin

receptor (IR) and insulin receptor substrate-1 (IRS-1) phosphorylation, and of PI 3-kinase and protein kinase B (PKB) targeting/activation (Elmendorf *et al.*, 1998) *(Sections 1.2.1-1.2.4)*. Instead GTPγS induces the tyrosine phosphorylation of a number of other signalling molecules including protein-tyrosine kinase-2, pp125 focal adhesion tyrosine kinase, pp130 Crk-associated substrate, paxillin and Cbl. Furthermore, in contrast to insulin, GTPγS has been reported to stimulate glucose transport both by increasing the rate of exocytosis and by appreciably decreasing the rate of endocytosis (Shibata *et al.*, 1995).

1.5.2 Dynamin

Dynamin is a large, 100-kDa GTPase, originally isolated from calf brain, in a search for novel microtubule-based motors, nearly 10 years ago (Shpetner and Vallee, 1989). More recently dynamin has been implicated in the endocytic uptake of receptors, associated ligands and the plasma membrane following exocytosis (Robinson *et al.*, 1996). This function of dynamin was discovered by studies on Drosphila with a temperature-sensitive mutation in the dynamin gene, *Shibire*. At non-permissive temperatures these flies rapidly display paralysis as a result of their inability to recycle synaptic vesicle membranes at the neuromuscular junction (Robinson *et al.*, 1996). Three dynamin isoforms have been identified to date, sharing 80% homology at the amino acid level; a brain-specific isoform, Dynamin I, a ubiquitous isoform, Dynamin II and a testis-specific isoform, Dynamin III (Urrutia *et al.*, 1997). Dynamins consist of a tripartite GTP binding site in the N-terminus, a pleckstrin homology (PH) domain and a C-terminal proline rich region (reviewed in Urrutia *et al.*, 1997). Each dynamin gene has several variably spliced gene products, and so it is interesting to speculate a role for each in related but distinct endocytic processes.

One of the first proteins to be shown to associate with dynamin was the cytoskeletal protein tubulin. In fact, tubulin polymers can stimulate GTPase activity on dynamin by 75-fold (Shpetner and Vallee, 1992). In addition to binding to the cytoskeleton, dynamin may also participate in cell signalling cascades by binding to SH3 domain-containing proteins, including the regulatory subunit (p85α) of PI 3-kinase *(Section 1.2.3)* via its proline-rich domain (Herskovits *et al.*, 1993). It has also been shown to bind to the plasma membrane adaptor complex AP2 *(Section 1.6.2)*, and can co-immunoprecipitate with the insulin receptor and IRS-1 via a common binding partner,

Grb2 (Ando *et al.*, 1994). One of the most intriguing properties of dynamin is its ability to self-assemble into helical filaments even in the absence of GTP (Hinshaw and Schmid, 1995). These 'spirals' have been seen *in vivo* around the necks of endocytic invaginations as electron dense 'collars'. The unique distribution of dynamin has led to speculation that it acts as a 'pinchase', severing the membrane to release vesicles into the cytoplasm, as a result of GTP hydrolysis. Indeed inhibition of GTP hydrolysis, using GTPγS or dynamin with a mutation in the GTP-binding domain, leads to the accumulation of membrane invaginations at the plasma membrane (reviewed in Warnock and Schmid, 1996).

GLUT4 is internalised via clathrin coated pits *(Sections 1.3.5 and 1.6.1)* by an unknown mechanism. Several groups have examined the role of dynamin I in GLUT4 endocytosis. To this end, wildtype and a GTPase negative mutants of dynamin (dynamin-K44E) were expressed in CHO cells expressing the insulin receptor and GLUT4 ($CHO^{IR\text{-}GLUT4}$) (Omata *et al.*, 1997), in primary rat adipocytes (Al Hasani *et al.*, 1998), and in 3T3-L1 adipocytes, (Kao *et al.*, 1998). All three studies showed an accumulation of GLUT4 at the cell surface under basal conditions in cells expressing the dynamin mutant. Furthermore insulin was only able to recruit GLUT4 from the intracellular pool to the plasma membrane in cells expressing the wild-type dynamin, and not in cells expressing the mutant. These results clearly demonstrate a role for dynamin in GLUT4 endocytosis, and illustrate that endocytosis may be required not only for the selective uptake of receptors and transporters but also as a means of balancing cell surface versus intracellular compartments and their respective components.

Only one group has studied the effects of the ubiquitous dynamin isoform (dynamin II) on GLUT4 endocytosis, (Volchuk *et al.*, 1998). These experiments demonstrated that dynamin II is expressed in 3T3-L1 adipocytes in both the plasma membrane and low density microsome fraction, (a fraction enriched in Golgi structures), and that insulin causes a decrease in the association of dynamin II with the plasma membrane of $\approx$ 50%. In addition, these authors have also assessed the role of amphiphysin in GLUT4 trafficking. Amphiphysin is an SH3 domain containing protein, which binds to the proline-rich region of dynamin, and is thought to be important in recruiting dynamin to sites of endocytosis. Microinjection of a fusion protein containing the SH3 domain of amphiphysin into 3T3-L1 adipocytes inhibits TfR endocytosis and increases cell surface

GLUT4. Furthermore a peptide containing the proline-rich domain of dynamin (which binds to amphiphysin) inhibits GLUT4 re-internalisation following insulin stimulation. Taken together, these data suggest that both dynamin II and amphiphysin play a role in GLUT4 endocytosis in 3T3-L1 adipocytes.

1.5.3 Rad GTPase

Rad is a small GTP-binding protein of the *Ras* superfamily, isolated from human muscle by subtraction cloning (Moyers *et al.*, 1996). The expression of Rad is increased in some type II diabetics raising the possibility that Rad plays an important role in glucose homeostasis. Overexpression of Rad in the insulin-responsive cell lines, C_2C_{12} murine myotubes and L6 rat myotubes, results in a 50-90% decrease in insulin-stimulated 2-deoxy-D-glucose transport, without a detectable change in GLUT4 translocation (Moyers *et al.*, 1996). These data suggest that Rad negatively modulates the intrinsic activity of GLUT4.

1.5.4 ARF GTPases

ADP-ribosylation factors (ARFs) are 20-kDa nucleotide binding proteins, members of the *Ras* GTPase superfamily, which were originally isolated as a consequence of their ability to stimulate the ADP-ribosyltransferase activity of the cholera toxin A subunit (CTA) (Kahn and Gilman, 1984). We now know that ARFs have a multitude of functions; they act as molecular switches for many vesicular trafficking pathways, are activators of specific phospholipase Ds (PLDs) and are involved in the recruitment of coat proteins onto budding vesicles (reviewed in Roth, 1999) *(Section 1.6.6.2)*.

Mammalian ARFs can be divided into 3 classes based on size, amino acid sequence, gene structure, and phylogenetic analysis; ARFs -1, -2 and -3 are in class I, ARFs -4 and -5 are in class II and ARF6 is in class III (Roth, 1999). ARFs exhibit a vectorial pattern of signalling, which results from the necessary sequence of GTP binding, hydrolysis of bound GTP and release of the GDP product *(Figure 1.5)*. ARFs act as binary switches, active in the GTP-bound form and inactive in the GDP-bound form. The most studied members of the ARF family are ARF1 and the atypical ARF, ARF6 (Chavrier and Goud, 1999).

ARF1 was initially found to be a component of COPI vesicles isolated from Golgi membranes, and was later shown to be necessary for the formation of these vesicles *in vitro* (Rothman and Wieland, 1996). In addition, much data has now indicated a role for ARF1 in the formation of clathrin-coated vesicles containing the adaptor proteins AP1 (Stamnes and Rothman, 1993) and AP3 (Ooi *et al.*, 1998) *(Section 1.6.2)*. A definitive role for ARF1 in the regulation of vesicular trafficking came from experiments *in vivo* using ARF mutants defective in either GTP-binding or GTP hydrolysis. Mutants defective in GTP-binding prevented coat proteins from binding to the Golgi, and this resulted in the retrograde transport of Golgi membranes to the ER. In contrast, mutants defective in GTP hydrolysis allowed binding of coat proteins to the membranes however this binding was irreversible, and prevented the fusion of vesicles with the Golgi membrane (Rothman and Wieland, 1996).

ARF6 is the least conserved of the ARF protein family. It is associated with, and appears to control the integrity of peripheral membranes (Chavrier and Goud, 1999). Several studies have indicated that ARF6 may cycle between the plasma membrane and an internal compartment, depending on its nucleotide status (Radhakrishna and Donaldson, 1997). In CHO cells, a GTP bound, constitutively active mutant of ARF6 (ARF6Q67L), is localised to the plasma membrane, where it causes extensive invaginations, inhibits transferrin internalisation, and induces a redistribution of TfRs to the plasma membrane (D'Souza-Schorey *et al.*, 1995; D'Souza-Schorey *et al.*, 1998). In contrast, a GDP bound ARF6 mutant (ARF6T27N) is associated with a peri-centriolar pool which contains TfRs and VAMP3 (D'Souza-Schorey *et al.*, 1995). In addition ARF6 binds to the actin cytoskeleton and induces actin rearrangement. This can be prevented by incubation with cytochalasin D, which redistributes ARF6 from the plasma membrane to the recycling endosomes (D'Souza-Schorey *et al.*, 1995).

1.5.5 ARF-GEFS

Under physiological conditions, exchange of GDP for GTP on ARFs is a rate-limiting step in ARF activation. However this exchange process is rapidly accelerated by the action of Guanine nucleotide exchange factors (GEFs), seven of which are now known (for review see Roth, 1999) *(Figure 1.5)*. ARF-GEFs exist in soluble and particulate forms and may be divided into three classes based on their size and their sensitivity to the fungal metabolite, brefeldin A. The large, 'sensitive' class contains the yeast

proteins Sec7p, Gea1p, Gea2p and the mammalian p200. The large 'insensitive' class contains the protein GBF1, recently identified by screening a cDNA library from a brefeldin A-resistant CHO mutant cell line (Claude *et al.*, 1999). The smaller proteins, ARNO1, GRP1 and cytohesin1 represent the final class and are all brefeldin A insensitive. These small proteins each contain a pleckstrin homology domain and may associate with specific membranes in response to the production of phosphoinositides. For example, GRP1, which was discovered as a result of a screen for mouse proteins which bind phosphoinositides (Klarlund *et al.*, 1997), associates specifically with phosphatidylinositol-3,4,5-trisphosphate (PIP_3). This lipid specificity may dictate recruitment of GRP1 to sites of PIP_3 production and connect receptor-activated PI 3-kinase signalling pathways with proteins that mediate biological responses such as membrane trafficking (Klarlund *et al.*, 1997).

All ARF-GEFs have a small catalytic Sec7 domain, which is responsible for guanine nucleotide exchange. However, when the Sec7 domain of ARNO is reacted with myristoylated ARF-GDP it fails to catalyse nucleotide exchange (Paris *et al.*, 1997). Only in the presence of liposomes does the reaction proceed. This observation has led to the suggestion that the myristoylated amino terminus of ARF inhibits nucleotide exchange unless there is lipid nearby. ARFs are distinct from many other *Ras*-related proteins in their conformation in the nascent state. In the inactive form ARF-GDP adopts a conformation in which the N-terminal myristate is bound to a pocket on the surface of the protein, and amino-acids 41-47 form a β-strand at the edge of a sheet of seven strands. In 1998, Goldberg solved the structure of active ARF-GTP, and showed that following activation amino acids 41-47 leave the sheet, and move to a position similar to other *Ras*-related proteins (Goldberg, 1998a). This extensive rearrangement requires that the N-terminus and myristate leave the binding pocket and that a loop between strands β2 and β3 invade the space. Also in 1998, Goldberg crystallised a complex of the Sec7 domain of Gea2p and ARF-GDP (Goldberg, 1998b). This structure revealed that, "the structure of ARF-GDP appears to be incompatible with the contours of the recognition site" of the Sec7 domain (Goldberg, 1998b). This indicates that ARF must undergo a conformational change, which facilitates entry into the Sec7-binding domain. Biochemical data mentioned above have indicated that ARF will not interact with the Sec7 domain in the absence of lipid. Thus either Sec7 can dislodge the myristoylated amino-terminus of ARF if there are lipids nearby to capture it, or the lipids themselves can draw it away from the binding pocket. The role of the myristate

on the N-terminus of ARF is therefore to regulate where and when ARF-GDP can be activated by ARF-GEFs. This can be further demonstrated by the observation that ARNO can catalyse nucleotide exchange, even in the absence of lipid micelles, when ARF is present without the first 17 amino acids at the N-terminus (Paris *et al.*, 1997).

1.5.6 ARF-GAPS

As well as ARF-GEFs, ARF function is aided by a number of ARF-GTPase activating proteins (ARF-GAPs), which catalyse GTP hydrolysis *(Figure 1.5)*. Since GTP-binding and hydrolysis are equally critical features of ARF action, it is intriguing that many more ARF-GEFS have been identified than ARF-GAPs (Moss and Vaughan, 1998). One possible reason is that ARF-GAPs appear to exhibit a much broader specificity, catalysing GTP hydrolysis on a number of ARF isoforms.

The N-terminal domain (130 amino acids) of the rat ARF-GAP p47 is sufficient for GAP activity. This domain contains the zinc finger motif, a signature for ARF-GAP proteins (Roth, 1999). In addition to the catalytic domain, a non-catalytic domain is also required for ARF-GAP function. This non-catalytic domain, situated at the C-terminus is required for faithful ARF activation due to its role in membrane targeting (Roth, 1999). Recently it has been shown that ARF1-GAP binds to membranes via an association with the transmembrane KDEL receptor, ERD2. The KDEL receptor was initially discovered as a receptor for soluble ER proteins, which are mistargeted to the Golgi. The first observation that KDEL receptors may also play a role in the secretory pathway came from studies of yeast mutants with deleted KDEL receptors. As expected, these mutants were unable to retrieve KDEL proteins from the Golgi back to the ER, but they also exhibited dysregulated transport through the Golgi (Semenza *et al.*, 1990). Later overexpression of KDEL receptors was shown to inhibit ARF1 activation by interacting with ARF1-GAP (i.e. preventing GTP hydrolysis on ARF1), via the non-catalytic domain. Interaction of KDEL receptors with ARF-GAPs is therefore important for regulating GAP recruitment and activity and for ARF1 inactivation on membranes (Aoe *et al.*, 1999).

Recently, a new family of proteins, the centaurins, has been described, which contain a zinc finger domain in the N-terminus, showing similarity to the rat liver ARF1-GAP, and to the yeast GAP protein, Gcs1. In addition to the zinc finger domain, the

Figure 1.5 Vectorial Sequence of ARF Activation. Association of ARF with ARF-GEFs allows the exchange of GDP for GTP. Some ARF-GEFs are brefeldin A (BFA) sensitive, other are not. ARF-GAPs associate with the membrane by binding to KDEL receptors. Once bound they stimulate GTP hydrolysis on ARF.

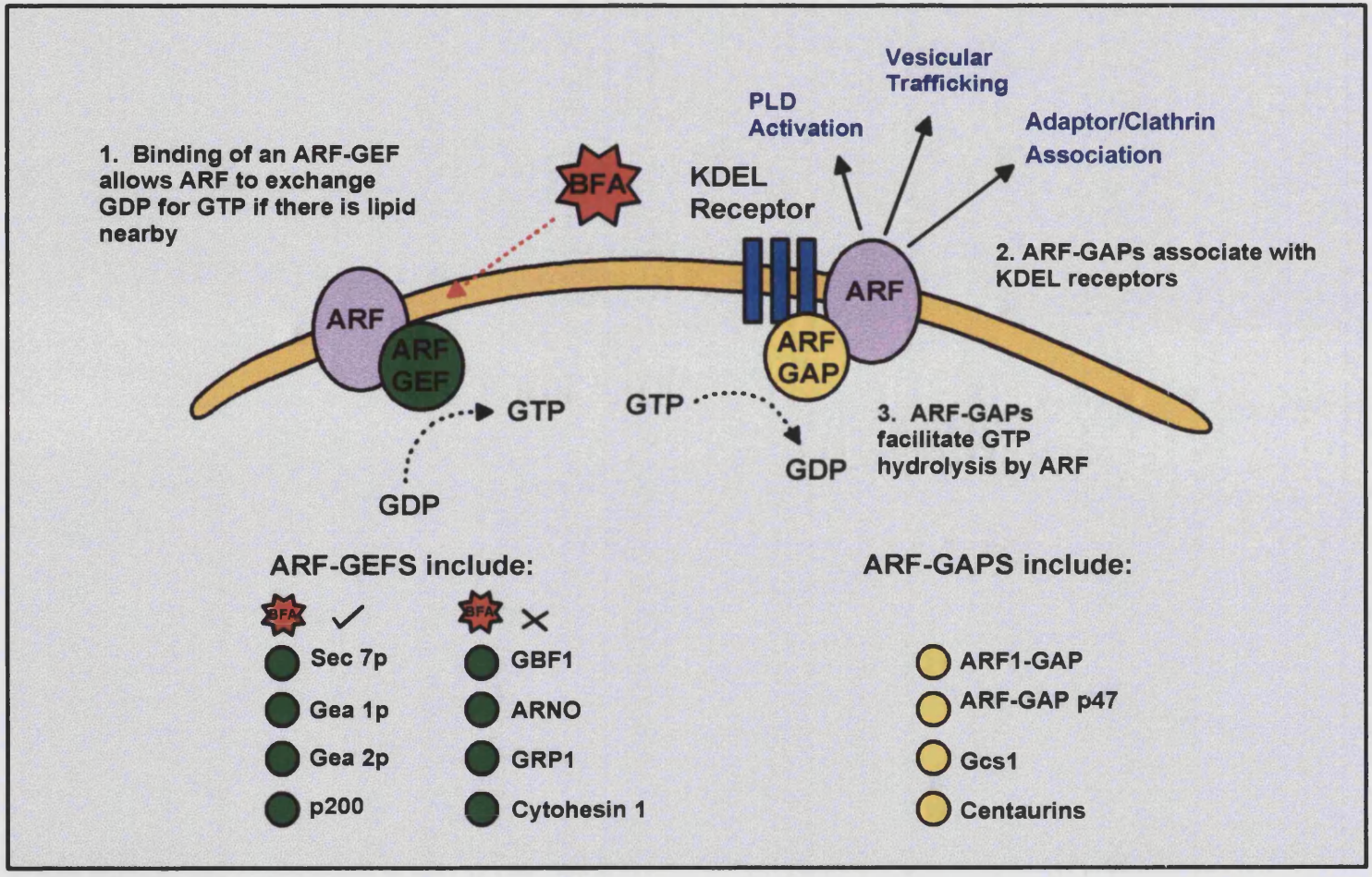

centaurins, also contain two pleckstrin homology domains designated PH-N and PH-C. Centaurin-α (also known as $p42^{IP4}$ or PIP_3-binding protein in other species) was originally purified from rat brain based on its ability to bind to affinity columns of IP_4 analogues, and was later shown to exhibit highest affinity for PIP_3 (Hammonds-Odie *et al.*, 1996). Using the human homologue of centaurin-α, centaurin-α_1, tagged with green fluorescent protein (GFP-centaurin-α_1) Venkateswarlu and colleagues (Venkateswarlu *et al.*, 1999), demonstrated that following PIP_3 production GFP-centaurin-α_1 rapidly translocates to the plasma membrane in PC12 cells. Furthermore, centaurin-α_1 was able to functionally complement a yeast strain lacking Gsc1 (Δ*gcs*1), indicating its potential role as an ARF-GAP (Venkateswarlu *et al.*, 1999).

1.5.7 ARF and GLUT4

For the past several years interest in the involvement of a putative ARF in GLUT4 trafficking has been growing. Since GLUT4 vesicles must bud from a number of different compartments, and some of these vesicles have been shown to be clathrin coated, the discovery of a function for ARF in GLUT4 trafficking has long been anticipated. Such a role has now been indicated in a recent publication analysing the effects of insulin and ARFs -5 and -6 on glucose transport (Millar *et al.*, 1999). In this study, a myristoylated ARF6 peptide was shown to inhibit insulin-stimulated glucose transport and GLUT4 translocation by ≈ 50%. A similar ARF5 peptide had no effect on GLUT4 translocation, but inhibited the appearance of both the TfR and GLUT1 at the cell surface. In addition ARF5 exhibited an insulin-induced redistribution from the cytosol to the plasma membrane, while the location of ARF6 at the plasma membrane was unchanged. These authors suggest that ARF5 is involved in the regulation of endosomal membrane traffic to the plasma membrane, while ARF6 controls the movement of GLUT4 in response to insulin (Millar *et al.*, 1999).

The discovery that the ARF-GEF, ARNO translocates to the plasma membrane in response to insulin increased excitement in this area of research. Like insulin-dependent GLUT4 translocation, ARNO is unaffected by brefeldin A, but sensitive to the PI 3-kinase inhibitors wortmannin and LY294002, and to co-expression of a dominant negative p85 mutant of PI 3-kinase (Venkateswarlu *et al.*, 1998). This suggests that the translocation of ARNO is as a consequence of insulin-stimulated PI 3-kinase activation and PIP_3 production, and strongly implies that ARNO acts as a PIP_3

receptor (Venkateswarlu *et al.*, 1998). Insulin-induced translocation of ARNO may enable it to interact with ARF6.

1.6 Coated Vesicles

1.6.1 Clathrin

One of the earliest steps in the transport of vesicles to their target membranes is the selection of their cargo. Usually this occurs by the concentration of the required protein via interactions with coat proteins, which are also required for vesiculation of the membrane. The vesicles then pinch off, and are trafficked to their appropriate membranes.

Thirty-five years ago, Roth and Porter first observed coated vesicles during their studies of yolk protein uptake in mosquito oocytes (Roth and Porter, 1964). With incredible foresight, they predicted that coat formation would be transient, would be responsible for the mechanical deformation of the membrane, and that components of the coat may have some bearing on the choice of cargo. Five years later, the coat was visualised using negative staining microscopy and was seen to consist of a spectacular lattice of polyhedral structures (Kaneseki and Kadota, 1969), which were later purified to near homogeneity and named clathrin (Pearse, 1975). Clathrin consists of both a heavy chain protein (HC) and two smaller polypeptide light chains (LC_a and LC_b) which assemble together (three heavy chains and three light chains) to form the basic clathrin assembly unit, the triskelion. Clathrin triskelions are heterogeneous in nature, as the distribution of the two different light chains is random (Hirst and Robinson, 1998).

At about the same time as the characterisation of clathrin, Brown and Goldstein were defining a role for clathrin coated vesicles in their studies of low-density lipoprotein (LDL) (Goldstein *et al.*, 1976). From this work, they found that LDL was endocytosed far more rapidly than could be accounted for by simple bulk-flow endocytosis, and proposed that LDL was internalised by receptor-mediated endocytosis. Later, they observed, using electron microscopy, that LDL was concentrated in clathrin-coated pits at the cell surface and that incubating samples at 37°C before fixing, resulted in the pinching off of invaginations to form coated vesicles, which were later uncoated (Anderson *et al.*, 1977). In the years that followed, a number of other proteins were

shown to internalise via clathrin coated pits, including GLUT4, the TfR and the epidermal growth factor receptor (EGFR) (reviewed in Rea and James, 1997; Hirst and Robinson, 1998).

1.6.2 Adaptor Proteins

The principle proteins that drive clathrin coat formation are known as adaptor proteins (APs). In 1979 Keen and colleagues showed that clathrin coats could be stripped from vesicles by treatment with 0.5 M Tris-HCl (Keen *et al.*, 1979). Using gel filtration, these researchers also showed that in addition to clathrin, a number of other 100 kDa polypeptides were components of the extracted vesicle coat. These polypeptides, named adaptins (APs), facilitated the formation of clathrin lattices *in vitro*, and were shown, by ultrastructural studies, to bridge the gap between clathrin and the vesicle membrane (Vigers *et al.*, 1986).

APs form heteromeric complexes which couple coated pit assembly to the entrapment of membrane receptors/transporters (Kirchhausen *et al.*, 1997). Four adaptor complexes have been characterised to date. AP1 localised to the TGN, AP2 localised to the plasma membrane, AP3 localised to the endosomal compartment and the newly described AP4, targeted to or near the TGN, (the latter two protein coats do not seem to involve clathrin) (reviewed in Kirchhausen *et al.*, 1997; Dell'Angelica *et al.*, 1999). All adaptor complexes consist of two 100 kDa adaptins (γ-and β1- (AP1), α- and β2 (AP2), δ- and β3- (AP3), ε- and β4 (AP4)), and in addition, a medium ≈ 45 kDa μ chain (μ1, μ2, μ3, μ4) and a small ≈ 20 kDa σ chain (σ1, σ2, σ3, σ4) *(Figure 1.6A)*. All adaptor subunits are derived from protein superfamilies, the most distantly related are the α-, γ-, δ- and ε-subunits, which are thought to direct the complexes from the cytosol onto the host membranes (Schmid, 1997).

1.6.3 Structure of Adaptor Complexes

Only the structure of the AP2 complex has been studied thus far, although based on biochemical evidence, the conformations of the other adaptor complexes are likely to be similar. Using rotary shadowing, AP2 appears as a brick-like 'head' flanked by two symmetrically placed 'ears'. The ears are attached to the head by ≈ 6 nm hinge-like flexible regions, corresponding to the C-terminal domains of the α2- and β2- adaptins

(Heuser and Keen, 1988). The bulk of the adaptor core is therefore composed of the N-terminals of both the α2- and β2- adaptins, along with the μ2 and σ2 polypeptides.

Little is known about how newly synthesised adaptor complexes assemble *in vivo*, however using the yeast two-hybrid system, much has been learnt about the interactions between the various subunits. These studies indicate that α- and γ-adaptins interact with both the σ- and β-subunits, and that β-subunits also interact with μ-subunits (Page and Robinson, 1995). Further interactions have been shown by studies using chimeras of α- and γ-adaptins, which demonstrate that the μ-subunit can be immunoprecipitated with these chimeras under non-denaturing conditions. Furthermore a stretch of amino acids between residues 130 and 330 of the α- and γ-adaptins, is important for selecting whether a chimera binds to μ1 and σ1 or to μ2 and σ2 (Page and Robinson, 1995). This in turn can dictate whether an adaptor complex binds to the plasma membrane or to the TGN. Interestingly more mammalian μ- and σ-subunits have been identified than their larger adaptin counterparts. The heterogeneity of the smaller subunits may be partly responsible for subtly targeting adaptor assembly onto distinct membranes (Schmid, 1997).

1.6.4 Function of Adaptor Complexes

In the absence of adaptors, clathrin can reassemble into cages *in vitro* (Keen *et al.*, 1979; Crowther and Pearse, 1981). However, the size of these cages varies considerably, and their formation will only occur under non-physiological conditions (low ionic Ca^{2+} buffer, pH < 6.5). Addition of adaptor proteins allows the assembly of uniform clathrin baskets in a less stringent, physiological environment (Zaremba and Keen, 1983). Incubation of coated vesicles with the uncoating ATPase Hsc70 strips clathrin from the membrane but adaptors remain. If the clathrin-extracted membrane is then treated with elastase to remove adaptors, clathrin can no longer rebind (Schlossman *et al.*, 1984; Moore *et al.*, 1987). These data suggest that adaptors bind directly to clathrin and mediate its association with the membrane. Considerable evidence indicates that it is the β subunits of the adaptor complex which are responsible for the clathrin-adaptor interaction. In binding assays, purified β2-adaptin interacts with clathrin with a stoichiometry of one to one, and can compete with the entire AP2 complex for clathrin binding (Ahle and Ungewickell, 1989). Interestingly AP3, which

Figure 1.6 Structure and Assembly of the Adaptor Protein AP1. A. Globular structure of AP1 showing ear-like appendages. The clathrin binding site is situated on the β-subunit and receptor tail signal sequences bind to the μ/β-subunits. B. AP1 binds to the TGN membrane following ARF binding and interacts with a putative docking protein.

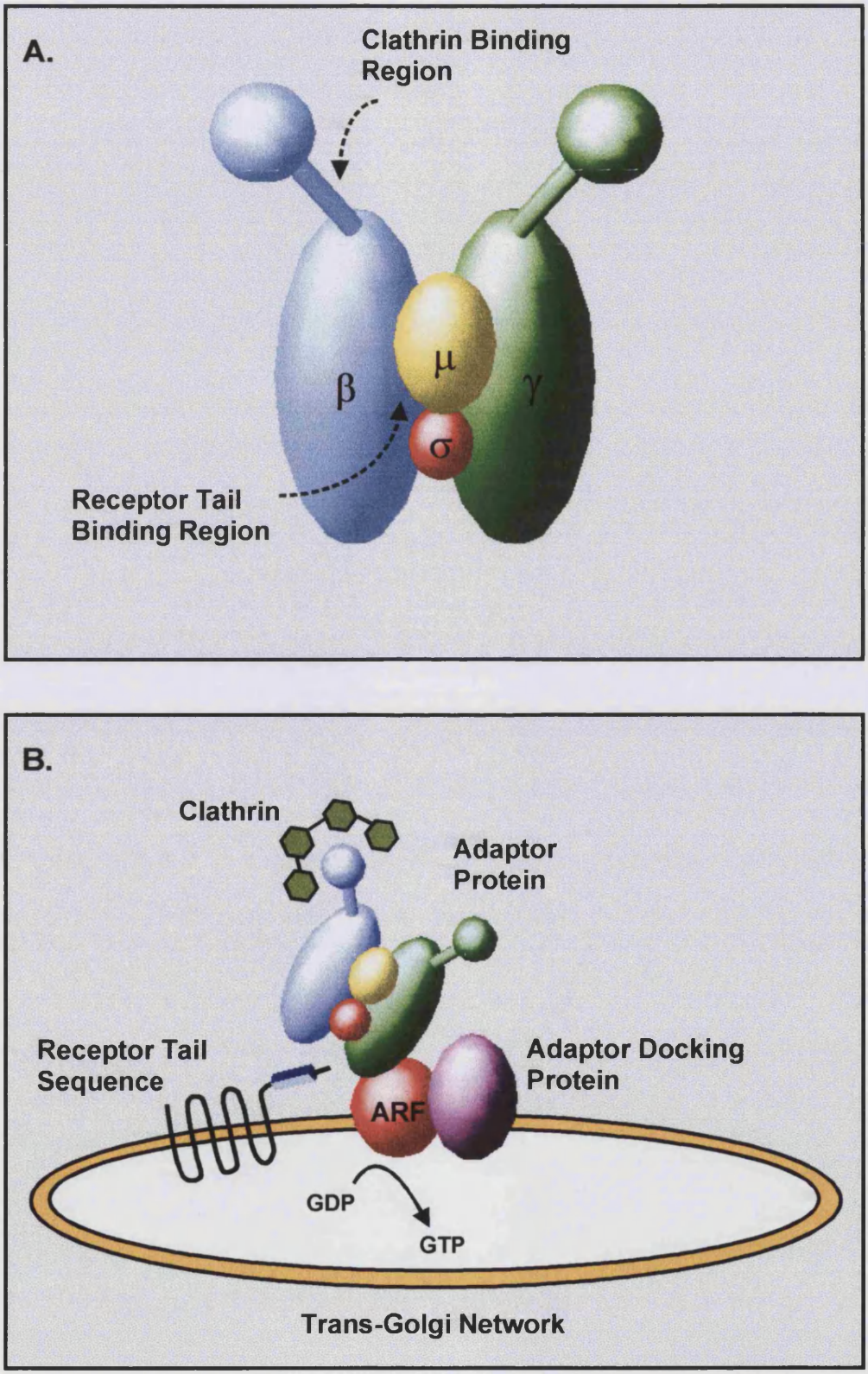

is located in endosomal clusters does not seem to contain a recognisable clathrin binding motif on the β3 hinge region, supporting the observation that this adaptor does not bind clathrin (Dell'Angelica *et al.*, 1997). Perhaps AP3 binds another unique coat protein or is sufficient in coating the vesicle on its own.

In addition to their association with clathrin, adaptors also bind to the cytoplasmic tails of transmembrane receptors and transporters. In 1985, the first study demonstrating such an interaction was performed. In this study the M6PR was shown to form aggregates with the plasma membrane adaptor complex AP2 when incubated under non-denaturing conditions (Pearse, 1985). Later, additional *in vitro* binding assays revealed that adaptors at both the plasma membrane and the TGN bind to receptor tails (reviewed in Schmid, 1997).

Most experimental data points to a role for the adaptor medium (μ) chain in receptor tail interactions. Screening of a yeast two-hybrid library for proteins, which associate with a triple repeat of the cytoplasmic tail of TGN38, 'captured' two clones, both of which encoded the μ2 subunit of AP2 (Ohno *et al.*, 1995). However a role for the β-subunit has also been suggested by the finding that purified asialoglycoprotein binds to the β2 subunit protein band on Far-Western blots (Beltzer and Spiess, 1991). Furthermore, the σ3A-subunit has been shown, using the yeast two-hybrid system, to act as a receptor for non-tyrosine phosphorylated IRS-1 *(Section 1.2.2)*, a component of the insulin-signalling cascade (VanRenterghem *et al.*, 1998) *(Figure 1.6B)*.

1.6.5 Adaptors and Trafficking Signals

Adaptor proteins have been shown to interact with the cytosolic tails of transporters and receptors which carry specific signals for their internalisation and intracellular targeting. The most well characterised are the di-leucine (LL) and tyrosine based motifs (YXXØ), and there is substantial evidence that these interact with all of the adaptor complexes via their μ- or β-subunits, presumably at differential binding sites within these subunits (for review see Kirchhausen *et al.*, 1997). A comparison of the abilities of μ1 and μ2 to interact with tyrosine based sorting sequences was performed using the yeast two-hybrid system (Ohno *et al.*, 1996). Under defined experimental conditions the μ2-subunit displayed higher avidity for tyrosine based sorting signals than μ1. Moreover

the two μ subunits were individually selective about the sequence environment surrounding the motif and the relative position of the aromatic amino acids. This suggests that subtle differences in a protein's sequence may be responsible for its association with adaptor complexes at different loci within the cell, perhaps adaptor proteins 'filter' trafficking proteins as they pass through consecutive compartments. Indeed many proteins including GLUT4 *(Section 1.3.5)* encode a great deal of sorting information within their sequences. This apparent overlap of function may reflect the need for a combinatorial method of selection at a variety of sorting depots. Alternatively different domains may be exposed under differing conditions. In this respect it is interesting to recall that GLUT4 has a phosphorylation site adjacent to its di-leucine motif *(Section 1.3.5)*, which may abrogate or enhance AP binding, depending upon its phosphorylation status. Indeed phosphorylation of a site 4 amino acids upstream of the LL motif in the M6PR enhances its sorting into a post-Golgi compartment (Mauxion *et al.*, 1996).

Recently the crystal structures of the YXXØ binding domain of μ2 complexed to peptides containing the signalling motifs of TGN38 and EGFR have been solved (Owen and Evans, 1998). This domain has a curved shape with 16 β-strands arranged into 2 sub-domains with pockets for the aromatic and hydrophobic amino acids. Surprisingly the YXXØ signal interacts with the binding site in an extended conformation and not in a β-turn as predicted from biochemical analysis. The tight β-turn adopted by signalling motifs in solution may therefore act as a method of regulation such that when the signal is not required for internalisation, the motif displays the closed conformation, which may be 'opened' by interaction with cognate adaptor complexes. Furthermore the medium chain binding pocket for tyrosine based motifs was found to exclude LL sequences (Owen and Evans, 1998).

In 1998 a study of peptides, derived from a number of different proteins, was used to analyse the interaction of adaptor proteins with di-leucine motifs (Rapoport *et al.*, 1998). Using an approach in which samples were first frozen before cross-linking by photo-irradiation, Rapoport and colleagues have revealed a specific interaction of di-leucine containing peptides (including a C-terminal peptide of GLUT4) with AP1. The site of binding was found to be on the β1 subunit, similar to that observed for the asialoglycoprotein (Beltzer and Spiess, 1991). In addition, medium chains (μ-subunits)

have also been shown to interact with LL motifs (Rodionov and Bakke, 1998). Thus APs contain at least two physically separate binding sites for sorting signals.

Overexpression of proteins containing signalling motifs can induce a plethora of trafficking defects including inefficient receptor internalisation, mis-targeting of proteins to the plasma membrane, mislocalisation of adaptins etc. Indeed high levels of overexpression of proteins containing either tyrosine or di-leucine based signals reduces the internalisation of the TfR (Nordeng and Bakke, 1999). Furthermore mutation of the overexpressed proteins to remove the signalling motif allows TfRs to internalise as normal, indicating that the clustering of proteins into coated pits and their sorting is saturable. One development in the past few years is the realisation that many signalling motifs are degenerate in nature and that this may be a critical feature for the coated vesicle sorting machinery. Thus even weak affinity for a motif may be sufficient for internalisation, since the organisation of a coat will bring together multiple copies of APs, and other component proteins, which will strengthen the initial interaction (Kirchhausen *et al.*, 1997).

1.6.6 Regulation of Adaptor Recruitment

1.6.6.1 Receptors for Adaptor Docking

Regulation of adaptor binding is tightly controlled: AP1 and AP4 bind to the TGN and TGN-related compartments, AP2 is localised at the plasma membrane, and AP3 binds to peripheral and endosomal membranes (Hirst and Robinson, 1998). How this is achieved is poorly understood, however some evidence indicates that the choice of cargo may potentiate membrane recruitment. For example, in cells lacking the M6PR, the total amount of AP1 binding to the TGN is decreased by 25% (Le Borgne *et al.*, 1993). Conversely, cells overexpressing the M6PR or the TfR have an increased abundance of clathrin lattices at the TGN and plasma membrane respectively (Miller *et al.*, 1991; Le Borgne *et al.*, 1993). However these proteins alone cannot provide the required specificity for adaptor recruitment, since they may be targeted with even greater efficacy to compartments that do not contain these adaptors. Indeed, at steady state the majority of the M6PR is in the late endosomes, whereas the TfR is confined to the recycling/early endosomes (Hirst and Robinson, 1998). One possibility is that adaptors bind to docking proteins and that it is these which provide the necessary

membrane selectivity. Some evidence to support this hypothesis was provided by the identification of a saturable, high affinity binding site for AP2 on brain membranes, (Virshup and Bennett, 1988). Furthermore, a possible candidate for an AP2 docking protein has come from work showing that AP2 can bind to agarose beads coated with recombinant synaptotagmin I (Zhang *et al.*, 1994a). Other approaches to identify adaptor receptors have used chemical cross-linking or adaptin affinity columns, (Seaman *et al.*, 1996; Mallet and Brodsky, 1996). Using both of these methods a TGN-specific protein of 75-80 kDa has been identified which selectively binds to AP1. However in both cases sequence information could not be obtained due to a lack of material. Thus no definitive docking proteins for AP1 have yet been elucidated (Seaman *et al.*, 1996; Mallet and Brodsky, 1996).

1.6.6.2 The Role of GTPγS and Brefeldin A

Budding of vesicles from their respective membranes must be finely controlled in order to maintain the normal composition of various compartments. Association of AP1 with membranes is stimulated by incubation with GTPγS and is inhibited by the fungal heterocyclic lactone, brefeldin A (Robinson and Kreis, 1992; Wong and Brodsky, 1992). In fact incubation of cells with brefeldin A induces severe morphological changes within the intracellular compartments, presumably as a result of the complete dispersion of adaptins from membranes to the cytosol (Robinson and Kreis, 1992; Wong and Brodsky, 1992). Members of the ARF family of small GTPases *(Section 1.5.4)* mediate the actions of GTPγS and brefeldin A on AP1. Brefeldin A interferes with ARF recruitment by preventing GDP.GTP exchange by ARF-GEFs (Rothman, 1996). Further evidence for the role of ARF in AP1 recruitment comes from experiments in which an ARF-depleted cytosol fails to sustain efficient AP1 recruitment, however full recruitment is restored by the addition of myristolyated ARF1 (Traub *et al.*, 1993). How ARF potentiates AP1 binding is unknown but may be linked to its ability to stimulate phospholipase D (PLD). This in turn may modulate membranes by increasing local levels of acidic phospholipids, which may regulate the interaction of adaptors with receptor tails *(Section 1.6.4)*.

In contrast to AP1, the association of AP2 with the plasma membrane, is unaffected by brefeldin A implying that ARF1 is not involved in AP2 recruitment. However GTPγS and exogenous PLD both result in mistargeting of AP2 to endosomal membranes, and

inhibition of PLD by neomycin (which binds to its cofactor PIP_2) inhibits binding of AP2 to both the endosomes and the plasma membrane (West *et al.*, 1997). These data although different from AP1 suggest a role for PLD and ARF in AP2 recruitment, perhaps mediated via the brefeldin A-insensitive ARF, ARF6.

Although treatment of cultured skeletal myotubes with brefeldin A causes fusion of endosomal-TfR with GLUT4-containing compartments *(Section 1.3.3)*, incubation of adipocytes with brefeldin A has no effect on the insulin-stimulated GLUT4 pathway, and only decreases basal transport moderately (Bao *et al.*, 1995). These results suggest that the basal recycling of GLUT4 (responsible for maintaining the intracellular location of the transporter) may include a membrane budding step that is brefeldin A-sensitive, but that the insulin-stimulated GLUT4 pathway is predominantly brefeldin A-insensitive.

Different membrane compartments show varying susceptibility to brefeldin A, indicating that the drug affects multiple subcellular targets (Wong and Brodsky, 1992). In addition, its effects can be prevented by pre-treatment with $[AlF_4]^-$ implicating heteromeric G proteins (as well as the small GTPase ARF) in the association of coats with their respective membranes, (Robinson.and Kries, 1992). Recently two groups have identified specific residues within the Sec7 domain which confer brefeldin A sensitivity on ARF-GEFs (Sata *et al.*, 1999; Peyroche *et al.*, 1999). Furthermore studies have shown that brefeldin A acts not by competing with ARF for the brefeldin A sensitive binding site on the Sec7 domain but by stabilising an abortive ARF-GDP-sec7 domain complex (Peyroche *et al.*, 1999).

1.6.6.3 Control of Adaptors by Phosphorylation

One molecular switch, which may regulate adaptor-membrane assembly, is phosphorylation. Many of the subunits of the adaptor complex are found phosphorylated in the cytosol whereas membrane bound APs are not (Wilde and Brodsky, 1996). This may indicate that phosphorylation leads to the disassembly of AP subunits from clathrin. Interestingly, the kinase activity, which converts adaptors to the phosphorylated state, is associated with the clathrin-coated vesicles themselves (Wilde and Brodsky, 1996).

Insulin causes the phosphorylation of a ≈ 125 kDa polypeptide component of the plasma membrane adaptor complex (Corvera and Capocasale, 1990). This phosphorylation occurs exclusively on serine residues and is seen within 2 min of insulin stimulation. The function of this insulin-induced phosphorylation event is unknown but may regulate the formation of clathrin-coated pits in response to insulin.

1.6.6.4 Control of Adaptors by Polyphosphoinositides

Adaptors bind polyphosphoinositides including PIP_3. The binding of PIP_3 is saturable and has highest affinity when APs are in their clathrin bound form. Using a bacterially expressed fusion protein encoding amino acids 5-80 of the N-terminus of AP2 Gaidarov *et al.* (Gaidarov *et al.*, 1996) demonstrated the importance of this region in PIP_3 binding. Interestingly this N-terminal domain is also close to a site thought to be responsible for membrane targeting (Page and Robinson, 1995).

As well as PIP_3, IP_6 can also bind to adaptors at physiological concentrations. When IP_6 is bound, adaptors and clathrin cannot form lattices. In the basal state, levels of PIP_3 are extremely low (Stephens *et al.*, 1991; Cross *et al.*, 1997). Upon receipt of a signal, PIP_3 is generated by the action of PI 3-kinase and the transient production of this acidic lipid may allow it to displace IP_6 from the adaptor binding site. With PIP_3 bound, adaptors and clathrin can assemble into polyhedral lattices and vesicles may pinch off from the donor membrane. This lipid exchange mechanism may regulate protein recycling by controlling the formation of clathrin coated vesicles in response to exogenous stimuli. Indeed, the PI 3-kinase vps34p has been implicated in clathrin-dependent vacuolar protein sorting in yeast (Schu *et al.*, 1993).

As well as modulating clathrin-adaptor binding, PIP_3 also regulates the interaction of adaptors with cytoplasmic receptor tails. PIP_3 generally enhances the binding of adaptor proteins to cytoplasmic tails containing tyrosine-based motifs (Rapoport *et al.*, 1997) while inhibiting the interaction of adaptors with LL motifs (Rapoport *et al.*, 1998). Since sites for both tyrosine and di-leucine based motifs exist on the core of the adaptor complex, it is possible that binding of a phosphoinositol molecule results in the opening of one site and the occlusion of the other.

1.6.7 Involvement of Cholesterol in Clathrin-Coated Vesicle Formation

Given the ability of clathrin and adaptors to self-assemble into cages, it was generally assumed that these proteins would play the major role in membrane deformation. However, fresh evidence has indicated a role for the lipid cholesterol in the mechanism of membrane curvature. In cells depleted of cholesterol by the use of beta-methyl-cyclodextrin flat coated membranes are observed by confocal microscopy of GFP-clathrin. These coated regions fail to detach from the plasma membrane, and the internalisation of the recycling endosomal marker, the TfR, is decreased by as much as 85%, without affecting transport back to the cell surface (Subtil *et al.*, 1999).

1.7 Mobilising GLUT4: Involvement of a Possible GLUT4-Vesicle Fusion Apparatus

"All the roads for membrane traffic may yet prove to be paved with the same kinds of molecules" speculated Rothman and collaborators fifteen years ago (Balch *et al.*, 1984). Since then a remarkable convergence of data has indeed revealed that the fundamental principles of membrane fusion and translocation between different vesicular pathways are conserved in eukaryotic cells.

One potential advantage of a specialised secretory compartment for GLUT4 is that the compartment itself will be mobile, fusing with acceptor membranes as a result of hormonal interjection (Rea and James, 1997). A useful paradigm for this comes from studies of small synaptic vesicles in neuroendocrine cells. In the brain, tiny vesicles rapidly transport neurotransmitter to the synapse in response to depolarising sensitisation (Rothman and Warren, 1994). Over the past several years much of the molecular circuitry, which has emerged from studies of these processes in neural tissues, has been shown to be replicated in the regulation of GLUT4, and analogous proteins have been characterised in many insulin-sensitive cells *(Figure 1.7)*.

1.7.1 NSF and α-SNAP

Early dissectors of the fusion apparatus showed that vesicle transport could be inhibited in CHO cells by treatment with N-ethylmaleimide (NEM), and that this could be circumvented by the addition of fresh cytosol (Glick and Rothman, 1987). These data

indicate that a cytoplasmic NEM-sensitive fusion protein is involved in protein trafficking. The N-ethylmaleimide-sensitive fusion protein (NSF) is a soluble tetramer purified by virtue of its ability to restore intercisternal Golgi transport in a cell free assay (Block *et al.*, 1988). In yeast, the Sec18 gene encodes NSF. Indeed the yeast protein encoded by this gene (Sec18p) can replace NSF in a mammalian system for cell-free Golgi transport, adding substance to the theory of universality of transport across species barriers. *In vivo*, NSF seems to play a role in nearly all steps in the secretory pathway, from the ER to the plasma membrane, and in endocytosis (Beckers *et al.*, 1989).

NSF itself does not bind to membranes, requiring the addition of further cytoplasmic elements. Using *in vitro* binding assays in brain extracts three soluble NSF attachments proteins (SNAPs) have been defined and designated α, β and γ (Clary *et al.*, 1990). α- and γ-SNAP have been identified in virtually all cell types whereas the β-isoform is confined to the brain (Whiteheart *et al.*, 1993). α-SNAP is the equivalent of the yeast protein Sec17p, shown by its ability to restore fusion activity to cytosolic extracts of yeast Sec17p mutants (Griff *et al.*, 1992). An important observation is that α- and β-SNAP bind competitively to the same site on alkaline extracted membranes indicating the existence of SNAP receptors which are integral membrane proteins (Sollner *et al.*, 1993).

Once bound NSF hydrolyses ATP. This hydrolysis results in the dissociation of NSF from the fusion apparatus. Originally NSF and α-SNAP were described as proteins responsible for facilitating vesicle targeting and fusion (Wilson *et al.*, 1991). However, current hypotheses include models in which NSF and α-SNAP play roles not in fusion *per se* but in 'priming' a pre- or post-fusion step, analogous to chaperones (Morgan and Burgoyne, 1995).

The *Drosphila comatose* mutant provides direct evidence for the involvement of NSF in exocytosis since the synaptic transmission defect observed in these flies is due to a temperature-sensitive mutation in *Drosphila* NSF-1 (Pallanck *et al.*, 1995). A role for NSF in GLUT4 trafficking has recently been proposed by Cushman and colleagues who observed that in rat adipose cells expressing an ATPase-deficient NSF, the translocation of epitope-tagged GLUT4 was markedly diminished (reviewed in St Denis and Cushman, 1998).

1.7.2 The SNARE Hypothesis

Every few minutes, vesicles with the surface area of the entire cisternae pass between the stacks in the Golgi apparatus. Maintaining the integrity of the cisternae in the face of this massive flux therefore requires a fusion mechanism of great specificity and organisation (Palade, 1975). The SNARE hypothesis was originally proposed by Rothman and colleagues who, using an affinity column of NSF/α-SNAP and a detergent solubilised brain extract, were the first to identify a novel group of protein receptors, now known as SNAP receptors or SNARES, (Sollner *et al.*, 1993). The hypothesis itself suggests that donor (vesicular) and acceptor membranes contain cognate SNAREs, which mediate selective binding and therefore appropriate targeting of proteins to their compartments. This in turn dictates that there must be a large gene family of vesicular- (v-) and target- (t-) SNARES, in order to achieve the intricate trafficking required by most cells. Indeed, the search for such proteins has been extremely fruitful with the discovery of numerous syntaxin, SNAP-25 and VAMP homologues. However it has also become clear that, despite the vast evidence for their absolute role in vesicular transport, SNAREs do not act alone. Indeed a number of additional moieties are required to modulate their assembly, in other words, to act as the 'fine control'.

1.7.3 Vesicle Associated Membrane Proteins (VAMPs)

In 1992, the first homologues of VAMP in insulin sensitive tissues were reported by Leinhard and colleagues (Cain *et al.*, 1992). Subsequently, adipocytes were shown to express both VAMP2 and VAMP3 (cellubrevin) and both were targeted in significant amounts (25-40% of their total pools) to GLUT4 vesicles, (Volchuk *et al.*, 1995). Studies employing neurotoxins such as botulinum neurotoxin isoform B (BoNTx/B) which cleaves both VAMP2 and VAMP3 have shown partial inhibition of GLUT4 translocation and glucose transport, (Tamori *et al.*, 1996). However, recently a more specific role for VAMP2 in the insulin-regulated movement of GLUT4 has been demonstrated by two independent studies. In the first study compartmental ablation (Martin *et al.*, 1996a), was used to demonstrate that a large proportion of VAMP2 (in contrast to VAMP3) resides in the non-ablated GLUT4 storage compartment. In the second analysis, GST fusion proteins of VAMPs were employed, and these indicated that only GST-VAMP2 inhibits insulin-stimulated GLUT4 translocation, (Martin *et al.*, 1998). The latter study also showed that a synthetic N-terminal peptide of VAMP2 was

sufficient to inhibit insulin-stimulated GLUT4 translocation, but had no effect on GTPγS stimulation of GLUT4 *(Section 1.5.1)* or insulin-stimulated translocation of GLUT1 *(Section 1.3.3)*. These results suggest that GLUT1 and GLUT4 traffic to the plasma membrane from different compartments, (supported by confocal microscopy highlighting their differential localisation). Furthermore selective cleavage of VAMP2 with IgA protease also leads to a loss of insulin-induced GLUT4 translocation as determined by GLUT4 fluorescence on plasma membrane sheets (Cheatham *et al.*, 1996). From these data, an obvious hypothesis would be that VAMP3 is responsible for the endosomal trafficking of GLUT4, whereas VAMP2 is necessary for its rapid translocation out of the GSVs and to the plasma membrane in response to insulin.

1.7.4 Syntaxins

Antisera against various syntaxin homologues have shown that the predominant syntaxin isoforms found at the adipocyte plasma membrane are syntaxins -2 and -4, with a much lower amount of syntaxin 3 (reviewed in Rea and James, 1997). To determine which (if any) of these syntaxins are capable of forming a fusion complex with GLUT4 vesicles, *myc*-tagged NSF and recombinant α-SNAP, were mixed with solubilised membranes and ATP, and subjected to immunoprecipitation using an antibody directed against the *myc* tag. The resulting fusion complex was shown to contain VAMPs -2 and -3, and syntaxin 4, (Timmers *et al.*, 1996). An absolute role for syntaxin 4 has subsequently been illustrated using microinjection of a peptide directed against syntaxin 4 (aa106-122) and a recombinant GST-fusion protein encoding the cytoplasmic tail of syntaxin 4, both of which block (40 % and 100 % respectively) insulin-stimulated GLUT4 translocation in 3T3-L1 adipocytes, (Macaulay et al., 1997; Cheatham *et al.*, 1996).

1.7.5 Syntaxin-Binding Proteins

In addition to VAMPs, other proteins have been identified in neural tissues, which are capable of binding to syntaxins. One such protein is synaptotagmin, a calcium binding protein which has been described by Martin and colleagues as a 'fusion clamp' (Martin *et al.*, 1995). These authors suggest that under conditions where fusion is not required synaptotagmin binds to syntaxin 1A and prevents it interacting with other members of the fusion complex. Upon depolarisation, there is rapid release of calcium, which

interacts with synaptotagmin resulting in a conformational change, which exposes syntaxin to the rest of the fusion itinerary. In adipocytes, calcium does not seem to play a role in GLUT4 translocation in response to insulin. Intriguingly, in muscle, exercise induced translocation of glucose transporter activity may involve calcium, (Holloszy and Narahara, 1967) *(Section 1.4)*, and as such the search for synaptotagmin homologues is on-going.

Other syntaxin-binding proteins include SNAP-25 and munc-18, homologues of which have already been identified by screening cDNA libraries in adipocytes. Syndet or SNAP-23 is a ubiquitously expressed homologue of SNAP-25 (Wang *et al.*, 1997). The interaction of syndet with components of the docking and fusion family has been studied using the technique of plasmon resonance (Rea *et al.*, 1998). Full length syndet was immobilised on a carboxymethylated dextran CM5 chip by thiol disulphide exchange. Cytoplasmic domains of syntaxin 4 and VAMP2 were passed over the chip in a small volume of running buffer, and binding of these proteins to syndet was measured by changes in surface plasmon resonance. Results indicate that syndet forms a tertiary complex with syntaxin 4 and VAMP2. In the same study the authors also showed that incubation of permeabilised 3T3-L1 adipocytes with a synthetic 24 amino acid peptide of syndet or microinjection of anti-syndet antibodies results in the inhibition of insulin-stimulated glucose transport in these cells. In contrast to this study, experiments using an *in vitro* binding assay Foster and colleagues failed to show a tripartite complex of syntaxin 4, VAMP2 and the rat homologue of syndet, SNAP-23 (Foster *et al.*, 1998). This is surprising since using similar 3-way binding assays the neuronal syntaxin 1A-SNAP-25-VAMP2 is readily detectable. However the differences between the neuronal studies and the plasmon resonance experiments which show a tertiary complex and the study by Foster and colleagues which does not, may be related to the half-life of the triad complex. In neurones, small synaptic vesicles fuse rapidly at the synapse. This swift exocytosis is due to the vesicles being tethered close to the plasma membrane in a pre-fusion-competent state awaiting a calcium signal. Thus the tertiary fusion complex in the neurone may need to be particularly stable as it is required to pre-assemble. In contrast the rate of exocytosis of non-neuronal vesicles is comparatively slow. Docking and fusion may therefore occur almost simultaneously and hence the tripartite association need not be strong. This may mean that the half-life of the assembled complex is too short to be detected by *in vitro* binding assays. The observation of the fusion complex by plasmon resonance demonstrates the sensitivity of

Figure 1.7 Assembly of the GLUT4 Vesicle Fusion Apparatus. In the resting state GLUT4 vesicle fusion with the plasma membrane is prevented by the interaction of Syntaxin 4 with Synip and SNAP-23. Insulin releases these fusion clamps allowing VAMP2 on the GLUT4 vesicles to bind to its cognate t-SNARES, (Syntaxin 4 and SNAP-23).

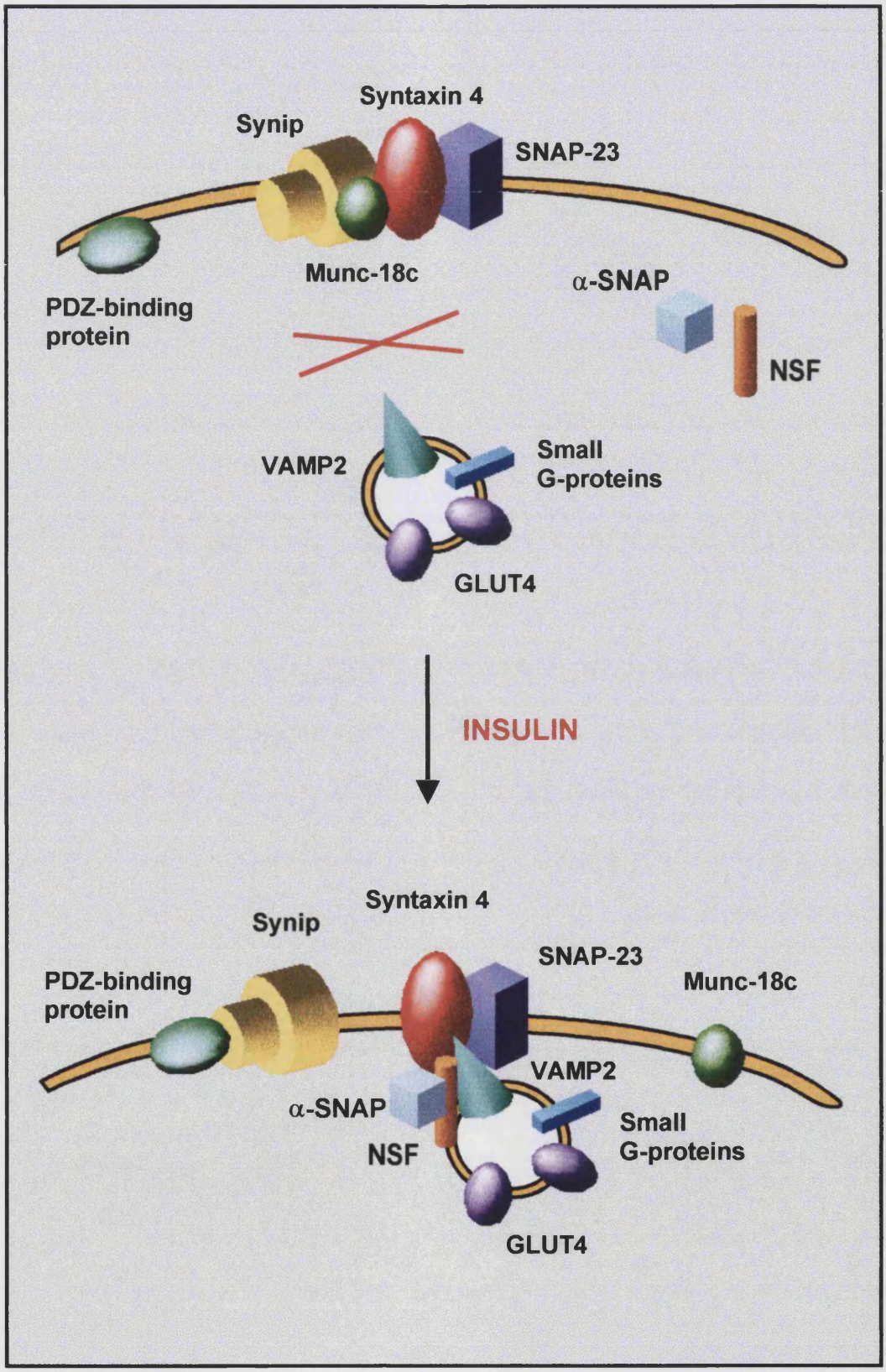

this technique and renders it invaluable in studies of this type. In muscle, in addition to syndet, there may also be an another SNAP25 homologue, (Wong *et al.*, 1997).

Three Munc-18 isoforms (Munc18-a, -b and -c), have been identified in adipocytes (Tellam *et al.*, 1995). Of these isoforms only Munc-18c is capable of interacting with syntaxin 4, (as shown by *in vitro* binding assays with recombinant Munc-18 fusion proteins), (Tellam *et al.*, 1997). Furthermore, Munc-18c and syntaxin 4 show remarkable overlap in terms of their subcellular distribution, being primarily targeted to the cell surface, (despite the lack of a membrane attachment domain in Munc-18c). In 1998, Kasuga and co-workers showed that overexpression of Munc-18c in 3T3-L1 adipocytes, by adenovirus-mediated gene transfer, results in the inhibition of insulin-induced GLUT4 translocation (but not GLUT1 translocation) in a virus dose dependent manner (Tamori *et al.*, 1998). The same year, another group showed that Munc-18c competes for the binding of syntaxin 4 with VAMP2 (Thurmond *et al.*, 1998). Immunoprecipitation experiments revealed that Munc-18c could co-immunoprecipitate with syntaxin 4 and that this complex was reduced in the insulin-treated state. Thus Munc-18c blocks fusion of GLUT4 vesicles by preventing VAMP2 from binding, and insulin releases this block by targeting Munc-18c to another site on the plasma membrane. This is analogous to the role of Munc-18a in the neurone. Here, Munc-18a and VAMP2 bind to syntaxin 1A in a mutually exclusive manner. Protein Kinase C (PKC) which stimulates calcium-dependent exocytosis phosphorylates Munc-18a preventing it from binding to syntaxin 1A (reviewed in Rea and James, 1997).

Recently, in addition to SNAP-23 (syndet) and Munc-18c another protein has been identified which plays an important role in GLUT4 vesicle fusion. Synip was identified using the yeast two hybrid system with syntaxin 4 as the bait (Min *et al.*, 1999). Northern blots hybridised with a radiolabeled probe consisting of part of the coding sequence of Synip revealed that it was only expressed abundantly in insulin-sensitive tissues. Transfection of differentiated 3T3-L1 adipocytes with cDNAs encoding both the full length Synip (Synip/WT) or the C-terminal domain of Synip (Synip/CT) showed that both constructs could co-immunoprecipitate with syntaxin 4 from basal cells. Treatment of cells with insulin resulted in a decrease in the Synip/WT: syntaxin 4 complex but no change in the co-immunoprecipitation of Synip/CT and syntaxin 4. The disruption of the Synip/WT: syntaxin 4 complex by insulin may be due to modulation of the N-terminus since insulin was unable to dissociate the Synip/CT domain from

syntaxin 4. Moreover, the binding of Synip to syntaxin 4 is unaltered by SNAP-23 but is inhibited by VAMP2. Overexpression of Synip/CT reduced insulin-stimulated glucose transport by ≈ 50%, presumably as a direct result of competition with endogenous Synip. The aberrant binding of Synip/CT to syntaxin 4 in the presence of insulin presumably blocks the ability of VAMP2 positive GLUT4 vesicles to dock at the plasma membrane. Since syntaxin 4 binds to both VAMP2 and VAMP3 with high affinity and is therefore conceivably involved in the fusion of vesicles derived from both the GLUT4 storage compartment and the endosomes, both Synip and Munc-18c may provide a means of manipulating/regulating the docking and fusion of these differential populations.

1.7.6 Phosphorylation of Proteins Involved in the Fusion Complex

As well as regulation at the level of protein-protein interaction, the fusion complex may also be regulated by post-translational covalent modifications such as phosphorylation. Indeed protein kinase A (PKA) can phosphorylate syntaxin 4 (Foster *et al.*, 1998) in an *in vitro* kinase assay. In its phosphorylated form syntaxin 4 is no longer able to associate with SNAP-23. This may add another tier of regulation to the fusion apparatus. For example, isoproterenol *(Section 1.9.5)*, an activator of stimulatory G-proteins and hence adenylate cyclase and PKA can inhibit glucose transport by the formation of an occluded population of GLUT4 vesicles (Vannucci *et al.*, 1992). One possible explanation for this phenomenon is that insulin stimulates the delivery of GLUT4 vesicles to the plasma membrane but since PKA is activated and hence syntaxin 4 is phosphorylated, the fusion of the vesicles with the plasma membrane is blocked (Foster *et al.*, 1998).

1.7.7 Rab GTPases

Rabs, a branch of the *Ras* superfamily of small GTPases, have been implicated in vesicle docking and fusion as regulators of SNARE pairing (Chavrier and Goud, 1999). Mutant forms of Rab can block transport of vesicles along a route or change the size of an organelle. Over forty members of the Rab family have been characterised in mammalian systems, each localised to surfaces of distinct membranes (Zerial and Stenmark, 1993). This vast number of Rab proteins reflects the complexity of docking and fusion events in mammalian cells.

In order to bind to membranes, Rabs must be prenylated on two cysteine residues at their C-termini. The enzyme which catalyses this prenylation is geranylgeranyltransferase (Anant *et al.*, 1998). Until both cysteines are modified, newly synthesised Rabs are bound in the cytosol by Rab escort proteins (REPs). REPs aid prenylation by presenting Rabs to geranylgeranyltransferase in the correct conformation. Following prenylation inactive Rab-GDP can anchor on to the membrane. Here, Rab-GDP is exchanged for Rab-GTP by Rab-specific nucleotide exchange factors (GEFs). Current models predict that Rab proteins catalyse membrane fusion in their GTP bound form, and are acted upon by a further two distinct classes of regulator proteins known as GTPase activating proteins (GAPs) and Guanine nucleotide dissociation inhibitors (GDIs) (Pfeffer, 1994). GAPs are responsible for returning Rabs back to their GDP bound state, following membrane fusion. GDIs retrieve Rabs from their fusion targets and recycle them back to their membranes of origin, where they may be re-activated by GEFs. At steady-state most Rabs are anchored on membranes, however some remain in the cytosol, stoichiometrically bound to GDI (for review see Chavrier and Goud, 1999) *(Figure 1.8)*.

Genetic experiments have linked Rabs to SNAREs. For example, although the yeast ER-to-Golgi Rab, Ypt1p is an essential gene product, overexpression of SNAREs can compensate for its loss (Schimmoller *et al.*, 1998). In addition, Rabphilin 3A, a protein that interacts with Rab3, shares high sequence homology with synaptotagmin, a syntaxin-binding protein which regulates calcium-dependent exocytosis in the neurone. It is interesting to speculate that Rabs may bind to v-SNAREs, while Rabphilins may interact with t-SNAREs, thus strengthening the overall fusion complex. The primary role of Rabs could therefore be to facilitate efficient SNARE binding, rather than as components of the fusion apparatus *per se* (Simons and Zerial, 1993). One interesting feature of Rab proteins is that GTP hydrolysis does not seem to be necessary for vesicle fusion to occur. Rather GTP loading of Rabs is the more important criteria. In fact a number of Rab effectors including the mammalian Rabaptin-5 and the yeast, exocyst, are predicted to 'clamp' Rabs in their GTP-bound conformation, thus ensuring that GTP hydrolysis does not pre-empt vesicle fusion (Schimmoller *et al.*, 1998).

Rab proteins involved in the endocytic pathway include Rab4 and Rab5, both of which are associated with the early endosomes. Overexpression of Rab5 increases the rate of endocytosis, and expands the early endosome pool. Therefore Rab5 is likely to be

involved in plasma membrane to early endosome, and homotypic endosome-endosome fusion (Bucci *et al.*, 1992). Conversely, overexpression of Rab4 increases the reflux of proteins from the endosome to the plasma membrane and leads to the formation of endocytic tubules. This implies that Rab4 is part of the recycling endosome (van der Sluijs *et al.*, 1992)

In 1993, Rab4 was shown to exhibit an insulin-induced redistribution from microsomal membranes to a soluble fraction (Cormont *et al.*, 1993). In addition, these authors also demonstrated that in the basal state, Rab4 could be detected on GLUT4 vesicles and that upon insulin-stimulation the amount of Rab4 on GLUT4 vesicles decreased. Later, the same group showed that insulin causes the phosphorylation of Rab4 by extracellular-signal-regulated kinase (ERK1), and suggested that this insulin-induced post-translational modification results in the movement of Rab4 from GLUT4 vesicles to the cytosol (Cormont *et al.*, 1994).

To study the role of Rab4 in insulin-stimulated GLUT4 translocation more precisely, 3T3-L1 adipocytes were transiently transfected with cDNAs of both an epitope-tagged GLUT4-myc and Rab4 (Cormont *et al.*, 1996a). Using this system, the authors were able to demonstrate that increasingly high concentrations of Rab4 (in which Rab4 was found targeted to the cytosol) inhibit the appearance of cell surface GLUT4 under insulin conditions. Thus they speculate that Rab4 is involved in the intracellular retention of GLUT4 and that overexpression of cytosolic Rab4 acts as a sink for a factor(s) involved in insulin-stimulated GLUT4 translocation. This hypothesis was strengthened by the observation that a mutant of Rab4 lacking the geranylgeranylation sites was effective at inhibiting insulin-stimulated GLUT4 translocation, even at low expression levels (Cormont *et al.*, 1996a). A similar study showed that a synthetic peptide corresponding to the C-terminal hypervariable domain of Rab4, inhibited insulin-stimulated glucose transport in rat adipocytes (Shibata *et al.*, 1996). Furthermore, even in the presence of an internalisation inhibitor, the C-terminal Rab4 peptide could still stunt insulin-induced GLUT4 translocation, suggesting that it act's upon GLUT4 recruitment at the exocytic limb (Shibata *et al.*, 1996). Likewise, antibodies against Rab4 also inhibit insulin-responsive glucose transport.

Figure 1.8 Lifecycle of Rab Proteins. Newly synthesised Rabs are bound by Rab Escort Proteins (REPs) until prenylated on two cysteine residues by geranylgeranyltransferase. Rabs bind to the membranes where GTPase nucleotide exchange proteins (ARF-GEFs) exchange GDP for GTP. GTP hydrolysis on Rabs is catalysed by GTPase activating proteins (ARF-GAPs) and this results in membrane fusion. Following fusion, Rabs are retrieved from their target membranes and are recycled back to their donor membranes by GDI proteins.

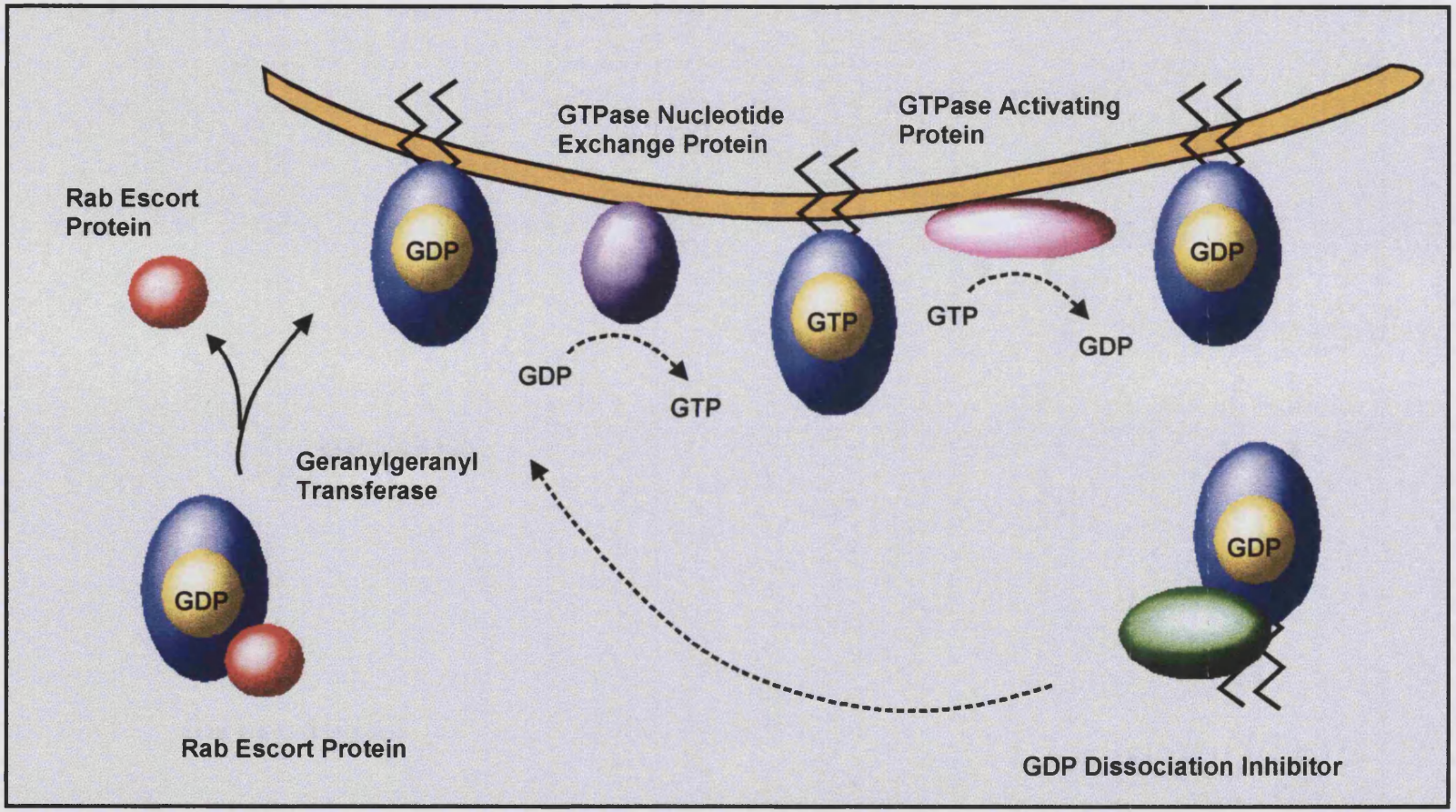

As well as insulin, exercise also induces GLUT4 translocation to the plasma membrane in skeletal muscle *(Section 1.4)*. However, only insulin stimulates Rab4 translocation (Sherman *et al.*, 1996), indicating that the regulation of GLUT4 by insulin and contraction may occur by different mechanisms. Interestingly, activation of PI-3-kinase by insulin leads to an increase in the GTPγS-loading of Rab4, (Shibata *et al.*, 1997). Furthermore, pre-incubation with wortmannin blocks the insulin-induced redistribution of Rab4 from the microsomal membranes to the soluble fraction.

Finally, Rab4 is important in the genesis of membrane ruffles *(Section 1.8)*. The GTP loading of Rab4, rather than its GTP hydrolysis, seems to be important for the insulin-induced association of Rab4 with actin, and for the concomitant GLUT4 translocation. Taken together, these data argue for a role for Rab4 via the cytoskeleton in insulin- but not exercise-sensitive GLUT4 trafficking pathways.

In addition to Rab4, Rab5 also exhibits an insulin-induced redistribution, decreasing by ≈ 50% from the microsomal membranes. However Rab5 is not found on immunoprecipitated GLUT4 vesicles (Cormont *et al.*, 1996b), and treatment of adipocytes with the PI 3-kinase inhibitor wortmannin *(Section 1.2.3)*, has no effect on the insulin-stimulated redistribution of Rab5. Recently a new class of proteins thought to act as membrane tethers has been described (Waters and Pfeffer, 1999). Use of PI 3-kinase inhibitors has led to the identification of one such tethering protein known as early endosome antigen 1(EEA1) (Patki *et al.*, 1997). This protein binds to both GTP-loaded Rab5 and to phosphatidylinositol 3-phosphate (PI-3-P). Binding of EEA1 to PI-3-P is mediated by a conserved zinc finger domain known as the FYVE domain (Patki *et al.*, 1998). Interestingly addition of excess EEA1 to an *in vitro* fusion assay can circumvent the requirement for both Rab5 and PI-3-P, allowing endosome fusion to occur even in the presence of wortmannin (which blocks the production of PI-3-P) and GDI (which sequesters Rabs) (Christoforidis *et al.*, 1999). Since treatment of cells with wortmannin leads to the formation of large swollen vacuoles (Shpetner *et al.*, 1996) it is possible that PI-3-P regulates EEA1 and therefore regulates fusion. Further evidence has recently placed the PI-3 kinase activated kinase PKB upstream of Rab5, thus it is possible that PIP_3 also indirectly regulates EEA1 (Barbieri *et al.*, 1998).

Additional information concerning the temporal involvement of Rabs in the fusion process suggests that their action is subsequent to NSF and α-SNAP and may be

required for the formation of the SNARE complex (Mayer and Whickner, 1997). Indeed a protein called Pra1 has recently been isolated (Martincic *et al.*, 1997) which is capable of interacting both with prenylated Rab GTPases and VAMP2, and may serve to couple these two protein families together in the control of vesicle docking and fusion. This protein is predominantly cytosolic but a small proportion cycles between the cytosol and the membrane. Although the intracellular location of Pra1 does not seem to alter in response to insulin in rat adipocytes (A.Gillingham, unpublished observation), it is possible that homologues of this protein will be found with specific roles in insulin-sensitive tissues.

1.7.8 Role of ATP

In addition to GTP, the nucleotide ATP is also known to be important in fusion and docking events. As well as activating cytosolic NSF, it also regulates the yeast protein Vps33p involved in fusion events between the prevacuolar compartment and the vacuole (Gerhardt *et al.*, 1998). Vps33p cycles between soluble and particulate forms in an ATP-dependent manner, which may facilitate the specificity of transport vesicle docking or targeting to the yeast vacuole/lysosome (Gerhardt *et al.*, 1998). As already discussed, many of the components of the fusion/docking repertoire are duplicated in cells and tissues, thus it will be of interest to determine if such a protein is required in insulin-induced GLUT4 translocation.

In conclusion, it is clear that many of the mechanisms employed in the release of neurotransmitter from small synaptic vesicles can be directly translated to explain, in part, the translocation of GLUT4 vesicles from the GSVs to the plasma membrane. The absolute role for members of a fusion apparatus in GLUT4 vesicle translocation has been convincingly demonstrated by a number of approaches. However, it is interesting to note that the inhibition of insulin-stimulated glucose transport, caused by disrupting the endogenous populations of SNAREs and SNARE regulators, is usually no more than 50%. This observation supports the view that the 'insulin sensitive' compartment is segregated from the recycling endosomal compartment, but also implies that the endosomes can partially respond to insulin or compensate for the loss of the GSVs *(Section 1.3.5)*. Alternatively other proteins including vesicle tethers may be able to compensate for the loss of endogenous SNAREs.

1.8 Role of the Cytoskeleton in GLUT4 Trafficking

It is not known where the primary site of insulin action is. It may be to promote vesicle fusion, however an equally plausible explanation is that insulin controls the actual movement of GLUT4 vesicles from deep within the cytoplasm to the plasma membrane. An advance in recent years in our understanding of the mobility of GLUT4 has been the discovery that an intact actin cytoskeleton is required for both insulin-stimulated glucose uptake and for the formation of membrane ruffles (Tsakiridis *et al.*, 1994). Cytochalasin D, a fungal metabolite which caps the barbed (polymerising) ends of the actin molecule, has been widely used to study the role of the actin cytoskeleton in GLUT4 trafficking. Incubation of L6 myotubes, with cytochalasin D can reduce insulin-stimulated glucose transport by between 50 and 80%, without effecting basal transport (Tsakiridis *et al.*, 1994; Wang *et al.*, 1998). In addition to cytochalasin D, latrunculin B, a structurally distinct marine macrolid which disassembles actin filaments by binding to free actin monomers, also inhibits insulin-stimulated glucose uptake to approximately the same extent (Wang *et al.*, 1998). The decrease in glucose transport induced by treatment with cytochalasin B has been shown to directly correlate with an inability of insulin to promote the movement of glucose transporters from the LDM to the cell surface. Furthermore incubation with cytochalasin D results in the failure of insulin to induce the formation of membrane ruffles, the role of which is presently unknown. Together these data provide compelling evidence for the role of actin filaments in glucose transport *(Figure 1.9)*.

An important molecule in the insulin signalling cascade is PI 3-kinase *(Section 1.2.3)*. Many factors besides insulin stimulate PI 3-kinase activity, for example, platelet-derived growth factor (PDGF) and epidermal growth factor (EGF), however none of these other stimuli induce the translocation of GLUT4 to the plasma membrane. Thus there must be a difference in the action of insulin and PDGF on PI 3-kinase. One fundamental difference is that insulin stimulates PI 3-kinase activity at an intracellular locus, while PDGF enhances PI 3-kinase activity at the plasma membrane (Clark *et al.*, 1998). In fact insulin causes an increase in PI 3-kinase p85α and p110β in the intracellular GLUT4 containing compartment, and this increase can be inhibited by cytochalasin D (Wang *et al.*, 1998). Moreover microinjection of a constitutively active mutant of PI 3-kinase (PI 3-kinase p110*) causes the translocation of GLUT4 to the plasma membrane in 3T3-L1 adipocytes and induces the formation of actin filament

ruffles (Martin *et al.*, 1996b). This effect is inhibited by wortmannin and by the use of a PI 3-kinase mutant with a point mutation in the kinase domain (Martin *et al.*, 1996b). These data suggest that the localisation of PI 3-kinase activity is important for insulin-stimulated GLUT4 translocation via the actin cytoskeleton.

In fact inhibition of PI 3-kinase by wortmannin has far-reaching implications in terms of general membrane morphology. For example treatment of mammalian cells with PI 3-kinase inhibitors causes a marked change in endosomal structure, highlighted by tubulation and enlargement of endosomes containing TfR (although it has little effect on TfR recycling) (Shpetner *et al.*, 1996). These wortmannin-induced morphological changes demonstrate the importance of PI 3-kinases in maintaining the integrity of intracellular compartments as well as in GLUT4 translocation *per se*. The deleterious effect of PI 3-kinase inhibitors can be blocked by incubation with $[AlF_4]^-$, implying that a heteromeric GTP binding protein somewhere downstream of PI 3-kinase is involved in endosomal organisation (Shpetner *et al.*, 1996).

As well as PI 3-kinase, other molecules have been implicated in the insulin-induced translocation of GLUT4 and/or actin rearrangement. These include the small GTPase Rab4 (Vollenweider *et al.*, 1997), and the general receptor for phosphoinositides 1 (GRP1) (Clodi *et al.*, 1998). In addition, a significant proportion of the t-SNARE SNAP-23 *(Section 1.7.5)* has been shown to co-sediment with detergent resistant cytoskeletal elements including actin (Foster *et al.*, 1999). Contrary to the role of PI 3-kinase which is presumably involved in the translocation of GLUT4 vesicles *per se*, the interaction of SNAP-23 with the actin cytoskeleton is more likely to facilitate the presentation of GLUT4 vesicles to the rest of the fusion apparatus at the plasma membrane.

The involvement of an intracellular scaffold in the maintenance of the internal population of GLUT4 has been shown visually using a green fluorescent protein chimera of GLUT4 (GFP-GLUT4) (Oatey *et al.*, 1997). Expression of GFP-GLUT4 in 3T3-L1 adipocytes under basal conditions and collecting images by time-lapse confocal microscopy has shown that the majority of the GFP-GLUT4 vesicles are static as if tethered to an intracellular structure. The authors speculate that the role of insulin is to release the 'anchor' on the GFP-GLUT4 vesicles allowing them to translocate to the plasma membrane.

Figure 1.9 The Role of the Cytoskeleton in GLUT4 Translocation. Insulin signalling results in the association of PI 3-kinase with tyrosyl phosphorylated IRS1 at an internal membrane site. GLUT4 which is tethered to the actin cytoskeleton by a putative tethering protein is released by the actions of insulin and can traffic to the plasma membrane where it interacts with its target SNAREs including SNAP-23.

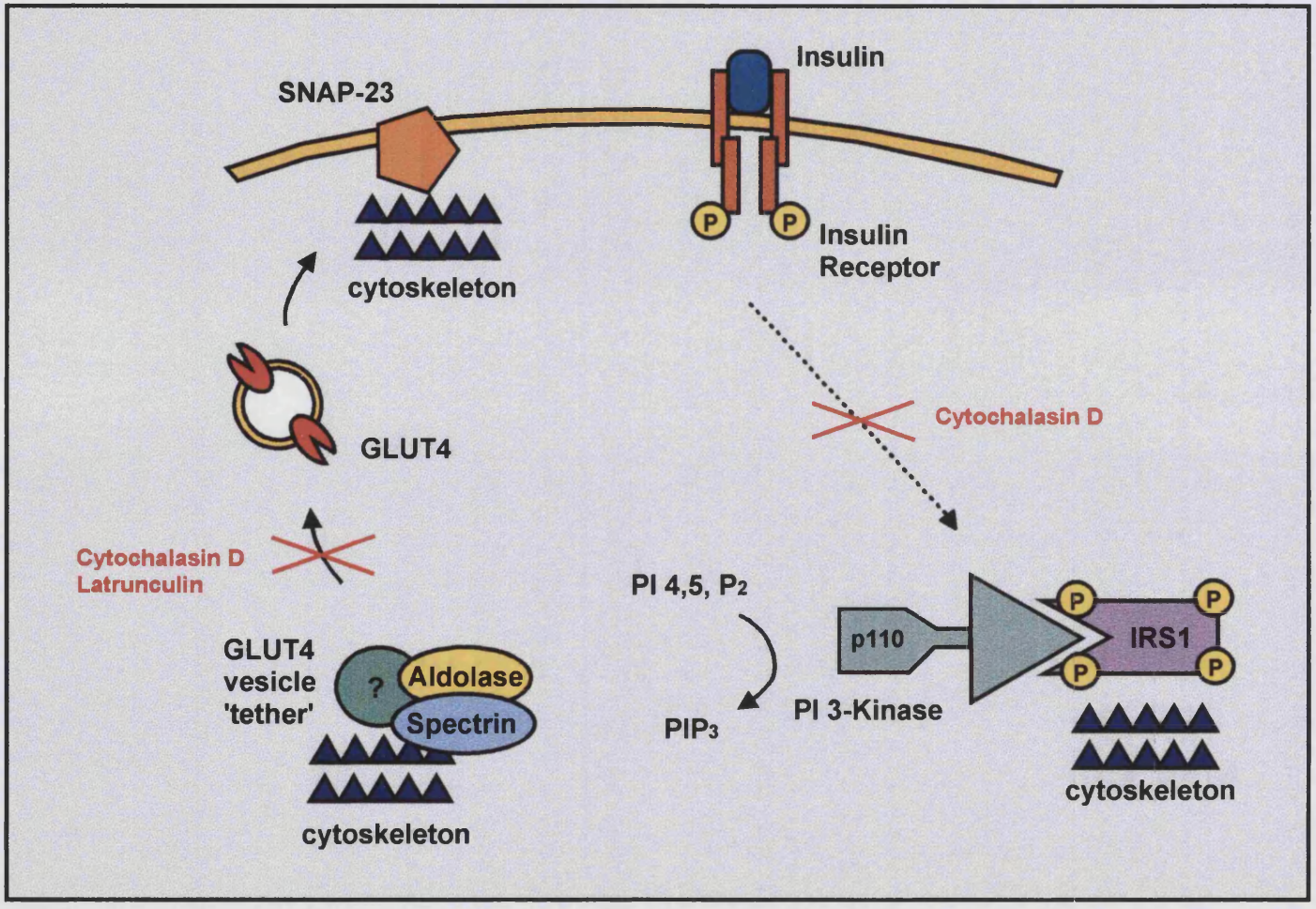

The search for proteins important in tethering GLUT4 is ongoing. One such protein may be spectrin which has been shown, by immunoblotting, to be associated with GLUT4 vesicles (Tsakiridis *et al.*, 1994). Another protein, which may act as the GLUT4 vesicle anchor, is fructose 1,6-bisphosphate aldolase. GST fusion proteins of the C-termini of GLUT1 and GLUT4, showed that aldolase associated selectively with GST-GLUT4, but not with GST-GLUT1. Introduction of the metabolic inhibitor 2-deoxy-D-glucose into permeabilised 3T3-L1 adipocytes disrupted the interaction between actin and aldolase, and inhibited insulin-stimulated GLUT4 exocytosis without affecting GLUT4 endocytosis (Kao *et al.*, 1999). In addition, microinjection of aldolase-specific antibodies can also inhibit GLUT4 translocation. It is interesting to note that data from our laboratory (Pryor, P.R., Koumanov, F. and Holman, G.D, unpublished observation) has shown that phosphatidylinositol 3,4,5 trisphosphate (PIP_3), the lipid product of PI 3-kinase binds specifically to aldolase. The use of aldolase as a GLUT4 vesicle tether may therefore couple insulin signalling via PI 3-kinase with a negative feedback mechanism for glucose metabolism.

1.9 The Importance of pH in Membrane Trafficking Events

At the turn of the century Metchnikoff showed by feeding litmus paper to protozoa, that bacteria and other foreign bodies ingested by the phagocytic cells of the immune system are transferred to acidic structures in the cytoplasm, where they are digested (Metchnikoff, 1893). Since then the importance of intracellular pH not only in the entry and immune response to pathogens but also in the function of the biosynthetic and endocytic pathway has been recognised and documented (Mellman, 1992).

In the endocytic pathway material entering from the plasma membrane traffics through increasingly acidic compartments from endosomes to lysosomes. Likewise proteins of the exocytic route follow a similar pH gradient from the ER to the secretory vesicles. The level of acidity varies between intracellular organelles and its function depends upon the membrane compartment in question. For example, in lysosomes the low pH favours the activation of enzymatic hydrolases; in chromaffin granules the proton gradient is used to provide energy for the transport of biogenic amines; and in receptor-mediated endocytosis the difference in the pH between the endosomes and the external environment is used to provide asymmetry in the recycling circuit between the two compartments (Mellman, 1992). In the latter case, the disparity in pH allows receptors

and their ligands to display differential association-dissociation kinetics depending on their acidic environment (Mellman, 1992). Acidification of endosomes is also required for the formation of endosome carrier vesicles (ECVs) which are responsible for shuttling proteins between the early and late endosomes (Clague *et al.*, 1994) *(Figure 1.10)*. Acidity in organelles is maintained by vacuolar ATP-dependent proton pumps and by ion-exchangers including the Na^+/H^+ exchanger, NHE1, both of which shall be discussed in detail in this section.

1.9.1 Characteristics of v-ATPases

The v-ATPases are composed of two complex functional domains *(Figure 1.11A)*. The V_1 domain, responsible for ATP hydrolysis, is a 570-kDa peripheral protein composed of 8 different subunits (A_3, B3, C-H). The A and B subunits participate in the formation of the nucleotide binding site, with the catalytic domain localised by mutational analysis to the A subunit and an auxiliary non-catalytic domain localised to the B subunit. Proton translocation across the membrane is mediated by V_0. This domain is a 260 kDa integral membrane complex consisting of 5 different subunits (a, d, c, c' and c''). Electron microscopic images examining the structure of the v-ATPase from *Neurospora,* have revealed that this protein consists of a globular head attached to the membrane by a central stalk, with additional projections emanating from the base of the stalk (Dschida and Bowman, 1992). The information for targeting the v-ATPase exists within the V_0 domain, which must be in the correct conformation to reach the vacuolar membrane. All the V_1 subunits except the H polypeptide are required for the assembly and attachment of V_1 to V_0.

Vacuolar proton pumps appear to be electrogenic and as such proton translocation can occur without direct molecular coupling to cations or anions. This means that acidification may be accompanied by the generation of a positive interior membrane potential. The exact mechanism, by which proton translocation is achieved, has not yet been established. However it is assumed that it will be similar to the rotary mechanism proposed for the F-ATPase of mitochondria. In this model the hydrolysis of ATP forces the rotation of the central subunits, and in doing so allows the transport of protons from one side of the membrane to the other (Vik and Antonio, 1994).

Figure 1.10 The Importance of pH in Intracellular Trafficking. The acidity of compartments increases along both the endocytic and biosynthetic pathways. The changes in pH aid receptor-ligand dissociation, binding of proteins such as ARF to membranes and activation of enzymes such as hydrolases.

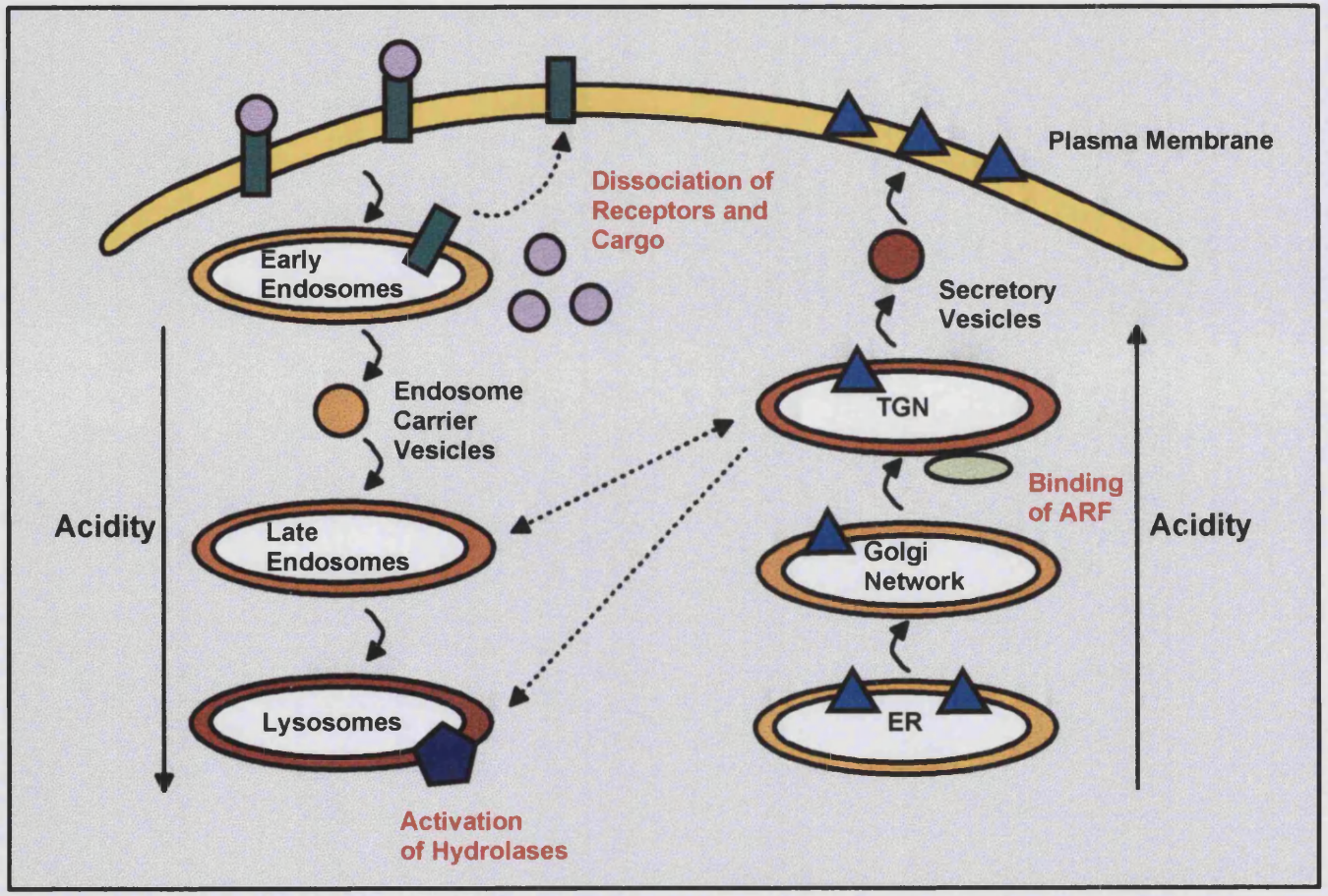

How does one pump help to maintain divergent intracellular compartments at different pH values? Several mechanisms have been proposed to explain this phenomenon: (1) The ATPase is able to rapidly dissociate and reassemble in response to stimuli. This mechanism is seen in yeast deprived of glucose. (2) Inhibitory disulphide bond formation at the v-ATPase catalytic site can regulate ATPase activity. Consistent with this hypothesis is the observation that oxidation of the v-ATPase from *Neurospora* leads to enzyme inactivation. (3) Altering the coupling efficiency of the ATPase can modulate function. For example, an increase in the coupling efficiency in the lemon fruit v-ATPase allows it to maintain a vacuolar pH of 2. (4) Small activator and inhibitor proteins have been detected, which modulate v-ATPase activity directly and (5) other ion channels, particularly Cl^- channels, which dissipate the membrane potential induced by proton translocation, may be regulated and this regulation may control intra-compartmental pH. Support for this theory comes from the observation that Cl^- conductance is modulated by protein kinase-A dependent phosphorylation (reviewed in Forgac, 1999).

1.9.2 Measurement of Vacuole Acidification

One of the most convenient methods to measure vacuolar acidification relies upon the properties of certain lipophilic weak bases. At neutral pH these reagents are uncharged and therefore membrane permeant. If allowed to equilibrate with cells or isolated organelles, these bases will accumulate within membrane vesicles that have acidic lumen. The degree to which the lipophilic base becomes concentrated within a compartment depends upon the magnitude of the transmembrane potential across it. One such reagent is the dye acridine orange. This dye can be used in optical measurements of pH since it exhibits a characteristic alteration in its absorbance spectra and fluorescence intensity as a consequence of increased concentration. As such, acridine orange has been exploited in morphological studies to identify acidic organelles in living cells (Mellman *et al.*, 1986).

1.9.3 Inhibitors of V-ATPases

In 1984 a variety of naturally occurring bafilomycins, including bafilomyin A_1, were isolated from the mycelium of *Streptomyces griseus* (Werner *et al.*, 1984) *(Figure 1.11A, lower panel)*. Bafilomycins are members of the plecomacrolide-defined class of

macrolide antibiotics which act as high affinity inhibitors of v-ATPases (Bowman *et al.*, 1988). Structure/activity studies (Drose *et al.*, 1993), have revealed that the macrolactone ring of bafilomycin A_1 strongly contributes to its ability to act as a v-ATPase inhibitor. Derivatives carrying an open hemiketal ring, such as bafilomycin D can still inhibit vacuolar ATPases but do so with much lower affinity. Using [H^3]-bafilomycin, the antibiotic binding site of the v-ATPase has been localised to the V_0 domain (Mattson and Keeling, 1999). Subsequently Zhang and colleagues (Zhang *et al.*, 1994b) have pinpointed the binding site to a 116-kDa subunit of the V_0 domain.

Bafilomycins can inhibit vacuolar ATPases without causing vacuolation. When added to cells in culture, plecomacrolides inhibit v-ATPases in a variety of organelles, increasing the luminal pH and causing a number of secondary effects including changes in the affinity of receptors for ligands, and in protein conformations and activities. For example, bafilomycin A_1 inhibits lysosomal acidification and degradation of endocytosed EGF in the mammalian cell lines BNL CL.2 and A431, whereas internalisation of EGF and its transport to the lysosomes is not affected (Yoshimori *et al.*, 1991).

TfR trafficking in CHO cells treated with bafilomycin A_1 has also been studied (Johnson *et al.*, 1993). In this case endosomal pH was seen to increase (neutralise) and TfR externalisation was decreased by 50% while internalisation was unaffected. The slow rate of TfR recycling seen in the bafilomycin A_1 treated cells could be completely abolished by substituting the two aromatic amino acids in the receptors internalisation motif *(Section 1.6.5)*, however there was no change in the localisation of the plasma membrane adaptor, AP2. The simplest explanation for these results, is that intravesicular acidification is important for regulating the interaction of receptors with proteins involved in their retention and/or trafficking. As discussed in relation to the LL motif in GLUT4 *(Section 1.3.5)* cytosolic proteins act as molecular anchors, retaining proteins within compartments. Thus it is equally plausible that cytosolic proteins which bind to tyrosine based motifs also exist. Perhaps the change in pH induced by bafilomycin A_1, allows the formation of protein-protein interactions which do not normally exist, and hence result in a decrease in the rate of TfR exocytosis. Furthermore, some proteins involved in trafficking may require vesicular acidification in order to bind and become activated. Included in this family of proteins are the small

GTPases ARF *(Section 1.5.4)* which are recruited to TGN membranes in response to a decrease in pH (Zeuzem *et al.*, 1992).

The effect of bafilomycin A_1 on the recycling of GLUT4 has also been examined (Chinni and Shisheva, 1999). Surprisingly, in this case, bafilomycin A_1 stimulated GLUT4 translocation from the intracellular pool to the plasma membrane in 3T3-L1 adipocytes. Bafilomycin A_1 also caused a change in distribution of GLUT1 and Rab4, but had no effect on non-insulin sensitive proteins. The effects of the v-ATPase inhibitor were independent of insulin receptor autophosphorylation and independent or downstream of PI 3-kinase (Chinni and Shisheva, 1999).

Thus the unique pH of a compartment may act as a signature for it, enabling proteins to identify 'where they are', and allowing specific interactions of receptors with auxiliary proteins along the trafficking pathway. This may be a mechanism for differential sorting of proteins within the endo- and exocytic pathways.

1.9.4 Molecular Physiology of Na^+/H^+ Exchangers

Na^+/H^+ exchangers (NHEs) catalyse the electrically silent countertransport of Na^+ and H^+, controlling the transmembrane movement of salt, water and acid-base equivalents. They are therefore important for cell volume control, Na^+ tolerance and pH regulation. Na^+/H^+ exchange was first demonstrated in 1972 in the bacterium *Streptococcus faecalis* and since that time the existence of the transporter in virtually all cell types has been described *(Figure 1.11B)* (for review see Wakabayashi *et al.*, 1997).

In 1989, the first cDNA for a Na^+/H^+ antiporter was cloned through genetic complementation of an exchange-deficient mouse fibroblast cell line (Sardet *et al.*, 1989). The cDNA sequence consists of a 2445 base pair open reading frame, encoding a protein of 90-kDa. This protein is now known as NHE1. Since then at least 6 mammalian NHE isoforms have been identified, NHEs 1-4 share 40% identity at the amino acid level. Based on hydropathy plots of their amino acid sequences, NHE proteins consist of 10-12 transmembrane spanning domains and a long cytoplasmic C-terminal tail, upon which several modulatory motifs are found (Wakabayashi *et al.*, 1997). Most NHE isoforms are primarily localised to the plasma membrane, but a

distinct subset of vesicles (≈ 20%) contain a Na^+/H^+ exchange activity, with similar kinetic properties to that found at the cell surface, (Nass and Rao, 1998).

The cloning of transporter cDNAs and the development of exchanger-deficient cell lines has enabled the study of the specific function of each isoform in a defined environment. All the cloned exchangers exhibit Michaelas-Menton kinetics for external H^+ when expressed in the exchange-deficient cell line, PS120, with K_m values in the range of 5 to 50 mM depending upon the species and isoform tested. In contrast, the concentration dependence to the internal H^+ is much steeper. Aronson and co-workers have proposed, based on the analysis of Na^+ transport by brush border membrane vesicles, that intracellular protons may act at an allosteric site on the exchanger as well as at the H^+ transport site itself (reviewed in Wakabayashi *et al.*, 1997). The cytoplasmic C-terminal domain (300 amino acids) although dispensable for Na^+/H^+ activity, controls the affinity of the transporter for these allosteric intracellular H^+ and is therefore sometimes known as the 'transducer unit'. Partial or complete deletion of the C-terminal cytoplasmic domain reduces the rate of Na^+/H^+ exchange on the N-terminus in response to certain hormones.

NHE1 is the only ubiquitously expressed NHE isoform (NHE2-4 being confined to epithelial cells). It is a glycoprotein of 90 kDa, and is mainly responsible for maintaining intracellular pH. NHE1 is acted upon by various growth factors and hormones, including insulin, (Noel and Pouyssegur, 1995), and is modulated by G-proteins of the Ras and Rho families, (Hooley *et al.*, 1996). Microinjection of antibodies against the carboxy-terminal 157 amino acids of NHE1 blocks activation of Na^+/H^+ exchange by hormones indicating that this part of the antiporter is required for hormone 'sensing'. How hormones elicit changes in Na^+/H^+ exchange is not known but may be due to signalling cascades including a PKC-dependent pathway and a tyrosine kinase pathway, (Incerpi *et al.*, 1994). PI 3-kinase may also be important in regulating the function and localisation of NHE isoforms. Recently Ma and co-workers showed, in cells expressing mutant PDGF receptors lacking PI 3-kinase- and PKC- dependent pathways, that both pathways were required for PDGF-induced activation of NHE1 (Ma *et al.*, 1994). In addition, treatment of polarised epithelial cells with the PI 3-kinase inhibitors wortmannin and LY294002, results in a marked inhibition of NHE-3 mediated H^+ extrusion, and the loss of NHE-3 from the cell surface due to impaired recycling (Kurashima *et al.*, 1998). Hormones and growth factors appear to regulate

NHE1 by phosphorylation of the protein on serine residues in the cytoplasmic tail. The importance of phosphorylation has been revealed by the use of okadaic acid, an inhibitor of protein phosphatase 1 and 2A (PP1 and PP2A), which can activate NHE1.

The Na^+/H^+ exchanger has been implicated in a number of pathophysiological conditions including cancer, hypertension and diabetes mellitus. In uncontrolled diabetes, where there may be high concentrations of extracellular glucose, the Na^+/H^+ activity of NHE1 is elevated, (Semplicini *et al.*, 1989). In addition, exposure of cells to insulin causes an increase in intracellular pH (pH_i), which has been suggested to be a result of activation of Na^+/H^+ exchange, since insulin causes an increase in Na^+ influx. Indeed insulin elicits an increase in the V_{max} of NHE1 in erythrocyte membranes by enhancing the serine/threonine phosphorylation of the cytosolic loop. This is in contrast to EGF and thrombin, which also increase the phosphorylation content of the NHE transporter, but do not effect its turnover rate (Canessa and Manriquez, 1997). However it occurs, alkalinization may function as a vital component of tissues response to insulin, much as pH changes are involved in the regulation of fertilisation, proliferation and metabolism in other cellular contexts, (Schaffer and Lodish, 1994).

1.9.5 Inhibitors of Na^+/H^+ Exchange: Implications for GLUT4 Translocation

I. Amiloride. Amiloride and its analogues are potent inhibitors of Na^+/H^+ exchange. They consist of a substituted pyrazine ring, and with a pKa of 8.7 they exist as monovalent cations at physiological pH. Counillon *et al.* have identified a single amino acid mutation in Na^+/H^+ exchangers isolated from amiloride-insensitive chinese hamster lung fibroblasts (Counillon *et al.*, 1993a). This $F^{167} \rightarrow L$ substitution occurs in the middle of putative transmembrane helix 4, which may represent the site of amiloride sensitivity.

Insulin stimulates Na^+/H^+ exchange in parallel with glucose transport and glycolysis (Fidelman *et al.*, 1982). Conversely, amiloride, which blocks Na^+/H^+ exchange, inhibits glucose transport (Fidelman *et al.*, 1982). However, amiloride is not absolutely specific for NHE1, also inhibiting a number of other ion transport systems. Therefore it is difficult to isolate the Na^+/H^+ pump, which in turn, leads to difficulties in interpreting the data.

II. HOE-694 and -642. In 1993, HOE-694 ((3-methylsulphonyl-4-piperidino-benzoyl) guanidine methanesulphonate), a novel compound with a structure distinct from amiloride was reported as a potent Na^+/H^+ pump inhibitor (Scholz *et al.*, 1993). Later cariporide mesilate or HOE 642 ((4-isopropyl-3-methanesulphonyl-benzoyl) guanidine methanesulphonate) was also identified as a specific NHE1 inhibitor (Scholz *et al.*, 1995) *(Figure 1.11B, lower panel).* Both compounds consist of a substituted benzene nucleus, and both have been shown to be beneficial in preventing cardiovascular damage during ischemia/reperfusion. Since these compounds are far more specific for NHE1 than amiloride (Counillon *et al.*, 1993b), they will provide useful tools for re-examining the role of this exchanger and of intracellular pH, in insulin-stimulated glucose transport and GLUT4 translocation.

III Isoproterenol. Isoproterenol inhibits Na^+/H^+ exchange via a β2-adrenergic receptor activation, which occurs through an adenylate cyclase stimulation and a cAMP-dependent mechanism, (Arsenis *et al.*, 1995). In addition, isoproterenol leads to a decrease in glucose transport and in the accessibility of insulin-stimulated GLUT4 at the adipocyte plasma membrane as judged by ATB-BMPA photolabelling, (Vannucci *et al.*, 1992). This effect occurs without an apparent change in the subcellular distribution of GLUT4 as determined by Western blotting. Thus these data suggest that insulin-stimulated glucose transporters can exist in two states in the plasma membrane, one which is functional and accessible to extracellular substrate, and one which is non-functional. Thus the effect of isoproterenol is to retarget insulin-stimulated GLUT4 into 'occluded', non-functional vesicles, (Vannucci *et al.*, 1992), possibly as a result of Na^+/H^+ pump inhibition.

Figure 1.11 Schematic Diagram of the v-ATPase and the Sodium-Proton Exchanger. A. Model of the v-ATPase in the plasma membrane showing the V_1 domain in blue and the V_0 domain in green. The lower panel shows the structure of the v-ATPase inhibitor bafilomycin A_1. (Adapted from Forgac, 1999). B. Model of the sodium-proton exchanger. The transporter consists of a membrane spanning N-terminal domain and a long cytoplasmic region at the C-terminus , The lower panel shows the chemical structure of the inhibitor HOE-642. (Adapted from Wakabayashi *et al.*, 1997).

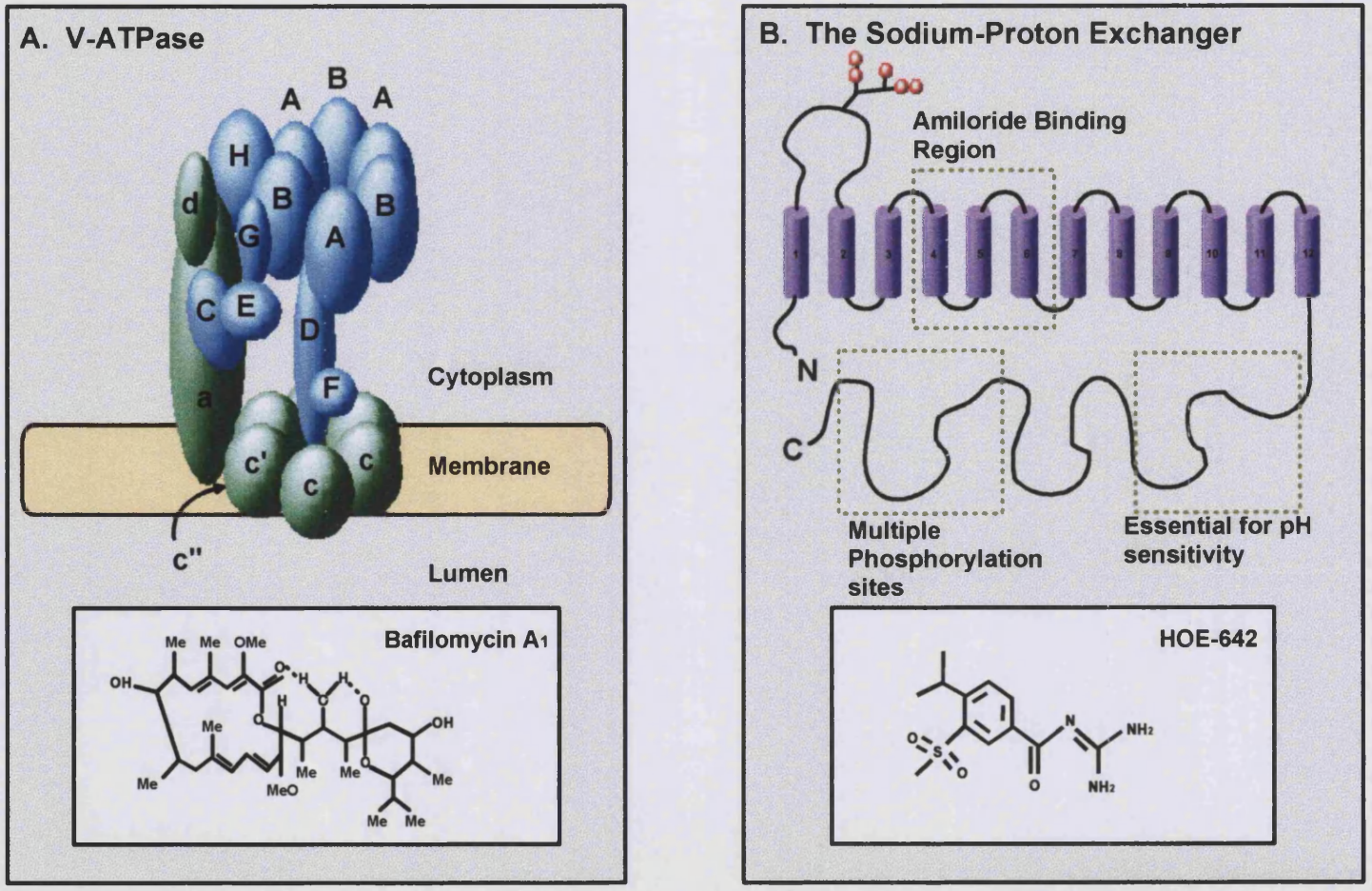

1.10 The Experimental Aims of the Work Described in this Thesis

The work described in this thesis has two main themes – the function of intracellular pH and the role of adaptor proteins in controlling intracellular trafficking and recycling of the glucose transporter, GLUT4. Initially an isolation protocol for cardiomyocytes was developed. Then, several studies were performed to confirm that the cells were insulin-responsive in terms of their glucose transport and GLUT4 translocation.

Investigations were undertaken to determine whether perturbations in the cellular pH would alter glucose transport and transporter translocation to the cell surface. Several techniques were employed. Firstly cells were stained with the acidotrophic dye acridine orange to establish that changes in pH had taken place. Then 2-deoxy-D-glucose and 3-*O*-methyl-D-glucose transport assays, cell surface photolabelling, subcellular fractionation and confocal microscopy were used to analyse changes in hexose transport and glucose transporter localisation.

Several studies with adipocytes were performed to establish a role for adaptor proteins in GLUT4 trafficking. Both Nycodenz and glycerol gradients were used to establish whether adaptor proteins and GLUT4 co-localise. A technique for immunoisolating GLUT4 vesicles was developed and characterised in order to examine whether a direct interaction between adaptor proteins and GLUT4 vesicles exist. Furthermore, the roles of GTPγS, temperature and brefeldin A on the association of adaptor complexes with GLUT4 vesicles were all investigated. In addition, an analysis of the association of the small GTPase ARF1 with GLUT4 vesicles was performed. Again gradient sedimentation and vesicle isolation protocols were employed. Moreover, the role of insulin on the association of adaptor proteins with GLUT4 vesicles was investigated and a number of approaches including chemical cross-linking and immunoprecipitation were used to analyse the interaction between the GLUT4 protein and the adaptor complexes.

2.0 Methods

2.1 Materials

2.1.1 Laboratory Chemicals

Radiolabelled sugars and ECL Western blotting detection reagents were purchased from Amersham Pharmacia Biotech. Optiphase Safe™ scintillation fluid was from LKB. Collagenase Type 1 from *Clostridium histolyticum* was from Worthington Biochemical Corporation or from Serva. Bovine Albumin Cohn Fraction V was purchased from Intergen Co. Fatty acid Free Bovine Serum Albumin and Thesit (Nonaethylene glycol dodecyl ether) were from Boehringer Mannheim. Protein molecular weight markers were from Sigma or New England BioLabs. Other reagents were of analytical grade and were purchased from Sigma, BDH or Fisons.

2.1.2 Antibodies

- The source of antibodies and their appropriate dilutions for Western blotting (*Section 2.9.3*) and immunoprecipitation (*Section 2.6.1*) are shown in the tables below. All antibodies were diluted in Tris-buffered saline buffer (0.09% (w/v) NaCl, 1M Tris-HCl, pH 7.4) containing 0.1% (v/v) Tween-20, 1% (w/v) BSA, and 0.02% (w/v) azide, unless otherwise stated.

- Rabbit antisera against GLUT1 and GLUT4 were raised in the laboratory of Dr. S.W. Cushman (National Institutes of Health, Bethesda, USA); using C-terminal peptides produced in our laboratory (Holman *et al.*, 1990).

Table 2.1 Source and Dilution of Antibodies Used for Western Blot Analysis

Antibody	Polyclonal/Monoclonal Purified/Serum	Source	Dilution for Western Blotting
Rabbit anti-σ1 subunit (AP1)	Polyclonal Purified	M.S. Robinson, University of Cambridge, U.K.	1:250 - 1:1000

Rabbit anti-γ subunit (AP1)	Polyclonal Purified	M.S. Robinson, University of Cambridge, U.K.	1:500 - 1:1000
Rabbit anti-α hinge (AP2)	Polyclonal Purified	B.J. Reaves, University of Bath, U.K.	1:250
Rabbit anti-β3A subunit (AP3)	Polyclonal Purified	M.S. Robinson, University of Cambridge, U.K.	1:500
Rabbit anti-μ3A subunit (AP3)	Polyclonal Purified	M.S. Robinson, University of Cambridge, U.K.	1:500
Mouse anti-ARF	Monoclonal (1D9) Purified	Alexis Corporation (U.K.) Ltd., Nottingham, U.K.	1:250-1:500
Rabbit anti-GLUT1	Polyclonal Purified	National Diagnostics, Germany.	1:1000
Rabbit anti-GLUT4	Polyclonal Serum and Purified	G.D.Holman, University of Bath, U.K.	1:4000
Mouse anti-GLUT4	Monoclonal (1F8) Purified	Biogenesis Ltd. Poole, U.K.	1:1000
Rabbit anti-Insulin Receptor α	Polyclonal	Santa Cruz Biotechnology Inc. U.S.A.	1:250
Mouse anti-Insulin Receptor Substrate 1	Monoclonal	Transduction Laboratories, Kentucky, U.S.A	1:250
Chicken anti-human NHE1	Polyclonal Serum	Alpha Diagnostics International Inc. San Antonio, U.S.A.	1:1000
Rabbit anti-PRA1	Polyclonal Serum	J.K.Ngsee, Loeb Reserach Institute, Ontario, Canada.	1:1000 - 1:2000
Rabbit anti-PI 3-Kinase p85α	Polyclonal	Transduction Laboratories, Kentucky, U.S.A,	1:250
Goat anti-Protein Kinase B (N)	Polyclonal	Santa Cruz Biotechnology Inc. U.S.A	1:500
Rabbit anti-αSNAP	Polyclonal Purified	J. Mitchell, University of Bath, U.K.	1:1000
Rabbit anti-syntaxin4	Polyclonal Purified	S. Oldfield, University of Bath, U.K.	1:5000
Mouse anti-TGN38	Monoclonal (2F 7.1) Purified	G. Banting, University of Bristol and P.Luzio, University of Cambridge, U.K.	1:1000
Mouse anti - Transferrin Receptor	Monoclonal (CD 71) Purified	Chemicon International Inc., U.S.A.	1:1000
Rabbit anti-VAMP2	Polyclonal (L220) Purified	M.A. Krepper, Renal Mechanisms Section, NIH, Washington D.C., U.S.A.	1:500- 1:1000 (made in TBS only)

Mouse anti-VAMP2	Monoclonal (CL69.1)Purified	R. Jahn, Max Planck Institute, Germany.	1:1000

Table 2.2 Source and Dilution of Secondary Antibodies Used for Western Blot Analysis

Antibody	Source	Dilution
Goat anti-chicken IgG peroxidase conjugate	Sigma ImmunoChemicals, St. Louis, U.S.A.	1:1000
Human anti-goat IgG peroxidase conjugate	Sigma ImmunoChemicals, St. Louis, U.S.A.	1:4000
Goat anti-mouse IgG peroxidase conjugate	Sigma ImmunoChemicals, St. Louis, U.S.A.	1:1000
Goat anti-rabbit IgG peroxidase conjugate	Sigma ImmunoChemicals, St. Louis, U.S.A.	1:4000

Table 2.3 Sources and Concentration of Antibodies Used for Immunoprecipitation

Antibody	Source	Concentration Required for Immunopreciptation
Rabbit anti-GLUT1	G.D. Holman, University of Bath, U.K.	100 µl serum / 1 ml adipocyte cell lysate
Rabbit anti-GLUT4	G.D. Holman, University of Bath, U.K.	20 µg purified antibody / 1 ml adipocyte cell lysate
Rabbit anti-GLUT4	G.D. Holman, University of Bath, U.K.	50 µl serum / 1 ml adipocyte cell lysate

2.1.3 Bis-mannose Photolabels

2-*N*-4-(1-azi-2,2,2-trifluoroethyl)-benzoyl-1,3-[^{3}H]bis(D-mannos-4-yloxy)-2-propylamine) (ATB-[^{3}H]-BMPA) (≈ 10 Ci/mmol) and the biotinylated derivative Bio-lc-ATB-BMPA were synthesised as described in (Clark and Holman, 1990; Koumanov *et al.*, 1998) by Professor G.D. Holman.

2.2 Isolation of Insulin Sensitive Cells

2.2.1 Preparation of Bovine Serum Albumin Solution

10 g of BSA (Fraction V) per 60 ml of double-distilled water was dissolved overnight at 4°C. The BSA was filtered through a Millipore type A membrane filter (0.8 μm pore size) under vacuum and the pH of the solution was adjusted to 7.6 with 10 M NaOH. Double distilled water was added to give a final BSA concentration of 10% (w/v). The BSA was divided into 40 ml aliquots and stored at -20°C until required.

2.2.2 Isolation of Rat Adipocytes

2.2.2.1 Preparation of Buffers

All buffers, unless otherwise stated, contained the following Krebs-Ringers-HEPES buffer (KRH) consisting of 140 mM NaCl, 4.7 mM KCl, 2.5 mM $CaCl_2$, 1.25 mM $MgCl_2$, 2.5 mM NaH_2PO_4, 10 mM HEPES. The pH was adjusted to 7.6 at 20°C. BSA was added as required. Buffer stock solutions were prepared as 10-time concentrates, one containing HEPES and NaH_2PO_4 (pH 7.6), and the other containing NaCl, KCl, $CaCl_2$ and $MgSO_4$, and were stored at 4°C for up to 1 month.

2.2.2.2 Preparation of Isolated Rat Adipocytes

Isolated adipose cells were prepared from the whole epididymal fat pads of male Wistar rats (180-200 g) as described, (Taylor and Holman, 1981; Simpson *et al.*, 1983). The rats were stunned and the necks dislocated. The epididymal fat tissue was quickly removed and rinsed in 1% (w/v) BSA/KRH buffer at 37°C. The washed tissue was placed in KRH buffer (4pads/ 5mls) containing 3.5% (w/v) albumin, 5 mM glucose, and 0.70 mg/ml collagenase (Worthington) and minced finely with scissors. The tissue suspension was shaken rapidly in a shaking water bath at 37°C for approximately 40 min until most of the tissue lumps were digested. The resulting cell suspension was filtered through a nylon mesh (250 μm mesh size, Lockertex), returned to 37°C and the cells were allowed to float. The infranatant buffer was removed using a needle (2 mm dia. x 100 mm) attached to a 20 ml plastic syringe, and 15-20 ml 1% (w/v) BSA/KRH buffer was added. The cells were gently resuspended and then allowed to float. This washing procedure was repeated 3-4

times. The cell suspension was adjusted to a cytocrit of 40%, (using a capillary tube which was centrifuged at 1500 *g* for 30 sec, and expressed as the ratio of the length of the packed cell fraction in the tube to the total length of the suspension in the tube).

2.2.3 Isolation of Rat Cardiac Myocytes

2.2.3.1 Preparation of Buffers

All buffers, unless otherwise stated, contained the following cardiomyocyte Krebs-Ringers-HEPES buffer (cKRH buffer): 6 mM KCl, 1 mM Na_2HPO_4, 0.2 mM NaH_2PO_4, 1.4 mM $MgSO_4$, 128 mM NaCl, 10 mM HEPES. Buffer stock solutions were prepared as 10-time concentrates, one containing HEPES, NaH_2PO_4, and Na_2HPO_4 (the pH was adjusted to 7.4 with 10 M NaOH), and the other containing NaCl, KCl, and $MgSO_4$. Stock solutions were stored at 4°C for up to 1 month.

Prior to use, the cKRH buffer was gassed with O_2 for 20 min. From the cKRH buffer, a number of other buffers were prepared on the day of use:

- *Buffer A:* cKRH buffer supplemented with 5.5 mM glucose, 2 mM ultrapure pyruvic acid (Sigma) and 20 mM inosine (Aldrich).
- *Buffer B:* buffer A supplemented with 0.7% (w/v) BSA, 1.1 mg/ml collagenase, 2.65 mg/ml hyaluronidase Type 1-S, 15 mM 2,3-butanedione monoxime (BDM).
- *Buffer C:* buffer A supplemented with 0.2 mg/ml DNAse I (Boehringer Mannheim), 15 mM 2,3-butanedione monoxime (BDM), 200 μM $CaCl_2$, and 2% (w/v) BSA.
- *Buffer D*: buffer A supplemented with 1 mM CaCl2 (physiological calcium concentration), and 2% (w/v) BSA.
- *Buffer E*: buffer A containing 1 mM CaCl2 and 2% (w/v) Fatty acid free Albumin, Fraction V, (Boehringer Mannheim).
- *Buffer F (no glucose or pyruvate):* cKRH Buffer containing 1 mM $CaCl_2$ and 2% (w/v) Fatty acid free Albumin, Fraction V, (Boehringer Mannheim).
- *Heparin Solution:* Heparin Grade 1A isolated from porcine intestinal mucosa was reconstituted in 0.9% (w/v) NaCl (1000 Units/ml) and filter sterilised through a 0.2 μm filter (Sartorius). Aliquots were stored at 4°C.

2.2.3.2 Preparation of Isolated Rat Cardiac Myocytes

Calcium-resistant[1], rod-shaped cardiomyocytes from adult male Wistar rats (260-280 g fed *ad libitum*) were prepared using a method originally described by (Fischer *et al.*, 1991) with some modifications. Briefly, animals were anaesthetised with 350 µl Sagatal™ (Pentobarbitone Sodium b.p., 60mg/ml, (Rhone Merieux)) before administration of 500 units of heparin solution via the tail vein. After 5 min the neck was dislocated and the heart rapidly removed into semi-frozen Buffer A (0-4°C). The heart was immediately mounted on to a catheter and perfused by the method of Langendorff, (Langendorff, 1895) with Buffer A, at 37°C, for 5 min in order to remove blood and metabolites from the coronary vessels and atrial and ventricular chambers. The perfusion was then switched to Buffer B equilibrated with oxygen and was recirculated by means of a peristaltic pump.

After 15 min 100 µM $CaCl_2$ was added to the recirculating buffer. The $CaCl_2$ concentration was raised to 200 µM after a further 3 min. The heart was perfused for a total of 18 min prior to its' removal from the catheter. The heart tissue was dissociated in a buffer containing 10 ml Buffer B and 10 ml Buffer C prewarmed to 37°C and under an oxygen atmosphere. Incompletely digested tissue was passaged gently through a 1 ml syringe and incubated for a further 10 min at 37°C. During this last incubation, the calcium concentration was increased in 200 µM steps until the final concentration was 800 µM.

The digested suspension was filtered through a 250 μm^2 nylon gauze (Lockertex,) and the cardiomyocytes were allowed to settle for 3-4 min to form a loose pellet. The supernatant was removed and the cells resuspended in 20 ml Buffer D. The cells were allowed to settle again for 3-4 min at room temperature and the supernatant was removed. The pellet was resuspended in 10 ml Buffer E and the cell suspension was incubated for 20-30 min at 37°C under an oxygen atmosphere to allow the cells to recover from the isolation procedure. Viability was assessed by counting the number of rod-shaped (viable) versus round-shaped (dead) cells under the light microscope.

[1] cardiac myocytes are designated "calcium tolerant" when they survive the reintroduction of calcium at physiological concentrations after a period of calcium-free incubation or perfusion (Fischer *et al.*, 1991)

2.3 Treatment of Isolated Cells with Insulin

2.3.1 Preparation of Insulin

Monocomponent porcine insulin was a gift from Dr. G. Daniellson, Novo Nordisk. 1.0 mg of insulin was dissolved in 1.0 ml of 0.03 M HCl and the solution made up to 3.0 ml with double-distilled water. 1.0 ml of this solution was then diluted to 50 ml with 1% (w/v) BSA/KRH buffer, pH 7.6. The resulting insulin solution (1 mM) was divided into 500 µl aliquots and stored at -20°C until required. The solution was not refrozen once it had been thawed.

2.3.2 Stimulation of Adipocytes with Insulin

20 nM insulin (1 mM stock, *Section 2.3.1.*) was used to stimulate isolated rat adipocytes (40% cytocrit), for 20 min at 37°C. Basal cells were also maintained at 37°C during this time.

2.3.3 Stimulation of Cardiac Myocytes with Insulin

Prior to manipulation the cells were washed once in Buffer F, (to reduce the glucose and pyruvate concentrations), and divided into the required number of aliquots. Cells designated 'insulin' were stimulated for 30 min with 30 nM insulin. During this time both basal and insulin-stimulated cells were maintained at 37°C, under oxygen pressure with gentle shaking.

2.4 Glucose Transporter Studies

2.4.1 Assay for 3-*O*-Methyl-D-Glucose Uptake in Rat Adipocytes

Uptake of 3-*O*-methyl-D-glucose was determined by the method of Whitesell and Gliemann, (Whitesell and Gliemann, 1979). 50 µl of a 40% adipocyte suspension was added to 10 µl of radiolabeled sugar (200 µM 3-*O*-methyl-D-glucose (33.3 µM final concentration) containing 0.15 µCi of 3-*O*- [^{14}C] methyl-D-glucose) in KRH buffer. Uptake was terminated by rapidly adding 3 ml 300 µM phloretin in albumin-free KRH

buffer (the phloretin was first dissolved in ethanol such that the final concentration of ethanol was 0.5% (v/v)). Timings of 10 s or less were carried out using a metronome set at 2 beats/sec. Uptake was measured for 3 s in insulin-stimulated cells and 120 s in basal cells (these times should give fractional filling values (F) of approximately 0.5). All measurements were carried out in triplicate.

"Background" values (b) (indicating extracellular trapped radioactivity) were determined by adding 3 ml of 300 μM phloretin in KRH buffer to the sugar before the addition of the cells. "Infinity" values (cpm_a) (indicating equilibrium distribution of radioactivity) were determined by incubating insulin-treated cells with sugar for at least 20 min. Approximately 1 ml of silicon oil (Dow Corning 100/200 cs, obtained from BDH) was layered on top of the buffer, and the tubes were centrifuged (MSE bench centrifuge, swing-out rotor) at 1000 *g* for 45 sec. The cell layer was removed from the top of the oil using small pieces of pipe-cleaner (5 mm), and placed in a scintillation vial. 8 ml of scintillation fluid (Optiphase Safe™) was added. The rate constant of sugar uptake (v/s) was calculated from the fractional filling (F) using the following equation, which assumes that the rate of filling (approaching equilibrium) is a single exponential function of time:

$$F = \frac{cpm_t - b}{cpm_a - b} \qquad \frac{V}{S} = \frac{(-\ln[1-F])}{t}$$

2.4.2 Assay of 2-Deoxy-D-glucose Uptake in Rat Cardiac Myocytes

Uptake was determined using a modification of the method described by Fischer, (Fischer *et al.*, 1991). Cells were either maintained in the basal state or insulin-stimulated as described, (*Section 2.3.2*). The cell suspension was divided into 900 μl aliquots in glass tubes (4.5 cm x 1.5 cm) with sealed lids, which were connected to an oxygen supply by means of a small needle. The transport assay was started by the addition of 2-deoxy-D-glucose to a final concentration of 100 μM (containing 0.5 μCi of 2-deoxy-D-[^{3}H]-glucose, (specific activity:1 mCi/ml) as a tracer). Sugar uptake was terminated by transferring the cell suspension to eppendorff microfuge tubes containing

100 µl 6.8 mM phloretin in Buffer F, (final concentration of phloretin was 400 µM). The samples were quickly mixed and immediately centrifuged at 3500 *g* for 1 min. The supernatants were removed and the cells were washed 3 times with 1 ml Buffer F containing 400 µM phloretin. Cells were lysed with 1 ml ice-cold 0.1 M NaOH, and aliquots were taken for protein determination, (*Section 2.9.5*).

The lids of the eppendorff tubes were removed and the entire tube placed in scintillation vials. Samples were counted in 8 ml of scintillant (Optiphase Safe^{TM},) in a Packard 1500 TRI-CARB or 1600 TR liquid scintillation counter. Background counts were determined by addition of cells to eppendorf tubes that contained 2-deoxy-D-glucose pre-mixed with 400 µM phloretin. These cells were washed and lysed exactly as described above.

2.4.3 Bis-Mannose Photolabelling Of Cell-Surface Glucose Transporters In Adipocytes

18.5 MBq (final concentration of label was 100 µM) ATB-[^{3}H]-BMPA or 500 µM Bio- lc-ATB-BMPA was added to 500 µl of cells (40% cytocrit) in 1% (w/v) BSA/KRH buffer in 35 mm polystyrene dishes (Nunc/Gibco BRL) at 18°C. Cells and label were mixed, then irradiated for 1 min in a Rayonet RPR-100 photoreactor containing 300 nm lamps. Following irradiation, the cells were washed into universal tubes (Sarstedt) with 20 ml 1% (w/v) BSA/KRH buffer at 18°C and pulse spun in a bench centrifuge (IEC centra-3) to 1000 *g*. The infranatant buffer was removed using a needle (2 mm dia. x 100 mm), and the cells were resuspended in 20 ml 1% (w/v) BSA/KRH buffer and washed once more. The cells were solubilised by the addition of 2% (w/v) Thesit in PBS buffer containing protease inhibitors at 18°C. The unsolubilised material was removed by centrifugation at 20,000 *g* for 20 min. The samples were processed as described in *Section 2.4.5*.

2.4.4 Bis-Mannose Photolabelling Of Cell-Surface Glucose Transporters In Cardiac Myocytes

Basal and insulin-stimulated cells (*Section 2.3.2*) were transferred to 35 mm diameter polystyrene dishes (Nunc/Gibco BRL) and incubated at 18°C for 5 min to slow transporter recycling. 18.5 MBq ATB-[^{3}H]-BMPA or 500µM Bio-lc-ATB-BMPA was

added to the samples. Cells were irradiated for 1 min in a Rayonet RPR-100 photoreactor containing a 50/50 distribution of 300 nm and 350 nm lamps. Following irradiation, cells were transferred to 15 ml falcon tubes and washed once with 15 ml Buffer F and twice with 15 ml HES buffer (20 mM HEPES pH 7.2, 1 mM EDTA, 255 mM sucrose plus protease inhibitors: 1 μg/ml leupeptin, 1 μg/ml aprotonin, 1 μg/ml pepstatin A, 1 μg/ml antipain, 100 μM (4-(2-aminoethyl) benzenesulfonyl fluoride (AEBSF)), at 18°C. Following the final wash, the cell pellets were resuspended in 500 μl HES buffer and homogenised with 30 strokes using a muscle homogeniser. The homogenates were transferred to 3 ml polycarbonate tubes and made up to a total volume of 3 ml with HES buffer. The samples were centrifuged at 541,000 *g* in a Beckman TL-100 benchtop ultracentrifuge with a TLA-100.3 fixed rotor for 30 min at 4°C. The resulting total membrane pellets were washed in 3 ml HES buffer plus protease inhibitors and the centrifugation step was repeated. The final pellets were resuspended in 800 μl PBS buffer (12.5 mM Na_2HPO_4, 154 mM NaCl, pH 7.2, containing protease inhibitors), and transferred to clean eppendorff tubes. 200 μl 10% (w/v) Thesit solution was added to the samples to give a final concentration of Thesit of 2% (w/v). The samples were rotated at room temperature for 20 min. Unsolubilised material was removed by centrifugation at 20,000 *g* for 20 min. The samples were processed as described in *Section 2.4.5.*

2.4.5 Processing Photolabelled Transporters

2.4.5.1 Immunoprecipitation of ATB-[^{3}H]-BMPA Labelled Transporters and Gel Slicing

ATB-[^{3}H]-BMPA-photolabelled glucose transporters from the solubilised supernatants of adipocytes or cardiomyocytes were immunoprecipitated using Protein A sepharose beads coupled to either GLUT1 or GLUT4 antibodies (*Section 2.6.1*). The resulting precipitates were resolved on a 10% SDS-PAGE gel. After staining and destaining (*Section 2.9.4*), lanes from the gel were cut into 0.66 cm slices and dried individually in open scintillation vials in an 80°C oven. Dried gel slices were solubilised with 500 μl 2% (v/v) NH_4OH in 30% (v/v) H_2O_2 in sealed vials at 80°C. 8 ml of scintillation cocktail (Optiphase Safe^{TM}) was added and ^{3}H counts determined using a Packard Tri-Carb 1600 Scintillation counter. A graph of slice number versus disintergrations per minute (d.p.m) was constructed. The radioactivity associated with the labelled transporters was determined by adding up the

counts from the slices that formed the peak and subtracting the counts from the same number of slices that contained no label (background counts).

2.4.5.2 Streptavidin Precipitation of Bio-lc-ATB-BMPA Labelled Glucose Transporters

50 µl of a 50% slurry of Immunopure streptavidin beads (Pierce) (stored in ethanol) were used per condition. The beads were washed twice with 1 ml ice-cold PBS buffer containing protease inhibitors, to remove the ethanol. The photolabelled transporters from solubilised supernatants of adipocytes or cardiomyocytes (*Sections 2.4.3 and 2.4.4*) were incubated with the streptavidin beads overnight at 4°C with end-to-end rotation. Following this incubation, the streptavidin beads were washed 4 times with 1ml PBS buffer containing 1% (w/v) Thesit, 4 times with 1ml PBS buffer containing 0.1% (w/v) Thesit and once with 1ml PBS buffer only. Bound biotinylated glucose transporters were eluted in 30 µl 'high SDS' sample buffer (62.5 mM Tris-HCl, pH 6.7, 3% (w/v) SDS, 50% (v/v) glycerol, 0.02% (w/v) bromophenol blue) by heating at 95°C for 30 min. The eluate was collected and the elution procedure was repeated. The resulting eluates were pooled and loaded carefully using sequencing tips on to 10% SDS-PAGE gels, transferred to nitrocellulose and blotted with GLUT1 or GLUT4 antibodies (*Sections 2.9.1 – 2.9.3*).

2.5 Subcellular Fractionation of Insulin Sensitive Cells

2.5.1 Subcellular Fractionation of Rat Adipocytes

This procedure was carried out essentially as described by Weber (Weber *et al.*, 1988). Briefly, cells were washed twice in HES buffer at 20°C and then resuspended in HES buffer to give a 40% cytocrit. The cells were rapidly homogenised (basal first) with 10 strokes of a 55 ml Potter-Elvehjem homogeniser, (Thomas Scientific), with a specific clearance of 150 µm. The homogenates and subsequent fractions were centrifuged in a Beckman TL-100 benchtop ultracentrifuge with a TLA-100.3 fixed rotor (or a TLS-55 swing-out rotor, where indicated). Initially, each sample was centrifuged at 17, 500 *g* for 20 min resulting in a crude membrane pellet, a microsomal/cytosolic fraction and a layer of fat. The microsomal/cytosolic fractions were removed, using 19 gauge needles attached to 5 ml syringes, and used for fractionation of the microsomal membranes. The pellets

Figure 2.1 Method for the Subfractionation of Rat Adipocytes. Adipocytes were homogenised and spun at 1000 *g*. The fat was removed and the resulting supernatant was centrifuged at 17,500 *g* for 20 min. The resulting supernatant was centrifuged at 49,000 *g* for 9 min to produce the high density microsomes (HDM). The supernatant from this spin was centrifuged at 541,000 *g* for 17 min to produce the low density microsomes (LDM) and the cytosol (CYT). The pellet from the original 17,500 g spin was resuspended in HES buffer and layered onto the top of a sucrose cushion which was centrifuged at 105,000 *g* for 20 min. The resulting plasma membranes were pelleted and washed twice by centrifugation at 74,000 *g* for 9 min.

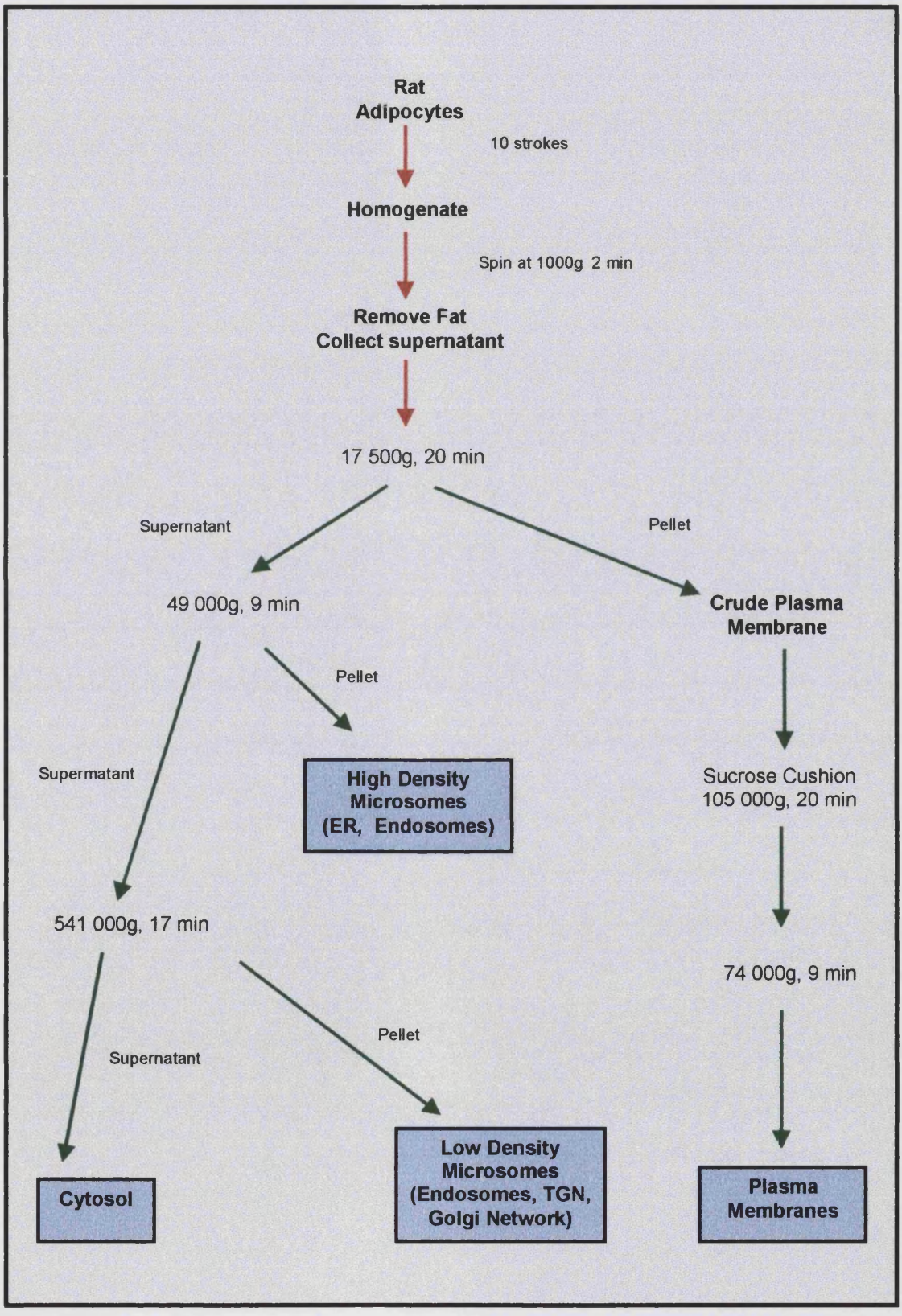

containing plasma membranes, mitochondria and nuclei were resuspended in 300 µl HES buffer and loaded onto 0.6 ml sucrose cushions (1.12 M sucrose (38.3% (w/v), 20 mM HEPES pH 7.2, 1 mM EDTA) and spun at 105, 000 *g* for 20 min in the swing-out rotor. The mitochondria and nuclei were recovered in the pellets. The plasma membranes were collected from the sucrose cushions, resuspended in HES buffer to 3 ml and centrifuged at 74, 000 *g* for 9 min. The resulting plasma membrane (PM) pellets were resuspended in 3 ml HES buffer and repelleted at 74,000 *g* for 9 min.

The supernatants (containing the microsomal membranes) obtained from the 17,500 *g* spin were centrifuged at 49, 000 *g* for 9 min to pellet the high-density microsomes (HDMs). The resulting post-HDM supernatants were centrifuged at 541, 000 *g* for 17 min to pellet the low-density microsomes (LDMs). Both microsomal fractions were resuspended in HES buffer. The remaining supernatants were the cytosol fractions. All fractions were assayed for protein content (*Section 2.9.5*), aliquoted and stored at -70°C.

2.6 Immunoprecipitation

2.6.1 Immunoprecipitation of Proteins

Immunoprecipitation of a required protein from cardiomyocytes or adipocytes was performed as follows: Cells were solubilised by incubation with 2% (w/v) Thesit in PBS buffer containing protease inhibitors for 20 min at room temperature. Any unsolubilised material was removed by centrifugation at 20, 000 *g* for 20 min at 4°C.

5 mg of Protein A-Sepharose CL-4B (Sigma) was washed and swollen in 1 ml PBS buffer, pH 7.2 for 10 min, then incubated for at least 2 h at 4°C with relevant affinity-purified antibodies or antiserum, (*Table 2.3*), in 1 ml PBS buffer containing protease inhibitors. Unbound antibodies were removed by washing the protein A-Sepharose pellets twice in 1 ml PBS buffer, pelleting by centrifugation at 3500 *g* for 1 min in a MSE microcentaur microfuge. Cell lysates were incubated with antibody-protein A-Sepharose conjugates for 2 h or overnight at 4°C.

The immunopellets were washed 6 times with 1 ml 1% (w/v) Thesit or Triton X-100 (v/v) in PBS buffer and once with 1 ml PBS buffer. The protein-antibody complexes were dissociated from the Protein A-Sepharose beads by incubating the immunopellets

for 20 min in 6 M urea electrophoresis sample buffer (6 M urea, 10% (w/v) SDS, 1% (w/v) bromophenol blue) and 100 mM 2-β mercaptoethanol at room temperature with occasional vigorous vortexing. Eluted proteins were analysed by SDS-PAGE, (*Section 2.9.1*).

2.6.2 Immunoprecipitation of GLUT4 Vesicles

2.6.2.1 Preparation of GLUT4 Vesicles on Staphylococcus aureus cells

GLUT4 vesicles were isolated on *Staphylococcus aureus* Cowan I cells (Staph cells) expressing Protein A. Initially Staph cells were prepared by heating to 95°C in extraction buffer (50 mM Tris-HCl, pH 7.2, 150 mM NaCl, 104 mM SDS, 10% (v/v) 2-β mercaptoethanol), at a ratio of 50 mg Staph cells per ml buffer. Staph cells were pelleted at 13, 400 *g* for 1 min and resuspended in extraction buffer. Cells were heated and centrifuged as before, then washed 3 times with 1 ml HES Buffer (10 mM HEPES, pH 7.2, 5 mM EDTA, 255 mM sucrose). Finally Staph cells were resuspended in HES buffer at 50 mg/ml and stored as 1 ml aliquots at -20°C until required.

Aliquots of Staph cells (40 µl) were incubated with 50 µl rabbit anti-GLUT4 serum or non specific rabbit serum (pre-immune control) in 1 ml HES buffer for 2 h at 4°C with end-to-end rotation. Staph cells were washed 3 times with 1 ml of HES buffer, centrifuging at 13, 000 *g* for 1 min between washes. Post-HDM supernatants were initially precleared by incubation with Staph cells coupled to rabbit IgG, for a minimum of 30 min at 4°C with rotation. Supernatants were then transferred to Staph cells bound with rabbit IgG (pre-immune control) or rabbit anti-GLUT4 IgG and rotated for 2 h at 4°C. Staph cells were subsequently washed once in HES buffer and twice in HES buffer containing 100 mM KCl. Vesicular proteins were solubilised by incubating Staph cell pellets with 100 µl 2% (w/v) Thesit in HES buffer at room temperature for 20 min. Bound GLUT4 protein was eluted by heating pellets to 95°C in sample buffer (62.5 mM Tris-HCl, pH 6.7, 1% (w/v) SDS, 50% (v/v) glycerol, 0.02% (w/v) bromophenol blue) with 20 mM dithiothreitol (DTT), for 5 min.

2.6.2.2 Preparation of GLUT4 Vesicles on Acrylamide beads

One ml of Reacti-Gel (GF-2000) support (acrylamide beads) (Pierce) was prepared by washing once with 20 ml ice cold double distilled H_2O and then once with 20 ml borate buffer (100 mM $NaBH_3$, 0.9% (w/v) NaCl, pH 8.5), using a Buchner funnel, and Whatman No. 1 filter paper. The acrylamide beads were then split into two aliquots; one was coupled to 500 µg purified rabbit anti-GLUT4 antibody (no azide) and the other to 500 µg purified rabbit IgG (Sigma), by rotation in borate buffer, overnight, at 4°C. The coupling buffer was then removed and the beads quenched for 1 h at 4°C with 2 M Tris-HCl, pH 8.0. Following this incubation, the beads were washed 4 times in PBS buffer (to remove Tris-HCl pH 8.0 buffer and unbound antibody), and stored at 4°C, as a 50% (w/v) slurry in PBS buffer, until required.

On the day of use, 50 µl of the 50% (w/v) slurry per condition, (both non-specific rabbit IgG and rabbit anti-GLUT4 antibody coupled beads) were blocked for at least 2 h with 2% (w/v) BSA in PBS buffer, at 4°C. The beads were then washed twice in PBS buffer and twice in HES buffer, pH 7.2, (pulse spinning to 2000 *g* between washes). Post-HDM supernatants were rotated with beads coated either in non-specific rabbit IgG (control) or rabbit anti-GLUT4 IgG (GLUT4 vesicles), for 2 h at 4°C (no pre-clearing step was required). Beads were washed once in HES buffer and twice in HES buffer containing 100 mM KCl. Vesicular proteins were solubilised by incubating beads with 100 µl 2% (w/v) Thesit in HES buffer at room temperature for 20 min. Bound GLUT4 protein was eluted by heating pellets to 95°C in sample buffer (62.5 mM Tris-HCl, pH 6.7, 2% (w/v) SDS, 50% (v/v) glycerol, 0.02% (w/v) Bromophenol Blue) with 20 mM dithiothreitol (DTT), for 5-10 min.

2.7 Gradient Centrifugation

2.7.1 Nycodenz Gradient Centrifugation

Post-HDM supernatants (*Section 2.6.1*) were analysed by Nycodenz velocity gradient centrifugation. The iso-osmotic medium 5-(N-2, 3-dihydroxypropylacetamido)-2,4,6-triiodo-N, N'-bis(2,3-dihydroxypropyl)isophthalamide (Nycodenz™) was prepared as a 27.6% (w/v) stock in Gradient buffer (20 mM HEPES, pH 7.5, 3 mM KCl and 0.3 mM

EDTA) and stored at room temperature. All other Nycodenz gradient solutions were prepared by diluting the 27.6% (w/v) Nycodenz stock solution with a sucrose diluent composed of 7.45% (w/v) sucrose in the Gradient buffer.

Table 2.4. Properties of Nycodenz™-Sucrose Gradients

% (w/v) Nycodenz™	27.6	18.4	13.8	9.2
Dilution ratio Nycodenz™: Sucrose Diluent	1:0	2:1	1:1	1:2
Density (g/ml) 20°C	1.148	1.105	1.086	1.066
Refractive index 20°C	1.3784	1.3669	1.3613	1.3553

Linear gradients (9.2 - 27.6% (w/v)) were constructed by layering 9 ml of each Nycodenz gradient solution, (1.148 g/ml to 1.066 g/ml) in to 38 ml polyallomer centrifuge tubes, (Beckman Instruments Inc., Palo Alto, USA), on ice. Gradients were sealed and placed on their sides for 1 h to allow rapid diffusion resulting in the formation of a smooth gradient. 2 ml of post-HDM supernatant per condition were dialysed overnight against Gradient buffer at 4°C, primarily to remove the sucrose. Gradients were then centrifuged at 4°C in a SW28 Titanium swing-out rotor (Beckman Instruments Inc.), at a speed of 63, 000 *g* for 2 h 30 min. Gradient fractions (1 ml) were collected from the bottom to the top of the tube by the use of a capillary tube and pump. Aliquots of each fraction (100 µl) were analysed by SDS-PAGE (*Section 2.9.1*) and Western Blotting, (*Section 2.9.3*).

2.7.2 Glycerol Gradient Centrifugation

Post-HDM supernatants from basal and insulin-treated rat adipocytes were diluted 5-fold in Gradient buffer II (10 mM HEPES, pH 7.2, 150 mM NaCl, 1 mM EGTA, 1 mM $MgCl_2$, 1 µg/ml leupeptin, 1 µg/ml aprotonin, 1 µg/ml pepstatin A, 1 µg/ml antipain, 100 µM (4-(2-aminoethyl) benzenesulfonyl fluoride (AEBSF), and loaded on to a 27.5 ml 5-25% (v/v) discontinuous glycerol gradient over an 8 ml 50% (w/v) sucrose cushion. The gradients were centrifuged at 80, 000 *g* for 16 h at 4°C. Gradient fractions (1 ml) were collected from the bottom of the tube. Aliquots of each fraction (100 µl) were

analysed for constituent proteins by SDS-PAGE (*Section 2.9.1*) and Western Blotting, (*Section 2.9.3*).

2.8 Confocal Microscopy

2.8.1 Indirect Immunofluorescence Microscopy

Following incubation with stimulatory or inhibitory compounds (indicated in the figure legends), cardiomyocytes (1 ml) were transferred to 15 ml falcon tubes, (if possible the cells were maintained in Buffer E containing glucose and pyruvate (*Section 2.2.3*)). The cells were fixed by incubation with 7.5 ml 4% (w/v) paraformaldehyde in PBS buffer pH 7.2 for 20 min at 20°C with gentle rocking. The cells were washed 3 times with 15 ml PBS buffer at 20°C spinning at 300 *g* for 1 min between washes. The cells were permeabilised in 7.5 ml Permeabilisation buffer (0.1% saponin, 1% (w/v) BSA, 3% (v/v) goat serum (Sigma) in PBS buffer pH 7.2) for 45 min with gentle rocking. Following permeabilisation the cells were centrifuged at 300 *g* and the pellets were resuspended in 250 µl Permeabilisation buffer and transferred to eppendorff tubes. 250 µl 4 µg/ml mouse anti-GLUT4 antibody (1F8 clone, Biogenesis Ltd., Poole) or rabbit anti-GLUT4 antibody was added to each sample (2 µg/ml final concentration) in Permeabilisation buffer. The samples were rocked gently for 60-90 min, then washed three times with 1 ml Permeabilisation buffer and incubated for 1 h with 500 µl 1:60 dilution of rhodamine labelled anti-mouse IgG antibody or fluorescein labelled anti-rabbit IgG antibody (Jackson Laboratories) in Permeabilisation buffer. The cells were washed 6 times with 1 ml Permeabilisation buffer and mounted onto a glass coverslip using Vector Shield mounting medium, (Vector Laboratories). Cardiomyocytes were viewed using a Zeiss confocal scanning microscope (LSM 510, Carl Zeiss Microscopy, Germany) with a 458/488 nm laser (for fluorescein labelled samples) or a 543 nm laser (for rhodamine labelled samples).

2.8.2 Vital Fluorescence Microscopy

Cardiomyocytes were stained with acridine orange following the method described by (Yoshimori *et al.*, 1991). Briefly, cardiomyocytes were incubated with acridine orange at a final concentration of 5 µg/ml in Buffer E (*Section 2.2.1.2)* for 10 min at 37°C with continuous gassing with O_2. The cells were subsequently washed twice with 15 ml 1%

(w/v) BSA/cKRH buffer, centrifuging at 300 *g* between washes. The cells were immediately mounted onto coverslips using Vector Shield mounting medium, (Vector Laboratories), and viewed using dual lasers for fluorescein and rhodamine (458/488nm and 543 nm) staining.

2.9 Protein Biochemistry Techniques

2.9.1 SDS-Polyacrylamide Gel Electrophoresis

Sample buffers (62.5 mM Tris-HCl, pH 6.7, 1% (w/v) SDS, 50% (v/v) glycerol, 0.02% (w/v) Bromophenol Blue) were prepared as 1-time, 3-time and 5-time concentrates and stored at room temperature. 10% (v/v) 2-β-mercaptoethanol or 20 mM dithiothreitol (DTT) (final concentration) were added as reducing agents, at the time of use. Protein samples (except those for glucose transporter analysis) were heated at 95°C for 2-3 min. Samples for GLUT1 and GLUT4 analysis were incubated with sample buffer and reducing agents at room temperature for 20 min. One exception to this rule was the study of glucose transporters biotinylated with Bio-lc-ATB-BMPA. In this case samples were heated to 95°C to dissociate the biotin-streptavidin interaction (*Section 2.4.5.2*).

Electrophoresis was carried out using the discontinuous buffer system of Laemmli (Laemmli, 1970), with either linear slab gels formed using the Protean II XI system with 16 cm plates, or the mini-PROTEAN II electrophoresis apparatus for minigels, (both Bio-Rad). Gels were prepared according to the manufacturers instructions, using the following buffer system: acrylamide/bis-acrylamide (30% (w/v) T, 2.7% (w/v) C)(National Diagnostics, Flowgen), resolving gel buffer (1.5 M Tris-HCl, pH 8.8, 0.4% (w/v) SDS), stacking gel buffer, (0.5 M Tris-HCl, pH 6.8, 0.4% (w/v) SDS), 10% (w/v) ammonium persulphate (APS) (Bio-Rad) and N,N,N,N'-tetramethylethylenediamine (TEMED) (Bio-Rad). For both systems the resolving gels (lower gel) were made to 0.375 M Tris-HCl, pH 8.8 and 0.1% (w/v) SDS, with acrylamide concentrations in the range of 7-15%. Stacking gels (upper gel) were made to 0.125 M Tris-HCl, pH 6.8 and 0.1% (w/v) SDS with acrylamide concentration of 6%, (or 4% when using ≤ 7% resolving gel). Polymerisation was initiated by the addition of TEMED and APS, both to 0.05% (v/v) (final concentration). The electrophoresis buffer was 25 mM Tris-HCl, pH 8.3, 192 mM glycine, 0.1% (w/v) SDS. Large gels were run at constant current (25

mA through the stacking gel and 35 mA through the resolving gel for 1.5 mm gels) for approximately 6 h until the bromophenol blue tracking dye had just run off the gel or overnight at 12 - 15 mA. Minigels were run at a constant 180 V for approximately 60 min.

Molecular weight markers were either High Molecular Weight markers (HMW markers) (Sigma) consisting of myosin (205 kDa), β-galactosidase (116 kDa), phosphorylase b (97.4 kDa), bovine albumin (66 kDa), ovalbumin (45 kDa) and carbonic anhydrase (29 kDa), or Broad range Protein markers (BMW markers) (New England BioLabs) consisting of myosin (212 kDa), MBP-β-galactosidase (158 kDa), β-galactosidase (116 kDa), phosphorylase b (97 kDa), serum albumin (66 kDa), glutamic dehydrogenase (55.6 kDa), maltose binding protein 2 (42.7 kDa), lactate dehydrogenase (36.4 kDa), triose phosphate isomerase (26.6 kDa), trypsin inhibitor (20 kDa), lysozyme (14 kDa), aprotonin (6.5 kDa) and insulin A, B chain (2.3-3.4 kDa)

2.9.2 Electrophoretic Transfer of Proteins to Nitrocellulose

SDS-polyacrylamide gel electrophoresis was carried out in the conventional manner. The stacking gel was removed and the resolving gel placed in continuous Transfer buffer, (39 mM glycine, 48 mM Tris base, 0.0375% (w/v) SDS and 20% (v/v) methanol, pH 8.8). Proteins were transferred using a Multiphor II NovaBlot electrophoretic transfer unit (Pharmacia LKB Biotechnology) by the semi-dry transfer method. Briefly, nine pieces of Whatman paper (3mm) (Munktell, Pharmacia Biotech) were soaked in Transfer buffer, pH 8.8, and placed at the anode of the transfer apparatus. A nitrocellulose sheet (Gelman Sciences, 45 μM pore size) soaked in Transfer buffer, was placed on the stack, followed by the gel. The final 9 sheets of filter paper were placed on the gel and the cathode placed on top of the stack. A fixed current (equivalent to the surface area of the gel ((cm^2) x 0.8)) was applied for a period of 1 h and 50 min. After which the electric current was turned off and the gel was placed in coomassie blue stain (*Section 2.9.4*) to check that the transfer was complete. The nitrocellulose filter was rinsed in water before staining with Ponceau S (0.1% (w/v) Ponceau S in 3% (v/v) trichloroacetic acid,) for 1-2 min to visualise protein bands. The positions of the molecular weight markers were recorded.

2.9.3 Western Blotting

The nitrocellulose membrane was rinsed briefly in Transfer buffer pH 8.8 to completely re-hydrate it, then washed in Tris-buffered saline buffer (0.09% NaCl, 1M Tris-HCl, pH 7.4) containing Tween-20 at a final concentration of 0.1% (v/v) (TBS-T) to remove the Ponceau S stain. The membrane was then placed in blocking solution consisting of 5% (w/v) dried skimmed milk powder in TBS-T, and incubated with gentle rocking for 30-60 min at room temperature or overnight at 4°C. This procedure blocks non-specific binding. The nitrocellulose was rinsed in TBS-T and incubated with the primary antibody, at the required dilution, (*Table 2.1*) in TBS-T containing 1% (w/v) BSA, for 60-90 min at room temperature. After extensive washing in TBS-T, the nitrocellulose was incubated for 30 min at room temperature with the secondary antibody at the required dilution (*Table 2.2*) in blocking solution. Once again the membrane was washed extensively.

Bands were visualised using enhanced chemiluminescence (ECL) or ECL Plus as described by the manufacturers (Amersham Pharmacia Biotech), and exposed to autoradiography film (Hyperfilm™ ECL™, Amersham Pharmacia Biotech.) until an image was apparent upon developing. In experiments where protein bands were quantified by densitometry, multiple exposures of the blots were performed to ensure that the analysis was performed in the linear range of signal densities.

2.9.4 Coomassie Blue Staining

Protein bands were visualised by staining with Coomassie brilliant blue reagent (0.2% (w/v) Coomassie blue R-250 in 10% (v/v) glacial acetic acid, 30% (v/v) MeOH, 60% (v/v) dH_2O) for 1 h, followed by destaining (30% (v/v) MeOH, 10% (v/v) glacial acetic acid, 60% (v/v) distilled H_2O). The gels were dried at room temperature between two layers of Biotrace membrane presoaked in destaining solution containing 8.7% (v/v) glycerol.

2.9.5 BCA Protein Determination

Protein concentrations were determined by the Pierce bicinchoninic (BCA) method of protein determination. The standard curve was made with 1-10 μg of BSA solution (1

mg/ml stock in 0.1 M NaOH) in 10 µl of 0.1 M NaOH prepared in a Microtitre plate (Labsystems, Helsinki, Finland). Reagent A (1% BCA-NO_2, 2% $NaCO_3.H_2O$, 0.16% Na_2tartarate, 0.4% NaOH, 0.95% $NaHCO_3$) and Reagent B (4% (w/v) $CuSO_4.5H_2O$) were mixed in the ratio 50:1 and 200 µl of this working solution was added to each of the standards, and to the samples. The plate was incubated at 37°C for 20 - 30 min or until sufficient colour development was apparent. The plate was read at 595 nm in a microplate spectrophotometer.

2.9.6 Data Analysis

Graphical data was plotted using GraphPad PRISM *version 3.0*, (GraphPad Software, Inc.,). Statistical analysis was carried out using the PRISM programme with paired one- and two- tailed t tests as indicated in the *figure legends*. Densometric analysis was performed using Molecular Analyst^{TM}/PC *version 1.5*, (Bio-Rad Laboratories).

3.0 Development of an Isolation Protocol for the Preparation of Insulin Sensitive Cardiac Myocytes

Studies of cells in suspension offer a number of advantages over whole organ experiments. In particular vascular factors are eliminated, cells are subject to homogenous environmental conditions and manipulation and control of the experimental conditions is facilitated. A plethora of methods has been available for isolating cardiomyocytes for many years. However most of these methods are hindered by the inability of isolated myocytes to remain viable in buffers containing physiological concentrations of Ca^{2+}. Moreover the study of glucose transport in functionally intact cardiomyocytes, as in adipocytes, is complicated by their sensitivity to the actions of unspecific factors during the isolation procedure and subsequent manipulation (Fischer *et al.*, 1991).

Most studies of glucose transport in isolated cardiomyocytes have reported an insulin-stimulated increase in glucose transport of 1.5 to 3-fold over control values (Lindgren *et al.*, 1982; Eckel *et al.*, 1983; Chen *et al.*, 1985; Shanahan *et al.*, 1986). However this hormone stimulates the rate of glucose transport in perfused rat heart by 6 to 8-fold (Zaninetti *et al.*, 1988). Moreover in skeletal muscle preparations and in adipocytes isolated under carefully controlled conditions insulin has been shown to stimulate glucose transport by up to 20- and 40-fold respectively (Whitesell and Abumrad, 1985; Zorzano *et al.*, 1986; Ploug *et al.*, 1987; Okuno and Gliemann, 1987). To date, only two methods have been published which claim to yield cardiomyocytes which are highly responsive to insulin (Haworth *et al.*, 1984; Fischer *et al.*, 1991). Using these methods as a starting point, a cardiomyocyte isolation procedure was set up in our laboratory.

Myocytes are the cells most commonly isolated from the adult heart, in which they comprise approximately 20% of the total cell number and 80% of the total cell mass (Jacobson and Piper, 1986). Ventricular cardiomyocytes can be identified by their elongated shape, cross-striations and mass of myofilaments. These cells tend to be irregular in shape with many branched protrusions and typically exhibit a rod-like morphology (*Figure 3.1A, green arrow*). Cells which do not survive the isolation procedure 'round up' and lose their structural integrity (*Figure 3.1A, blue arrows*). At

Figure 3.1 Isolation of Rod-Shaped Cardiomyocytes. Cardiomyocytes were isolated using a procedure originally described by Fischer and colleagues (Fischer *et al.*, 1991), with some further modifications. Following rapid removal, the heart was perfused with a KRH buffer to wash out blood and metabolites from the chambers. The perfusion buffer was then switched to one containing collagenase and hyaluronidase to digest the tissue. Following a period of perfusion, the heart was removed from the apparatus and further digestion was carried out in a waterbath. A. Viable cells display a rod-shaped morphology (indicated by the green arrow), while dead cells 'round up' (indicated by the blue arrows). B. A magnified view of a single cardiomyocyte (x 40), showing complex striations and irregular shape.

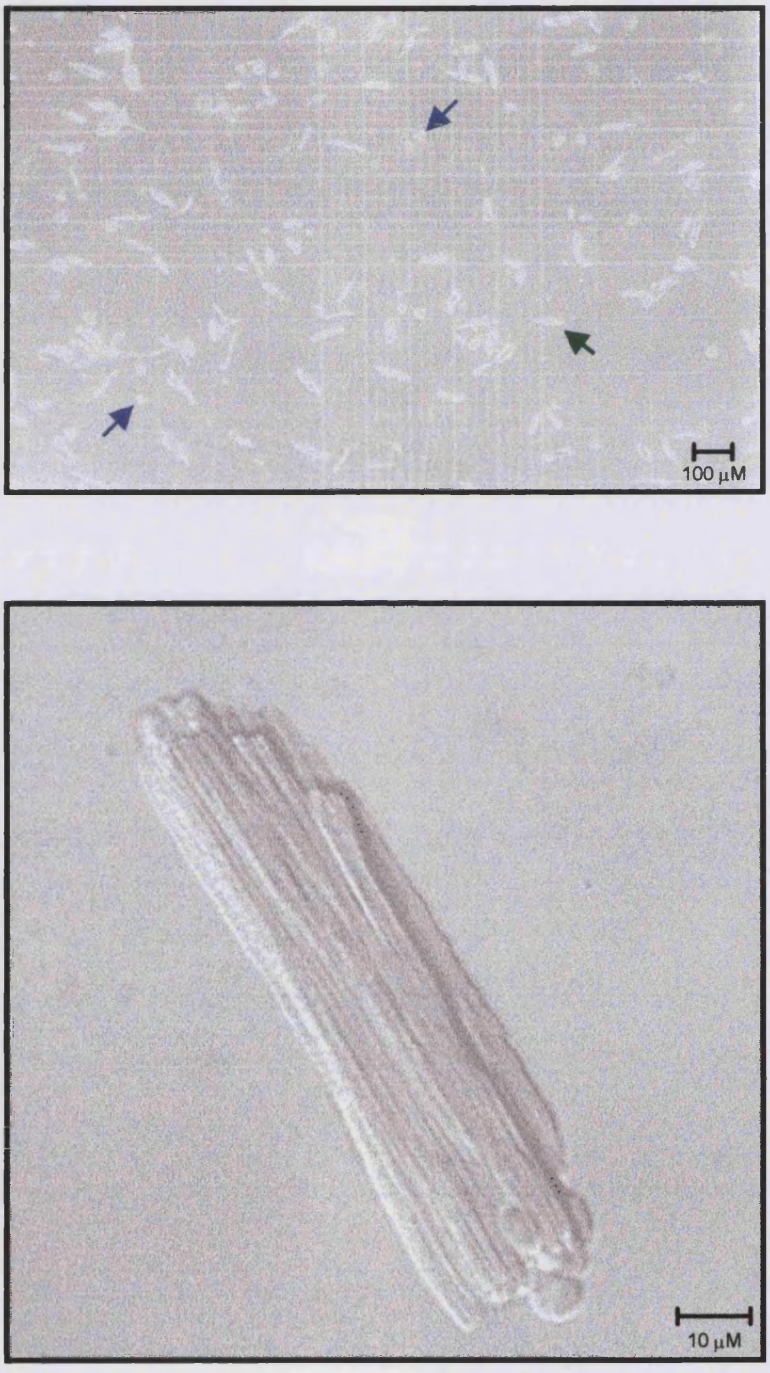

high magnification the irregularity of a typical cardiomyocyte can be clearly seen (*Figure 3.1B)*. In this figure parts of the myocyte appears blurred, being out of the focal plane, while other regions have a sharp distinct appearance. Myocytes isolated from rat heart are usually binucleate, although a single nucleus is seen in approximately 20% of cells and this is strain and species specific. Heart muscle cells range in length from 35 to 130 μM and in width from 12 to 30 μM, although cells as wide as 90 μM have been documented (reviewed in Dow *et al.*, 1981).

3.1 Testing Conditions Required for Efficient Insulin-Stimulated Glucose Transport

In order to isolate a population of viable, insulin sensitive cardiomyocytes, a number of variables were examined in detail, and shall be discussed here. The basic isolation protocol consisted of washing the blood and metabolites from the heart by retrograde perfusion via the aorta (with Buffer A) as originally described over 100 years ago (Langendorff, 1895) (*Figure 3.2*). The heart was then exposed to a perfusion buffer containing proteolytic enzymes (Buffer B). Once the tissue was soft it was removed from the catheter and treated mechanically (in Buffers B and C) to disperse the cells. This method results in the isolation of a larger number of cells that immersing small chunks of myocardial tissue directly into the dissociating buffer (Piper *et al.*, 1990). The cells were then washed in Buffers D and E to remove proteolytic enzymes and non-viable cells. The viability of the preparation was assessed by examining the numbers of rod-shaped (living) versus spherical (dead) myocytes by light microscopy. This simple test has been suggested to be more reliable than the exclusion of dyes such as trypan blue in adult ventricular myocytes (Nag *et al.*, 1983; Cheung *et al.*, 1985).

(i) Choice of Collagenase

Bacterial collagenase is common to nearly all methods of cell isolation (Dow *et al.*, 1981). Interestingly crude collagenase is more effective than the purified enzyme in digesting heart tissue indicating that a combination of collagenases (e.g. collagenase A-α and collagenase B-α) and contaminating proteolytic enzymes are required. These proteolytic enzymes are responsible for cleaving the external connections that hold the cardiomyocytes together, however they may also damage the cell themselves. Therefore the use of such reagents should be minimised, being just long enough to

permit digestion of the extracellular matrix, but not so long as to damage the cell itself. Since optimal combinations of proteolytic enzymes have yet to be described, commercially available crude enzyme preparations were tested for yield and viability of isolated myocytes. However the isolation of large numbers of myocytes was not the only criteria tested, as trace elements in crude collagenase preparations, such as metals and trypsin can stimulate basal levels of glucose transport (Fischer *et al.*, 1991). As such, batches were tested for their suitability with respect to insulin stimulation of glucose transport in isolated myocytes, as well as to the speed of the digestion and the yield of myocytes obtained.

(ii) Duration of the Isolation Procedure and Minimising Temperature Changes

A quick preparation is required to minimise the time when oxygen and substrate supplies are interrupted. However during the perfusion step itself a normal supply of oxygen and substrates cannot be maintained. This is because the microvascular bed is rapidly dissolved, abolishing the normal microcirculation. Thus tissue dissociation should be as rapid as possible. A tail vein injection of heparin was found to markedly improve the success rate of the cellular isolation and improved the insulin: control ratio, presumably as a result of its ability to inhibit blood clot formation and therefore to prevent anoxia/ischemia within the heart chambers. The heparin injection also aided the speed of the digestion, decreasing the time when energy supplies were limited.

During the isolation procedure and subsequently, care was taken to avoid changes in temperature which are known to increase the basal rate of glucose transport in rat adipocytes (Whitesell and Abumrad, 1985; Okuno and Gliemann, 1987). Thermal equilibration of the perfusate buffer at 37°C was assured by a water-jacketed delivery system. The mounted heart was also encased in a water jacket maintained at 37°C (*Figure 3.2*).

Figure 3.2 Schematic Diagram of a Heart Perfusion Apparatus. Buffer is gassed with oxygen and circulated via a peristaltic pump through a perfusion chamber where it is warmed to 37°C. The buffer then enters the heart which is mounted on a catheter and surrounded by a 37°C water jacket. Digestion of the heart is monitored by changes in pressure measured using a mercury-based pressure gauge.

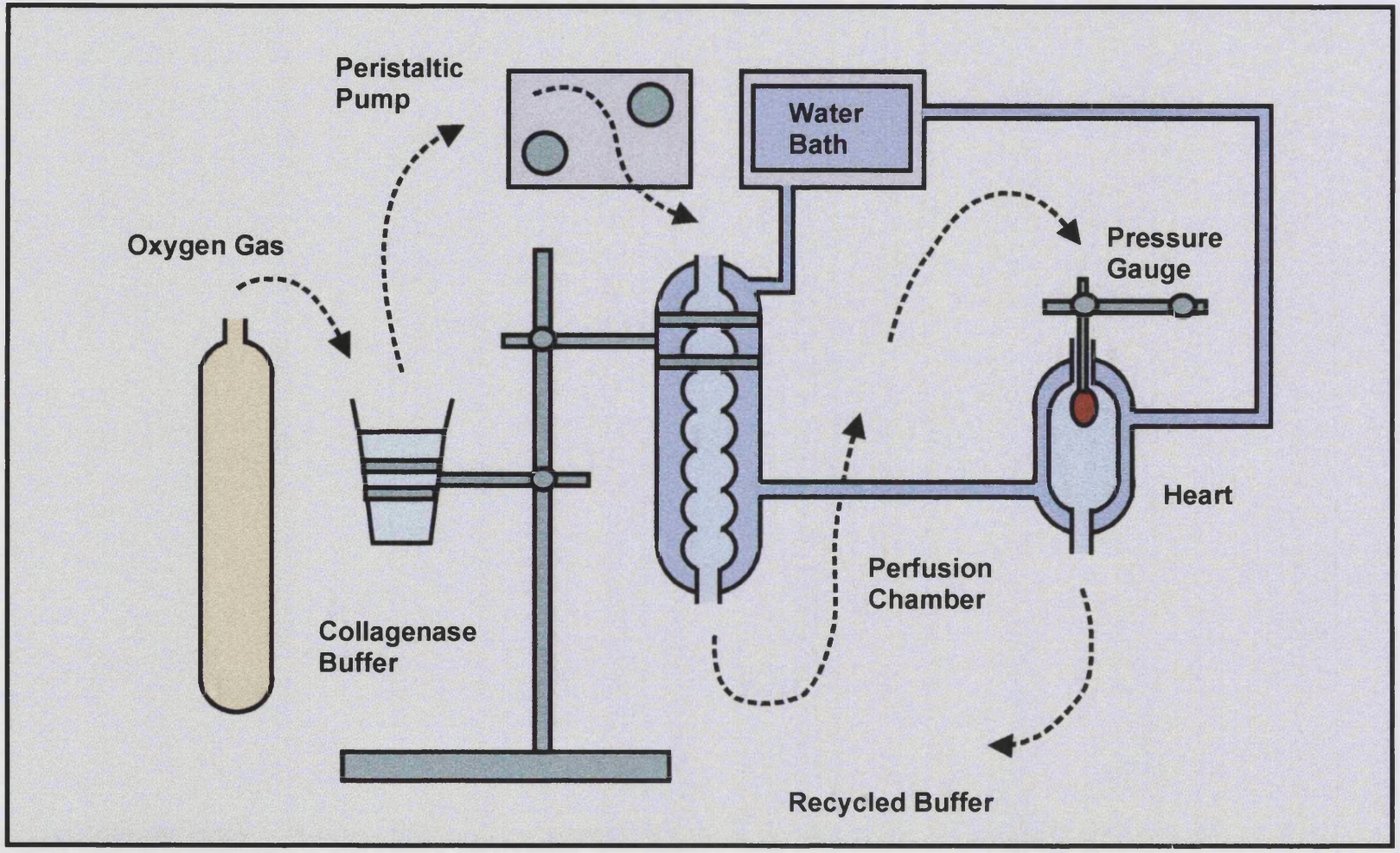

(iii) The Re-introduction of Calcium (The Calcium Paradox)

Cell cohesion depends upon the presence of calcium. Therefore during the isolation of myocytes it is necessary to remove almost all of the perfusate calcium in order to cause cell separation. However when physiological concentrations of calcium are re-introduced the cells are intolerant, and round up. This is known as the 'calcium paradox'. A number of factors have been proposed to be responsible for this. These include transient leaking from the sarcolemma, low Ca^{2+} in the perfusate that favours hyperpermeability and ischemic conditions which may reduce the activity of sarcolemmal ion pumps (Piper *et al.*, 1990). These conditions lead to an increase in the intracellular Na^{+} concentration during the perfusion. Upon re-addition of Ca^{2+}, Na^{+}/Ca^{2+} exchange leads to rapid Ca^{2+} overload and this inhibits relaxation processes that are normally initiated when Ca^{2+} dissociates from troponin binding sites. This in turn leads to hypercontracture and deterioration of the cells (Altschuld *et al.*, 1980; Haworth *et al.*, 1982), due to separation of the intercalated discs and of the basement membrane and plasma membrane components of the sarcolemma. Such gross loss of cellular architecture explains the irreversibly of the paradox.

In order to avoid the calcium paradox traces of calcium must remain in the perfusion buffer, and the buffer and cells should be kept warm in order to promote the efflux of intracellular Na^{+}. Usually there is no need to add addition Ca^{2+} to the perfusate buffer as some calcium is already present. This Ca^{2+} comes from endogenous Ca^{2+}, Ca^{2+} in the collagenase, Ca^{2+} in the albumin and in the salts. Potassium is also required in the perfusate to ensure recovery from the calcium paradox, (consistent with the observation that hypokalemia produces myofibrillar contractions and the appearance of myofibrillar insertion plaques at the intercalated discs (Emberson and Muir, 1969)). In addition magnesium can protect against contracture and sustain the phosphocreatine concentration (Dow *et al.*, 1981).

Early restoration of Ca^{2+} is beneficial. Haworth and colleagues found that addition of Ca^{2+} to the recirculating perfusate after 10 min of Ca^{2+}-free perfusion had no effect on cell mortality and resulted in the isolation of a higher number of Ca^{2+}-tolerant cells (Haworth *et al.*, 1989). Therefore a stepwise re-calcification was performed, beginning at a relatively early stage of the perfusion (after approximately 15 min of tissue digestion).

Cells which become hyperpermeable or 'leaky' may contract spontaneously due to the flow of ions across the damaged sarcolemma (Dani *et al.*, 1979). This contraction has a phasic property passing down the cells in a wave-like manner (Reiser *et al.*, 1979), in contrast to the beat induced by electrical stimulation which is characterised by synchronous, uniform sarcomere shortening (Krueger and Wittenberg, 1979). The myocytes prepared using our isolation protocol do not beat spontaneously even in the presence of 1 mM Ca^{2+}. However they can be induced to contract by stimulation in an electrical field (*Section 3.4*). This indicates the presence of a membrane potential in the quiescent state, and demonstrates that the cells are viable and intact.

(iv) Use of BDM

2,3-butanedione monoxime (BDM) is a nucleophilic agent which has been used as a component of cardioplegic solutions (Mulieri *et al.*, 1989). It possesses a 'phosphatase-like' activity and induces a rapid, dose-dependent and reversible abolition of the cytosolic continuity existing between cells via gap junctional channels (Verrecchia and Herve, 1997). Furthermore BDM has been shown to inhibit Ca^{2+} (Coulombe *et al.*, 1990), Na^{+} (Sada *et al.*, 1985) and K^{+} (Lopatin and Nichols, 1992) currents. Indeed treatment of frog skeletal muscle with BDM causes the release of Ca^{2+} from the sarcoplasmic reticulum (Horiuti *et al.*, 1988). The actions of BDM may be through the dephosphorylation of cellular phosphoproteins such as ion channels and connexins at gap junctions. Thus BDM may protect against the calcium paradox by inhibiting ion channels during the isolation procedure. Therefore consistent with the method of Fischer and colleagues (Fischer *et al.*, 1991), BDM was added to Buffers B and C.

(v) Choice of Albumin (Use of Fatty Acid Free BSA)

Some albumin batches are harmful to cells and others stimulate basal glucose transport in myocytes (Fischer *et al.*, 1991). This is consistent with observations made in rat adipocytes (Okuno and Gliemann, 1987). Thus albumin batches were tested for their suitability to isolate insulin-responsive adipocytes and these batches were used in Buffers B to D for the isolation of cardiomyocytes. A further complication in choosing an albumin batch for use in the isolation of insulin-responsive cardiomyocytes is that free fatty acids found in albumin preparations can acutely inhibit glucose utilisation in cardiac muscle *in vivo* (Jenkins *et al.*, 1988). Minimal basal transport rates have been reported in the presence of fatty acid free bovine serum albumin from Boehringer

(Fischer *et al.*, 1991). However due to the expense of this reagent it was used in the final buffers only (Buffers E and F), in which cells were allowed to recover following the isolation procedure and in which glucose transport assays were performed.

Initial experiments were performed as closely as possible to the method described by Fischer and co-workers (Fischer *et al.*, 1991) with some small modifications due to the lack of facilities. For example, instead of an orbital shaker, cells were dispersed in a shaking water bath in glass vials connected directly to an oxygen supply by means of small blunt-ended needles. Following isolation cells were allowed to recover from the procedure for 30 min at 37°C. The cells were then washed once in Buffer F (which did not contain glucose or pyruvate), then either left untreated (basal) or treated with 30 nM insulin for 30 min at 37°C. Following this incubation 100 μM 2-deoxy-D-glucose plus a tracer of 2-deoxy-D-[^{3}H]-glucose was added to the cells and glucose uptake was measured over a period of 10 min. Glucose transport was terminated by the addition of phloretin. In early experiments only a small increase in the insulin:basal ratio was observed (*Figure 3.3A, blue panels*). Many of the cells appeared round, and the yield of myocytes was relatively low being of the order of 2 x 10^6 cells.

3.1.1 The Effects of Trypsin

It has been reported that cells are more tolerant to Ca^{2+} when trypsin is added during the final stages of tissue digestion (Haworth *et al.*, 1989). Several reasons have been reported to explain this observation. Firstly, the number of damaged cells can be reduced by the addition of trypsin since damaged cells are more quickly digested than intact cells. Secondly it has been shown that the gap junctions of Ca^{2+}-susceptible cells often retain shreds of junctional regions from the cells with which it was formerly contiguous (Fry *et al.*, 1979). These unseparated gap junctions, which are exposed to the external buffer, may be sites of Ca^{2+} entry. Thus trypsin may remove these membrane shreds enabling gap junctions to close. Thirdly and as already mentioned Ca^{2+} susceptibility may be due to a high concentration of internal Na^+ which gives rise to a high rate of Ca^{2+} uptake following its re-introduction (Altschuld *et al.*, 1980). Addition of trypsin at the same time as Ca^{2+} has been shown to aid in the retention of K^+ (Haworth *et al.*, 1982). Furthermore leaking of Na^+ and K^+ is at a much lower rate in trypsin treated cells than in untreated cells (Haworth *et al.*, 1982). Thus it has been suggested that the levels of intracellular Na^+ in trypsin-treated cells are lower than those

in control cells (Haworth *et al.*, 1982) and this results in the isolation of a greater number of 'calcium-tolerant' cells.

In order to ascertain whether the loss of cell viability in early cell isolations was due to the calcium paradox, trypsin was added to Buffer C at a concentration of 2 mg/ml. Since tryptic digestion of insulin receptors has been reported (Eckel, 1989), the cells were only incubated with the enzyme for a short period before the reaction was terminated by the addition of Buffer D containing 10 μg/ml trypsin inhibitor. Following isolation the cells were again incubated at 37°C for 30 min, before glucose uptake was determined using 2-deoxy-D-glucose (*Figure 3.3A, yellow panels*). Trypsin increased the yield and calcium tolerance of the myocytes but also increased the basal glucose transport. This is consistent with earlier findings (Haworth *et al.*, 1984).

3.1.2 The Effects of Hyaluronidase and DNAse

Hyaluronidase has been used by a number of authors in combination with collagenase to aid the digestion of cardiac tissue (Haworth *et al.*, 1982; Jacobson and Piper, 1986). This raises the possibility that N-acetylglucosamine-glucuronic acid polymers are major inter-myocyte molecules. Thus hyaluronidase was added to the dissociating buffer (Buffer B). Addition of hyaluronidase resulted in a marked increase in the number of cells isolated (6-8 $x10^6$ cells/heart). This increase in cell number was probably due to a decrease in the time of the perfusion and hence a decrease in the time in which substrates and oxygen are limited. However some batches of cells appeared 'sticky' and rapidly formed clusters. This made them difficult to handle in suspension. This 'stickiness' was due to the release of DNA from damaged cells. Thus the cells were incubated with deoxyribonuclease (DNAse), which prevented the clumping from occurring. The combination of hyaluronidase and DNAse decreased the need for excessive mechanical agitation to fully disperse the cells. The decreased mechanical stimulation and the rapid perfusion of the heart resulted in an increase in insulin-stimulated glucose transport to a level which was approximately 1.9-fold higher than control values (*Figure 3.3B, red panels*).

Figure 3.3 The Effects of Trypsin, DNAse and Hyaluronidase on Insulin-Stimulated Glucose Transport in Cardiomyocytes. Cardiomyocytes were prepared as described in *Sections 3.1.1 and 3.1.2.* Following isolation, cells were allowed to recover from the procedure by incubation at 37°C for 30 min with continuous O_2 gassing. Cells were then stimulated with 30 nM insulin for 30 min at 37°C or were left untreated (basal). 2-Deoxy-D-[^{3}H]-glucose uptake was performed as described in *Methods 2.4.2.*

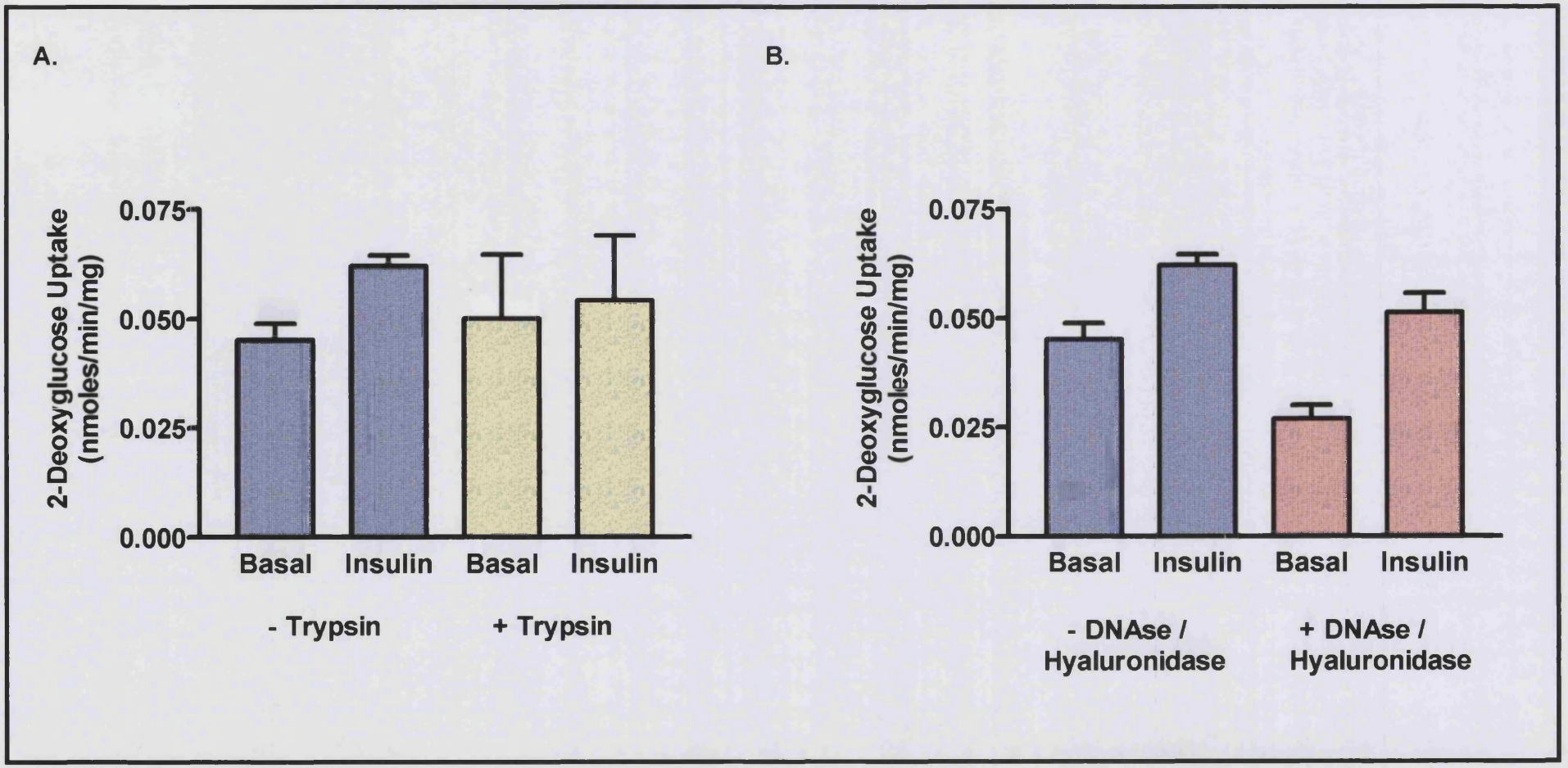

3.1.3 Centrifugation

A small decrease in the level of mechanical agitation appeared to increase the viability of the myocytes and increase their susceptibility to insulin, consistent with earlier findings in rat adipocytes (Whitesell and Abumrad, 1985; Okuno and Gliemann, 1987). Thus all steps which involved a level of mechanical stimulation were examined and it was decided to attempt to eliminate all centrifugation steps from the isolation protocol. One difficulty caused by the removal of the centrifugation steps was how to enrich the myocyte preparation with rod-shaped cells and remove dead myocytes. The study of cell responses to regulatory processes such as insulin stimulation can be severely complicated by the presence of damaged cells in the preparation, which distort the results. The enrichment of rod-shaped cells was achieved by the addition of a series of steps in which the cells were allowed to settle by gravity through an albumin-rich buffer (Buffers D and E). The dead cells that remained floating were aspirated and the remaining cells were resuspended. 70-80% of the cells isolated using this method were rod-shaped. Furthermore insulin-stimulated glucose transport measured by the uptake of 2-deoxy-D-glucose was increased to 4.1-fold over unstimulated controls (*Figure 3.4A, green panels*).

3.1.4 The Effects of Inosine

In order to ensure that the levels of intracellular ATP were maintained during the isolation procedure, inosine was added to all of the buffers as an alternative energy source. This reagent has been previously used as an energy substitute in models of insulin resistance in cell culture (Hresko *et al.*, 1998). The use of inosine resulted in an increase in cell viability and 'robustness'. Measurements of insulin-stimulated glucose transport in myocytes isolated in the presence of inosine revealed an increase in glucose uptake of 11.2-fold over basal controls (*Figure 3.4B purple panels*).

The results of the 2-deoxy-D-glucose transport assays are shown in Table 3.1. It is clear from this data that the increases in glucose transport in insulin-stimulated cells over unstimulated controls are due entirely to a reduction in the levels of basal transport. No change in the level of insulin stimulation was achieved, consistent with earlier studies in cardiomyocytes (Fischer *et al.*, 1991).

Figure 3.4 The Effects of Centrifugation and Inosine on Insulin-Stimulated Glucose Transport in Cardiomyocyte. Cardiomyocytes were prepared as described in *Sections 3.1.3 and 3.1.4*. Following isolation, cells were allowed to recover from the procedure by incubation at 37°C for 30 min with continuous O_2 gassing. Cells were then stimulated with 30 nM insulin for 30 min at 37°C or were left untreated (basal). 2-Deoxy-D-[^{3}H]-glucose uptake was performed as described in *Methods 2.4.2*.

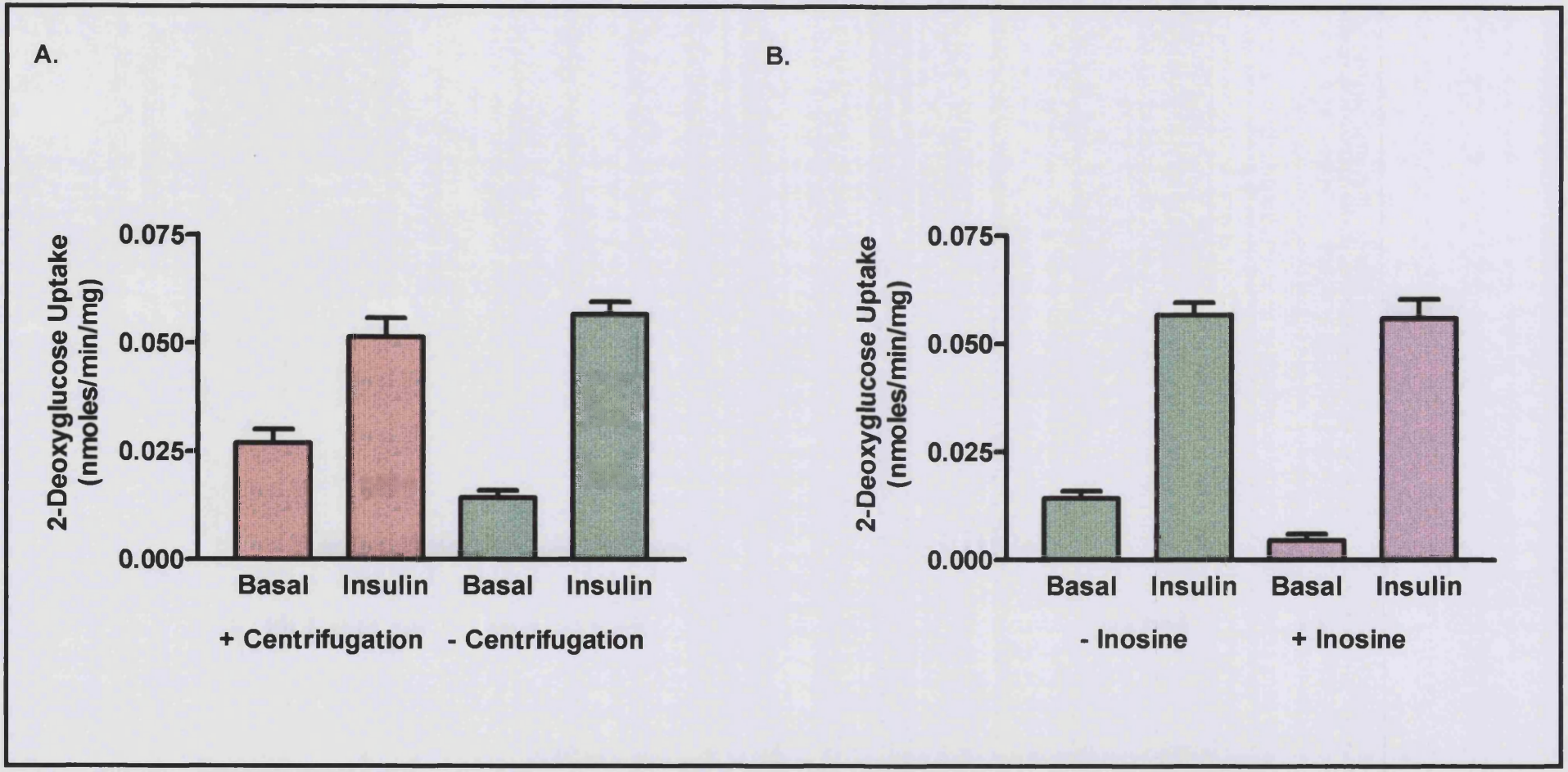

Table 3.1 Insulin-Induced Increases in Glucose Transport in Isolated Cardiomyocytes: Comparison of Different Methods.

Condition	Basal (nmoles/min/mg)		Insulin (nmoles/min/mg)		Insulin:Control Ratio
	Mean	s.e.m.	Mean	s.e.m.	
No additions	0.045	0.004	0.062	0.003	1.4
Trypsin	0.050	0.015	0.054	0.014	1.1
DNAse/ Hyaluronidase	0.027	0.003	0.051	0.005	1.9
No Centrifugation	0.014	0.002	0.057	0.002	4.1
Inosine	0.005	0.002	0.056	0.005	11.2

3.1.5 Insulin-Stimulated Glucose Transport is Linear and is Sensitive to Cytochalasin B

Cytochalasin B is a potent inhibitor of glucose transport (Lindgren *et al.*, 1982). Since it is hydrophobic (*Figure 3.5A, top panel*) it can pass through the plasma membrane interacting with the endofacial glucose binding sites of transporters both at the cell surface and within the cell. Cytochalasin B is therefore a useful reagent for assessing the concentration of 2-deoxy-D-glucose that is taken up into cells in a non-specific manner. Thus following isolation, cells were either left untreated (basal), or treated with 30 nM insulin for 30 min. Prior to the addition of the 2-deoxy-D-glucose, the cells were split into aliquots and some were treated with 10 μM cytochalasin B for 5 min. 2-Deoxy-D-glucose transport was then measured over a period of 30 min.

Cytochalasin B inhibited both basal and insulin-stimulated glucose transport. The rate of transport in cytochalasin B-treated cells was equivalent to approximately 30% of the rate of transport in basal cells (*Figure 3.5A*). The level of 2-deoxy-D-glucose transport, when the non-specific uptake of sugar was considered, is shown in *Figure 3.5B*. These experiments also showed that glucose transport is linear in cells obtained by this

Figure 3.5. The Effect of Cytochalasin B on Basal and Insulin Stimulated Glucose Transport in Cardiomyocytes. Cardiomyocytes were prepared as described in *Methods 2.2.3*. Following isolation, cells were allowed to recover from the isolation procedure by incubation at 37°C for 30 min with continuous O_2 gassing. Cells were then stimulated with 30 nM insulin for 30 min at 37°C or were left untreated (basal). The cells were then split into two aliquots and one aliquot from each condition was treated with 10 μM cytochalasin B for 5 min before the addition of 2-Deoxy-D-[^{3}H]-glucose. 2-Deoxy-D-[^{3}H]-glucose uptake was performed as described in *Methods 2.4.2*. A. Transport data from all four condition namely basal (●), insulin (●), basal + cytochalasin B (●) and insulin + cytochalasin B (●). B. Shows the same data but with the cytochalasin B data subtracted from the respective basal (●) and insulin (●) samples. The structure of cytochalasin B is shown in the grey panel.

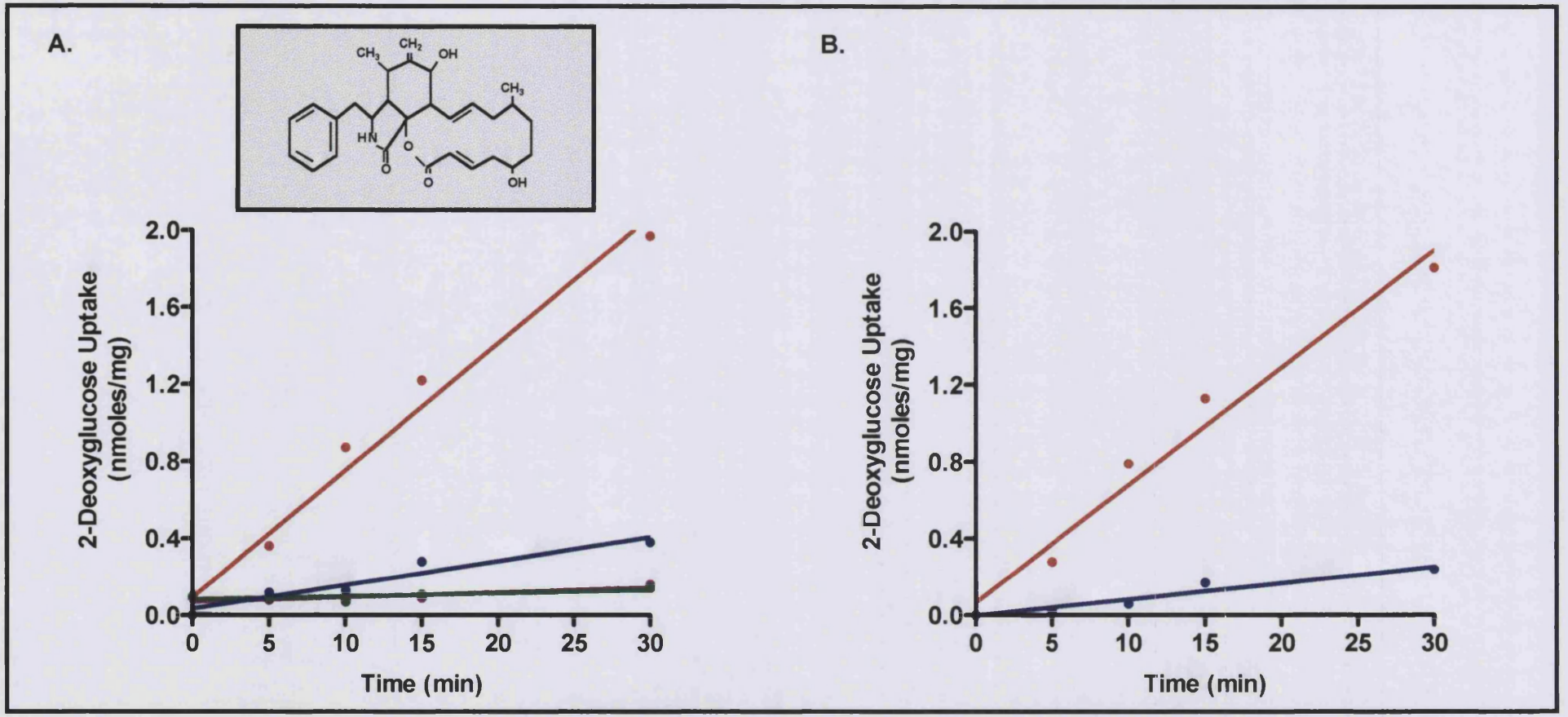

modified isolation procedure (without inosine) over a period of at least 30 min (*Figure 3.5*).

3.2 Photolabelling Cardiomyocytes with Bis-Mannose Photolabels

3.2.1 The Use of ATB-[^{3}H]-BMPA

Since its first report, ATB-[^{3}H]-BMPA (*Figure 3.6A, top panel*) has been used extensively to study the properties of glucose transporter isoforms. The photolabel displays a high affinity for the erythrocyte glucose transporter GLUT1 (with a K_i of approximately 300 μM) as well as for the insulin sensitive isoform GLUT4 (the K_i for basal and insulin-stimulated glucose transport in rat adipocytes is 247 μM) (Holman *et al.*, 1990). Furthermore, the photolabel is cell impermeant and therefore only labels cell surface glucose transporters.

To assess whether the changes induced by insulin on glucose transport were due to changes in the levels of glucose transporters at the plasma membrane, cells (isolated in the absence of inosine) were transferred to petri-dishes and mixed with 18.5 MBq of ATB-[^{3}H]-BMPA (the final concentration of the label was 100 μM). The cells were then irradiated for 3 min in a photoreactor with 350 nm lamps, then washed to remove unbound tritiated label, solubilised in a detergent buffer and subjected to isoform specific antibody immunoprecipitation with antibodies against GLUT1 and GLUT4. The precipitates were resolved by SDS-PAGE, and the gel was sliced into 0.66 cm slices. The slices were dried and solubilised in a solution composed of H_2O_2 and NH_3 at 80°C. The solubilised gel slices were allowed to cool, then scintillant was added and the radioactivity was determined using a scintillation counter.

Using this method a single broad peak was observed at approximately 45 kDa for both GLUT1 (*Figure 3.6A*) and GLUT4 (*Figure 3.6B*). These peaks could be abolished by the addition of 500 mM D-glucose with the photolabel (data not shown) and were therefore determined to represent GLUT1 and GLUT4 protein labelled at the cell surface. As expected, upon insulin stimulation an increase in the incorporation of the photolabel was observed, suggesting an increase in glucose transporters at the cell surface. The insulin-stimulated translocation of GLUT1 and GLUT4 to the cell surface was approximately 2-fold and 3.5-fold respectively (*Figure 3.6*).

Figure 3.6 Photolabelling Cardiomyocytes with ATB-[^{3}H]-BMPA. Cardiomyocytes were prepared as described in *Methods 2.2.3.* Following isolation the cells were either left untreated (●) or treated with 30 nM insulin (●) for 30 min at 37°C. Cells were then transferred to petri-dishes and photolabelled with 18.5 Mbq ATB-[^{3}H]-BMPA. Cells were washed and solubilised in a Thesit detergent buffer. Following solubilisation glucose transporters were immunoprecipitated on protein A sepharose beads coupled with either anti-GLUT1 antibodies (A) or anti-GLUT4 antibodies (B). The precipitates were washed, eluted and resolved by SDS-PAGE. The resulting gel was dried, sliced and solubilised in a H_2O_2/NH_3 solubilisation buffer. Liquid scintillant was added and the radioactivity was counted in a Packard 1600 TR scintillation counter. The structure of ATB-BMPA is shown in the grey panel.

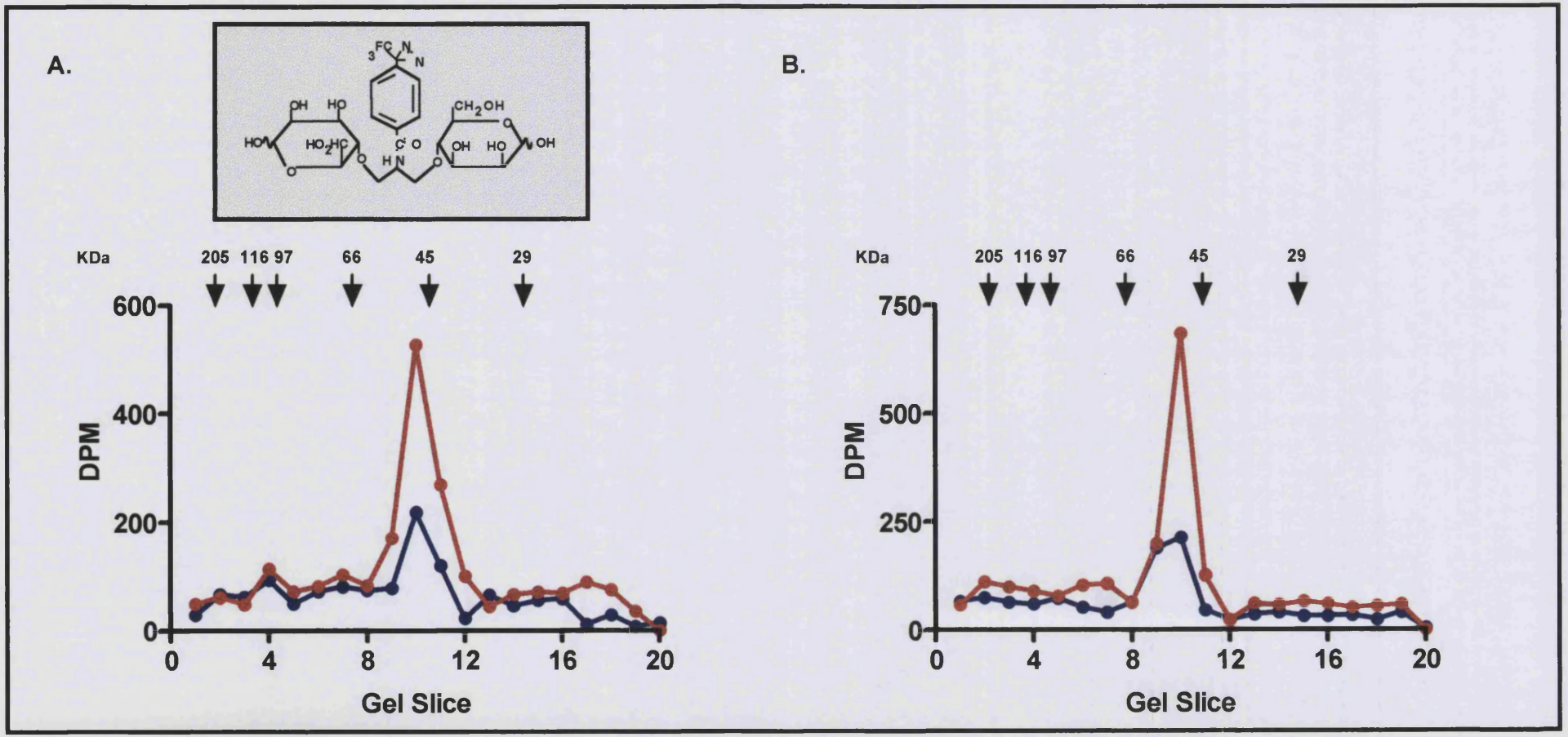

3.2.2 The Use of Bio-lc-ATB-BMPA

One of the disadvantages of the original bis-mannose derivatives is their dependence on radioactivity as the mode of detection. A problem associated with this is that despite the efficiency of the photolabel to crosslink to the transporter, (approaching 100%), only a small fraction of the total label added to a solution occupies the binding site (this is because of the relatively low affinity of the hexose analogues for the binding site). Therefore, large quantities of tritiated compound have to be added to solutions and extensive washings of cells and membranes have to be performed in order to reduce the background radioactivity. Thus new cell-impermeant bis-mannose photolabels have now been developed with biotinyl groups attached to ATB-BMPA by a hexanoic acid spacer (Bio-lc-ATB-BMPA) (*Figure 3.7A*). The K_i value for the inhibition of glucose transport activity in insulin-stimulated rat adipocytes using the new photolabel is very similar to that previously reported for ATB-[^{3}H]-BMPA, being 273 ± 28 μM (Koumanov *et al.*, 1998).

Thus photolabelling of cardiomyocytes (isolated with inosine) was performed exactly as described for the ATB-[^{3}H]-BMPA photolabel, except that the final concentration of the label was 500 μM and a 50:50 mixture of 350 nm and 300 nm lamps were used for 1 min. Following UV irradiation-induced cross-linking, the biotinylated glucose transporters were detected utilising the interaction of the biotin moiety for streptavidin molecules. Thus myocytes were solubilised in a detergent buffer and biotinylated transporters were precipitated on streptavidin beads. The resulting precipitates were analysed by SDS-PAGE and Western blotting with antibodies against GLUT4. An aliquot of cells irradiated without photolabel (unlabelled), solubilised and precipitated on streptavidin beads was run as a control. No bands were detected in this lane of the Western blot (*Figure 3.7A*). In contrast a single band migrating just above the 45 kDa marker was observed in both the basal and insulin-stimulated cardiomyocyte samples which had been photolabelled. Insulin increased the level of cell surface GLUT4 by approximately 5.4-fold as judged by densitometry (*Figure 3.7B*).

Figure 3.7 Photolabelling Cell Surface GLUT4 in Cardiomyocytes using Bio-lc-ATB-BMPA. Cardiomyocytes were prepared as described in *Methods 2.2.3*. Following isolation cells were either left untreated (B) or treated with 30 nM insulin for 30 min (I). Cells were transferred to petri-dished and photolabelled with 500 μM Bio-lc-ATB-BMPA (shown in A, top panel). Some cells were irradiated without photolabel (U). Cells were washed and solubilised in Thesit detergent buffer. Following solubilisation, biotinylated glucose transporters were precipitated on streptavidin beads. The precipitates were washed, eluted and resolved by SDS-PAGE. The resulting gel was transferred to nitrocellulose and Western blotted with antibodies against GLUT4 (A). The Western blot was analysed by densitometry, shown in B.

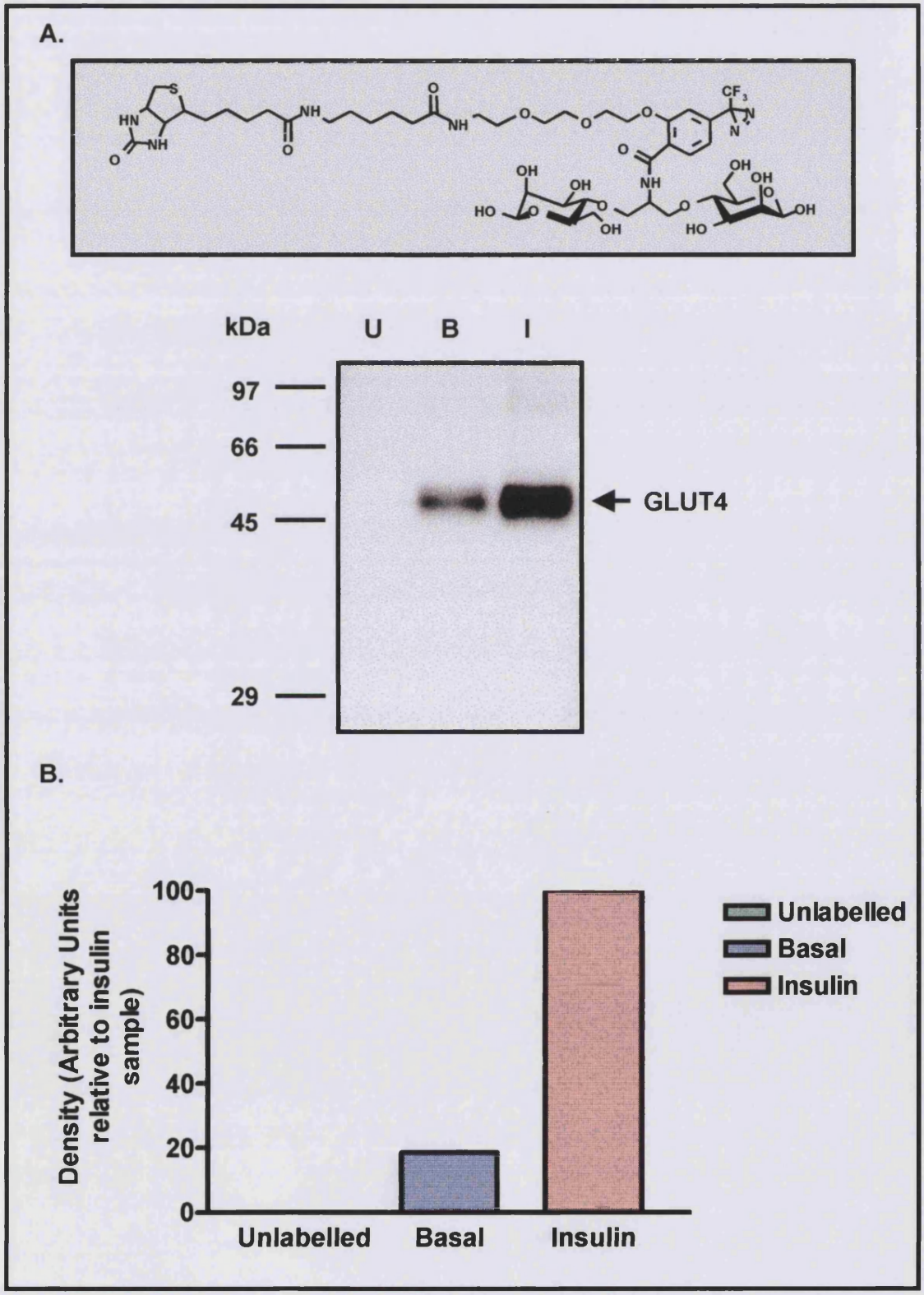

3.3 Confocal Microscopy of Basal and Insulin-Stimulated Cardiomyocytes

An immunocytochemical analysis of GLUT4 in cardiac myocytes was also performed. Cells were either left untreated or treated with 30 nM insulin for 30 min at 37°C. Cardiomyocytes were then fixed by incubation in 4% paraformaldehyde, followed by permeabilisation with 0.1% saponin. Cells were incubated with monoclonal mouse anti-GLUT4 antibodies for 1.5 h, then washed extensively before incubation with rhodamine-conjugated anti-mouse antibodies. Following this incubation the cells were washed again, mounted and viewed using a Zeiss laser scanning microscope.

As expected GLUT4 in basal unstimulated cells was predominantly intracellular (*Figure 3.8A*). The fluorescent pattern was particularly intense around the perinuclear region (indicated by the arrow), which probably represents the *trans*-Golgi network, or an endosomal sorting station. In addition, the pattern of GLUT4 staining was striated which may indicate that the transporters are bound to some sort of myofibril scaffold. Treatment of cells with insulin, resulted in a marked translocation of immunoreactive GLUT4 to the cell surface and periphery (*Figure 3.8C*), with a loss of labelling from around the nucleus. These results were confirmed using a different set of primary antibodies directed against the C-terminus of GLUT4. In this case the secondary antibodies were labelled with fluorescein (*Figure 3.8B and D*).

3.4 Contraction-Stimulated Glucose Transport in Cardiomyocytes

Stimulation of GLUT4 translocation to the plasma membrane of skeletal muscles has been suggested to occur by two mechanisms, one activated by insulin and insulin-like factors and the other activated by contraction and hypoxia (Hayashi *et al.*, 1997). When these two pathways are stimulated simultaneously glucose transport and GLUT4 translocation are increased in an additive manner (Lund *et al.*, 1995). Insulin-stimulated glucose transport appears to be mediated at least in part by PI 3-kinase because it is inhibited by wortmannin (Clarke *et al.*, 1994). In contrast, contractile or hypoxia-mediated glucose transport are not affected by wortmannin (Lund *et al.*, 1995; Yeh *et al.*, 1995).

Figure 3.8 Analysis of the Distribution of GLUT4 in Cardiomyocytes. Cardiomyocytes were isolated as described in *Methods 2.2.3.* The cells were then either left untreated (A, B) or treated with 30 nM insulin for 30 min (C, D). The myocytes were fixed with paraformaldehyde, permeabilised with saponin and probed with either mouse antibodies against GLUT4 and rhodamine-conjugated secondary antibodies (shown in red) or rabbit antibodies against GLUT4 and fluorescein-conjugated secondary antibodies (shown in green). The samples were viewed using a Zeiss confocal microscope (LSM 510) with 458/488 nm and 543 nm lasers.

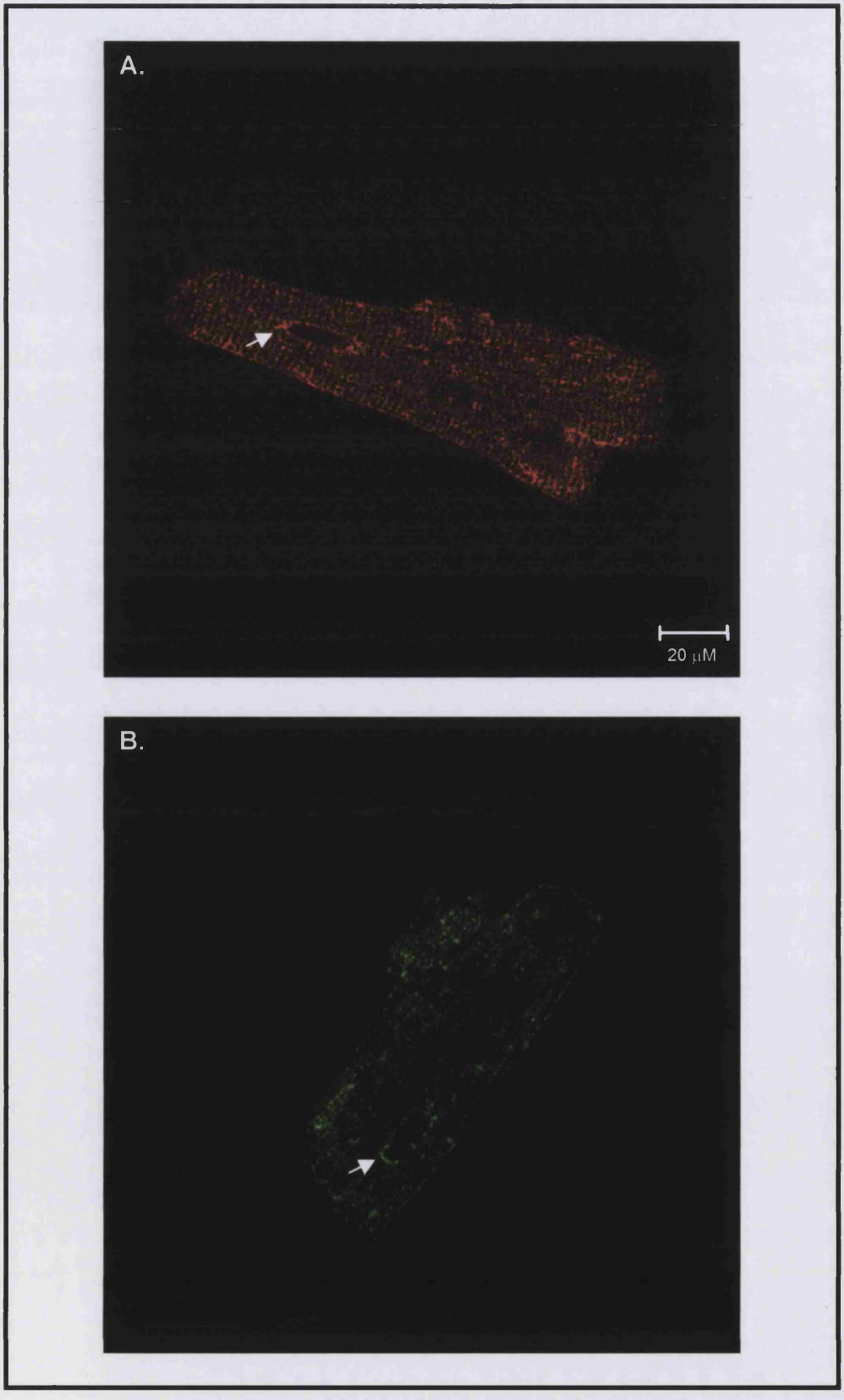

Figure 3.8 cont. Analysis of the Distribution of GLUT4 in Cardiomyocytes.

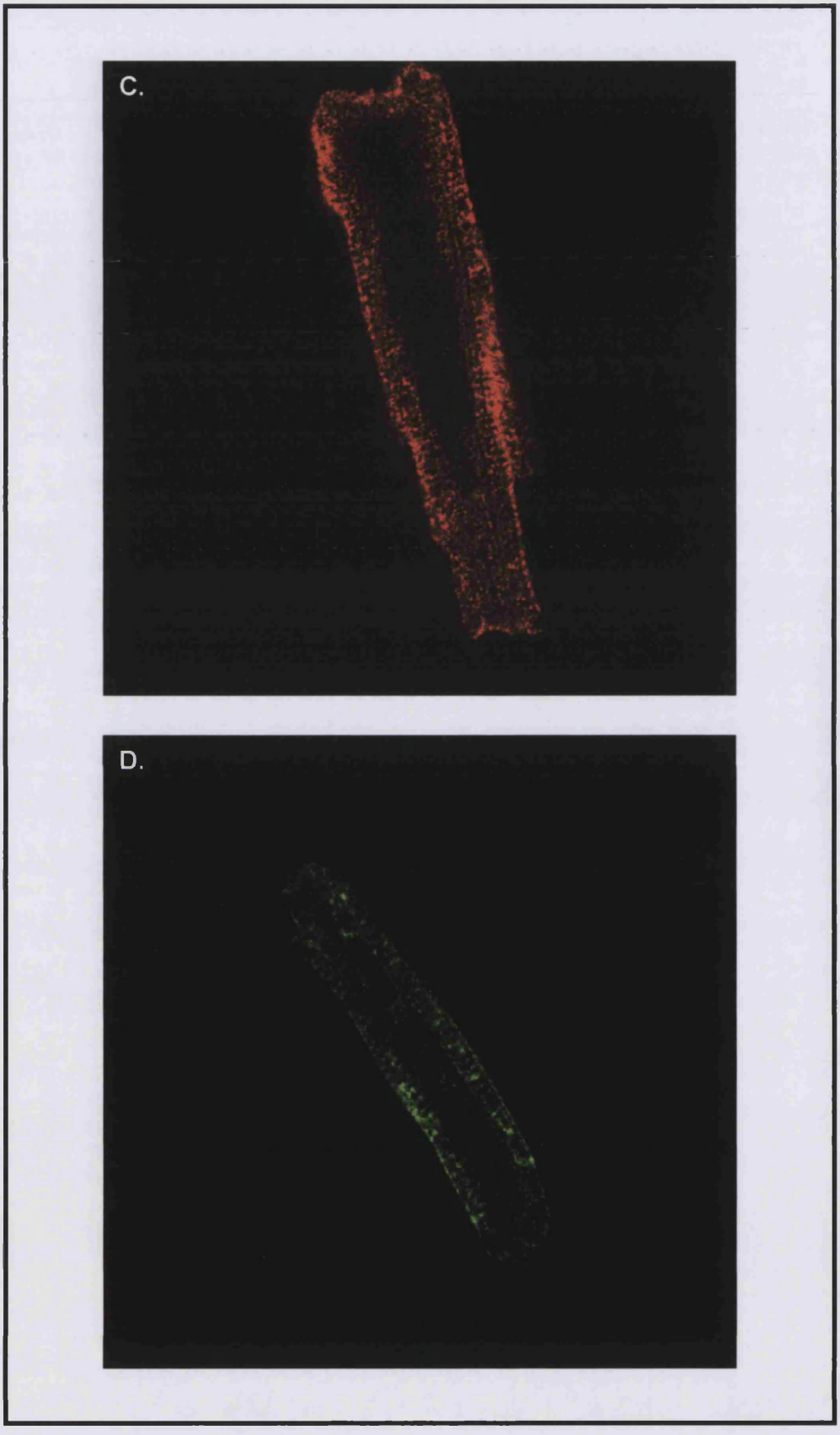

Only one study has addressed the issue of contraction-stimulated glucose transport in isolated cardiac myocytes. Using field stimulation of adult ventricular cardiomyocytes the effect of contractile activity on 3-*O*-methyl-D-glucose uptake was addressed (Kolter *et al.*, 1992). Cells that had been subjected to a contraction stimulus of 5 Hz for 5 min exhibited an increase in glucose transport of 224% over control values (Kolter *et al.*, 1992). However, somewhat controversially, insulin failed to produce a significant additional stimulation of glucose transport. Furthermore in a later study, the same group reported that treatment of cardiomyocytes with wortmannin completely blocked the contraction-induced stimulation of glucose transport, (Till *et al.*, 1997), in contrast to established studies in skeletal muscle (Lund et al., 1995; Yeh *et al.*, 1995).

To re-address the issue of whether cardiac muscle is indeed different to skeletal muscle with respect to contraction-stimulated glucose transport, a contraction chamber was developed (*Figure 3.9A and B*). This chamber consisted of a perspex box with two platinum electrodes through which an electrical current was passed. The cell suspension was placed between the electrodes and stirred gently with a flea to allow for oxygen diffusion. The cells were stimulated with biphasic pulses (5 Hz, 150 V of 165 μs duration) and viewed using a light microscope. Cells were quiescent in the resting state but contracted synchronously when an electrical current was passed between the electrodes.

A preliminary experiment (*Figure 3.9C*) revealed that contracting the cells at a frequency of 5 Hz for 5 min increased their glucose transport rates by 1.5-fold over controls. However the level of glucose transport in the basal cells in this experiment was particularly high and therefore the level of contraction-induced stimulation was probably underestimated. At present the reasons for this are unclear. Consistent with earlier results (Kolter *et al.*, 1992), the combined effects of 30 nM insulin and contraction (5 Hz for 5 min) did not significantly increase glucose transport above the levels induced by 30 nM insulin alone (*Figure 3.9C*). Subsequent preliminary experiments have revealed that shorter pulse times (under 30 sec) can also stimulate glucose transport and appear less damaging to the cells (data not shown).

Figure 3.9 The Effect of Contraction on Glucose Transport in Cardiomyocytes. Cardiomyocytes were prepared as described in *Methods 2.2.3*. Following isolation cells were either left untreated (basal), treated with 30 nM insulin for 30 min (insulin), stimulated for 5 min with a 5 Hz, 150 V biphasic pulse of 165 μs duration (contraction) or a combination of both 30 nM insulin and the contraction stimulus (insulin + contraction). 2-Deoxy-D-[^{3}H]-glucose transport was measured as described in *Methods 2.4.2*. The results shown here are of a single preliminary experiment.

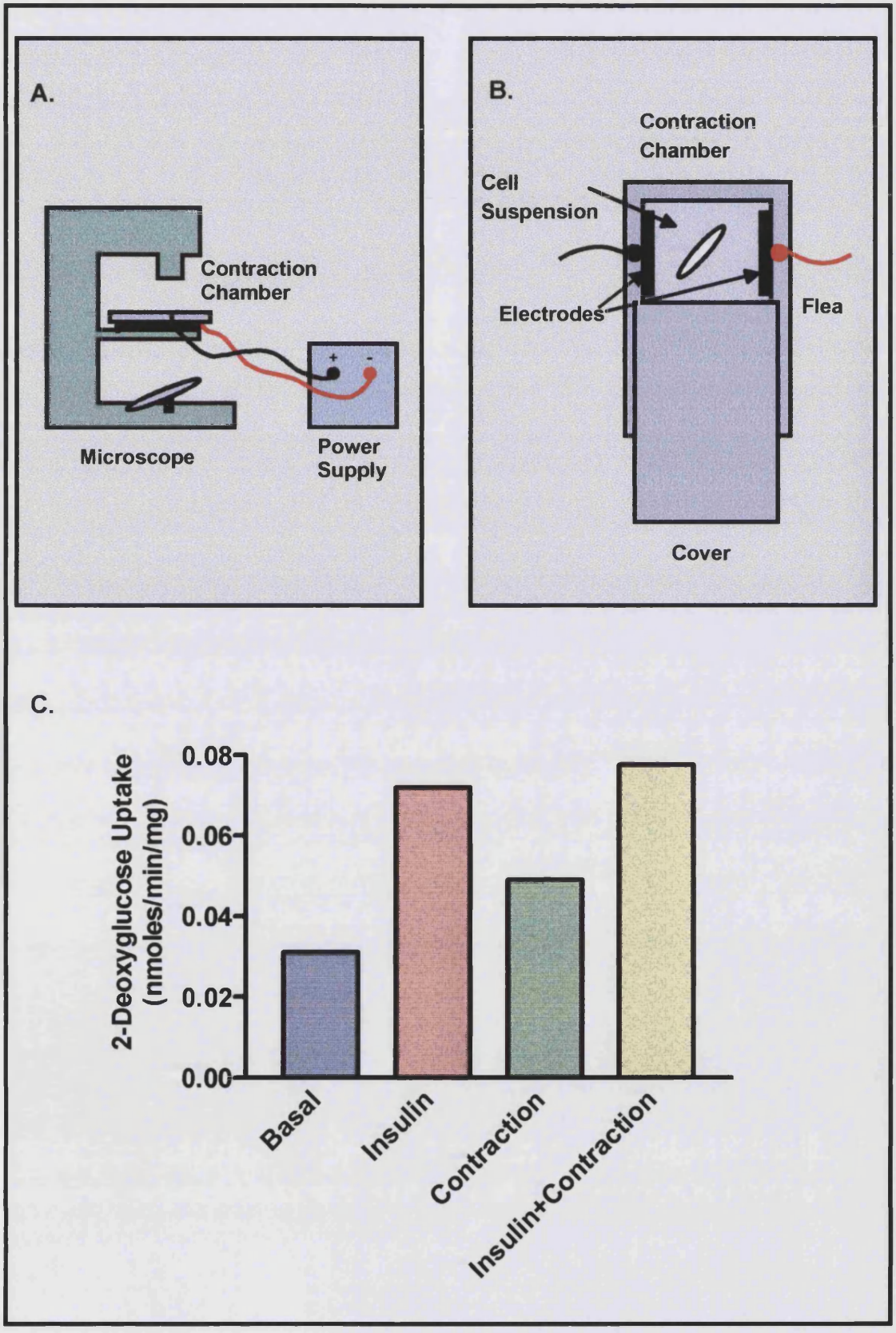

3.5 Discussion

Although heart, skeletal muscle and adipose tissue are all insulin sensitive, the majority of studies of glucose transport and insulin action have been performed in adipocytes, (Whitesell and Gliemann, 1979; Suzuki and Kono, 1980; Cushman and Wardzala, 1980). This is mainly due to the establishment of an effective protocol for the isolation of highly insulin responsive adipose cells that are relatively easy to manipulate under defined conditions. In contrast techniques to isolate functionally intact cardiac myocytes have been rather more difficult to establish for a number of reasons. For example, heart muscle cells are firmly connected to one another by intercalated discs and an established extracellular matrix (Piper *et al.*, 1990). Indeed it took over 200 years to resolve the debate as to whether the heart was catenary or syncytial, such is the nature of the close interactions between the cells (Dow *et al.*, 1981). Furthermore the cardiomyocyte is a large, rigid cell which is more easily damaged by mechanical impact than many other cell types (reviewed in Piper *et al.*, 1990). However a number of isolation protocols have now been documented and several of these have been characterised with respect to glucose transport (Lindgren *et al.*, 1982; Eckel *et al.*, 1983; Haworth *et al.*, 1984; Fischer *et al.*, 1991).

The isolated cardiomyocytes obtained by the modified procedure described in this chapter are calcium tolerant and highly responsive to insulin with respect to glucose transport. The stimulation observed upon treatment with maximally effective concentrations of hormone is higher than the effects reported by most groups and similar to those obtained by Haworth (Haworth *et al.*, 1984) and Fischer (Fischer *et al.*, 1991), upon whose methods the protocol was initially based (*Table 3.2*).

The high insulin : control ratio obtained in these myocytes is probably due to a relatively low basal level of transport, rather than a stronger response to insulin. Indeed the level of insulin stimulation remained constant, while basal transport was shown to decrease as the isolation protocol was optimised (*Table 3.1*). This is because methodological artefacts are more likely to accelerate hexose influx than to inhibit it (Haworth *et al.*, 1984).

Table 3.2. Insulin-Stimulated Glucose Uptake: A Comparison of Published Studies.

Authors	Insulin : Basal Ratio
(Lindgren *et al.*, 1982)	2 – 3
(Eckel *et al.*, 1983)	1.5 – 1.8
(Chen *et al.*, 1985)	1.4 – 1.5
(Haworth *et al.*, 1984)	≈ 10
(Bihler *et al.*, 1985)	1.7 – 2.2
(Geisbuhler *et al.*, 1987)	≈ 2.5
(Fischer *et al.*, 1991)	8 – 20
This work	4 – 15

It has long been known that the use of appropriate chemicals and minimal mechanical agitation is important for the isolation of adipocytes with a low basal glucose transport rate (Whitesell and Abumrad, 1985; Okuno and Gliemann, 1987). This work indicates that these restrictions are also fundamental in the isolation of cardiomyocytes which can respond markedly to insulin. It is hoped that further manipulation of the isolation conditions may lead to the isolation of myocytes which are able to respond to insulin at a level approaching that observed in adipocytes.

Cytochalasin B –insensitive glucose uptake accounts for approximately 20-30% of the total non-inhibited basal glucose uptake in these cells. This is consistent with values obtained in adipocytes (Okuno and Gliemann, 1987; Suzuki, 1988). In adipocytes, this relatively high rate of cytochalasin B-insensitive glucose uptake is attributed both to the actions of non-mediated diffusion and to another transporter, possibly a fructose transporter (Okuno and Gliemann, 1987). This raises the possibility that this is also the case in cardiac myocytes.

It is noteworthy that insulin-stimulated an increase in both the cell surface content of GLUT1 and GLUT4, consistent with previous studies (Fischer *et al.*, 1997). ATB-[^{3}H]-BMPA incorporation was increased approximately 2-fold for GLUT1 and 3.5-fold for GLUT4. These values are slightly lower than those already reported (Fischer *et al.*, 1997). A number of possible reasons can be proposed for this. Firstly, the myocytes were isolated without inosine (as this was discovered to be beneficial at a later stage). This may have increased the numbers of transporters at the cell surface under basal conditions consistent with results from the glucose transport assays (*Table 3.1*). Secondly the cells were irradiated for 3 min. This could lead to an increase in photolabelled transporters as they recycle between the plasma membrane and the internal membranes, distorting the 'snapshot' results. Later experiments employing the biotinylated photolabel Bio-lc-ATB-BMPA were performed on cells isolated in the presence of inosine. In this case the duration of the irradiation was reduced to 1 min and a shorter (and therefore stronger) UV wavelength was employed. Under these conditions the insulin: control ratio for GLUT4 labelling increased to 5.2-fold, similar to previous reports (Fischer *et al.*, 1997).

Immunocytochemical analysis of GLUT4 in isolated cardiomyocytes revealed that the transporter resides in an internal locus in the basal state. Upon insulin stimulation the insulin-sensitive transporter was found to translocate to the plasma membrane and the cell periphery. The pattern of staining was punctate and vesicular. The distribution of GLUT4 observed in our cardiomyocyte preparation supports studies performed in adipocytes (Slot *et al.*, 1991a) and cardiac muscle (Slot *et al.*, 1991b). In these cells the insulin-responsive glucose transporter is found in the *trans*-Golgi reticulum (TGR) and in an intracellular tubulovesicular compartment from where it undergoes insulin dependent movement to the cell surface (Rea and James, 1997).

Initial experiments have shown that contraction can also stimulate glucose transport in isolated cardiomyocytes. Future work could concentrate on the controversial observation that the contraction and insulin stimuli do not appear to be additive in cardiac myocytes (Kolter *et al.*, 1992; Till *et al.*, 1997). Trafficking in cardiac myocytes could be analysed by using biotinylated photolabels. Plasma membrane transporters from cells stimulated with insulin, with contraction or with a combination of both stimuli could therefore be tagged and the rate of loss of transporters from the cell surface measured by taking advantage of the biotin-avidin interaction (*Figure*

Figure 3.10 Method for Studying the Trafficking of GLUT4 in Insulin-Responsive Cells. Cell surface GLUT4 is biotinylated using the photolabel Bio-PEG80. Avidin is then added at various timepoints. The cells are solubilised and the biotin label is detected. The longer the period between the photolabelling and the addition of avidin the higher the biotin signal. From measurements taken at various timepoints the rate of internalisation can be determined. Right hand panels show erythrocytes labelled with Bio-PEG80 and detected using fluorescein-conjugated anti-biotin antibodies (C). The detection of the photolabel is abolished by the addition of Neutravidin at a concentration of 0.2 mg/ml (D).

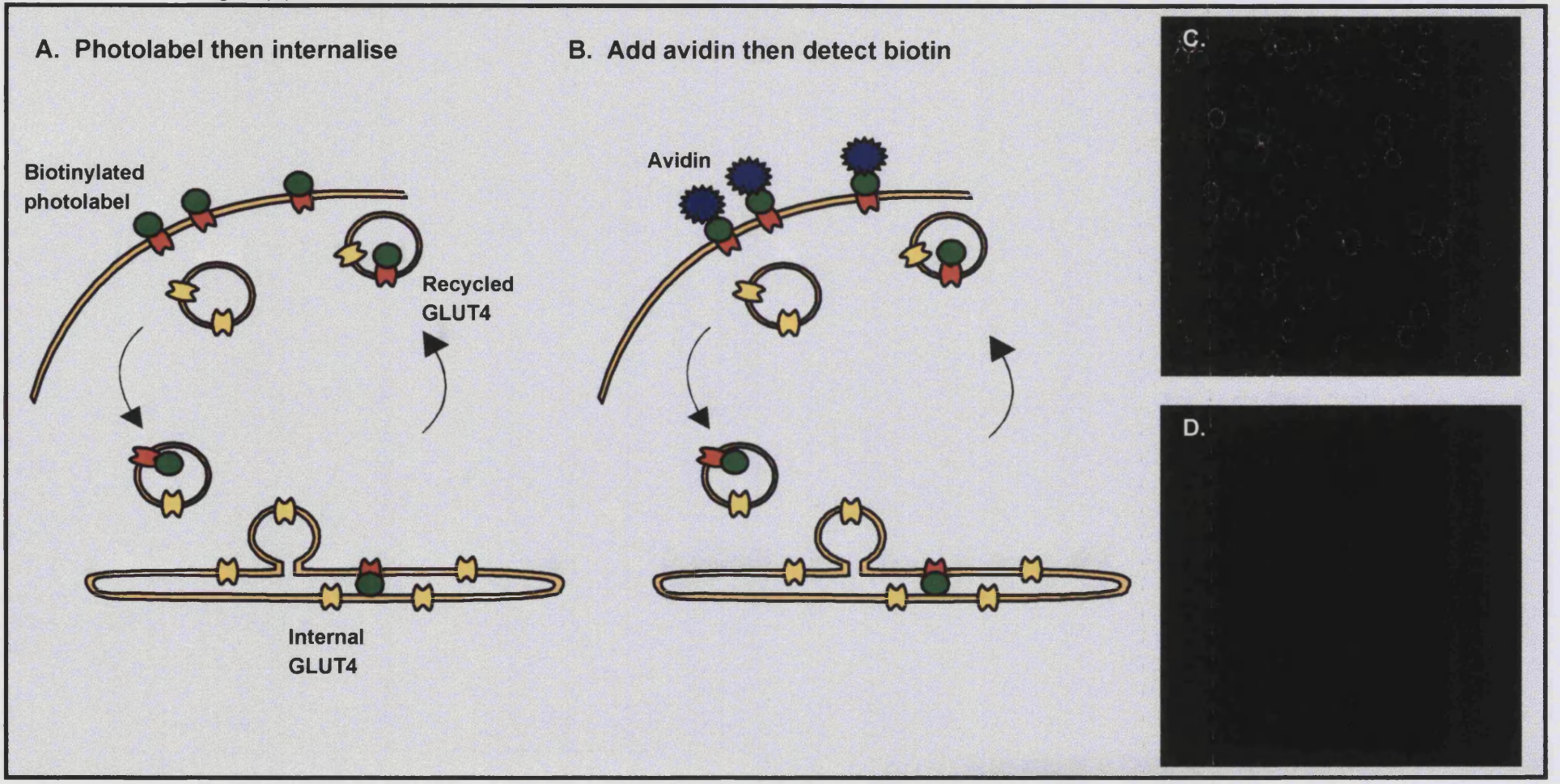

3.10A, B). If the stimulatory effects of insulin and contraction are mediated via separate pools then the combined rates of decay of transporters from the cell surface should be the same as the sum of the individual decays. If the rate of decay is slower then this is indicative of transporter mixing. However if the insulin- and contraction-mediated signalling pathways are non-additive but there is upstream convergence of signalling, then it may be difficult to differentiate between the two pools using kinetic experiments.

Another approach is to address the issue of separate insulin and contraction pools at the morphological level using confocal microscopy. The highly organised nature of the myocyte lends itself perfectly to such an analysis. Thus a combination of anti-GLUT4 and anti-biotin antibodies could be employed to detect any differences in the localisation of photolabelled glucose transporters that respond to insulin compared with those that are stimulated by contraction. In particular GLUT4 localisation could be compared to the markers giantin and the TfR, which were used to show that two distinct GLUT4 pools reside in skeletal muscle, one stimulated by insulin and one by exercise (contraction) (Ploug *et al.*, 1998). Initial experiments using erythrocytes labelled with Bio-PEG80, a new photolabel with a long (500 Å) spacer arm, have revealed the potential of such an approach. Here, photo-tagged erythrocytes could be detected with fluorescein-conjugated anti-biotin antibodies (*Figure 3.10C*), whereas the addition of 0.2 mg/ml Neutravidin blocked this detection (*Figure 3.10D*).

In summary, the ability to isolate functionally intact, insulin responsive myocytes has provided a new model for the study of both insulin-regulated and contraction-regulated processes in our laboratory.

4.0 The Role of Intracellular pH in the Regulation of Glucose Transport Activity and Glucose Transporter Translocation

4.1 Studies with the Sodium-Proton Pump Inhibitor HOE-642 (Cariporide) in Cardiac Myocytes

Intracellular pH is controlled by two major ion transport mechanisms. In the presence of HCO_3^-, intracellular pH (pH_i) is regulated by the activation of Cl^-/HCO_3^- and Na^+/H^+ exchange mechanisms whereas in the absence of HCO_3^-, Na^+/H^+ antiport is the only mechanism available to regulate pH_i by exchanging extracellular Na^+ for intracellular H^+ (Arsenis *et al.*, 1995). The Na^+/H^+ antiporters (NHEs) are a family of proteins that are thus responsible for the regulation of cellular pH and volume (Grinstein and Rothstein, 1986). The most well characterised of these Na^+/H^+ pumps is NHE1. This pump is quiescent above a certain cellular pH and is activated by acidification of the cytosol. It is also activated by a variety of growth factors and hormones, and by hyperosmotic shrinking. Activation by these stimuli is mediated not by prior acidification of the cytosol but by an alkaline shift of the pH-dependence of the antiporter. This in turn leads to alkalinisation of the cytosol above the normal set point (Wakabayashi *et al.*, 1997). Like many hormones, insulin activates the Na^+/H^+ exchanger in a variety of cells, and this is one of the earliest responses of cells to insulin stimulation (Arsenis and Tarvin, 1986).

Amiloride is an inhibitor of Na^+/H^+ exchange. Early studies have shown that treatment of cells with amiloride not only inhibits insulin-induced alkalinisation of the cytoplasm, but also markedly reduces insulin-stimulated glucose transport into these cells (Klip *et al.*, 1986; Goto *et al.*, 1993). This occurs both by inhibition of GLUT4 translocation, and by a decrease in the 'effectiveness' of insulin on the insulin-signalling pathway (Goto *et al.*, 1993). However the actions of amiloride are not absolutely specific for Na^+/H^+ exchangers and as such it is difficult to assess whether the inhibition of glucose transport activity is as a direct consequence of Na^+/H^+ inactivation or mediated by secondary effects of the drug.

Recently the discovery of a new class of NHE inhibitors has allowed the re-examination of the involvement of Na^+/H^+ antiport in glucose transporter regulation. These

compounds constitute a class of benzoyl guanidine derivatives which include the drugs HOE-694 and HOE-642 (Cariporide). These inhibitors have an affinity for NHE1 which is two or more orders of magnitudes higher than for the isoforms NHE2 and NHE3 (Counillon *et al.*, 1993b). Furthermore these compounds have recently been shown to inhibit NHE activity in perfused rat heart *in vivo* (Scholz *et al.*, 1993; Scholz *et al.*, 1995).

4.1.1 Changes in the Intracellular pH Assessed with the Acidotrophic Dye Acridine Orange

In order to study the effects of Na^+/H^+ exchange activity on glucose transport, cardiomyocytes were first analysed for changes in pH induced by insulin, and by inhibition of the NHE1 antiporter. Modulation of the intracellular pH induced by insulin and HOE-642 was analysed by vital staining with acridine orange. This dye is an acidotrophic weak base which is taken up by living cells and accumulates in acidified compartments. At low concentrations acridine orange fluorescence is green, however when allowed to accumulate the fluorescence changes to orange. When unstimulated cardiomyocytes were stained with 5 μg/ml acridine orange for 10 min at 37°C, the nuclei and in particular the nucleoli and the cytoplasm displayed green fluorescence, whereas orange/red fluorescence was observed in a granulated pattern dispersed within the cytoplasm. This distribution pattern suggests that the orange fluorescence is due to acidified lysosomes. Furthermore a compartment of intermediate acidity, which stained yellow was observed in the perinuclear region, and may represent an endosomal sorting station or the *trans*-Golgi network (*Figure 4.1A*). Treatment of cardiomyocytes with 30 nM insulin for 30 min at 37°C before addition of the acridine orange stain caused a complete disappearance of the orange fluorescence, whereas the green fluorescence remained, (*Figure 4.1B*). A small number of yellow compartments around the nucleus also remained. Addition of 20 μM HOE-642 for 10 min at 37°C, prior to the addition of insulin, resulted in a marked decrease in cytoplasmic pH, indicated by the yellow colour of the acridine orange stain (*Figure 4.1C*). The number and colour of the granular compartments within the cytosol was reminiscent of the unstimulated control cells (*Figure 4.1A*). This suggests that HOE-642 has blocked the activation of the Na^+/H^+ pump by insulin, resulting in a failure of the cell to increase the cytosolic pH.

Figure 4.1 The Effect of HOE-642 on the Intracellular pH As Judged By Vital Fluorescence. Cardiomyocytes were prepared as described in *Methods 2.2.3*. The cells were either left untreated (A), treated with 30 nM insulin for 30 min (B), or treated with both 30 nM insulin and 20 μM HOE-642 (C). The cells were then incubated for 10 min with 5 μg/ml acridine orange, then washed and mounted in Vectorshield. The cells were viewed using a Zeiss confocal scanning microscope (LSM510) with dual lasers set at 458/488 nm and 543 nm.

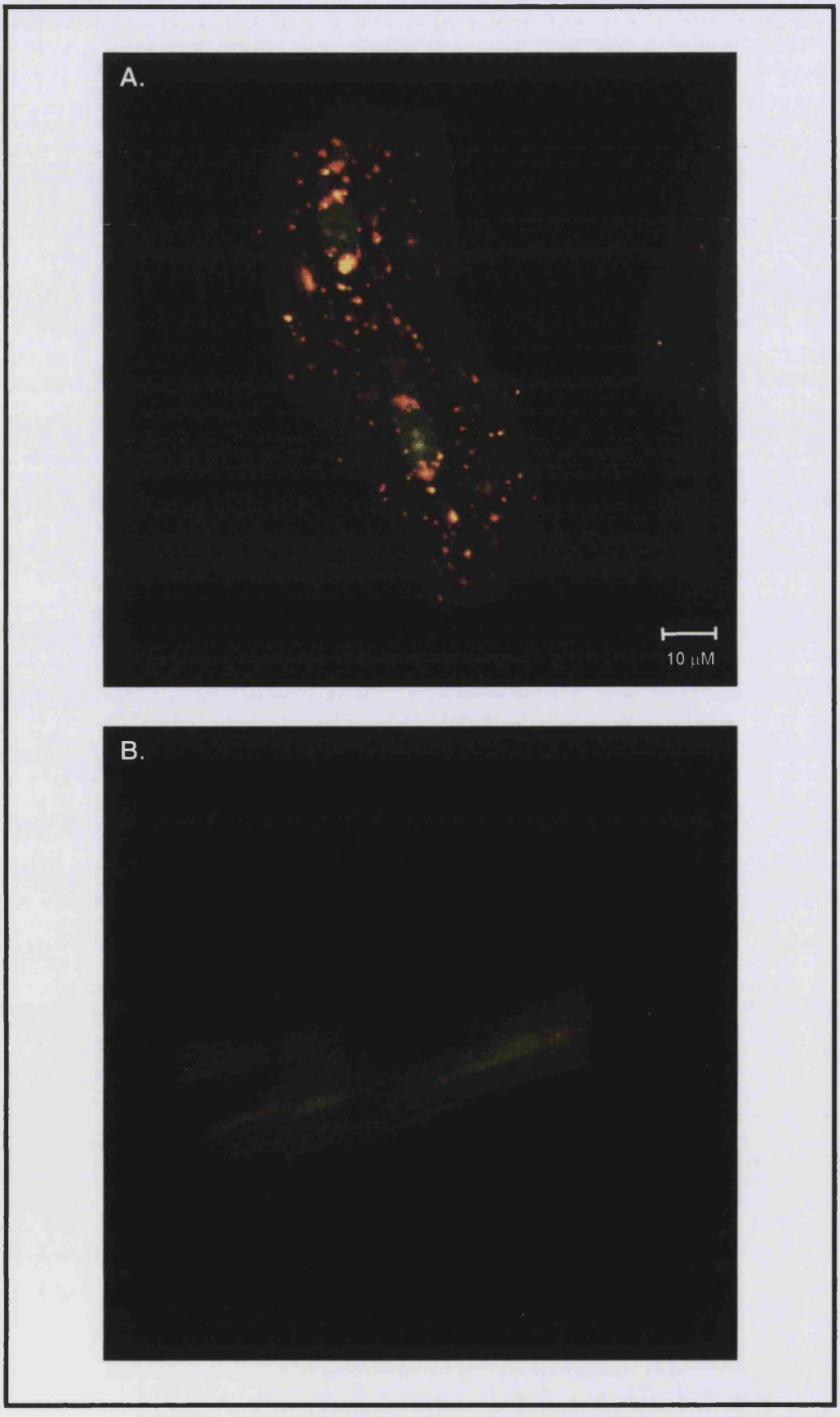

Figure 4.1 cont. The Effect of HOE-642 on Intracellular pH As Judged By Vital Fluorescence.

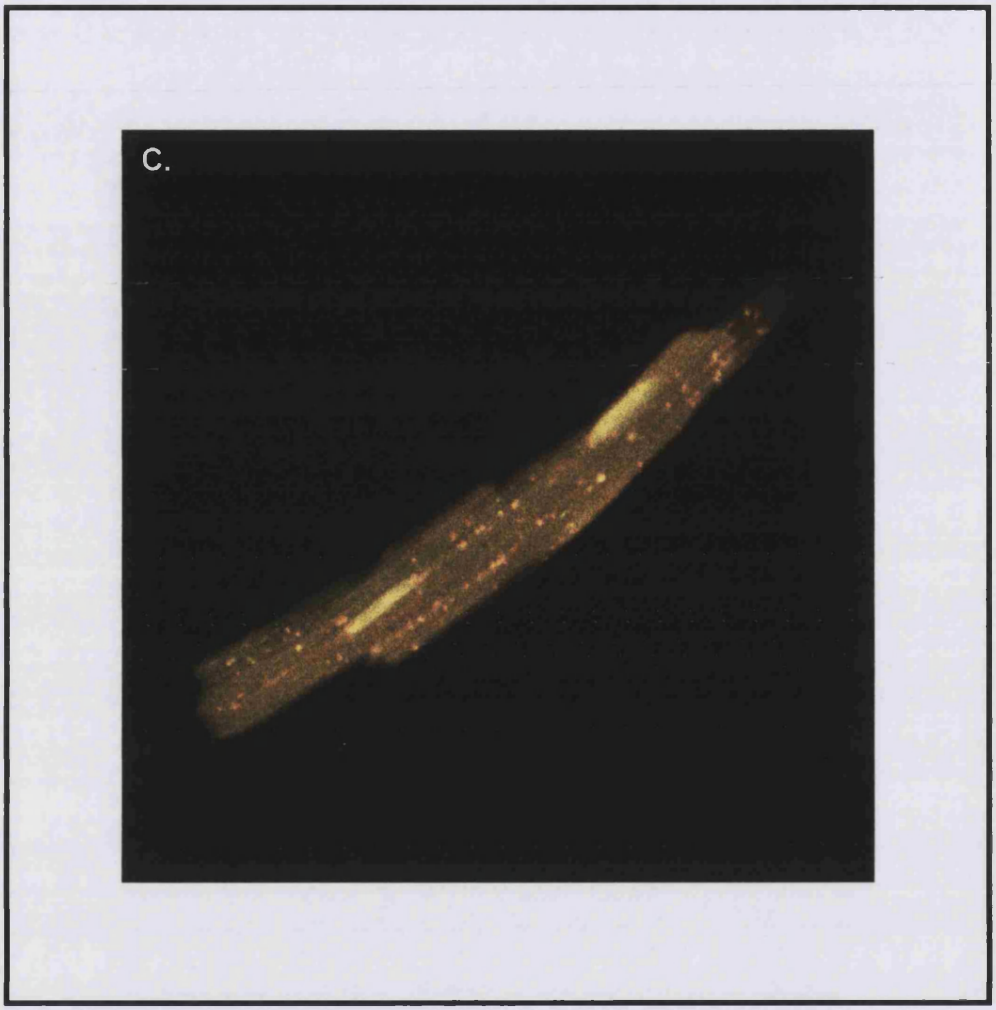

4.1.2 Inhibition of Insulin-Stimulated Glucose Uptake in Cardiac Myocytes Treated with HOE-642

To directly test whether NHE1 activity is necessary for the activation of glucose transport in response to insulin, the uptake of 2-deoxy-D-glucose into cardiomyocytes was analysed. Thus following isolation, cells were either left untreated (basal), treated with 30 nM insulin for 30 min, treated with 20 μM HOE-642 for 10 min or treated with a combination of both 20 μM HOE-642 and 30 nM insulin. All samples were incubated at 37°C for a total of 40 min. Rates of basal and insulin-stimulated 2-deoxy-D-glucose uptake in cardiomyocytes are shown in *Figure 4.2*. In agreement with previous findings insulin increased glucose transport activity ≈ 6 fold above rates measured for basal glucose uptake (Fischer *et al.*, 1991). The absolute rates of 2-deoxy-D-glucose uptake being 0.010 ± 0.0026 nmoles/min/mg of protein and 0.059 ± 0.0034 nmoles/min/mg of protein for basal and insulin-stimulated cardiomyocytes respectively.

We have previously demonstrated in cardiomyocytes that 2-deoxy-D-glucose uptake is linear for at least 30 min under the experimental conditions used in this study (*Section 3.1.5*). Furthermore, others have shown that when the total intracellular concentration of 2-deoxy-D-glucose is less than 20 mM, then only 2% of the total intracellular 2-deoxy-D-glucose is present in the unphosphorylated form (Hansen *et al.*, 1995). Thus the rate of 2-deoxy-D-glucose uptake should accurately reflect glucose transport activity.

Treatment of cardiomyocytes with HOE-642 prior to the addition of insulin, resulted in a marked inhibition of insulin-stimulated glucose transport by ≈ 35% (*Figure 4.2*), whereas HOE-642 treatment had little or no effect on basal glucose transport activity. The absolute rates for 2-deoxy-D-glucose being 0.011 ± 0.0034 nmoles/min/mg of protein and 0.039 ± 0.0047 nmoles/min/mg of protein for HOE-642 treated samples from basal and insulin-stimulated cells, respectively.

4.1.3 The Effect of HOE-642 on Cell-Surface Levels of GLUT4 and GLUT1

To determine whether there was a correlation between HOE-642 inhibition of glucose transport activity and glucose transporter translocation to the plasma membrane, the cell impermeant photolabel Bio-lc-ATB-BMPA was employed. This photolabel only labels

Figure 4.2 Inhibition of Insulin-Stimulated Glucose Uptake in Cardiac Myocytes Treated with HOE-642. Cardiomyocytes were prepared according to *Methods 2.2.3*. Cells were treated with 20 μM HOE-642 for 10 min at 37°C where appropriate before stimulation with 30 nM insulin for 20 min at 37°C, or were left untreated. 2-Deoxy-D-[^{3}H]-glucose uptake was measured as described in *Methods 2.4.2*. The results shown are from 4 independent experiments (paired, two-tailed t-test with 95% confidence intervals).

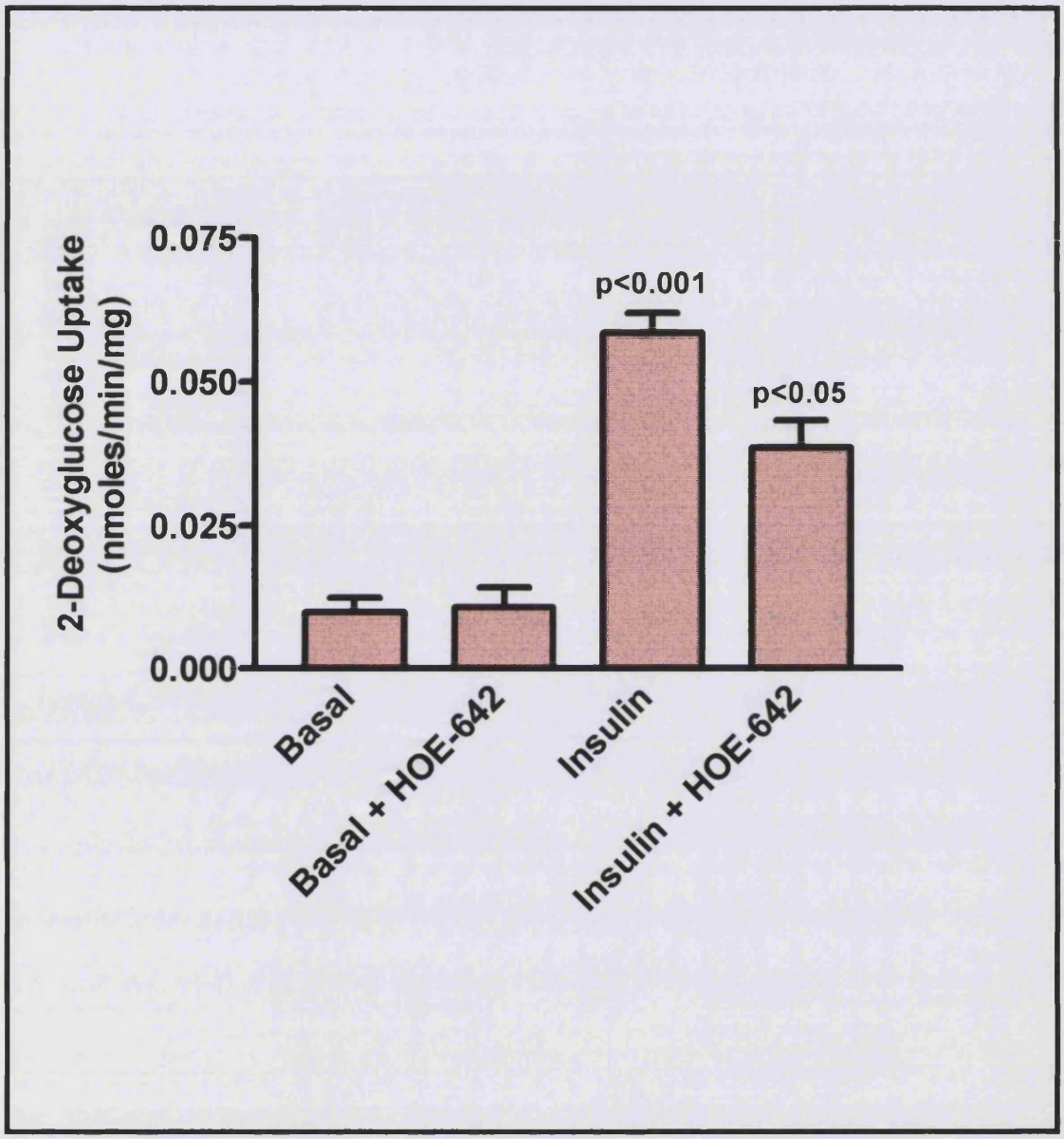

the transporters accessible at the plasma membrane, and as such is a useful tool to analyse changes in the distribution of glucose transporters between the intracellular compartments and the plasma membrane. Following incubation either with 30 nM insulin, with 20 μM HOE-642 or with a combination of both reagents at the same concentrations, cardiomyocytes were labelled with 500 μM Bio-lc-ATB-BMPA by photo-irradiation. The cells were then washed extensively to remove unincorporated biotinylated reagent, and solubilised in a detergent buffer. Following this incubation insoluble material was removed by centrifugation and a small volume of this supernatant was retained for analysis. Biotin-tagged transporters were precipitated on streptavidin beads, then eluted and resolved by SDS-PAGE and Western blotting with antibodies against GLUT1 and GLUT4. The results of representative experiments are shown in *Figures 4.3 and 4.4.*

Analysis of GLUT1 by photolabelling showed that insulin caused an approximately 2.5-fold increase in the levels of this transporter at the plasma membrane (*Figure 4.3*). This is in agreement with other studies which have used the ATB-[^{3}H]-BMPA label to analyse cell surface GLUT1 in cardiomyocytes (Fischer *et al.*, 1997). Surprisingly treatment of cardiomyocytes with HOE-642 followed by insulin resulted in little change in the plasma membrane content of GLUT1, indeed in some cases a slight augmentation of cell-surface GLUT1 was observed (*Figure 4.3A*). To check that an equal amount of protein had been added to the streptavidin beads and that HOE-642 had no significant effect on the total intracellular concentration of GLUT1, an equal volume of the detergent solubilised supernatant (retained prior to the streptavidin precipitation) was analysed by SDS-PAGE and Western blotting with antibodies against GLUT1. No change in the amount of immunoreactive GLUT1 was observed in any of the samples analysed (*Figure 4.3B*).

Next we examined changes in plasma membrane GLUT4. GLUT4 at the cell surface increased following insulin stimulation by approximately 4.6-fold over basal levels (ranging between 3- and 6-fold over 4 separate experiments). Again this is in agreement with published studies showing that insulin increases cell surface GLUT4 by ≈ 5.7 fold in cardiomyocytes (Fischer *et al.*, 1997). In contrast to GLUT1 but in agreement with the transport activity data, the level of GLUT4 at the plasma membrane decreased following HOE-642 and insulin treatment in combination, by approximately 36% (*Figure 4.4A*). No change in the total amount of GLUT4 was detected in the

Figure 4.3 The Effect of HOE-642 on the Cell Surface Levels of GLUT1 As Judged By Photolabelling. Cardiomyocytes were prepared as described in *Methods 2.2.3*. The cells were either left untreated (B), treated with 30 nM insulin (I), or treated with both 20 μM HOE-642 and 30 nM insulin (IH). The cells were photolabelled with 500 μM Bio-lc-ATB-BMPA, washed and solubilised in a Thesit detergent buffer. Photo-tagged GLUTs were precipitated on streptavidin beads. The resulting precipitates were analysed by SDS-PAGE and Western blotting with antibodies against GLUT1 (A). A small amount of solubilised protein from before the streptavidin precipitation was kept to check for equal loading (B). The material from the streptavidin precipitation was analysed by densitometry (C). The results shown are representative of 2 separate experiments.

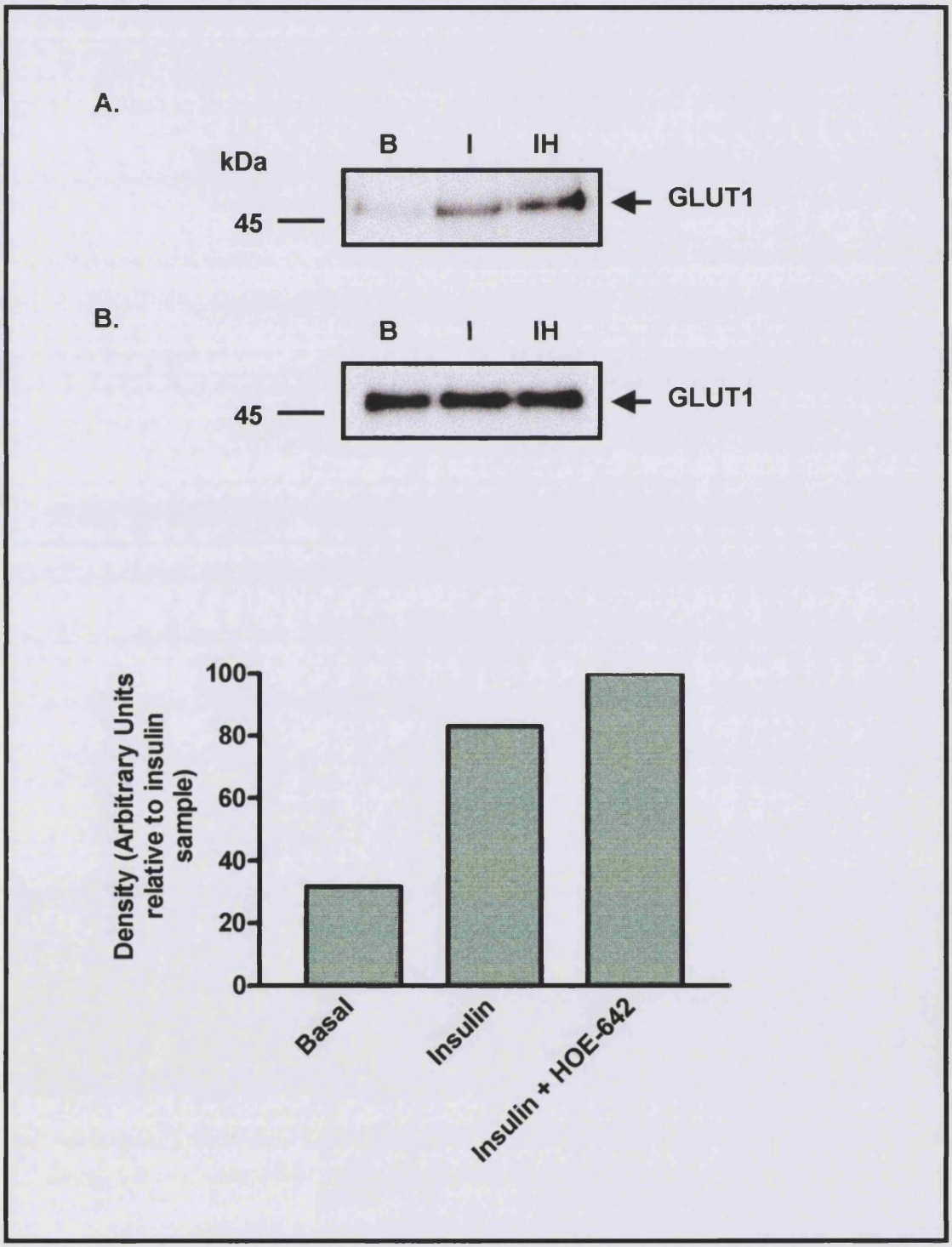

Figure 4.4 The Effect of HOE-642 on the Cell Surface Levels of GLUT4 As Judged By Photolabelling. Cardiomyocytes were prepared as described in *Methods 2.2.3*. The cells were either left untreated (B), treated with 30 nM insulin (I), or treated with both 20 μM HOE-642 and 30 nM insulin (IH). The cells were photolabelled with 500 μM Bio-Ic-ATB-BMPA, washed and solubilised in a Thesit detergent buffer. As a control an aliquot of cells was irradiated without photolabel (U). Photo-tagged GLUTs were precipitated on streptavidin beads. The resulting precipitates were analysed by SDS-PAGE and Western blotting with antibodies against GLUT4 (A). A small amount of solubilised protein from before the streptavidin precipitation was kept to check for equal loading (B). The material from the streptavidin precipitation was analysed by densitometry (C). The results shown are representative of 4 separate experiments.

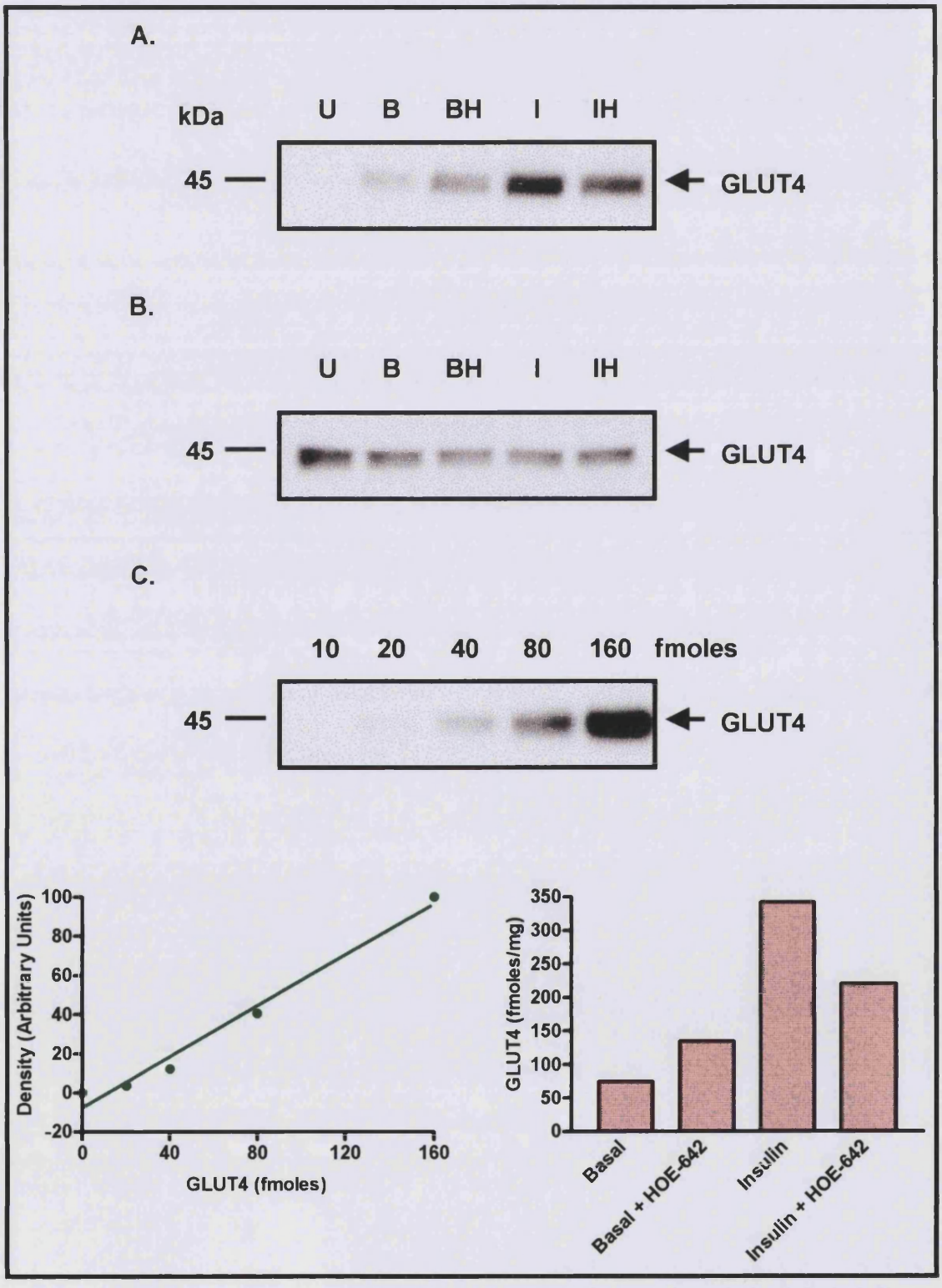

detergent solubilised supernatants indicating that (a) an equal amount of protein had been incubated with the streptavidin beads and (b) HOE-642 has no significant effect on the total amount of GLUT4 in cardiomyocytes.

In order to determine an approximation for the amount of GLUT4 at the cell surface of cardiomyocytes under the conditions tested, we compared a standard curve of low density microsomal protein (LDM) with photolabelled samples by SDS-PAGE and Western blotting with an antibody raised against GLUT4. LDM protein is known to contain approximately 60 pmoles of GLUT4 per mg (Simpson et al., 1983; Holman *et al.*, unpublished observation). Densitometric analysis of these Western blots indicated that under basal conditions approximately 74.4 fmoles of GLUT4 per mg of membrane protein were present at the cell surface. Upon insulin stimulation this increased to 341.4 fmoles of GLUT4 per mg of membrane protein. Treatment with HOE-642 in conjunction with insulin decreased the level of GLUT4 at the cell surface to 219.8 fmoles per mg of membrane protein (*Figure 4.4C*).

4.1.4 Distribution of the Insulin-Sensitive Glucose Transporter GLUT4 Revealed by Confocal Microscopy

To confirm the photolabelling results, the distribution of GLUT4 in cardiomyocytes was analysed by confocal microscopy. Thus following isolation, cardiomyocytes were either left untreated (basal), treated with 30 nM insulin for 30 min, or treated with a combination of 20 μM HOE-642 for 10 min and 30 nM insulin for 30 min. Cardiomyocytes were then fixed by incubation in 4% paraformaldehyde, followed by permeabilisation with 0.1% saponin. Cells were incubated with monoclonal mouse anti-GLUT4 antibodies for 1.5 h, then washed extensively before incubation with rhodamine conjugated anti-mouse antibodies. Following this incubation the cells were washed again, mounted and viewed in Vectorshield. The results shown are representative of 10 cells selected at random per condition per experiment, and of two independent experiments. All cells were viewed in approximately the same focal plane.

As expected GLUT4 in basal unstimulated cells was predominantly intracellular (*Figure 4.5A*). The fluorescent pattern was vesicular with particularly intense labelling around the perinuclear region (indicated by the arrow), which presumably represents the

Figure 4.5 The Effect of HOE-642 on the Distribution of GLUT4 in Cardiomyocytes. Cardiomyocytes were prepared as described in *Methods 2.2.3*. The cells were either left untreated (A), treated with 30 nM insulin (B), or treated with 20 μM HOE-642 followed by 30 nM insulin for 30 min (C). The cells were fixed with paraformaldehyde, solubilised with saponin and probed with mouse antibodies against GLUT4. The cells were then washed and incubated with rhodamine-conjugated anti-mouse antibodies. As a control some cells were treated with the secondary antibody alone (D). The samples were viewed using a Zeiss laser scanning microscope (LSM510) with 543 nm lasers.

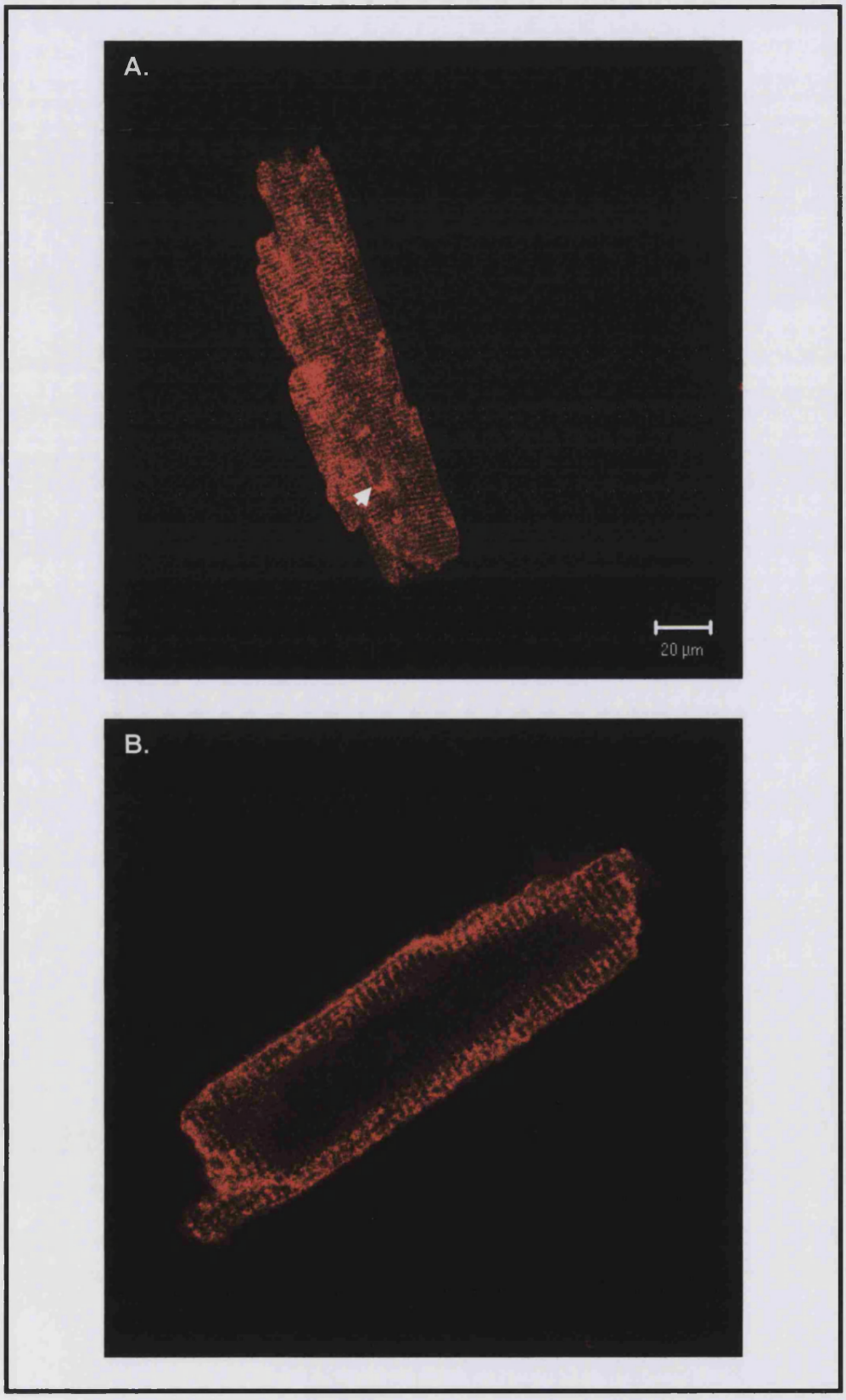

Figure 4.5. cont. The Effect of HOE-642 on the Distribution of GLUT4 in Cardiomyocytes.

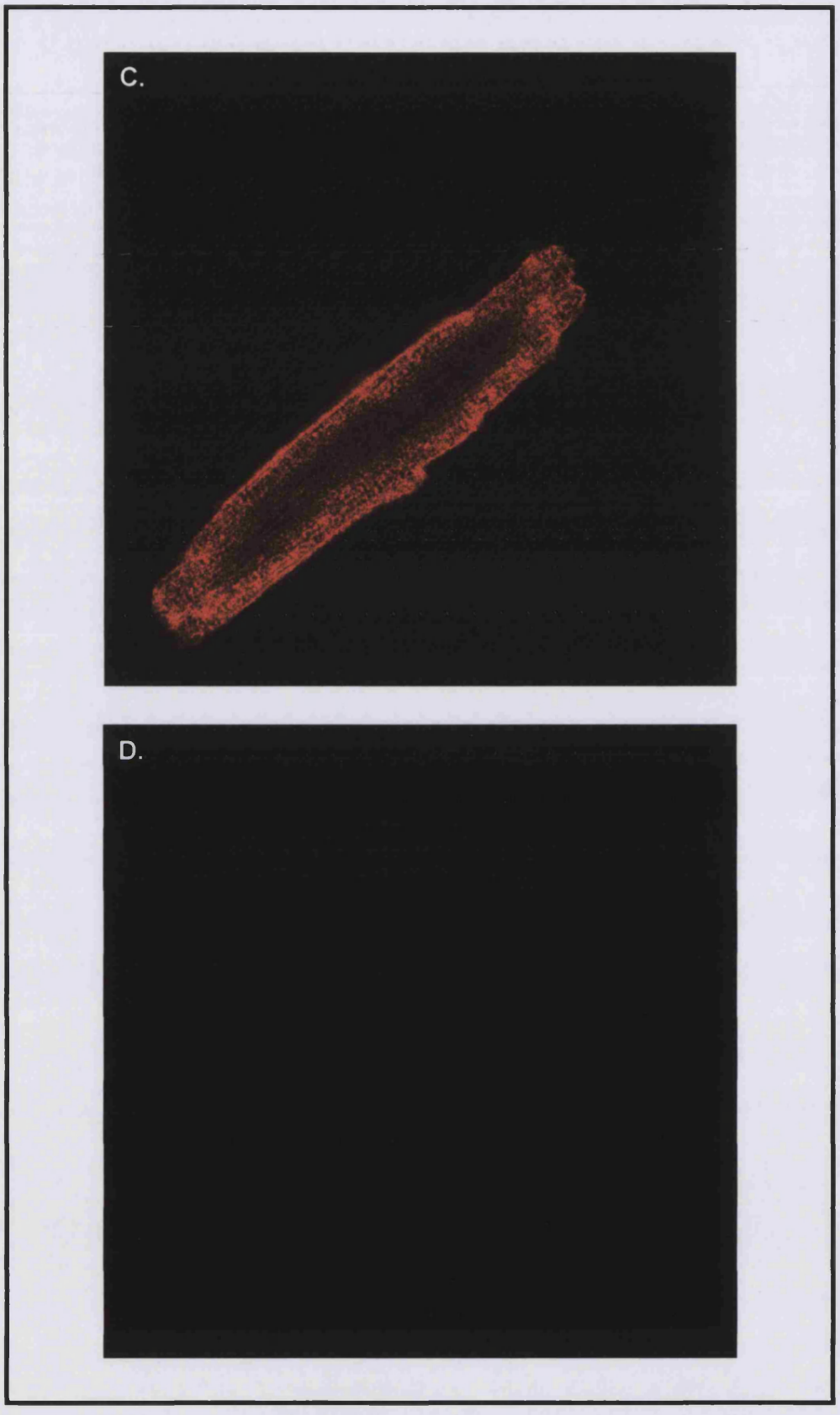

trans-Golgi network, or an endosomal sorting station. GLUT4 was also localised below the plasma membrane. GLUT4 appeared to distribute to striations and displayed a labelling pattern reminiscent of the arrangement of actin filaments. Following insulin stimulation a sizeable proportion of GLUT4 was redistributed to the plasma membrane, and to peripheral tubulo-vesicular structures in the cytoplasm. These structures appeared punctate and connected as if on 'strings' (*Figure 4.5B*). This in agreement with immunolocalisation studies in cardiac muscle (Slot *et al.*, 1991b) which showed that under basal conditions less than 1% of the total GLUT4 is localised to the various domains of the plasma membrane (sarcolemma, intercalated discs and transverse tubules). Following insulin stimulation GLUT4 increased at the cell surface and transverse tubules by 42-fold (Slot *et al.*, 1991b).

Treatment of cardiomyocytes with HOE-642 in conjunction with insulin, failed to block the re-distribution of GLUT4 to the plasma membrane. In some cases the pattern of GLUT4 was less striated, and more vesicular. Some fluorescence around the perinuclear region remained and GLUT4 was seen to run in 'rows' between the two poles of the myocyte, perhaps associated with microtubules (*Figure 4.5C*). Control experiments in which only the secondary antibody was incubated with the cardiomyocytes revealed little non-specific staining (*Figure 4.5D*).

4.2 Studies of the Sodium-Proton Pump Inhibitor HOE-642 in Rat Adipocytes

4.2.1 Inhibition of Insulin-Stimulated Glucose Uptake in Rat Adipocytes Treated with HOE-642

The confocal microscopy results in cardiomyocytes prompted us to analyse the effects of HOE-642 on insulin-stimulated glucose transport and GLUT4 translocation in another insulin-responsive cell, from which sufficient material could be obtained for subfractionation analysis. Thus adipocytes were first tested for their ability to respond to HOE-642 by analysis of 3-*O*-methyl-D-glucose uptake in cells either left untreated (basal), treated with 20 μM HOE-642, treated with 20 nM insulin or treated with a combination of both reagents. 3-*O*-methyl-D-glucose uptake was assayed over a 90 s period for basal and basal/HOE-642 samples and over a 3 s period for insulin and insulin/HOE-642 samples to allow analysis of sugar uptake over the linear region of the

Figure 4.6 Inhibition of Insulin-Stimulated Glucose Transport in Rat Adipocytes Treated with HOE-642. Adipocytes were prepared according to *Methods 2.2.2.* Cells were then treated with 20 μM HOE-642 for 10 min at 37°C or were left untreated. Following the HOE-642 incubation, adipocytes were treated with 20 nM insulin for 20 min or were left untreated. ^{14}C-3-*O*-methyl-D-glucose uptake was performed as described in *Methods 2.4.1.* The results shown are representative of 3 separate experiments.

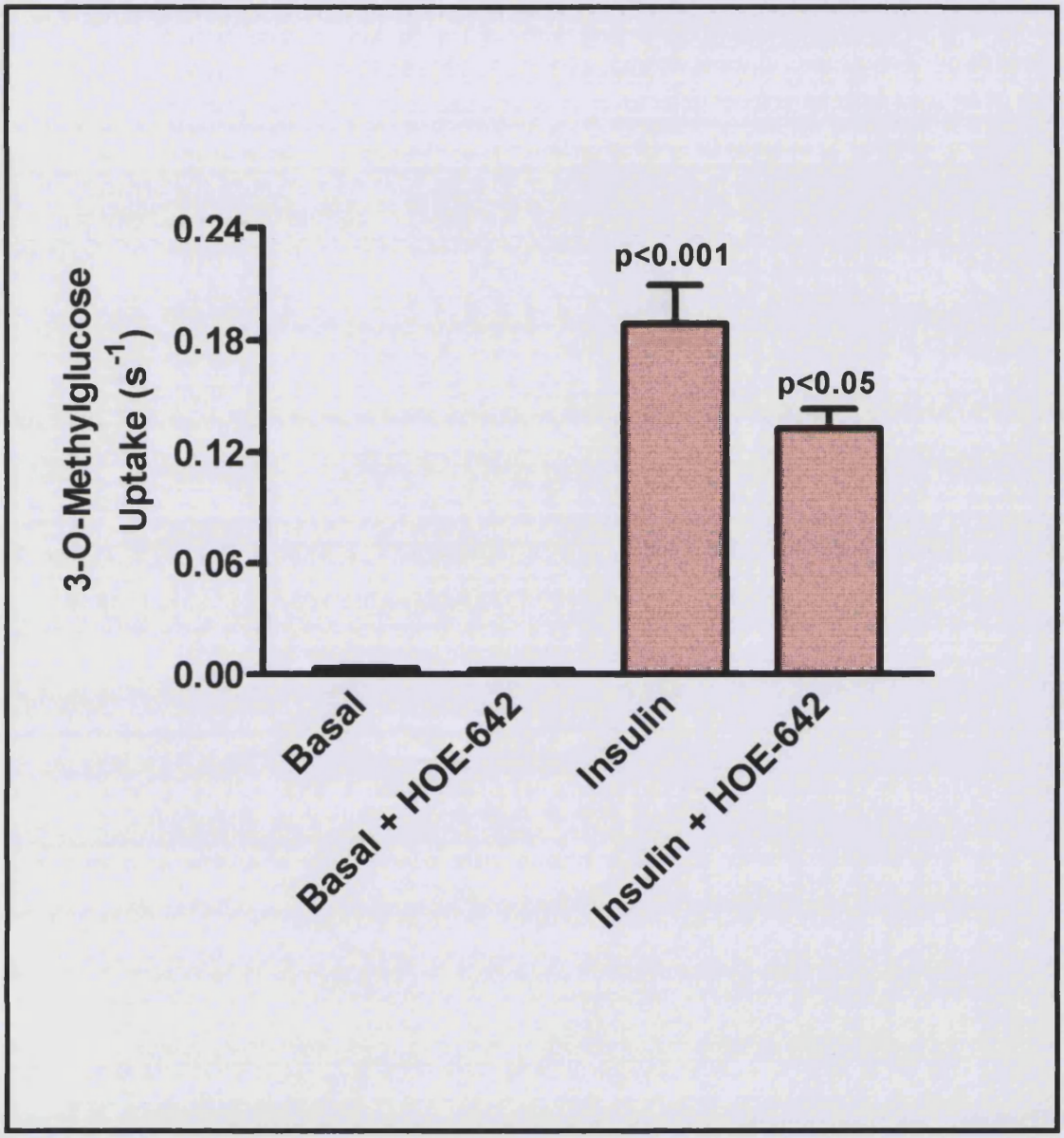

3-*O*-methyl-D-glucose transport curve (Whitesell and Gliemann, 1979; Taylor and Holman, 1981).

The rates of 3-*O*-methyl-D-glucose uptake are shown in *Figure 4.6.* Insulin increased the rate of 3-*O*-methyl-D-glucose uptake by approximately 58-fold over basal levels, similar to rates demonstrated previously (Holman *et al.*, 1990). The absolute values for transport being 0.0032 ± 0.0005 s^{-1} and 0.1887 ± 0.0206 s^{-1} for basal and insulin-stimulated adipocytes, respectively. Addition of HOE-642 inhibited insulin-stimulated glucose transport by approximately 30%, while HOE-642 had little effect on 3-*O*-methyl-D-glucose transport in basal adipocytes. The absolute rates of transport being 0.0024 ± 0.0005 s^{-1} and 0.1322 ± 0.0106 s^{-1} for HOE-642 samples from basal and insulin-stimulated adipocytes, respectively. This is in good agreement with the effects of HOE-642 observed in cardiomyocytes (*Section 4.1.2*).

4.2.2 The Effect of HOE-642 on Cell Surface Levels of GLUT4 in Rat Adipocytes

To examine whether the inhibition of insulin-stimulated glucose transport in rat adipocytes observed by treatment with HOE-642 was due to a reduction in accessible glucose transporters at the cell surface, plasma membrane GLUT4 was analysed by photolabelling with Bio-lc-ATB-BMPA. Insulin increased GLUT4 at the cell surface 7.3-fold over basal levels. This is lower than previously published photolabelling results performed with the ATB-[^{3}H]-BMPA photolabel in which insulin was shown to increase cell surface GLUT4 by 15-fold over basal control levels (Holman *et al.*, 1990). However these results indicate that an increase in GLUT4 translocation to the cell surface alone is not completely sufficient to compensate for the increase in glucose transport activity observed following insulin stimulation. This implies that the intrinsic activity of the glucose transporters can be modulated by the actions of insulin.

Pre-treatment of adipocytes with HOE-642 followed by insulin stimulation resulted in a decrease in cell surface labelling of GLUT4 by approximately 30% (*Figure 4.7A*), closely paralleling the results obtained in cardiomyocytes (*Figure 4.4*). Furthermore, HOE-642 had no effect on the total levels of GLUT4 detected in the solubilised supernatants from adipocytes (*Figure 4.7B*). In a second experiment serial dilutions of LDM protein were performed to produce a standard curve of GLUT4 which was compared with photolabelled GLUT4 in adipocyte plasma membranes. Thus in basal

Figure 4.7 The Effect of HOE-642 on the Cell Surface Levels of GLUT4 in Adipocytes As Judged By Photolabelling. Adipocytes were prepared as described in *Methods 2.2.2.* The cells were either left untreated (B), treated with 20 nM insulin (I), or treated with both 20 μM HOE-642 and 20 nM insulin (IH). The cells were photolabelled with 500 μM Bio-lc-ATB-BMPA, washed and solubilised in a Thesit detergent buffer. As a control an aliquot of cells was irradiated without photolabel (U). Photo-tagged GLUTs were precipitated on streptavidin beads. The resulting precipitates were analysed by SDS-PAGE and Western blotting with antibodies against GLUT4 (A). A small amount of solubilised protein from before the streptavidin precipitation was kept to check for equal loading (B). The material from the streptavidin precipitation was analysed by densitometry (C). The results shown are representative of 2 independent experiments.

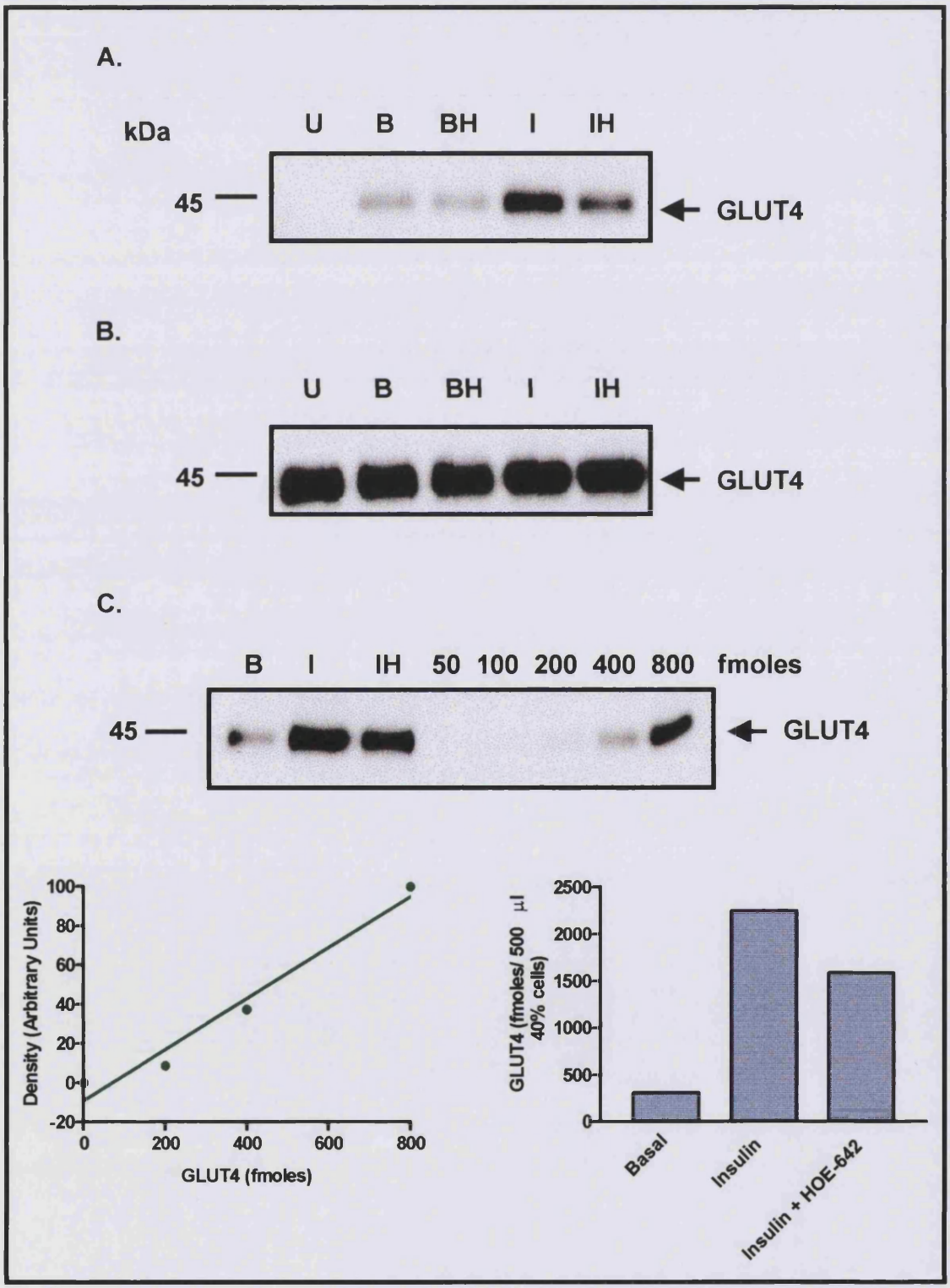

cells 309.3 fmoles of GLUT4/ 500µl 40% cells were detected in the plasma membrane. This increased to 2242.1 fmoles of GLUT4/ 500µl 40% cells upon stimulation with insulin, and was inhibited by HOE-642 to a level of 1583.8 fmoles of GLUT4/ 500µl 40% cells (*Figure 4.7C*).

4.2.3 Subfractionation of Rat Adipocytes Treated with HOE-642

Adipocytes contain a large single lipid droplet that displaces their cytoplasm to the periphery and gives them the shape of a small ring, measuring 2.55 ± 0.25 pl/cell (Arsenis *et al.*, 1995). Thus the scant cytosolic space in adipose cells complicates their analysis by confocal microscopy and as such the levels of GLUT4 in the plasma membrane and low density microsomes were determined by subcellular fractionation. As well as facilitating the analysis of GLUT4 distribution in adipocytes, the use of fractionation also gave us an independent, alternative method to confocal microscopy, with which to address this issue.

Adipocytes were either left untreated, treated with 20 nM insulin or with 20 nM insulin and 20 µM HOE-642. The cells were then fractionated (*see Methods, Section 2.5.1*) by centrifugation to give four subcellular fractions: the plasma membrane (PM), the low density microsomes (LDM), the high density microsomes (HDM) and the cytosol (Weber *et al.*, 1988). GLUT4 in the plasma membranes and the low density microsomes was analysed by SDS-PAGE and Western blotting.

In the basal state, immunoreactive GLUT4 was primarily localised to the low density microsomal fraction, with little GLUT4 at the plasma membrane. Upon insulin stimulation GLUT4 translocated to the plasma membrane with a paralleled decrease in the low density microsomes. Pre-treatment of adipocytes with HOE-642 did not significantly effect the redistribution of GLUT4 from the low density microsomes to the plasma membrane upon insulin stimulation (*Figure 4.8*). Thus the subfractionation data obtained from adipocytes correlates with the confocal micrographs of GLUT4 in cardiomyocytes.

Figure 4.8 Subfractionation of Rat Adipocytes Treated with HOE-642. Adipocytes were prepared as described in *Methods 2.2.2*. Once isolated, the cells were either left untreated (B), treated with 20 nM insulin (I), or treated with both 20 μM HOE-642 and 20 nM insulin (IH). The cells were then subfractionated as described in *Methods 2.5.1* to produces the low density microsomes (LDM) and the plasma membrane (PM). 20 μg of each of these fractions was analysed by SDS-PAGE and Western blotting with antibodies against GLUT4. The results shown are representative of 2 separate subfractionations. Data for basal (■), insulin (■) and insulin + HOE-642 (■) from the densitometric analysis of both subfractionations is shown in the lower panel with the results normalised to the basal LDM fraction. The minimum and maximum values are indicated by the error bars.

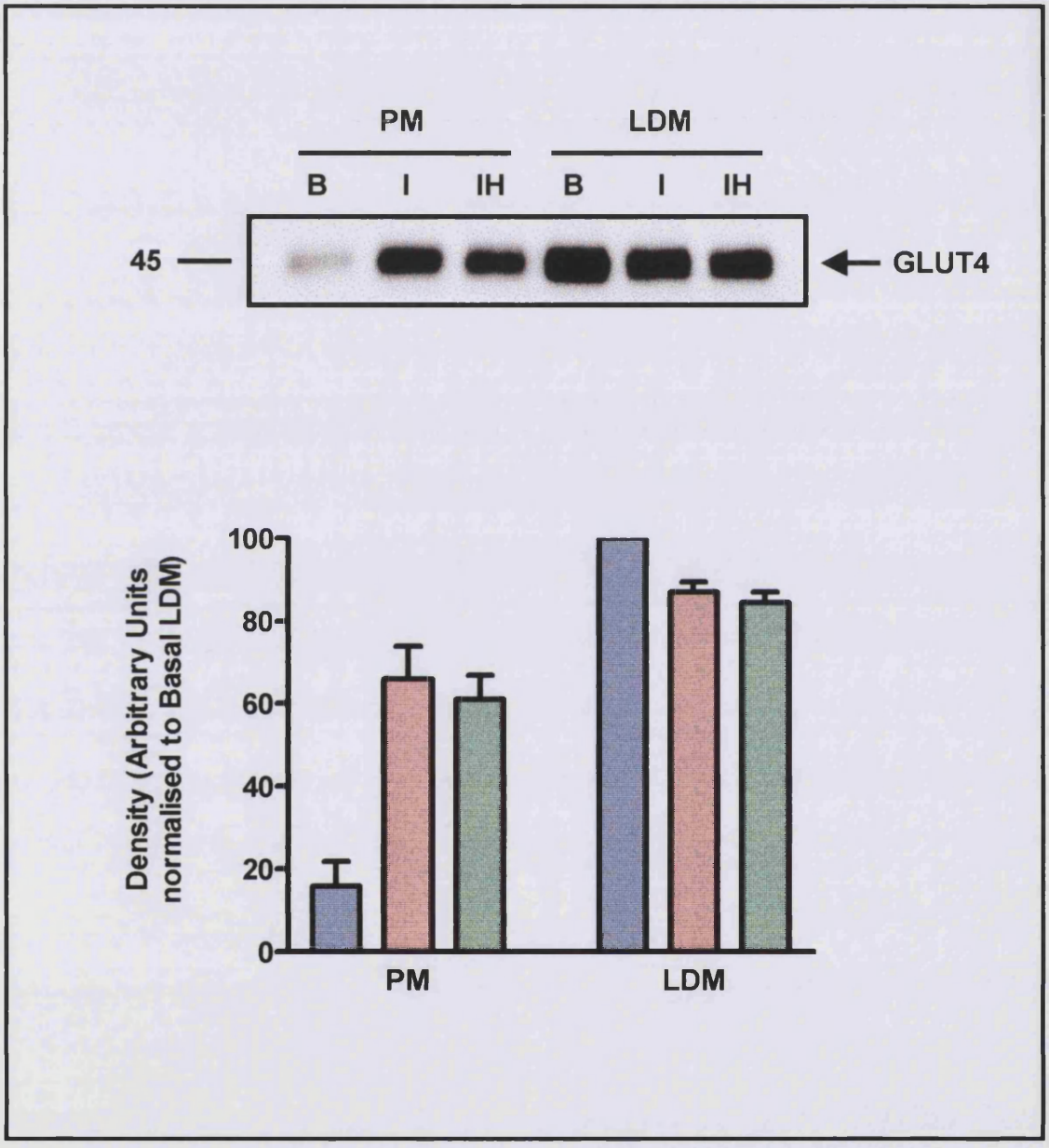

4.2.4 Comparison of the Effects of HOE-642 and Isoproterenol in Rat Adipocytes

Catecholamines belong to a group of hormones that cause insulin resistance by inhibiting insulin receptor binding and glucose transport activity in rat adipocytes (Arsenis and Tarvin, 1986). For example, isoproterenol attenuates insulin-stimulated glucose transport, particularly when adenosine is inactivated by adenosine deaminase. Furthermore treatment of adipocytes with isoprenaline results in the formation of an occluded population of vesicles which cannot be detected by photolabelling in intact adipocytes but which is detected by Western blotting of subcellular fractions or by photolabelling isolated membranes (Vannucci *et al.*, 1992). These alterations occur with a concomitant decrease in extracellular pH (Marjomaki *et al.*, 1994). In accordance with these observations, several studies have shown that isoproterenol inhibits NHE1 activity in rat adipocytes and that this inhibition occurs through activation of a β2-adrenergic receptor mechanism, which is achieved by adenylyl cyclase stimulation and a cAMP dependent pathway (Arsenis *et al.*, 1995).

Thus a comparison of the inhibition of insulin-stimulated glucose transport induced by isoproterenol, with that induced by HOE-642 in cells treated with adenosine deaminase was performed. As expected insulin-induced a massive increase in 3-*O*-methyl-D-glucose transport over basal levels (≈ 40-fold). Isoproterenol decreased insulin-stimulated 3-*O*-methyl-D-glucose transport by 73.6% from 0.1773 ± 0.0064 s^{-1} to 0.0467 ± 0.0199 s^{-1}. Similarly, although not to such a great extent, HOE-642 inhibited insulin-stimulated 3-*O*-methyl-D-glucose transport by ≈ 50%. The inhibition in the presence of adenosine deaminase was higher, than that observed in its absence (*Section 4.2.1*).

4.2.5 Localisation of the Sodium-Proton Pump in Rat Adipocytes

HOE-642 may alter membrane traffic by disrupting pH gradients in acidic vesicular compartments. Indeed many intracellular organelles including endosomes, clathrin coated vesicles, Golgi and other endomembrane structures contain specific ion pumps and channels to maintain their unique intraorganellar pH. Furthermore it has not yet been established whether NHE1 is sequestered in an intracellular compartment and translocated to the plasma membrane upon stimulation (Lin and Barber, 1996). Moreover a pharmacological profile for cloned NHE4 with respect to HOE-642 has yet

Figure 4.9 Comparison of the Effects of Isoproterenol and HOE-642 on Insulin-Stimulated Glucose Transport in Rat Adipocytes. Adipocytes were prepared according to *Methods 2.2.2*. An aliquot of cells was removed (B) and the remainder were washed once in KRH supplemented with 200 nM adenosine. Cells were either left untreated (B), treated with 20 nM insulin (IA), treated with 20 nM insulin plus 1 μM isoproterenol and 1 U/ml adenosine deaminase (IA+ADA+Iso) or treated with 20 nM insulin plus 20 μM HOE-642 and 1 U/ml adenosine deaminase (IA+ADA+HOE-642) for 30 min at 37°C. Following treatment ^{14}C-3-*O*-methyl-D-glucose uptake was performed as described in *Methods 2.4.1*, except that cells were adjusted to give a 15% cytocrit. The results shown are representative of 3 separate experiments (paired, two-tailed t-tests with 95% confidence intervals).

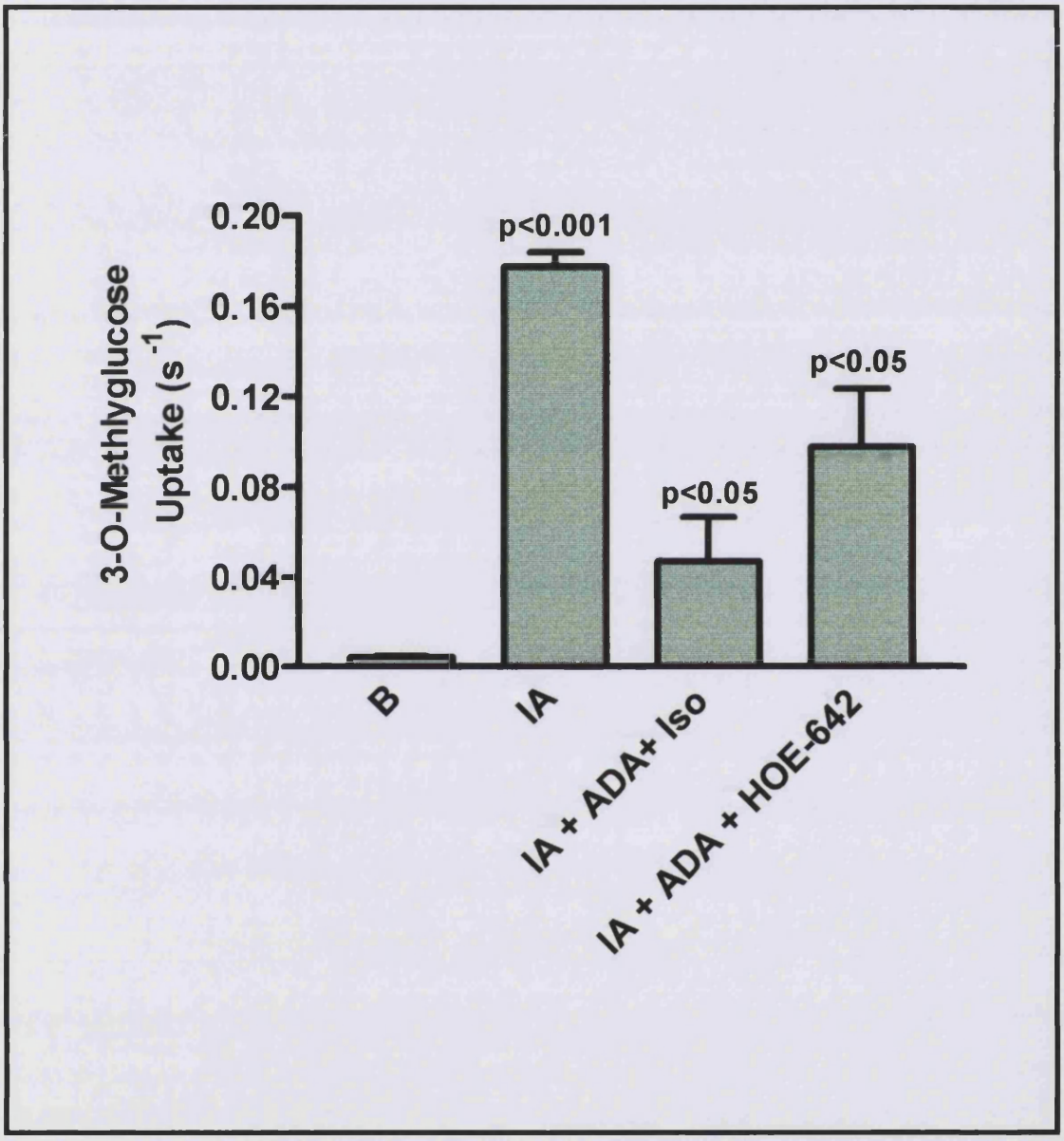

to be produced (Loh *et al.*, 1996). The yeast homologue of this Na^+/H^+ antiporter Nhx1 is located exclusively intracellularly (Nass and Rao, 1998) and so an involvement of the mammalian equivalent in glucose transport cannot be ruled out. Thus, an investigation into the possibility that GLUT4-vesicles might be endowed with a NHE pump was undertaken. Initially plasma membrane and low density microsomal fractions were analysed for NHE1 content by SDS-PAGE and Western blotting. Clear signals for NHE1 were detected in both the plasma membrane and LDM fractions. Indeed a slight decrease in NHE1 in the LDM fraction was observed in the insulin-stimulated sample, although no significant increase in immunoreactive NHE1 in the plasma membrane was detected (*Figure 4.10A*).

Since NHE1 was clearly detected in the low density microsomal fraction, we next tested whether NHE1 was directly associated with GLUT4 vesicles. To this end GLUT4 vesicles were immunoprecipitated on acrylic beads coated with non-specific rabbit IgG (NS) or affinity purified rabbit GLUT4 antibodies (GLUT4). Vesicle associated proteins were solubilised in a detergent buffer (soluble). Bound GLUT4 was eluted by denaturing the GLUT4 antibodies by heating to 95°C for 5 min in SDS-sample buffer supplemented with 20 mM DTT (insoluble). Both the detergent soluble and insoluble fractions were resolved by SDS-PAGE and analysed by Western blotting with antibodies against GLUT4 and NHE1. Mouse and chicken antibodies were used for the Western blotting of GLUT4 and NHE1 respectively, to obviate interference by the heavy chain of the immmunoprecipitating polyclonal antibody. As illustrated, significant amounts of GLUT4 vesicles were found immunoadsorbed to the beads only when anti-GLUT4 antibodies were used, and not when non-specific rabbit IgG was employed (*Figure 4.10B, top panel*). Extensive characterisation of this system for immunoprecipitating GLUT4 vesicles has been performed and is detailed (*Chapter 5, Sections 5.3.1, 5.3.2 and 5.3.5*). The efficiency of this method of GLUT4 vesicle immunoadsorption is 67%.

The immunoprecipitated vesicles were tested for the presence of NHE1. As illustrated in *Figure 4.10B, lower panel*, no NHE1 was detected on immunoprecipitated GLUT4 vesicles, whereas a clear signal was obtained in the control total membrane standard resolved in lane 1. Thus immunoprecipitated GLUT4-organelles are devoid of NHE1 activity. The ostensible absence of the NHE1 exchanger from GLUT4 vesicles suggests that either (a) a separate compartment endowed with NHE pumps is essential for the

Figure 4.10 Localisation of the Sodium-Proton Pump NHE-1 in Rat Adipocytes. A. Basal and insulin treated adipocytes were homogenised and subfractionated by differential centrifugation as described in *Methods 2.5.1* to produce the low density microsomes (LDM) and the plasma membrane (PM). 20 μg of each fraction was resolved by SDS-PAGE and analysed by Western blotting with a polyclonal antibody against NHE-1. B. GLUT4 vesicles were immunoadsorbed on acrylic beads coated with non-specific IgG (NS) or affinity purified anti-GLUT4 antibodies (GLUT4). Vesicle associated proteins were eluted in a detergent buffer (soluble). Proteins bound to the beads were released by heating at 95°C for 5 min (insoluble). Both the soluble and insoluble material was resolved by SDS-PAGE and analysed by Western blotting with antibodies against GLUT4 and NHE-1. A 50 μg total membrane control (TM) was run in lane 1. The results shown are representative of 2 independent experiments.

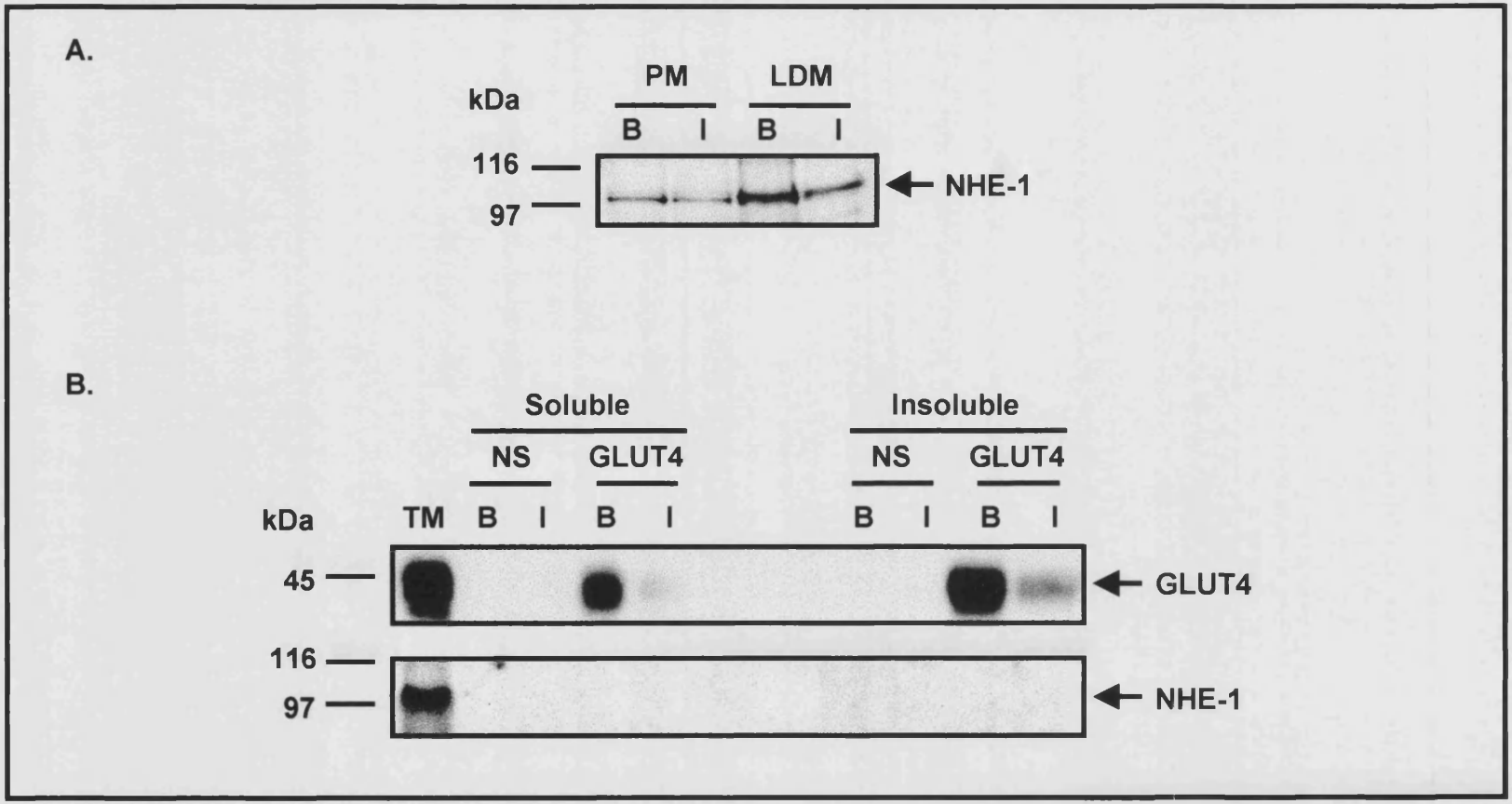

translocation and activation of glucose transporters, (b) that another NHE exchanger, possible NHE4, is active in these organelles or (c) that global effects on the cytoplasmic pH, perhaps involving perturbations of the insulin-signalling pathway are responsible for the inhibition of insulin-stimulated glucose transport.

4.2.6 The Effect of HOE-642 on the Distribution of Signalling Molecules at the Plasma Membrane

The insulin-inhibiting effects of HOE-642 may results from interference within steps of the insulin-signalling pathway or by mis-localisation of signalling molecules. Thus an investigation into whether the distribution of the insulin receptor was altered by treatment of adipocytes with HOE-642 was performed. Plasma membranes obtained from basal, insulin-stimulated and HOE-642/insulin-treated adipocytes were resolved by SDS-PAGE and analysed by Western blotting with an antibody against the α-subunit of the insulin receptor.

As demonstrated in *Figure 4.11, top panel* levels of insulin receptors present in the plasma membrane fractions were slightly decreased following insulin stimulation due to insulin-induced insulin receptor internalisation. This is in agreement with previous studies which have shown that approximately 10% of the insulin receptors at the plasma membrane are internalised following administration of insulin (Heller-Harrison *et al.*, 1995; Chinni and Shisheva, 1999). However treatment of cells with HOE-642 and insulin appeared to inhibit this insulin-induced receptor internalisation. Since the effects on insulin receptor internalisation induced by insulin are small, these experiments would need to be repeated many times in order to be confident that HOE-642 behaves in a manner similar to the unstimulated samples.

Since targeting of 'non-functional' GLUT4 to the cell periphery in HOE-642/insulin-treated cells was observed we next investigated whether other components of the insulin-signalling pathway were mis-targeted to the plasma membrane. Insulin receptor substrate-1 (IRS-1), PI 3-kinase and protein kinase B (PKB) which are localised primarily to the low density microsomes and the cytosol, were all detected in the plasma membrane fraction derived from basal adipocytes at low concentrations. The levels of IRS-1 and PKB at the plasma membrane decreased following insulin stimulation, however no change in the association of PI 3-kinase was observed. Plasma membrane

Figure 4.11 The Effect of HOE-642 on the Distribution of Insulin Signalling Molecules at the Plasma Membrane. Adipocytes were prepared as described in *Methods 2.2.2*. Following isolation adipocytes were treated with 20 nM insulin (I), with 20 μM HOE-642 and 20 nM insulin (IH) or were left untreated (B). The adipocytes were then homogenised and subfractionated as described in *Methods 2.5.1* to produce the plasma membrane fraction (PM). 50 μg of plasma membrane from each condition (B, I and IH) were resolved by SDS-PAGE and analysed by Western blotting with antibodies against the insulin receptor α-subunit, the insulin receptor substrate-1, PI 3-kinase p85α-subunit and Protein Kinase B.

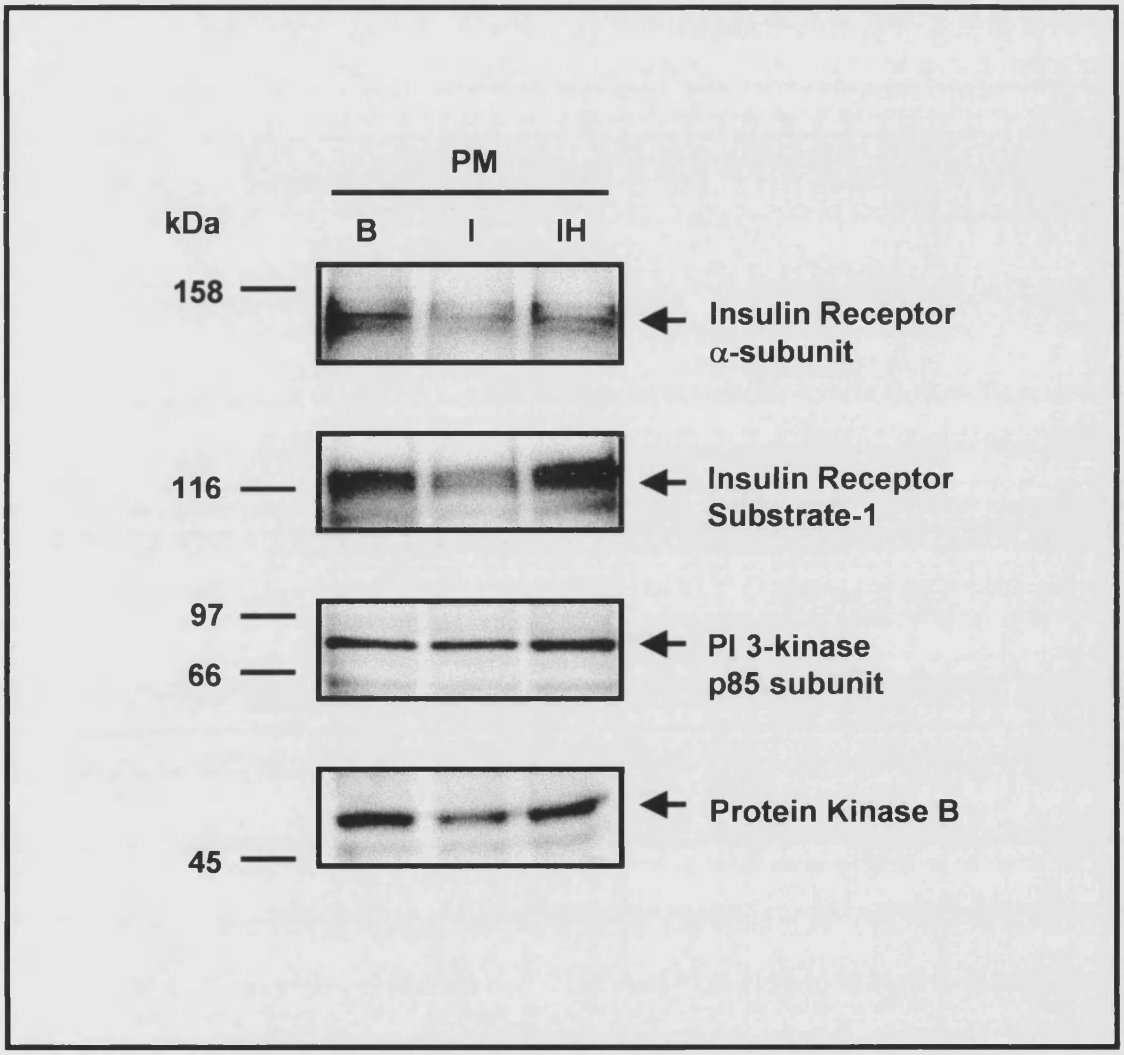

fractions derived from HOE-642/insulin-treated adipocytes displayed a distribution of signalling molecules similar to basal adipocytes, perhaps indicating that changes in cytosolic pH induced by HOE-642 perturb elements of the insulin-signalling pathway. Further experiments could examine whether the activity of signalling molecules (e.g. phosphorylation of tyrosine residues on the insulin receptor and IRS-1) are altered by the actions of HOE-642.

4.3 Studies with the Vacuolar ATPase Inhibitor Bafilomycin A_1

GLUT4 has been localised to a number of endosomal-tubulovesicular structures by immunoelectron microscopy (Slot *et al.*, 1991a; Slot *et al.*, 1991b). These and other biochemical data (Malide *et al.*, 1997; Millar *et al.*, 1997) suggest that the interaction of GLUT4 with certain membrane compartments is responsible for the formation of a specialised GLUT4 population. One of the features of endosomal, and endosomal-like organelles including Golgi and lysosomes is their controlled pH. Although the exact mechanism by which endosomal pH regulates membrane trafficking has yet to be elucidated, it is well established that endosomal pH is required for the dissociation of ligands from their receptors and for the recycling of a number of membrane receptors back to the plasma membrane (Mellman, 1996). Recently an investigation into the role of pH in the function of endosomal and endosomal-like membranes in GLUT4 trafficking was performed (Chinni and Shisheva, 1999). Using 3T3-L1 adipocytes these authors examined the distribution of GLUT4 following administration of the v-ATPase inhibitor, bafilomycin A_1. Incubation of 3T3-L1 adipocytes with this inhibitor resulted in an increase in GLUT4 at the plasma membrane, and thus it was proposed that bafilomycin A_1 exhibits insulinomimetic effects (Chinni and Shisheva, 1999).

4.3.1 Changes in Intracellular pH Assessed with the Acidotrophic Dye Acridine Orange

To further examine the role of intra-organelle acidification in GLUT4 trafficking, changes in the intracellular pH of cardiomyocytes induced by treatment with bafilomycin A_1 were analysed. To this end, isolated cardiomyocytes were either left untreated (basal), treated with 30 nM insulin for 30 min, treated with 100 nM bafilomycin A_1 or treated with a combination of insulin and bafilomycin A_1, before staining with acridine orange. As already documented (*Section 4.1.1*) in basal

Figure 4.12 The Effect of Bafilomycin A_1 on the Intracellular pH As Judged By Vital Fluorescence. Cardiomyocytes were prepared as described in *Methods 2.2.3*. The cells were either left untreated (A), treated with 30 nM insulin for 30 min (B), treated with 100 nM bafilomycin A_1 (C) or treated with both 30 nM insulin and 100 nM bafilomycin A_1 (D). The cells were then incubated for 10 min with 5 μg/ml acridine orange, then washed and mounted in Vectorshield. The cells were viewed using a Zeiss confocal scanning microscope (LSM510) with dual lasers set at 458/488 nm and 543 nm.

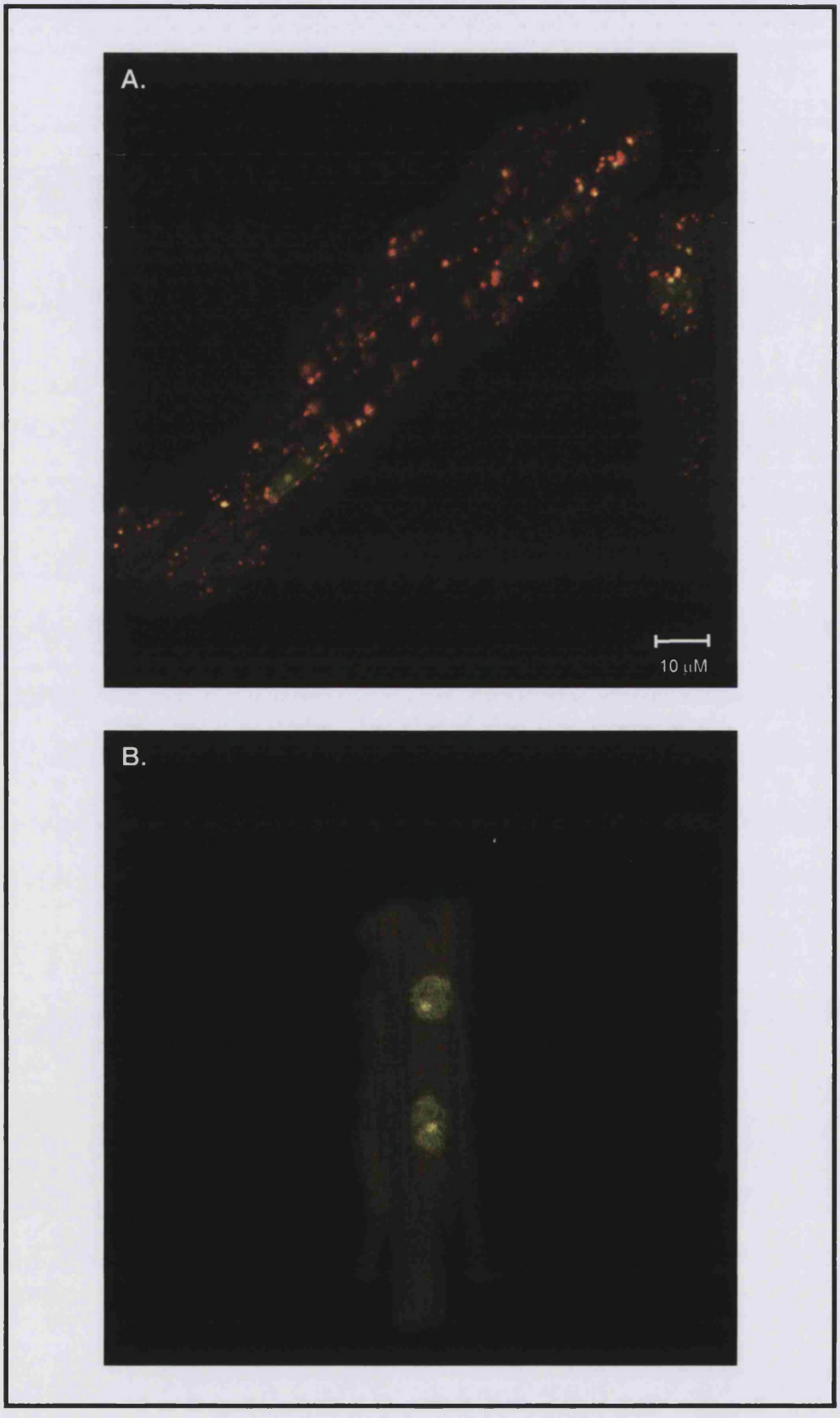

Figure 4.12 cont. The Effects of Bafilomycin A_1 on Intracellular pH As Judged By Vital Fluorescence.

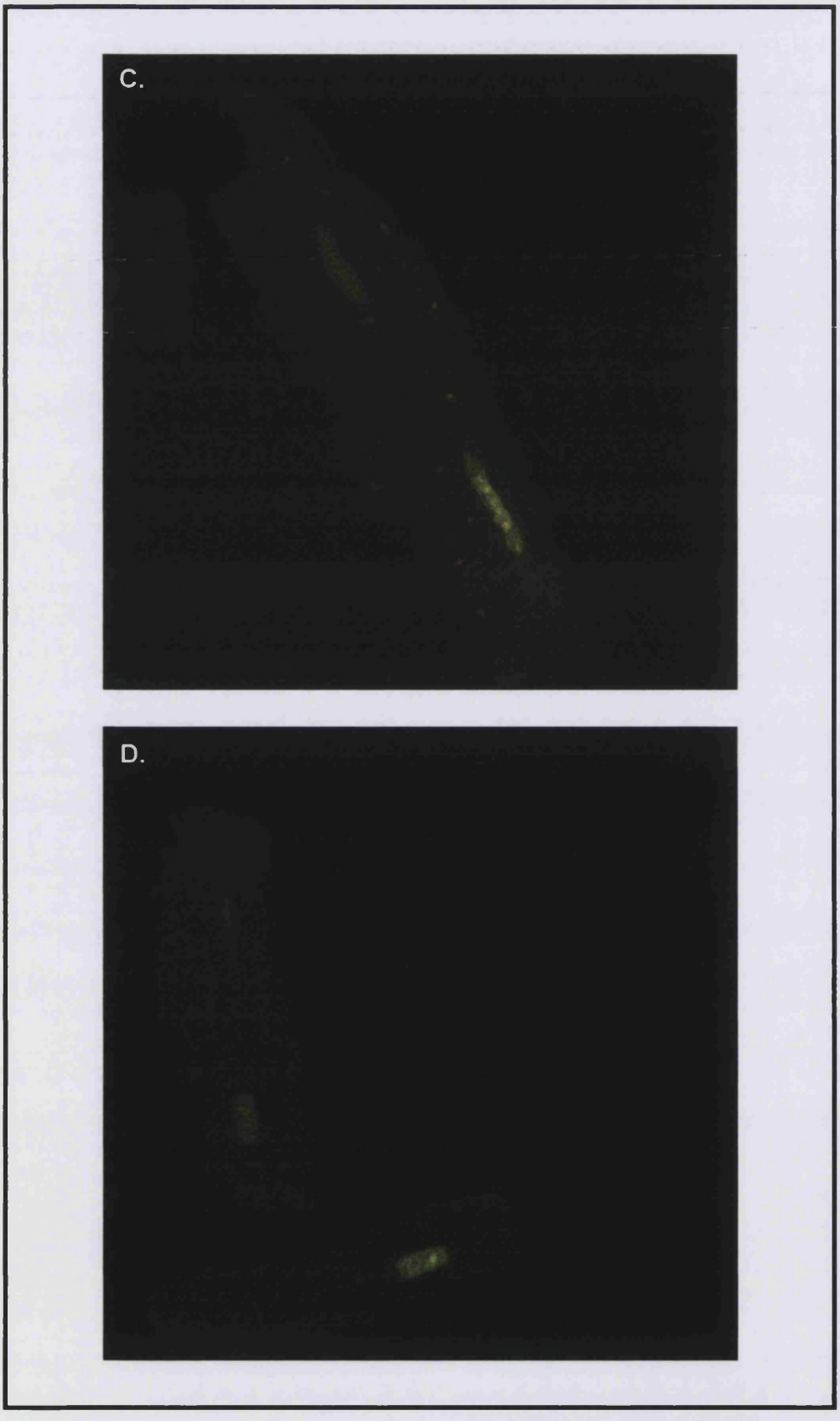

cardiomyocytes the cytoplasm, nuclei and nucleoli exhibited green fluorescence while a number of large red/orange vesicular structures were observed dispersed throughout the cytoplasm, and clustered around the nuclei (*Figure 4.12A*). Upon administration of insulin a marked decrease in red/orange labelling was observed, while the cytoplasm and nuclei remained green (*Figure 4.12B*). These results are supported by earlier studies which indicate that insulin induces a rapid alkalinisation of the cytoplasm, detectable in < 2 min and sustained for up to 1 h (Klip *et al.*, 1986).

Incubation of cells with bafilomycin A_1 effectively inhibited the acidification of the lysosomal/endosomal structures with only a small number of yellow organelles visible (*Figure 4.12C*). This is in good agreement with studies of the effect of bafilomycin A_1 detected by acridine orange staining in A431 and BNL CL.2 cells (Yoshimori *et al.*, 1991). Treatment of cardiomyocytes with insulin and bafilomycin also prevented the accumulation of acridine orange in endosomal/lysosomal compartments as expected (*Figure 4.12D*).

4.3.2 Inhibition of Insulin-Stimulated Glucose Uptake in Cardiac Myocytes by Bafilomycin A_1

In the study documenting the effects of bafilomycin A_1 on GLUT4 trafficking in 3T3-L1 adipocytes (Chinni and Shisheva, 1999), a direct measurement of the effect of bafilomycin A_1 on glucose transport was not performed. Thus we decided to test whether bafilomycin A_1 altered the rate of 2-deoxy-D-glucose transport in cardiomyocytes. Low concentrations of bafilomycin A_1 marginally increased the level of basal glucose transport. However in contrast to Chinni and Shisheva who saw an increase in GLUT4 at the cell surface upon increasing concentrations of bafilomycin A_1 (Chinni and Shisheva, 1999), the rates of 2-deoxy-D-glucose transport did not increase, indeed a decrease back to the basal level was observed (*Figure 4.13A*). Furthermore, and again in contrast to the results obtained in 3T3-L1 adipocytes, the level of stimulation by bafilomycin A_1 was small in comparison to the level of stimulation induced by insulin, (*Figure 4.13A and B*). Bafilomycin A_1 increased 2-deoxy-D-glucose transport by 1.4-fold over basal levels, whereas insulin increased basal 2-deoxy-D-glucose transport by 5.9-fold. The absolute values for transport being 0.0084 ± 0.0016 nmoles/min/mg of protein, 0.0119 ± 0.0027 nmoles/min/mg of protein and 0.0494 ± 0.0054 nmoles/min/mg of protein for basal, bafilomycin A_1-treated and

Figure 4.13 Inhibition of Insulin-Stimulated Glucose Uptake in Cardiac Myocytes by Bafilomycin A_1. Cardiomyocytes were prepared according to *Methods 2.2.3*. A. Cells were either left untreated, treated with 30 nM insulin or treated with various concentrations of bafilomycin A_1. The top panel compares the level of stimulation induced by bafilomycin A_1 with insulin. The lower panel is a titration curve of bafilomycin A_1 without insulin. B. Cells were either left untreated (B), treated with 30 nM insulin (I) or treated with 20 nM insulin and 100 nM bafilomycin A_1 for 30 min at 37°C. In all cases 2-deoxy-D-[^{3}H]-glucose uptake was measured as described in *Methods 2.4.2*. The results shown in B are representative of 3 separate experiments (paired, two tailed t-test with 95% confidence intervals).

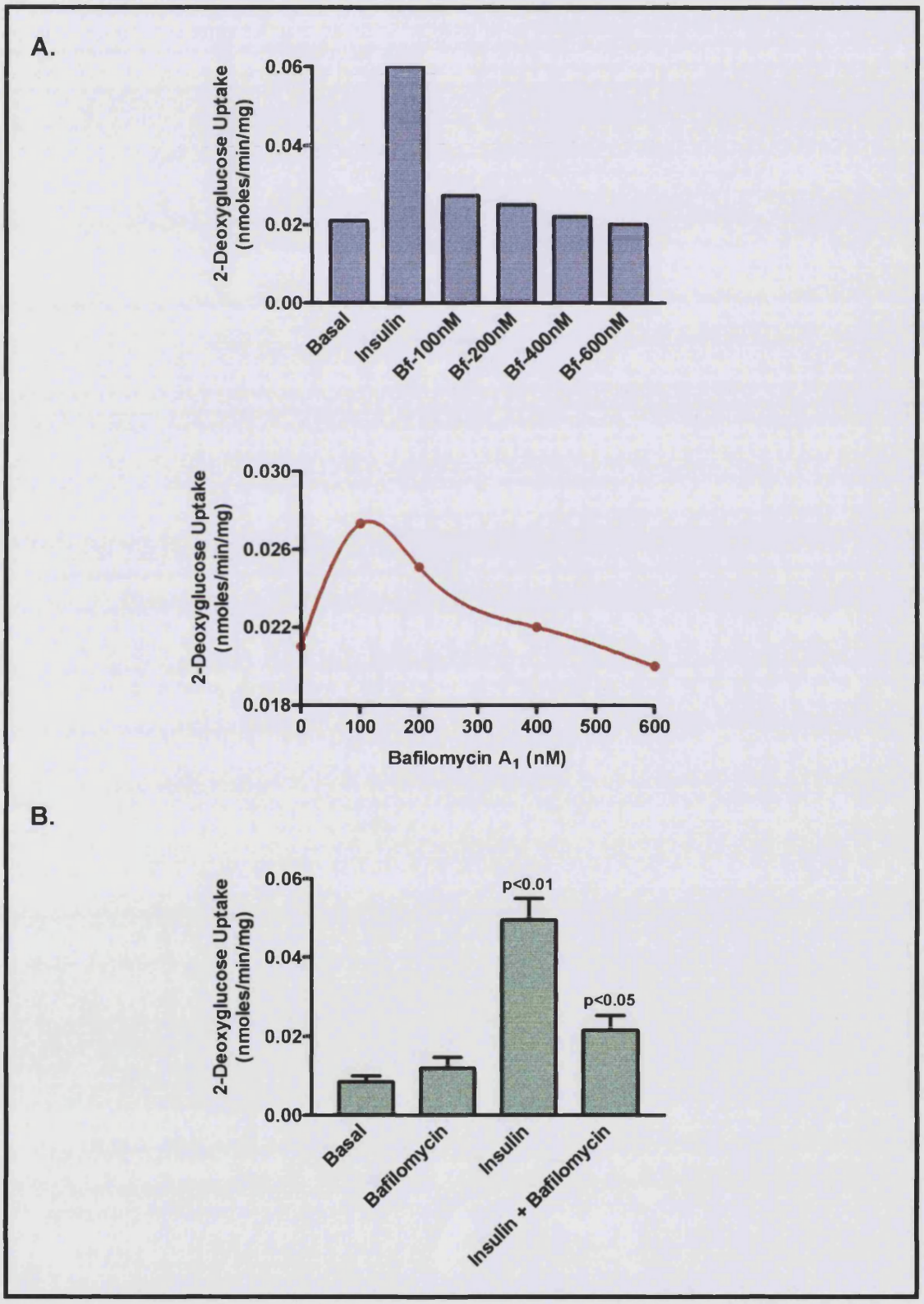

insulin-treated cardiomyocytes, respectively. Unexpectedly treatment of cardiomyocytes with insulin and bafilomycin A_1 resulted in a decrease in 2-deoxy-D-glucose transport of approximately 60%, to 0.0215 ± 0.0036 nmoles/min/mg of protein, compared with the insulin sample.

4.3.3 The Effect of Bafilomycin A_1 on Cell-Surface Levels of GLUT4 in Cardiomyocytes

To determine whether the effects of bafilomycin A_1 on glucose transport are due to a loss of functional GLUT4 from the cell-surface, GLUT4 at the plasma membrane was photo-tagged with Bio-lc-ATB-BMPA. Thus following cell isolation, myocytes were either left untreated or treated with 30 nM insulin, with 100 nM bafilomycin or with a combination of both reagents (at the same concentrations), then photolabelled with 500 μM Bio-lc-ATB-BMPA. The cells were washed, solubilised and precipitated on streptavidin beads. Following an overnight incubation the precipitated transporters were eluted and resolved by SDS-PAGE. Biotinylated transporters were analysed by Western blotting with antibodies against GLUT4.

Preliminary experiments indicated that both bafilomycin A_1 and bafilomycin A_1 in combination with insulin, reduce the number of glucose transporters present at the cell surface. Comparison of the inhibition induced by bafilomycin A_1 with that induced by HOE-642 suggests that direct perturbation of organelle pH is more potent in inhibiting GLUT4 activity at the plasma membrane, than the global effects on the cytoplasmic pH induced by HOE-642 (*Figure 4.14*).

4.3.4 Distribution of the Insulin-Sensitive Glucose Transporter GLUT4 Revealed by Confocal Microscopy

To further analyse the distribution of GLUT4 following bafilomycin A_1 treatment, cardiomyocytes were analysed by confocal microscopy. Thus following incubation with bafilomycin A_1, with insulin or a combination of both reagents, myocytes were fixed in 4% paraformaldehyde and permeabilised with 0.1% saponin. The cells were then probed with mouse monoclonal antibodies against GLUT4, washed and incubated with rhodamine-conjugated anti-mouse antibodies. The myocytes were washed again, then mounted and viewed in Vectorshield.

Figure 4.14 The Effect of Bafilomycin A_1 on the Cell Surface Levels of GLUT4 in Cardiomyocytes As Judged By Photolabelling. Cardiomyocytes were prepared as described in *Methods 2.2.3.* The cells were either left untreated (B), treated with 20 μM HOE-642 (BH), treated with 30 nM insulin (I), treated with 20 μM HOE-642 and 30 nM insulin (IH), treated with 100 nM bafilomycin A_1 (Bf) or treated with both 100 nM bafilomycin A_1 and 30 nM insulin. The cells were photolabelled with 500 μM Bio-lc-ATB-BMPA, washed and solubilised in a Thesit detergent buffer. Photo-tagged GLUTs were precipitated on streptavidin beads. The precipitates were analysed by SDS-PAGE and Western blotting with antibodies against GLUT4 (A). The results were analysed by densitometry (B).

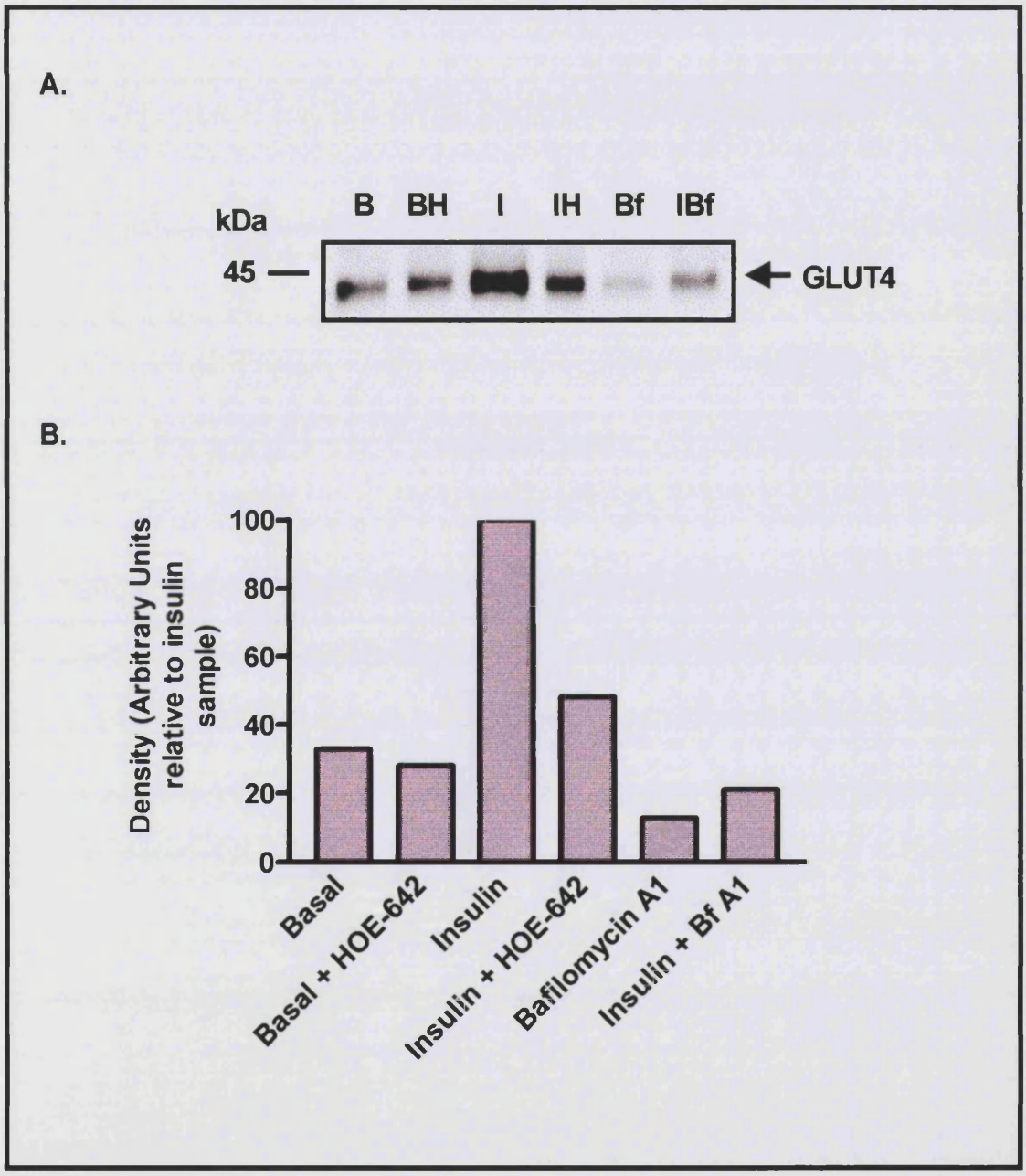

As already shown, GLUT4 labelling in basal cardiac myocytes was intracellular and concentrated around the nuclei and along transverse striations (*Figure 4.15A*). Upon insulin stimulation a marked translocation of GLUT4 from the intracellular locus to the plasma membrane was observed (*Figure 4.15B*). Likewise and in agreement with the subfractionation data obtained in 3T3-L1 adipocytes (Chinni and Shisheva, 1999), bafilomycin A_1 alone and in conjunction with insulin, caused the re-location of GLUT4 to the cell periphery. These findings suggest that GLUT4 activity at the plasma membrane can be partially dissociated from the cell-surface content of GLUT4. Thus either the intrinsic activity of GLUT4 is subject to regulation i.e. by a conformational change allowing glucose (and glucose analogues) to bind, or GLUT4 exists in an occluded population of vesicles, close to but not completely associated with the plasma membrane. This latter suggestion is supported by the observation that following insulin stimulation in rat adipocytes GLUT4 enters the plasma membrane rapidly and then there is a slower transition to a caveolae-enriched subdomain of the plasma membrane where glucose transport takes place (Gustavsson *et al.*, 1996).

Figure 4.15 The Effect of Bafilomycin A_1 on the Distribution of GLUT4 in Cardiomyocytes. Cardiomyocytes were prepared as described in *Methods 2.2.3*. The cells were either left untreated (A), treated with 30 nM insulin (B), treated with 100 nM bafilomycin A_1 (C) or treated with 100 nM bafilomycin A_1 followed by 30 nM insulin for 30 min (D). The cells were fixed with paraformaldehyde, solubilised with saponin and probed with mouse antibodies against GLUT4. The cells were then washed and incubated with rhodamine-conjugated anti-mouse antibodies. The samples were viewed using a Zeiss laser scanning microscope (LSM510) with 543 nm lasers.

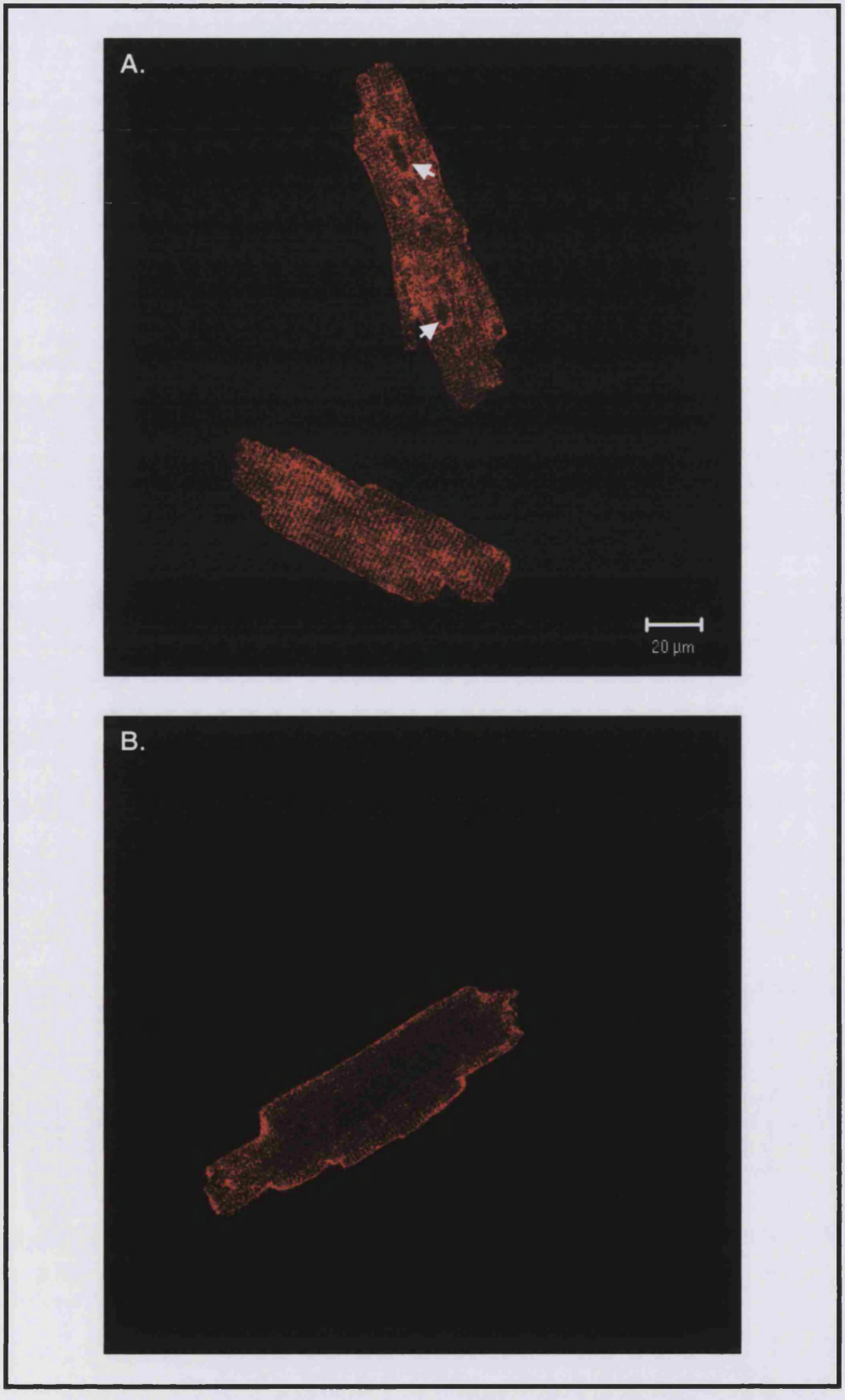

Figure 4.15 cont. The Effect of Bafilomycin A_1 on the Distribution of GLUT4 in Cardiomyocytes.

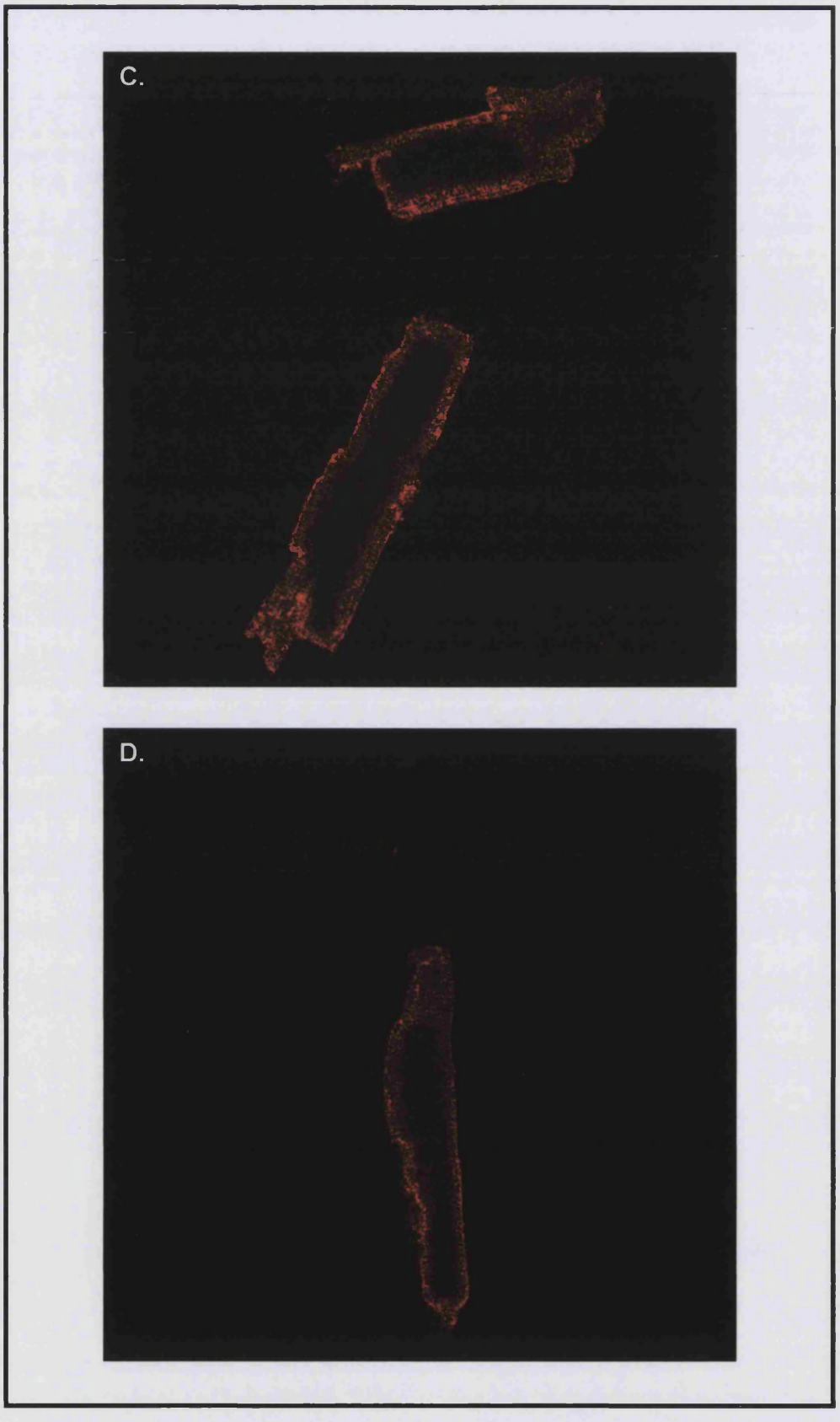

4.4 Discussion

Many organelles including clathrin-coated vesicles, endosomes, the Golgi apparatus, multivesicular bodies and secretory granules are acidified to varying degrees (Mellman *et al.*, 1986). These elements of the endocytic and exocytic pathways contain various ion channels and proton pumps which precisely control inter-organelle acidification (Forgac, 1989). The functions served by pH have been the subject of intense investigation and several physiological roles have been established. These include receptor-ligand dissociation and receptor recycling (Mellman *et al.*, 1986).

Much of what is known about the functions of intracellular pH has been learned from classical studies employing weak bases (e.g. chloroquine, NH_4Cl) or ionophores (e.g. monesin) to dissipate pH gradients (Mellman *et al.*, 1986; Maxfield and Yamashiro, 1991). Treatment of cells with these agents leads to concurrent endosome alkalinisation and decreased numbers of cell-surface receptors, however receptor internalisation is unaffected. Furthermore in the presence of these compounds a number of proteins are seen to accumulate in endosomes. These include the TfR (Stoorvogel *et al.*, 1987), TGN38 (Chapman and Munro, 1994) and the cation-independent mannose-6-phosphate receptor, indicating that dissipation of the pH gradient has affected receptor externalisation (Johnson *et al.*, 1993). However in some cases transport continues, for example, neither weak bases nor monesin block Fc-receptor recycling (Mellman *et al.*, 1984). Moreover chloroquine inhibits insulin-induced translocation of GLUT4 to the cell surface independent of its effects on endosomal pH (Romanek *et al.*, 1993). Thus much remains to be elucidated concerning the role of intracellular pH on protein trafficking.

Insulin plays an important role in Na^+ metabolism, and as such has been implicated in a number of clinical conditions associated with Na^+ imbalance. These include Na^+ wasting in poorly controlled diabetes, natriuresis of starvation and increased Na^+ reabsorption in hypertensive patients with type II diabetes (Arsenis *et al.*, 1995). In addition insulin stimulates glucose transport activity and glycolysis and raises the intracellular pH by activating the Na^+/H^+ antiport in various cells including muscle and fat (Mukherjee and Mukherjee, 1981; Fidelman *et al.*, 1982).

Amiloride which inhibits glucose transport and glycolysis blocks Na^+/H^+ exchange (Fidelman *et al.*, 1982; Klip *et al.*, 1986; Klip *et al.*, 1988) by acting as a competitive inhibitor (Holman *et al.*, unpublished observation). However the effects of amiloride are diverse and as such this study was undertaken to determine whether inhibition of Na^+/H^+ exchange activity alone would attenuate insulin-stimulated glucose transport. This was achieved using the selective NHE1 inhibitor HOE-642.

In the absence of HCO_3^-, the Na^+/H^+ exchanger is the only mechanism for maintaining intracellular pH (pH_i) and pH_i recovery following an acid load (Aronson, 1985). Thus to isolate the Na^+/H^+ exchanger all experiments were performed in nominally HCO_3^- free buffer. Under these conditions, HOE-642 markedly inhibited insulin-stimulated glucose transport, and the ability of the exofacial photolabel Bio-lc-ATB-BMPA to detect functional GLUT4 at the cell surface. However using both subfractionation of adipocytes and by confocal microscopical analysis of GLUT4 in cardiomyocytes a substantial translocation of GLUT4 to the cell periphery could be demonstrated. The mechanism by which this occurs appears to involve a reversible occlusion or disruption of the exofacial sugar-binding site of the glucose transporter protein.

It is now well established that insulin stimulates glucose transport by inducing the translocation of GLUT4 from an intracellular storage compartment to the plasma membrane (Suzuki and Kono, 1980; Cushman and Wardzala, 1980). However the magnitude of GLUT4 translocation, as determined by Western blotting of GLUT4, or cytochalasin B binding to plasma membranes does not always fully account for the increase in glucose transport activity measured in intact cells (Simpson *et al.*, 1983). The discrepancy between transporter number and activity is more marked when the actions of catecholamines such as isoprenaline (which inhibits Na^+/H^+ exchange) in conjunction with insulin are analysed (Kuroda *et al.*, 1987). This initially led to the hypothesis that these catecholamines alter the intrinsic catalytic activity of glucose transporters in the plasma membrane (Kuroda *et al.*, 1987). In addition, labelling cells with the cell impermeant bis-mannose photolabel ATB-[^{3}H]-BMPA, has shown that like HOE-642, isoprenaline decreases the number of 'active' glucose transporters at the cell surface, while subfractionation data shows little change in the plasma membrane content of these glucose carriers (Vannucci *et al.*, 1992). Taken together these data imply that isoprenaline induces an alteration but not a loss of glucose transporters in the plasma membrane of intact cells such that they can neither bind photolabel nor transport

glucose. One interpretation of these results is that neither isoprenaline nor HOE-642 affect the stimulation of GLUT4 to the plasma membrane by insulin, but that they both prevent the full 'activation' of transporters by the formation of a pre-fusion competent population of vesicles (Vannucci *et al.*, 1992). This model is consistent with the observation that isoprenaline alters the V_{max} of glucose transporters without effecting the apparent K_m for 3-*O*-methyl-D-glucose (Smith *et al.*, 1984). Alternatively HOE-642 and isoprenaline may induce a conformational change in the glucose transporter protein itself, such that it can no longer bind sugar.

The mechanism by which isoprenaline and HOE-642 induce the formation of the 'masked' population of vesicles is unknown but may occur by a common inhibition of Na^+/H^+ exchange. Alternatively the potential involvement of heteromeric G-proteins in the isoprenaline-induced occluded state has been implicated from the actions of pertussis toxins and cholera on this system (Honnor *et al.*, 1992). However as yet no direct interaction between a G-protein and GLUT4 has been observed, and as such this system requires further study. Another possible explanation for the occluded state stems from the observation that isoprenaline can induce the activation of adenylyl cyclase and hence PKA. In turn PKA can phosphorylate the t-SNARE syntaxin 4 at the plasma membrane, thus blocking the interaction of syntaxin 4 and VAMP2 and therefore inhibiting the fusion of GLUT4 vesicles with the plasma membrane (Foster *et al.*, 1998).

Treatment of cardiomyocytes with low doses of isoproterenol leads to mild acidification of their cytosol. During this time, late endosomes show signs of fragmentation and microtubule-dependent movement towards the cell periphery, while the subcellular distribution of lysosomes is unchanged (Marjomaki *et al.*, 1994). Ultrastructural data reveal that these small vesicles are formed by the vesiculation of large perinuclear late endosomes and that treatment of cells with nocodazole, following acidification results in fewer vesicles at the periphery. Since a movement of GLUT4 to the cell surface following treatment of cells with HOE-642 was observed, it may be the case that inhibition of Na^+/H^+ exchange leads to fragmentation of endosomes and the passive movement of GLUT4 vesicles to the cell exterior. Since there must also be a block in fusion with the plasma membrane or in the priming of fusion, GLUT4 vesicles remain associated with microtubules in the cytoplasm. It would therefore be of interest to test whether treatment of cardiomyocytes with nocodazole following acidification, inhibits

the movement of GLUT4 vesicles. Furthermore if inhibition of Na^+/H^+ exchange alone results in the fragmentation of endosomes one could speculate that treatment of basal cells with HOE-642 would lead to a similar translocation of vesicles to the cell periphery. This requires further experimentation, however it is interesting to note that basal myocytes treated with HOE-642 exhibit a slight increase in glucose transport activity, which may be a result of aberrant fusion of some of these endosomal fragments with the plasma membrane.

Kinesin has been shown to be responsible for centrifugal elongation of lysosomes along tubules (Hollenbeck and Swanson, 1990). From the data in this chapter it is not possible to conclude which proteins or factors are responsible for the movement of GLUT4 to the cell surface in the presence of HOE-642. GLUT4 tethers have been postulated including spectrin (Tsakiridis *et al.*, 1994) and aldolase (Kao *et al.*, 1999), although the precise roles of these proteins in GLUT4 trafficking remain to be elucidated, and as yet no information regarding their control by changes in pH has been reported.

It is well documented that the regulation of intracellular pH in the myocardium is of particular importance for several physiological processes. Firstly a change in intracellular pH induces an alteration in contractility (Orchard and Kentish, 1990). Secondly activation of the Na^+/H^+ pump, one of the major regulators of intracellular pH after ischemia induced acidosis, plays a key role in the development of alterations related to reperfusion (Karmazyn and Moffat, 1998). The drug HOE-642 is known to possess cardioprotective properties during ischemia and reperfusion (Scholz *et al.*, 1995). The protective effects of HOE-642 were originally assumed to be due to the prevention of intracellular sodium and calcium ion overload. However more recently the actions of HOE-642 have been attributed to its ability to prevent the recovery of intracellular pH from anoxic acidification during re-oxygenation (Russ *et al.*, 1996). Thus low intracellular pH during re-oxygenation appears to be beneficial and may be cardioprotective (Russ *et al.*, 1996). In this study we have shown that HOE-642 significantly inhibits insulin-stimulated glucose transport, thus the question arises as to how this can be reconciled with the apparent beneficial attributes of this drug during times of ischemia and reperfusion. If insulin-stimulated glucose transport were inhibited by HOE-642, would this not be detrimental to the ischemic heart? One explanation for this is that in addition to insulin, anoxia also stimulates glucose

transport and GLUT4 translocation albeit by a different, PI 3-kinase independent mechanism (Yeh *et al.*, 1995). Furthermore anoxia actually results in the acidification of the intracellular cytosol. Thus the signalling pathways to glucose transport by anoxia and insulin differ, in fact are opposite, in terms of their effects on cytosolic pH: insulin increasing the pH of the cytoplasm, while anoxia decreases it. The inhibition of insulin-stimulated glucose transport in cardiomyocytes by HOE-642 may therefore be compensated for in the anoxic/ischemic heart by the translocation of glucose transporters to the plasma membrane in response to an ischemia-stimulated pathway. This could be tested by photolabelling and glucose transport studies in the absence and presence of HOE-642 in the ischemic heart.

In this study acridine orange staining of non-ischemic cardiomyocytes treated with HOE-642 and insulin resulted in a yellow fluorescence distributed throughout the cytoplasm, and bright staining within vesicular structures. This yellow fluorescence may be caused by a decrease in pH following NHE1 inhibition, however at this time we cannot rule out that the unusually bright staining was due to an interaction between HOE-642 and the acridine orange stain. Acridine orange staining of cells treated with HOE-642 alone needs to be performed to address this issue.

Subcellular fractionation of adipocytes revealed that NHE1 could be detected in both the plasma membrane and the low density microsomes. However no NHE1 was detected on immunoprecipitated GLUT4 vesicles from freshly isolated adipocytes. This indicates that either a subset of GLUT4 vesicles containing NHE1 are regulated by the actions of HOE-642, that another compartment containing NHE1 is required for GLUT4 trafficking, that another HOE-642 sensitive NHE exchanger is present on GLUT4 vesicles, possibly NHE4, or that global cytosolic pH changes, due to plasma membrane localised NHE1, affect GLUT4 trafficking.

Treatment of 3T3-L1 cells with the v-ATPase inhibitor bafilomycin A_1 has been reported to induce the translocation of GLUT4 to the cell surface (Chinni and Shisheva, 1999). Unexpectedly we found that incubation of cardiomyocytes with bafilomycin A_1 caused little stimulation of glucose transport and in the presence of insulin resulted in a substantial inhibition of glucose transport. Furthermore, preliminary photolabelling results indicate that like HOE-642, bafilomycin A_1 causes a decrease in the number of functional transporters detected at the plasma membrane by the exofacial photolabel,

Bio-lc-ATB-BMPA, while confocal analysis of bafilomycin A_1 treated cells reveals a movement of GLUT4 vesicles to the cell periphery. Since these results are similar to those observed for HOE-642 inhibition of NHE1, it is interesting to speculate that there is a link between NHE1 and the v-ATPases. Indeed in early endosomes, regulation of the v-ATPase has been proposed to be due to the generation of a membrane potential by the Na^+/K^+ ATPase (Fuchs *et al.*, 1989). In fat and muscle, insulin stimulation of the Na^+/H^+ pump increases the intracellular Na^+ concentration and subsequently activates the Na^+/K^+ exchanger (Resh *et al.*, 1980; Rosic *et al.*, 1985). Therefore v-ATPases may be indirectly regulated by the actions of Na^+/H^+ pumps via Na^+/K^+ ATPases.

Studies of receptor recycling in numerous cell types have shown that bafilomycin A_1 inhibits receptor externalisation. For example, in CHO cell lines treated with bafilomycin A_1 endosomal pH is increased and TfR recycling back to the plasma membrane is markedly reduced (Johnson *et al.*, 1993). More detailed analysis of TfR recycling in bafilomycin A_1 treated cells has revealed that removal of transferrin in sorting endosomes and the accumulation of TfRs in recycling endosomes continues normally but that the rate of exit of TfRs from the recycling compartment to the plasma membrane is reduced by 50%. Bulk membrane flow is also reduced in bafilomycin A_1 treated cells but not to the same extent as TfR recycling (Presley *et al.*, 1997).

The slowed recycling of TfRs when the pH is perturbed requires the presence of the cytoplasmic domain of the TfR containing the tyrosine based internalisation motif, YTRF, which is also critical for efficient uptake of the receptor via clathrin-coated pits (Collawn *et al.*, 1990). A simple explanation for these results is that a block in intravesicular acidification leads to a receptor tail interaction involving the tyrosine-based internalisation motif, which does not normally occur. This mechanism is not mediated by any noticeable change in the localisation of the plasma membrane clathrin adaptor protein, AP2, (Johnson *et al.*, 1993) but may be due to the interaction of receptors with other adaptor proteins (AP1, AP3 or AP4), or by association with unidentified cytosolic adaptin-like proteins. Other studies also support the involvement of acidification in receptor tail recognition and controlled recycling via interactions with internalisation motifs (Basu *et al.*, 1981). Since GLUT4 contains a number of trafficking motifs, in particular a phenylalanine based motif in its N-terminus and a di-leucine sequence in its C-terminus, it would be interesting to examine the involvement of these internalisation signals in the regulation of GLUT4 trafficking by pH. This

could be achieved by analysing the trafficking of GLUT1/GLUT4 chimeras or of GLUT4 mutants with point mutations in these amino acid motifs.

How might these receptor-protein associations be regulated by acidification? Several proteins have been shown to undergo pH-sensitive changes in conformation (Turkewitz *et al.*, 1988), so one explanation may be that endosome acidification induces an overall conformational change in the receptor which alters the association of its tail with cytosolic proteins. However since it has been shown that the position of the internalisation motif within a receptors cytoplasmic tail can be altered without changing its recycling kinetics (McGraw *et al.*, 1991) and because endosomal alkalinisation can disrupt the externalisation of a number of receptors and transporters, it seems more likely that the change in conformation induced by acidification is exhibited by the putative cytosolic protein. Thus a protein other than the recycling receptor may be required to transmit the necessary information concerning luminal pH. To this end, it is interesting to note that treatment of pancreatic acrinar cells with bafilomycin A_1 inhibits the Mg.ATP induced distribution of ARF to the cytoplasmic face of the *trans*-Golgi network, where it is required for vesicle coating and budding (Zeuzem *et al.*, 1992). An alternative explanation for the role of pH in protein trafficking is that changes in acidification allow receptors to aggregate. Thus when receptor tails containing internalisation motifs are present in high enough concentrations, aberrant interactions with cytosolic adaptin-like proteins may occur (*Figure 4.16*).

Previously it has been demonstrated that glucose transporters and vacuolar-type H^+ pumps do not coexist in the same membrane (Romanek *et al.*, 1993). However the efficiency of the immunoprecipitation procedure used to recover GLUT4 vesicles in this published study was only 52%. Thus approximately half of the GLUT4 vesicles were not isolated using this technique and it is feasible that this subset of vesicles contain v-ATPases. If GLUT4 vesicles do not contain ion channels or proton pumps then perhaps another sorting station regulated by pH is necessary for GLUT4 translocation. Indeed GLUT4 passes through a number of compartments in order to generate and maintain the GSVs and many of these are regulated by pH.

Use of weak bases and inhibitors such as bafilomycin A_1 have inherent problems, since these reagents disrupt pH in all the acidified compartments of the cell. This leads to changes in organelle morphology. Furthermore in the case of bafilomycin A_1 v-

Figure 4.16 The Role of pH in GLUT4 Vesicle Trafficking. Intracellular pH is modulated by a number of ion channels and proton pumps. Inhibition of v-ATPases by bafilomycin A_1 and the sodium-proton exchanger (NHE-1) by HOE-642 reduces insulin-stimulated glucose transport due to the formation of an occluded population of GLUT4 vesicles at the plasma membrane. The occlusion of GLUT4 vesicles at the cell surface may be due to the inability of vesicles to dissociate from vesicle tethers, by inappropriate association of GLUT4 with adaptor proteins or cytosolic adaptor-like proteins or by inhibition of vesicle fusion due to the modulation of Syntaxin 4 by phosphorylation.

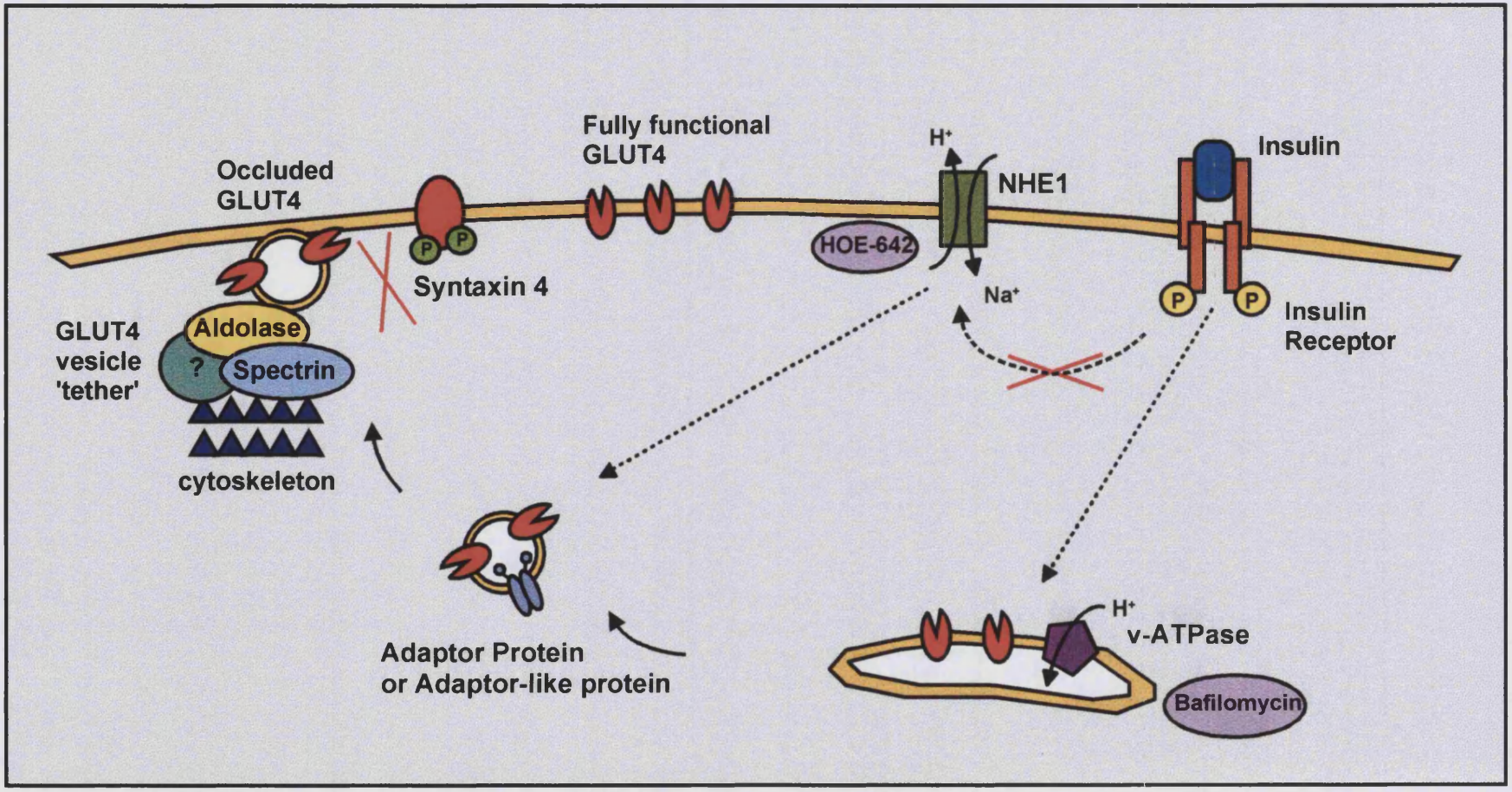

ATPases in different organelles may be differentially inhibited, making interpretations of results difficult. Recently a new method for selective perturbation of pH within organelles has been described (Henkel *et al.*, 1999). This method uses the expression of the M2 protein of the influenza virus to alter intracellular pH. Since the M2 protein is an acid activated proton selective channel, it will disrupt the pH gradient across organelle membranes in which it is expressed. At low multiplicity of infection delivery of proteins from the TGN to the cell surface is disrupted, but there is no change in the rate of TfR internalisation. At higher multiplicity of infection M2 accumulates in both the TGN and the endosomes, and TfR trafficking is attenuated. Since the experiments presented here have indicated a role for pH in GLUT4 trafficking, perhaps this method could be used to dissect this role in more detail.

The results documented in this chapter show a partial dissociation of insulin-stimulated glucose transport and GLUT4 translocation. Studies of the overexpression of human GLUT1 in the skeletal muscle of transgenic mice have also shown that glucose transport and GLUT4 translocation can be separated (Hansen *et al.*, 1998). In these studies basal glucose transport in human GLUT1 expressing transgenic mice is increased, however insulin-stimulated glucose transport is diminished. Photolabelling of glucose transporters in skeletal muscles from transgenic mice reveals that insulin can cause a redistribution of GLUT4 to the plasma membrane in line with control non-transgenic mice. These results are different from those presented here in that they show that non-functional glucose transporters at the plasma membrane can be labelled by ATB-BMPA. However this study further supports the idea that dissection of GLUT4 translocation and glucose transport activity, by whatever mechanism, is possible.

Early Western blotting and photolabelling studies have demonstrated that the appearance of GLUT1 and GLUT4 at the cell surface occurs prior to the stimulation of glucose transport in adipocytes (Clark *et al.*, 1991) and 3T3-L1 adipocytes (Yang *et al.*, 1992). The lag period between precipitation of transporters at the cell surface and the increase in carrier activity has been attributed to a population of glucose transporters in occluded precursor/fusion-incompetent states or bound to regulatory proteins which prevent the full exposure of the transporter to the extracellular environment. A recent study (Gustavsson *et al.*, 1996), has shown that insulin-induced translocation of GLUT4 to the plasma membrane fraction is followed by a slower transition of the transporter into a detergent resistant caveolae-rich region of the plasma membrane. The insulin-

stimulated appearance of transporters in the caveolae-rich fraction occurs in parallel with enhanced glucose uptake by cells (Gustavsson *et al.*, 1996). Thus the actions of HOE-642 and bafilomycin A_1 may be to prevent the transition of transporters from the plasma membrane into the cavaelae-rich domain, where they become activated.

The results presented here indicate that steps in the trafficking of GLUT4 are controlled by changes in pH. Perhaps the pH of a compartment aids its identification by specifying interactions between membrane transporters (e.g. GLUT4) and the cytosolic proteins which are required for efficient trafficking. These proteins may include clathrin, adaptins and members of the small GTPase families including Rabs and ARFs. The unique pH established within the lumen of consecutive compartments of the endocytic and exocytic pathways may therefore act as a 'sensor' for families of cytosolic proteins which direct transporters and receptors through the labyrinth of compartments to their target destinations. This sorting mechanism may be dependent on the strength of interactions of proteins with internalisation motifs in receptor tails, and these associations may be modulated by changes in pH.

5.0 The Association of Adaptor Proteins and ARF with GLUT4 Vesicles

5.1 Subcellular Distribution of Adaptor Proteins in Subcellular Fractions of Rat Adipocytes

The aim of this study was to identify which, if any, of the known adaptor complexes are required for GLUT4 vesicles coating and budding (*see Introduction, Section 1.6*). In order to achieve this, it was first necessary to examine the distribution of adaptor proteins in subcellular fractions of rat adipose cells. Adipocytes were fractionated by differential centrifugation (Weber *et al.*, 1988) to produce four fractions: the plasma membrane (PM), the low density microsomes (LDM), the high density microsomes, (HDM), and the cytosol (CYT). The protein recovered in each of these fractions is shown in *Figure 5.1A*, being approximately 300-400 μg per rat for both the PM and LDM fractions, 80 μg per rat for the HDM fraction and 1.3.mg per rat for the cytosol.

Aliquots of 20 μg from each of the subcellular fractions were resolved by SDS-PAGE and analysed by Western blotting with rabbit polyclonal antibodies raised against GLUT4, AP1, AP2 and AP3 (*Figure 5.1B*). As expected GLUT4 was predominantly localised to the LDM in untreated basal adipocyte fractions. Upon insulin stimulation GLUT4 translocates to the PM, with a concomitant decrease in the LDM fraction (*Figure 5.1B*). All of the adaptor complexes were detected in all of the subcellular fractions to varying extents (*Figure 5.1B*). However since an equal amount of protein from each fraction was loaded onto the gel but the recovery of the protein in each fraction varied, the Western blots were analysed by densitometry and normalised for protein recovery. The percentage of the total adaptor population in each fraction in basal adipocytes corrected for protein recovery is shown in *Figure 5.1C*. AP1 which associates with the TGN, (Kirchhausen *et al.*, 1997) was recovered primarily in the LDM fraction (≈ 34%) and the cytosol (≈ 48%). AP2 pelleted with the plasma membrane fraction (≈ 47%) or remained in the cytosol (≈ 44%). The majority of the AP3 complex, which colocalises with markers of the endosomal compartment (Simpson *et al.*, 1997), was detected with the LDM protein (≈ 30%) and in the cytosol (≈ 54%).

Figure 5.1 The Distribution of GLUT4 and Adaptor Proteins AP1, AP2 and AP3 in Subcellular Fractions of Rat Adipocytes. Basal and insulin stimulated adipocytes were homogenised and subfractionated as described *in Methods 2.5.1* to produce the plasma membrane (PM), the low density microsomes (LDM), the high density microsomes (HDM) and the cytosol (CYT). A. Table to show the total protein obtained in each fraction by the subfractionation procedure. Results are given as the mean ± s.e.m. B. 20 μg of protein from each fraction was analysed by SDS-PAGE and Western blotting for GLUT4, AP1, AP2 and AP3. C. Graph to show the percentage of each adaptor protein detected in each fraction from basal cells, corrected for protein recovery. The results shown are representative of 3 separate experiments for AP1 and AP3, and 2 experiments for AP2.

A.

Subcellular Fraction	Protein Recovery (μg / rat)
Plasma Membrane (PM)	371.3 ± 17.8
Low Density Microsomes (LDM)	390.3 ± 15.4
High Density Microsomes (HDM)	77.0 ± 2.5
Cytosol (CYT)	1333.3 ± 145.3

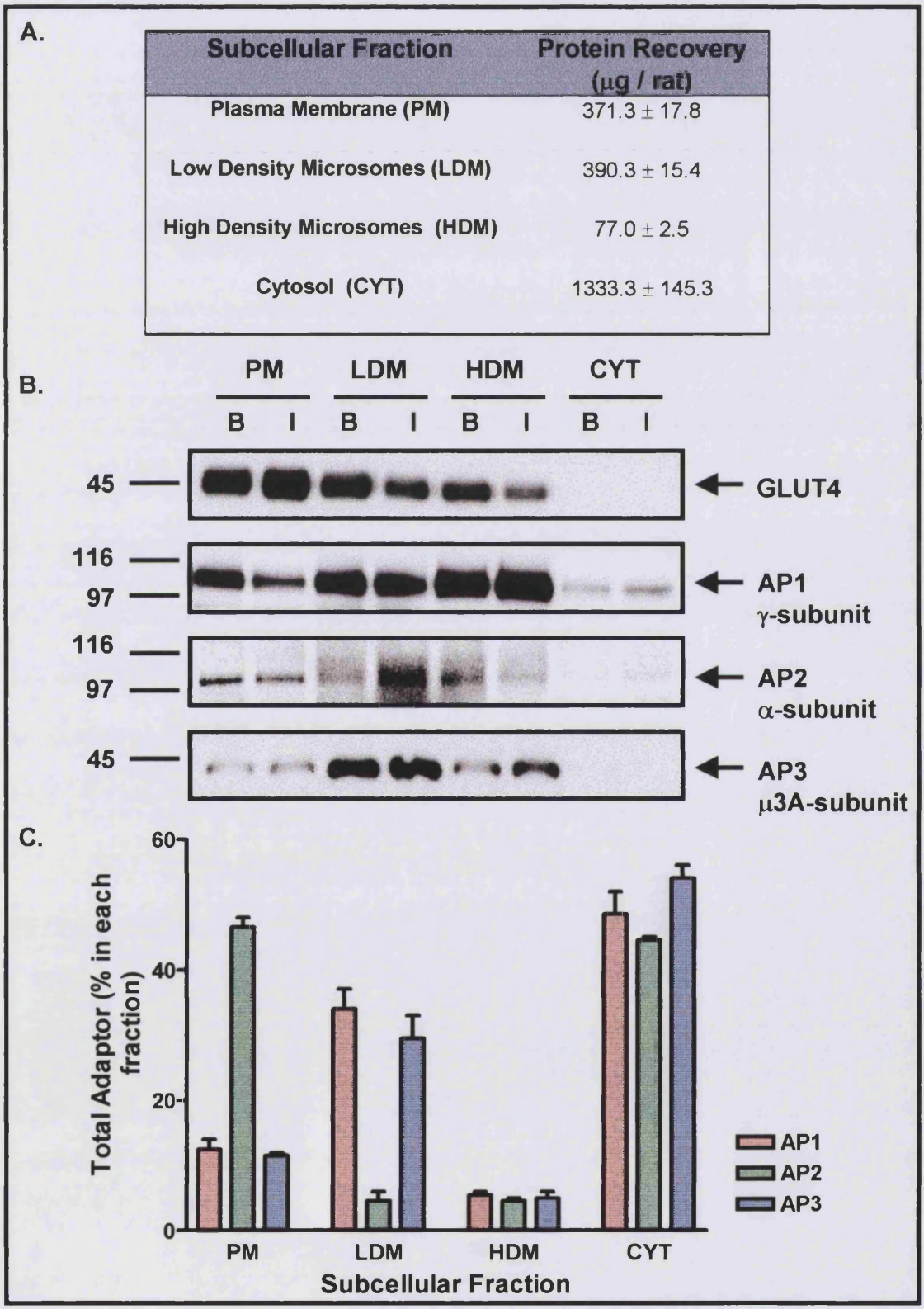

5.2 Characterisation of Post-HDM Supernatants on Gradients

5.2.1 Sedimentation of GLUT4 Vesicles on Nycodenz Gradients

Efforts were initially focussed on two adaptor protein complexes, namely the TGN specific adaptor complex, AP1 and the endosomal adaptor complex, AP3. EM studies show that GLUT4 is localised to both the TGN and to endosomal compartments (Slot *et al.*, 1991a). Furthermore confocal microscopy has revealed partial co-localisation of GLUT4 with γ-adaptin, a subunit of the AP1 complex (Malide *et al.*, 1997). In addition, a recent study of synthetic peptides has demonstrated a direct association of the β1-subunit of AP1 with a C-terminal GLUT4 peptide (Rapoport *et al.*, 1998). Our interest in the AP3 adaptor complex, stems from the observation that although it is important for vesicles budding it does not appear to associate with clathrin (Dell'Angelica *et al.*, 1997). Similarly the majority of GLUT4 vesicles are not found associated with clathrin (Malide *et al.*, 1997). Finally both of these adaptor complexes are enriched in the LDM and the cytosol, both of which can be isolated together, and are collectively referred to as the post-HDM supernatant.

In order to further examine the distribution of AP1 and AP3 with GLUT4, the post-HDM supernatant from basal adipocytes was fractionated on a linear 9-27% Nycodenz gradient. Nycodenz was selected for the sedimentation of GLUT4 vesicles, since unlike sucrose, it forms an iso-osmotic gradient over the density required. This avoids subjecting vesicles to unnecessary osmotic stress and results in the recovery of intact structures. As Nycodenz gradient separation of intracellular membrane fractions from the post-HDM supernatants of rat adipose tissues had not been previously studied, the system was characterised by comparing the sedimentation of GLUT4, with markers of the endosomal compartment (TfR) and of secretory vesicles (VAMP2) (*Figure 5.2*).

GLUT4-containing fractions form a broad band in the centre of the gradient, peaking between fractions 29 and 35. Very little of the GLUT4 peak colocalised with the TfR which was localised to a low density region of the gradient. GLUT4 partially co-sedimented with VAMP2 on these gradients. However the VAMP2 peak was narrower than the GLUT4 peak, suggesting that the latter may be a mixture of membrane vesicles some of which contain VAMP2, and some of which do not. TGN-38, a marker of the

Figure 5.2 Nycodenz Gradient Sedimentation of GLUT4 Vesicles. Plasma membranes and high density microsomes were removed from basal rat adipocyte homogenates (*Methods 2.5.1*). The remaining fraction (the post-HDM supernatant) was layered onto the top of a 9-27% Nycodenz gradient, which was centrifuged for 2.5 hrs at 63,000*g*. Fractions were collected from the bottom to the top of the gradient, and analysed by SDS-PAGE and Western blotting with antibodies against GLUT4, VAMP2 and TfRs. None of these proteins could be detected in fractions 1-19 and therefore only fractions 20-39 are shown. Densitometric analysis of the Western blotting data are shown in the right hand panels. The results shown are representative of 5 separate experiments.

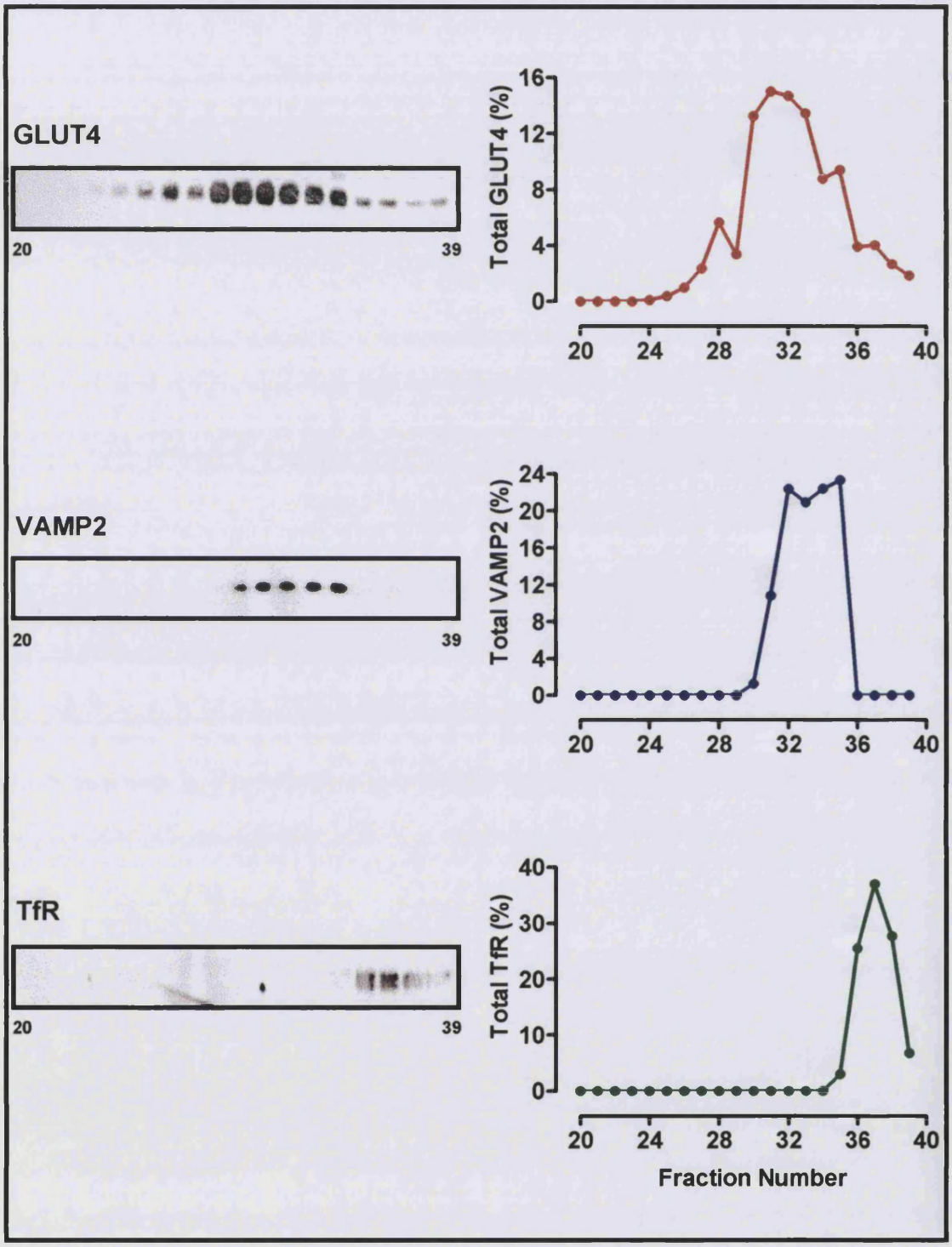

Figure 5.3 The Effects of GTPγS on the Fractionation of GLUT4 vesicles and Adaptor Complexes on Nycodenz Gradients. Plasma membranes and high density microsomes were removed from basal rat adipocyte homogenates (*Methods 2.5.1*) and the remaining post-HDM supernatant was maintained without additions (-) or was treated with 600 μM GTPγS and an ATP regenerating system for 30 min at 37°C (+). The samples were returned to ice to arrest the coating reaction and then loaded onto a 9-27% Nycodenz gradient, which was centrifuged for 2.5 hrs at 63,000*g*. Fractions were collected from the bottom to the top of the gradient, and analysed by SDS-PAGE and Western blotting with antibodies against GLUT4, the AP1 γ-subunit and the AP3 μ3A-subunit. None of these proteins could be detected in fractions 1-19 and therefore only fractions 20-39 are shown. Densitometric analysis of the Western blotting data from GTPγS treated (●) or untreated (●) samples is shown in the right hand panels. The results shown are representative of 3 separate experiments. The distribution of GLUT4 on the gradient is compared with the VAMP2 and TfR markers on Figure 5.2.

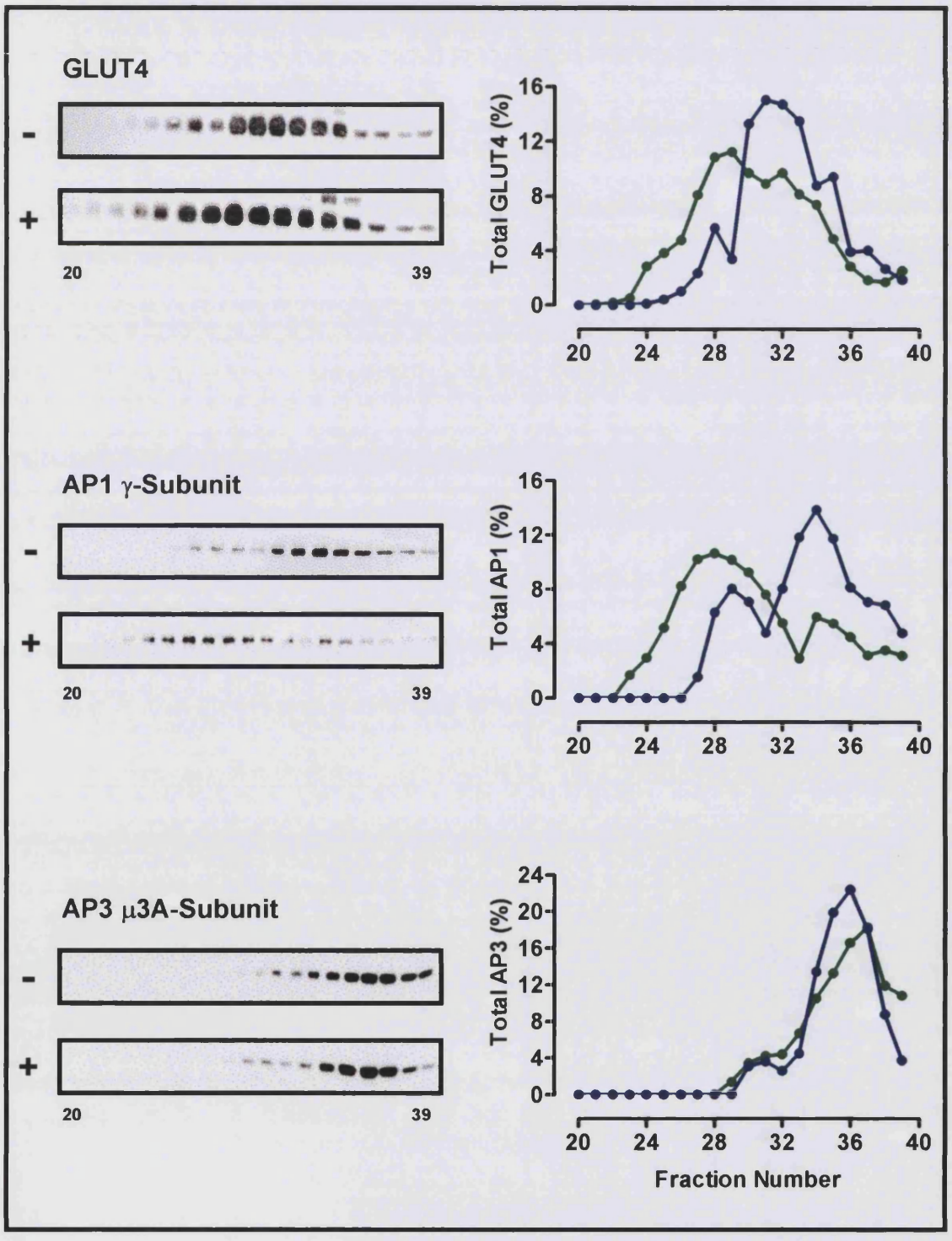

trans-Golgi network migrated to a region which partially overlapped with the peaks of both GLUT4 and the TfR (data not shown). Both AP1 and AP3 partially co-localised with GLUT4 on Nycodenz gradients (*Figure 5.3*). AP1 formed two peaks the first sedimenting at fractions 29-31, and the second, less dense peak distributing to fractions 33-36. The latter peak co-localised with GLUT4. AP3 is predominantly localised to the top of the gradient, peaking at fraction 36.

AP1 recruitment to purified Golgi membranes can be stimulated by incubation with GTPγS and inclusion of an ATP regenerating system (Traub *et al.*, 1993; Zhu *et al.*, 1998). To investigate whether GTPγS can drive a coating reaction in which adaptor subunits associate with GLUT4 vesicles, the post-HDM supernatant from adipose cells was treated with GTPγS in the presence of an ATP regenerating system consisting of 1mM ATP, 8 mM creatine phosphate and 31U/ml creatine phosphokinase type III (Diaz *et al.*, 1989), for 30 min at 37°C before addition to the Nycodenz gradient. A high percentage of the GLUT4 reactivity was shifted to a denser region of the gradient following GTPγS treatment. Similarly there was an increase in AP1 in the denser of its two peaks. Thus following incubation of the post-HDM supernatant with GTPγS in the presence of an ATP regenerating system, co-sedimentation of GLUT4 with AP1 was markedly increased. In contrast to the clear alteration in AP1 distribution on the Nycodenz gradient upon GTPγS treatment, little change in the sedimentation of AP3 was observed (*Figure 5.3*).

5.2.2 Sedimentation of GLUT4 vesicles on Glycerol Gradients

Since at least two different adaptor protein complexes co-sediment with GLUT4 on Nycodenz gradients, attempts were made to confirm these results using a different gradient system and to analyse whether the adaptor associated pools could be further resolved. To this end, post-HDM supernatants from basal adipocytes were layered onto a stepwise 5-25% glycerol gradient containing a 50% sucrose cushion, and centrifuged in a swing-out rotor at 80, 000 *g* for 16 h. One ml fractions were collected from the bottom to the top of the gradient and resolved by SDS-PAGE. The fractions were analysed by immunoblotting with a panel of antibodies against GLUT4, VAMP2, the TfR and Rab4. Under these conditions the GLUT4 vesicles were found to fractionate as two populations, the major pool located just above the sucrose cushion in a dense region

Figure 5.4 Glycerol Gradient Sedimentation of GLUT4 Vesicles. Plasma membranes and high density microsomes were removed from basal rat adipocyte homogenates (*Methods 2.5.1*). The remaining fraction (the post-HDM supernatant) was layered onto the top of a 5-25% glycerol gradient with a 50% sucrose pad, which was centrifuged for 16 hrs at 80,000*g*. 1ml fractions were collected from the bottom to the top of the gradient, and analysed by SDS-PAGE and Western blotting with antibodies against GLUT4, VAMP2, TfRs and Rab4. Densitometric analysis of the Western blotting data are shown in the right hand panels. The results shown are representative of 2 separate experiments.

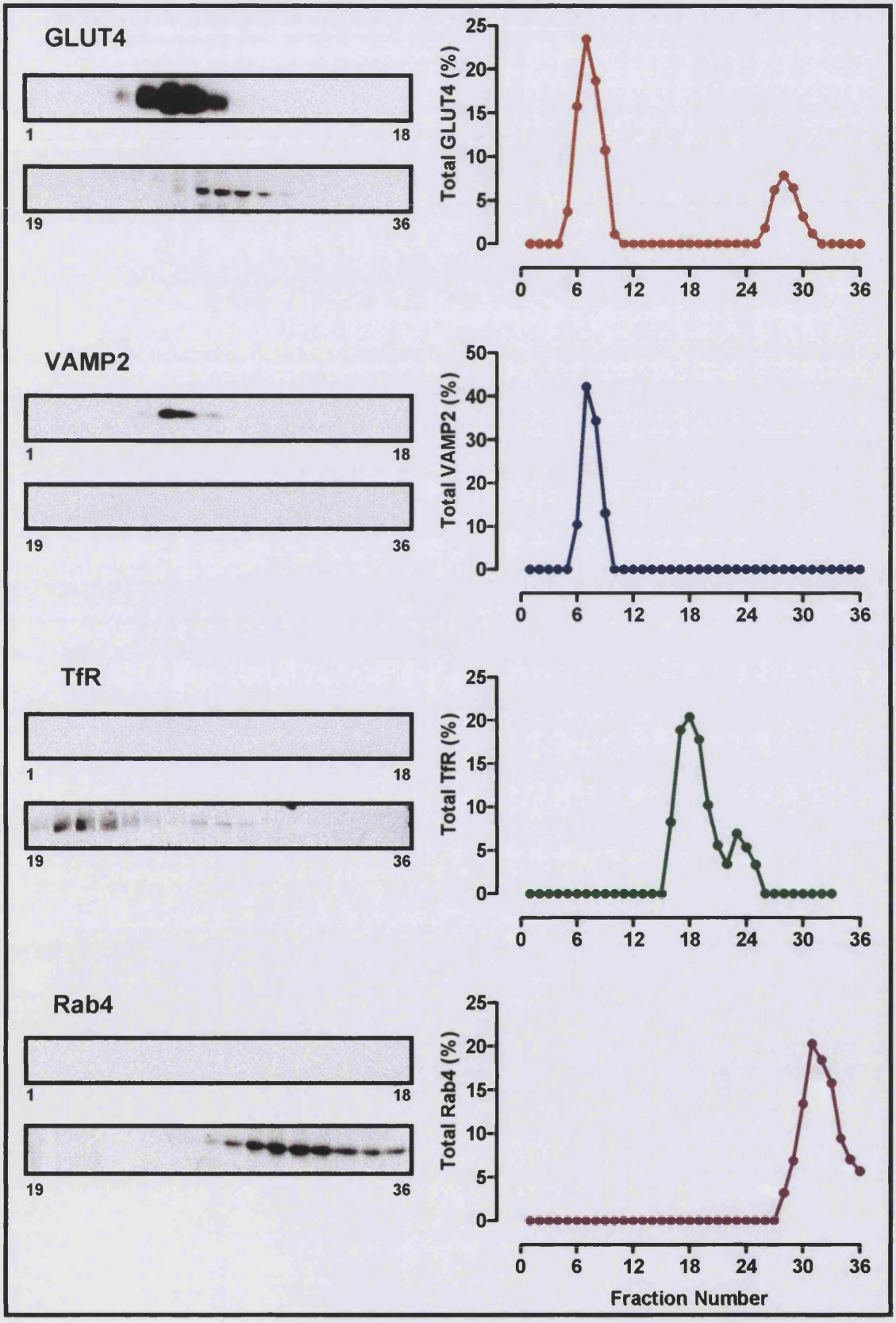

of the gradient and the minor pool in fractions 26-31 (*Figure 5.4*). VAMP2 co-localised with GLUT4 in fractions 5-10, as a single sharp peak. Immunoreactive TfRs were localised to fractions 17-25, and consisted of a peak with a small shoulder. Again GLUT4 and the TfRs did not co-migrate on this gradient, confirming a separation of the endosomal compartment containing TfRs and the specialised GLUT4 pool. Rab4, a marker of the cytosol, was localised to fractions 29-36, peaking at fraction 31.

Analysis of AP1 and AP3 on glycerol gradients, showed that the majority of these complexes co-sediment with the minor pool of GLUT4 in fractions 26-31. Some of this 'low density' peak must represent cytosolic adaptor proteins. AP3 but not AP1 partially co-localised with the major GLUT4 pool in fractions 5-10. Following incubation of the post-HDM supernatant with GTPγS and an ATP regenerating system for 30 min at 37°C, AP1 could also be detected in fractions which co-sediment with the major GLUT4 pool, although there was little change in the association of AP3 with this pool. Following GTPγS treatment, the peak of GLUT4 in the dense region of the gradient became sharper and more concentrated. Thus partial dissociation of two populations of GLUT4 vesicles has been achieved: a high density AP3-associated GLUT4 vesicles population, and a low density GLUT4 vesicle population, which can be recruited to the major GLUT4 pool upon stimulation with GTPγS by association with AP1.

5.3 Characterisation of GLUT4 Vesicles

5.3.1 Components of the GLUT4 Vesicles

In order to examine whether adaptor subunits associate directly with GLUT4 vesicles, it was first necessary to assess our ability to immunoprecipitate GLUT4 vesicles from rat adipocytes. Adipocytes were therefore fractionated to produce the post-HDM supernatant containing the LDM and the cytosol. GLUT4 vesicles were immunoisolated from this fraction (in which they comprise approximately 3% of the total vesicle population (Zorzano *et al.*, 1989)), using acrylic beads derivatised with affinity purified antibodies directed against the C-terminal tail of GLUT4 at a concentration of 1 mg/ml. As a control, non-specific rabbit IgG was immobilised on the support at the same concentration. Following a 2 h incubation at 4°C with end-to-end rotation, the beads were washed and bound vesicular proteins were solubilised in 1% Thesit in HES buffer. GLUT4 was released from the beads following denaturation of

Figure 5.5 The Effects of GTPγS on the Fractionation of GLUT4 vesicles and Adaptor Complexes on Glycerol Gradients. Post-HDM supernatants were maintained without additions (-) or were treated with 600 μM GTPγS and an ATP regenerating system for 30 min at 37°C (+). The samples were loaded onto a 5-25% glycerol gradient, which was centrifuged for 16 hrs at 80,000*g*. Fractions were collected and analysed by Western blotting for GLUT4, the AP1 γ-subunit, the AP3 μ3A-subunit and ARF. Densitometric analysis of the Western blotting data from GTPγS treated (●) or untreated (●) samples is shown in the right hand panels. The distribution of GLUT4 on the gradient is compared with the VAMP2, TfR and Rab4 markers on Figure 5.4.

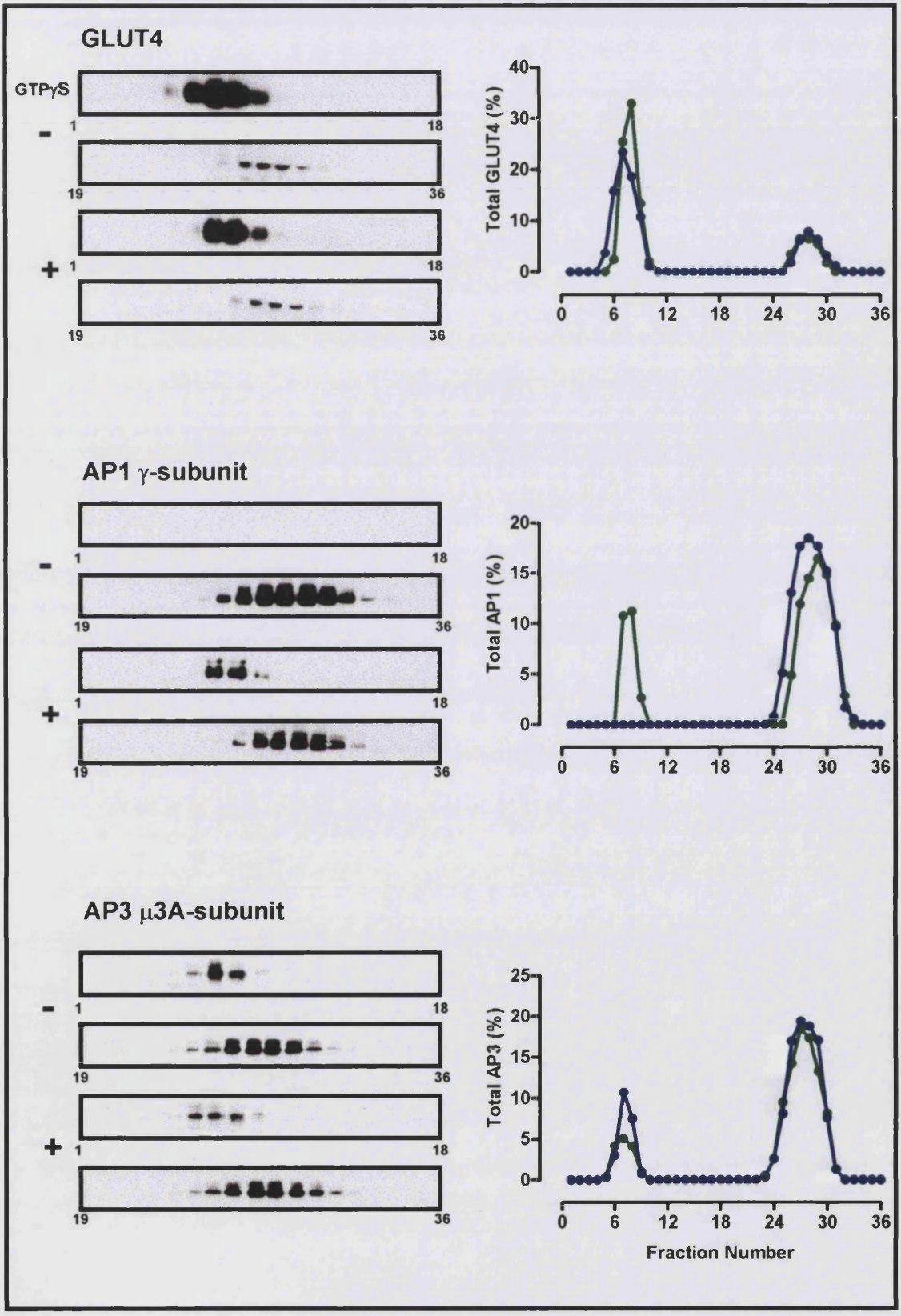

the antibodies by heating at 95°C for 5 min in electrophoresis sample buffer containing 20 mM DTT. Both the detergent extract and the GLUT4 eluate were analysed by SDS-PAGE and Western blotting with appropriate antibodies (*Figure 5.6A*).

GLUT4 was detected using a mouse monoclonal antibody (clone 1F8), to avoid any possible cross-contamination of GLUT4 with IgG from the immunoisolation procedure, the heavy chains of which migrate by SDS-PAGE to roughly the same position as GLUT4. Use of the acrylic beads resulted in only a small amount of IgG release since anti-GLUT4 antibodies are covalently coupled to the beads via an uncharged N-alkylcarbamate linkage.

As expected there was a decrease (of approximately 50%) in the yield of GLUT4 vesicles immunoadsorbed from post-HDM supernatants prepared from insulin-stimulated (I) cells compared with their basal unstimulated (B) counterparts (*Figure 5.6A*). This results as a consequence of the insulin-induced translocation of GLUT4 vesicles from the intracellular storage compartment to the cell surface and their subsequent fusion with the plasma membrane.

In order to test the integrity of the vesicles, the detergent solubilised material was immunoblotted with antibodies against VAMP2, a known component of GLUT4 vesicles and against α-SNAP, an important cytosolic factor which binds to vesicles prior to their docking and fusion with target membranes. The presence of both proteins as markers for fusion competent vesicles has been previously demonstrated (Cain *et al.*, 1992; Mastick and Falick, 1997), and both were detected in the detergent solubilised material indicating the presence of intact vesicles in the precipitates (*Figure 5.6A*). In addition, low levels of the t-SNARE, syntaxin 4 were also detected on GLUT4-specific immunoprecipitates (data not shown). This is presumably as a result of the interaction between syntaxin 4 and the GLUT4 v-SNARE, VAMP2. Indeed this has been previously demonstrated, (Kandror and Pilch, 1996).

To directly examine the association of adaptor complexes with isolated GLUT4 vesicles, the solubilised material was immunoblotted with antibodies to the γ- and σ1-subunits of AP1, and to the μ3A-subunit of AP3. Clear signals were obtained with GLUT4 vesicle samples isolated immediately at 0-4°C (*Figure 5.6B*) or in vesicles maintained at 37°C for 30 min before the immunoadsorption (*Figure 5.8A*). No

Figure 5.6 Analysis of GLUT4 Vesicle Associated Proteins. GLUT4 vesicles were immunoadsorbed from the post-HDM supernatants of basal (B) and insulin-stimulated (I) cells using acrylic beads covalently coupled with either non-specific rabbit IgG (NS) or with affinity purified rabbit anti-GLUT4 antibodies (GLUT4). Vesicle associated proteins were eluted by solubilisation in 1% Thesit in HES buffer and resolved by SDS-PAGE. A. Markers of intact GLUT4 vesicles were analysed by Western blotting with polyclonal antibodies against VAMP2 and α-SNAP and a monoclonal antibody against GLUT4 (clone 1F8). B. The association of adaptor complexes with GLUT4 vesicles was analysed by Western blotting with polyclonal antibodies against both the σ1- and γ-subunits of AP1 and the μ3A-subunit of AP3.

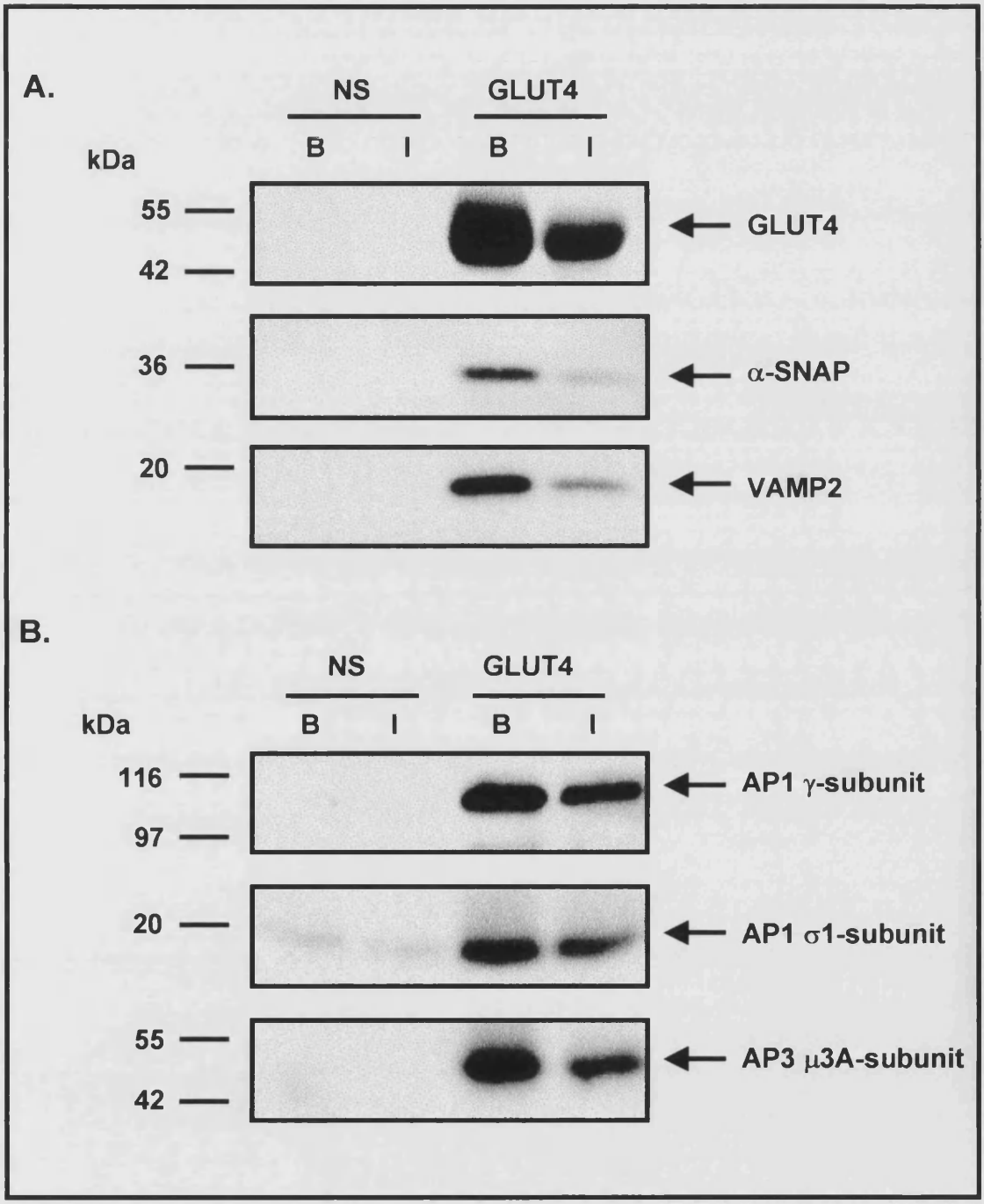

association was found in material isolated from the non-specific control precipitation. Additional experiments showed that the majority of the adaptor protein subunits were eluted from the beads with Thesit (data not shown). Furthermore, adaptor association was resistant to a salt wash using HES buffer containing 100 mM KCl (*Figure 5.6B*).

5.3.2 The Efficiency of the Acrylic Beads to Immunoprecipitate GLUT4 Vesicles

Following characterisation of GLUT4 vesicles immunoadsorbed on to acrylic beads, the efficiency of the immunoadsorption procedure was addressed. Thus after immunoprecipitation of the GLUT4 vesicles onto acrylic beads covalently coupled to either non-specific rabbit IgG or affinity purified rabbit anti-GLUT4 antibodies, the remaining supernatants were centrifuged at 541, 000 *g* for 17 min. The resultant LDM pellets were solubilised in 1% Triton X-100 in PBS buffer for 20 min at 20°C, then assayed for protein content. Equal protein (20 μg) from the remaining LDM of both GLUT4- and IgG-coupled acrylic beads was resolved on a 10% minigel, transferred to a nitrocellulose membrane and compared by Western blotting and scanning densitometry with a standard curve of LDM protein (5-20 μg).

The amount of GLUT4 detected in the remaining LDM pellets of basal and insulin samples rotated with acrylic beads coated with non-specific IgG corresponded to approximately 17.2 and 16.3 μg of the LDM protein standard respectively. In the remaining LDM pellets of basal and insulin samples rotated with beads coated with anti-GLUT4 antibodies, the values were 6.7 and 5.6 μg respectively. Thus the efficiency of the acrylic beads to immunoprecipitate GLUT4 vesicles is approximately 67% (*Figure 5.7*).

5.3.3 Quantification of Adaptor Proteins on GLUT4 Vesicles

In order to quantify the proportion of immunoadsorbed adaptors, a series of dilutions of the post-HDM supernatant (*Figure 5.8B*) were compared with the immunoadsorbed material (*Figure 5.8A*). These data indicated that GLUT4 vesicles isolated from basal cells and then maintained for 30 min at 37°C associate with 1.4% of the total AP1 γ-subunit and 0.9% of the total AP3 μ3A subunit from post-HDM supernatants. When corrected for GLUT4 vesicle recovery these percentages increase to 2.1% and 1.3% for AP1 and AP3 respectively. Since GLUT4 vesicle protein comprises only 3% of the

Figure 5.7 Analysis of the Recovery of GLUT4 Vesicles by Acrylic Beads. GLUT4 vesicles were isolated by immunoprecipitation on acrylic beads coated with either non-specific rabbit IgG (NS) or with affinity purified rabbit anti-GLUT4 antibodies (GLUT4). Following immunoprecipitation of the vesicles the remaining supernatant was centrifuged at 541,000*g* for 17 min to pellet the remaining low density microsomes (rLDM). The rLDM membranes were solubilised in 1% Triton X-100 and 20 μg aliquots were loaded onto a 10% gel with a standard curve of LDM protein. Western blotting was performed with a polyclonal antibody against GLUT4 and is shown in A. The blot was analysed by densitometry and the results are shown in B. The data shown is representative of 3 separate experiments.

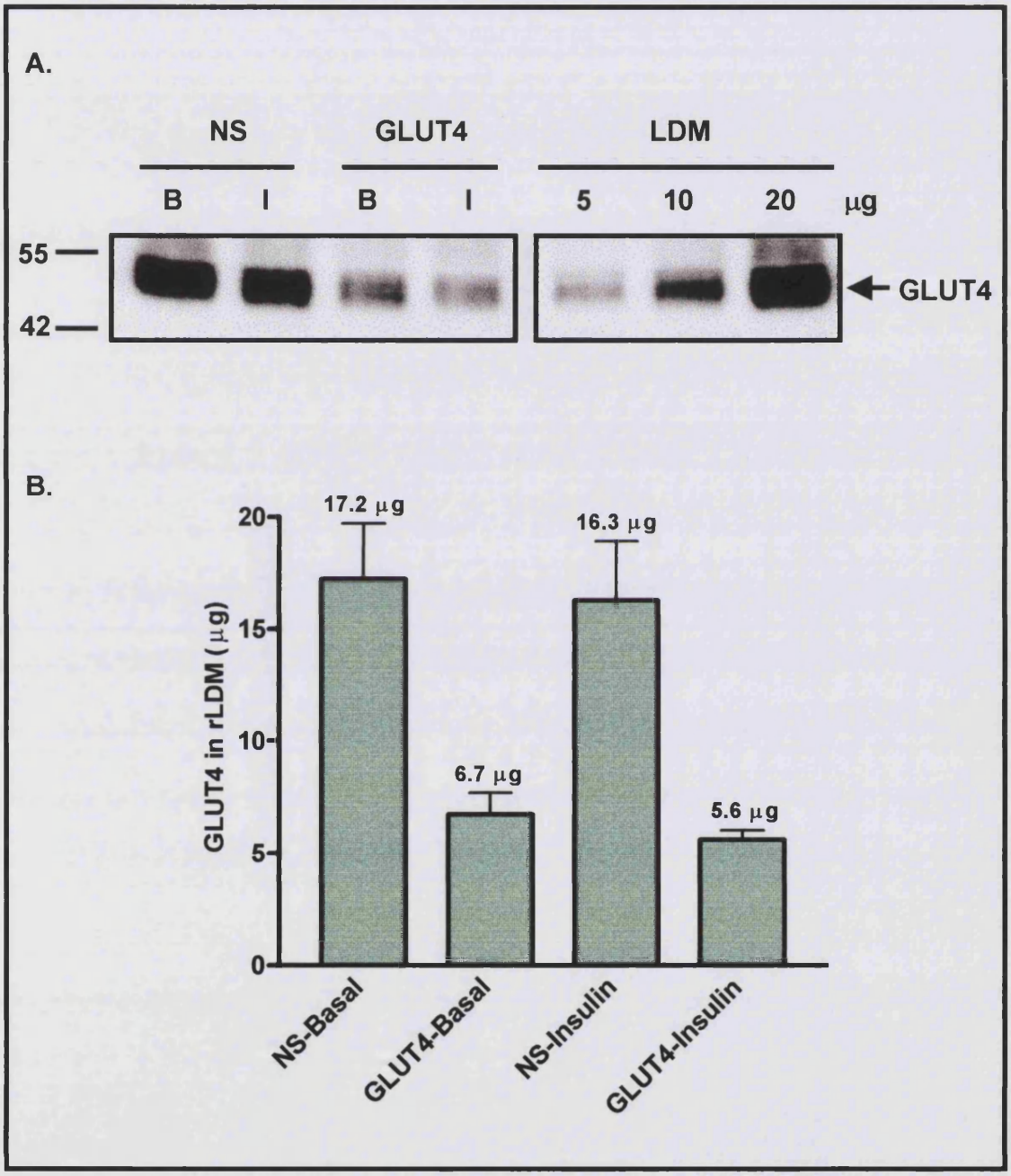

total microsomal protein present in this fraction (Zorzano *et al.*, 1989), the levels of AP1 and AP3 are highly significant, and suggest a role for these adaptor complexes in the regulation of GLUT4 vesicle sorting and trafficking.

AP2 is predominantly recruited to the plasma membrane, where it plays an important role in clathrin mediated endocytosis (Hirst and Robinson, 1998). Since GLUT4 is continually recycling between an intracellular locus and the cell surface (Satoh *et al.*, 1993), the association of GLUT4 with AP2 was analysed *(Figure 5.8)*. In this case the Thesit solubilised material was examined by Western blotting using an antibody against the hinge region of the 100 kDa α-subunit of AP2 (Ball *et al.*, 1995). Only minor amounts of AP2 on GLUT4 vesicles could be detected, comprising <0.2% of the total AP2 pool in the post-HDM supernatant. In order to assess this small signal, it was necessary to over-expose the detection film for the dilutions of the post-HDM supernatant (*Figure 5.8*).

5.3.4 The Effect of a Liposome Wash on the Association of Adaptor Proteins with GLUT4 vesicles.

To examine whether the association of adaptor proteins with GLUT4 vesicles was due to a lipid or protein interaction, the effect of a liposome wash on AP1 and AP3 recruitment was examined. A 6 mM liposome stock solution was prepared according to the method of Helms and colleagues (Helms *et al.*, 1993). Briefly, 9 mg egg lecithin was resuspended in 2 ml HES buffer and sonicated in 10 s bursts with 20 s rest periods until the solution was clear. Following immunoadsorption of the vesicles onto acrylic beads coupled to either non-specific rabbit IgG or affinity purified anti-GLUT4 antibodies, the beads were washed in HES buffer. The beads were then incubated with 1 mM phosphotidylcholine liposomes for 10 min at 4°C. The vesicles were washed again, and vesicle associated proteins were solubilised in a detergent buffer. The proteins were analysed by SDS-PAGE and Western blotting with antibodies against GLUT4, the γ-subunit of AP1 and the μ3A-subunit of AP3, (*Figure 5.9*). No change in the levels of immunoadsorbed GLUT4 vesicles were detected, nor was there any significant decrease in the levels of AP1 or AP3 recruitment to the GLUT4 populated membranes. This suggests that the interaction between GLUT4 and the adaptor proteins is specific. Furthermore fewer AP1 adaptors were recovered on GLUT4 vesicles isolated in the presence of a buffer in which HEPES was replaced by Tris (data not

Figure 5.8 Quantification of the Amount of each Adaptor Complex Associated with GLUT4 Vesicles. GLUT4 vesicles were immunoadsorbed from post-HDM supernatants of basal (B) and insulin stimulated (I) rat adipocytes using acrylic beads covalently coupled to either non-specific IgG (NS) or affinity purified rabbit anti-GLUT4 antibodies (GLUT4). Densitometric scanning was used to compare the vesicle associated material (left panel) with the levels of adaptor subunits found in the post-HDM supernatant (right panels). The results shown are representative of 4 independent experiments.

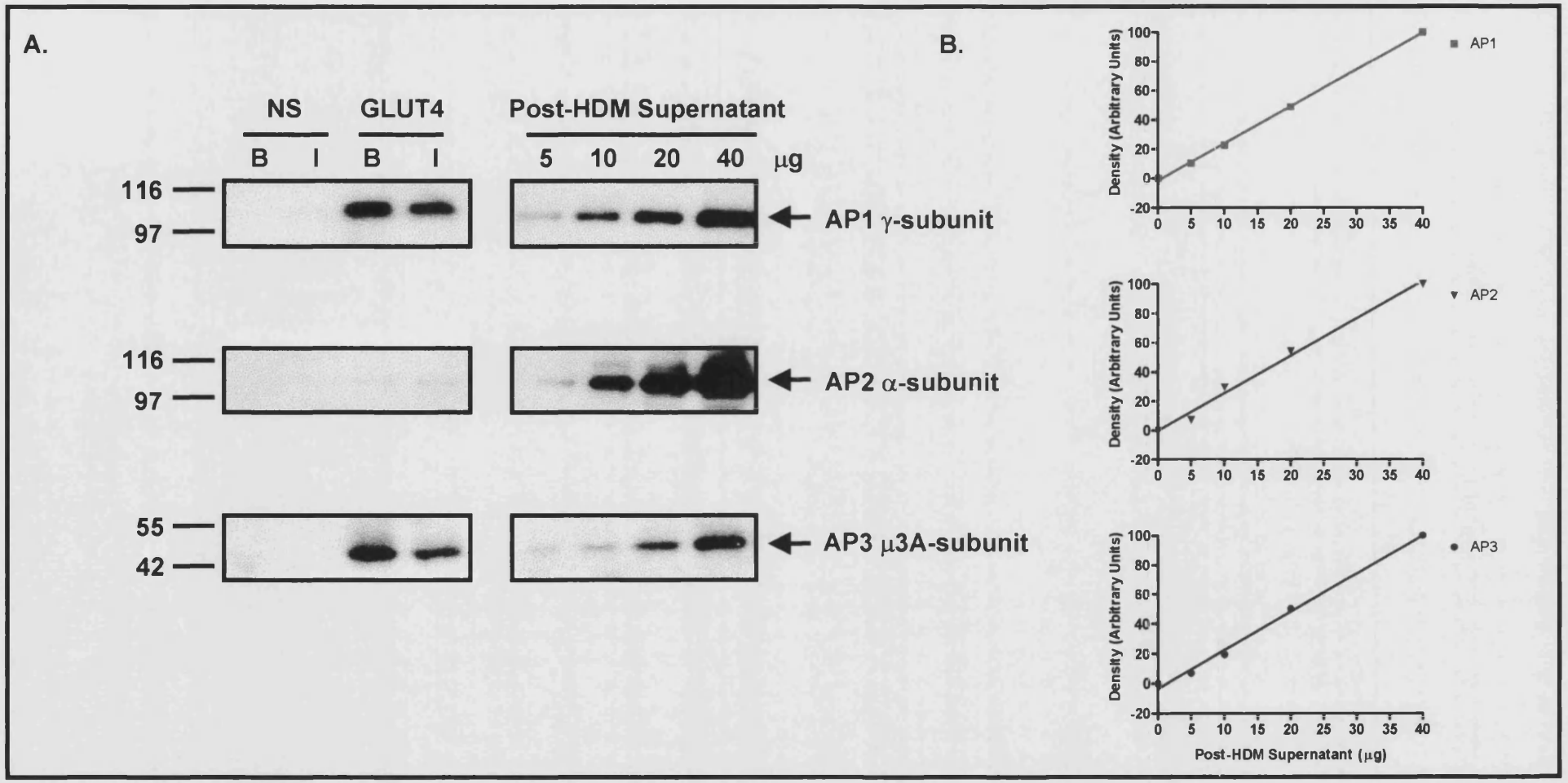

Figure 5.9 The Effect of a Liposome Wash on the Association of Adaptor Proteins with GLUT4 Vesicles. Plasma membranes and high density microsomes were removed from basal (B) and insulin treated (I) homogenates by centrifugation to give post-HDM supernatants. GLUT4 vesicles were immunoadsorbed from these post-HDM supernatants by acrylic beads covalently coupled to either non-specific rabbit IgG (NS) or affinity purified rabbit anti-GLUT4 antibodies (GLUT4). The adsorbed vesicles were then incubated with 1 mM phosphatidylcholine liposomes for 10 min at 4°C. Vesicle associated proteins were eluted and resolved by SDS-PAGE and Western blotting with antibodies to GLUT4, the γ-subunit of AP1 and the μ3A-subunit of AP3. The results shown are representative of 2 separate experiments.

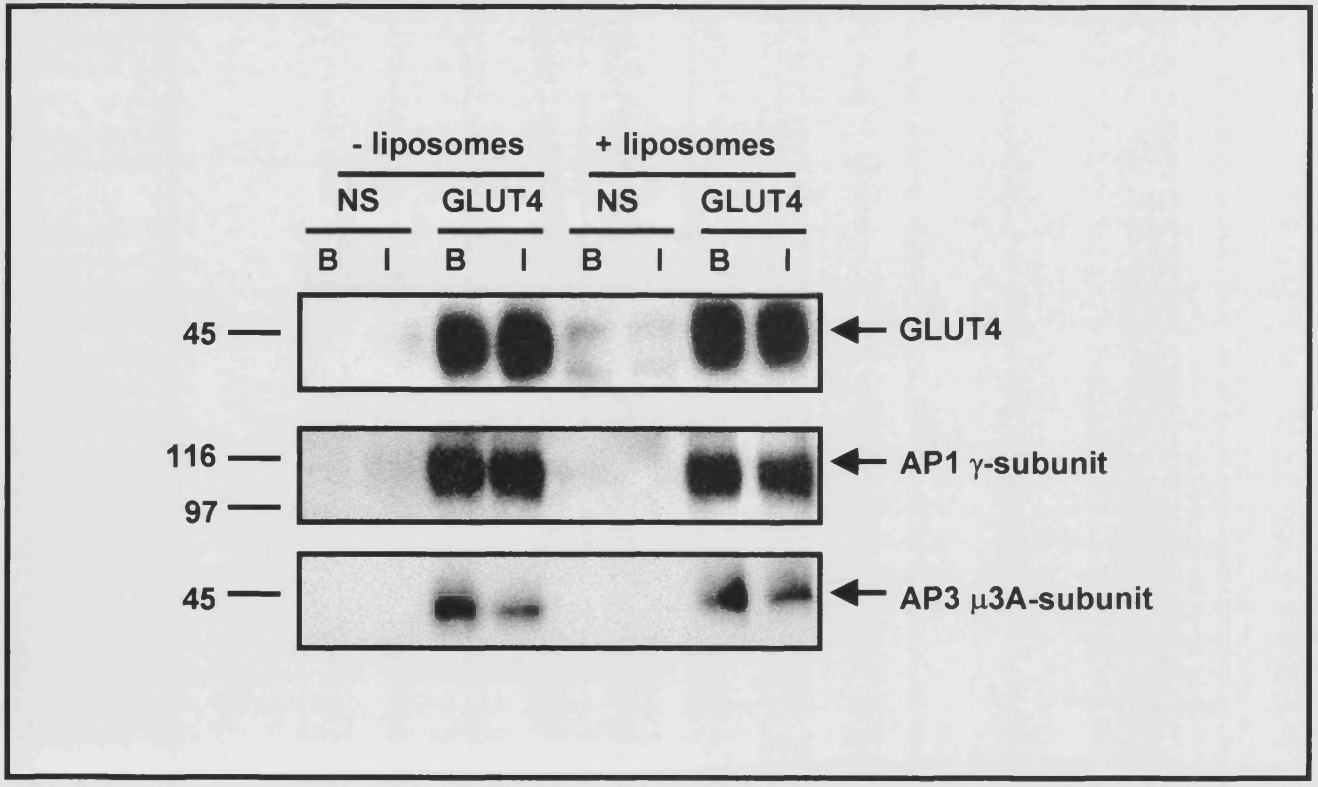

shown), consistent with the known effects of Tris on the binding of adaptors to their target membranes (Dittie *et al.*, 1996; Zhu *et al.*, 1998).

5.3.5 GTPγS Treatment Increases the Association of AP1 with GLUT4 Vesicles

Recruitment of adaptor proteins to the TGN has been reconstituted *in vitro*, and is stimulated by GTPγS and this stimulation is enhanced by ATP (Traub *et al.*, 1993; West *et al.*, 1997; Zhu *et al.*, 1998). To examine the possibility of GTPγS enhanced *in vitro* recruitment of adaptor proteins onto GLUT4 vesicles, vesicles were immuno-isolated from post-HDM supernatants of basal and insulin-stimulated cells that had either been treated with 100 μM or 600 μM GTPγS in the absence or presence of an ATP regenerating system. Control samples were left untreated (*Figure 5.10A*). Following incubation of all of the samples at 37°C for 30 min to stimulate adaptor recruitment, the preparations were returned to ice for 5 min to arrest the coating reaction. The vesicles were subsequently immunoadsorbed onto acrylamide beads coupled to affinity purified anti-GLUT4 antibodies and bound vesicle proteins were eluted and analysed by SDS-PAGE and Western blotting.

Immunoblotting for AP1 was performed using antibodies against the γ-, μ1- and σ1 subunits. The recruitment of all of the subunits of AP1 was enhanced by incubation of the post-HDM supernatants with GTPγS, and further stimulated by the addition of an ATP regenerating system in conjunction with the GTPγS. The association of the γ-subunit of AP1 with GLUT4 vesicles was increased ≈ 4-fold following the GTPγS and ATP regeneration incubation (*Figure 5.10B*) suggesting that there is a requirement for both a GTP binding protein (possibly a GTPase) and an ATPase in AP1 recruitment. There was no significant difference in the fold-change of GTPγS driven recruitment of adaptors onto GLUT4 vesicles prepared from basal compared with insulin-treated adipose cells. The lower levels of adaptor recruitment onto the vesicles prepared from insulin-treated cells reflected the lower levels of GLUT4 vesicles present (*Figure 5.10A top panel*). In contrast to the GTPγS enhanced recruitment of AP1, no significant change in the association of AP2 or AP3 with GLUT4 vesicles was observed (*Figure 5.10B*).

Figure 5.10 The Effects of GTPγS and an ATP Regenerating System on the Recruitment of Adaptor Complexes onto GLUT4 Vesicles in a Cell-Free System. Post-HDM supernatants of basal (B) and insulin stimulated (I) adipose cells were either left untreated (no additions) or treated with 100 μM or 600 μM GTPγS in the absence or presence of an ATP regenerating system (rATP). GLUT4 vesicles were then immunoadsorbed on acrylic beads coated with affinity purified anti-GLUT4 antibodies. Vesicle associated proteins were eluted and resolved by SDS-PAGE. Western blotting was performed with antibodies against GLUT4 and the γ- μ1- and σ1-subunits of AP1 and the μ3A-subunit of AP3.

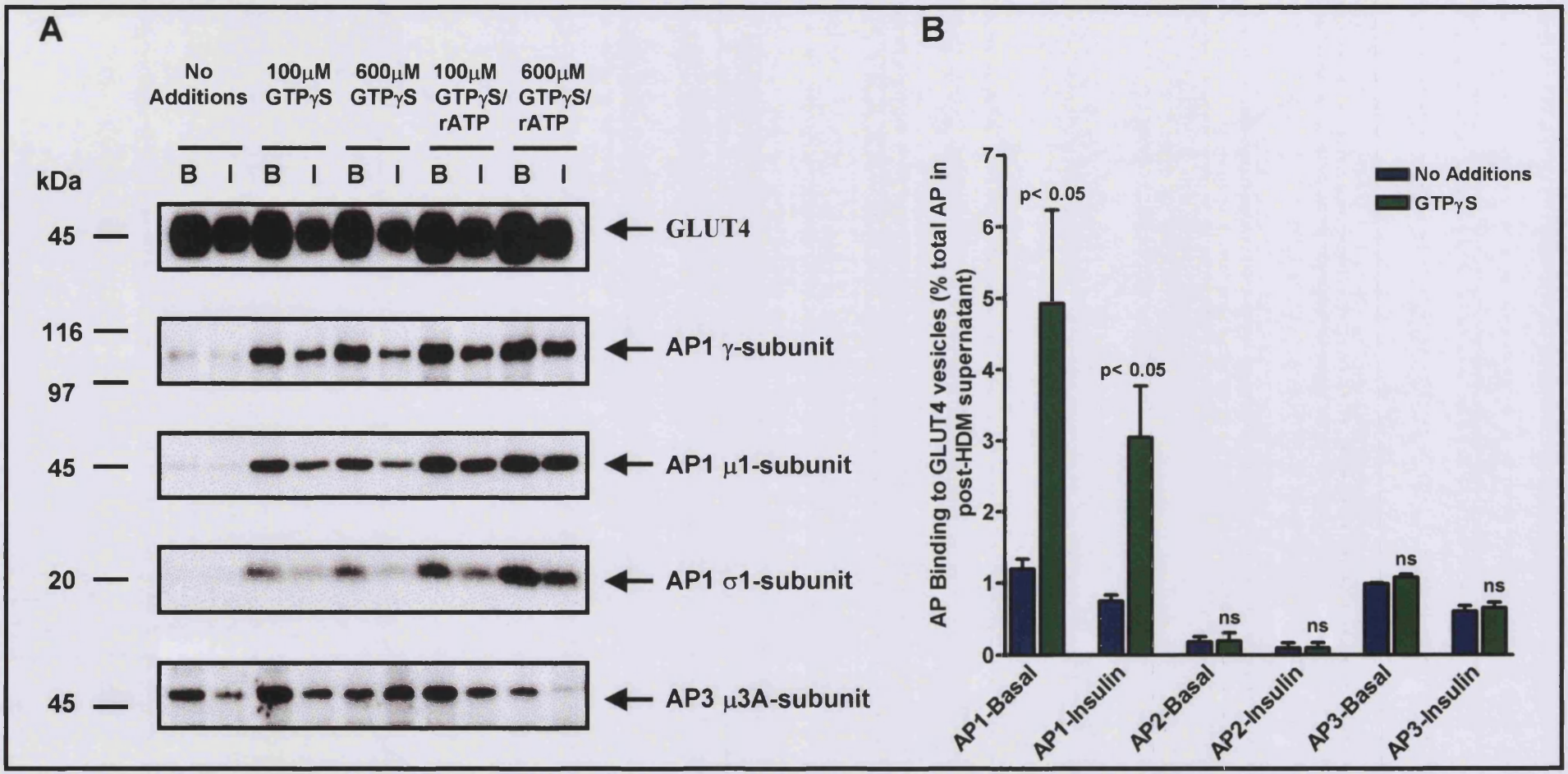

Figure 5.11 The Association of GLUT4 Vesicles with the Insulin Receptor and TGN38. Post-HDM supernatants of basal (B) and insulin stimulated (I) adipose cells were either left untreated (no additions) or treated with 100 μM or 600 μM GTPγS in the absence or presence of an ATP regenerating system (rATP). GLUT4 vesicles were then immunoadsorbed on acrylic beads coated with affinity purified anti-GLUT4 antibodies. Vesicle associated proteins were eluted and resolved by SDS-PAGE. Western blotting was performed with antibodies against the insulin receptor α-subunit, a marker of the plasma membrane and against TGN38, a marker of the *trans*-Golgi network. 50 μg of total adipocyte membranes (TM) was run in lane 1 as a control.

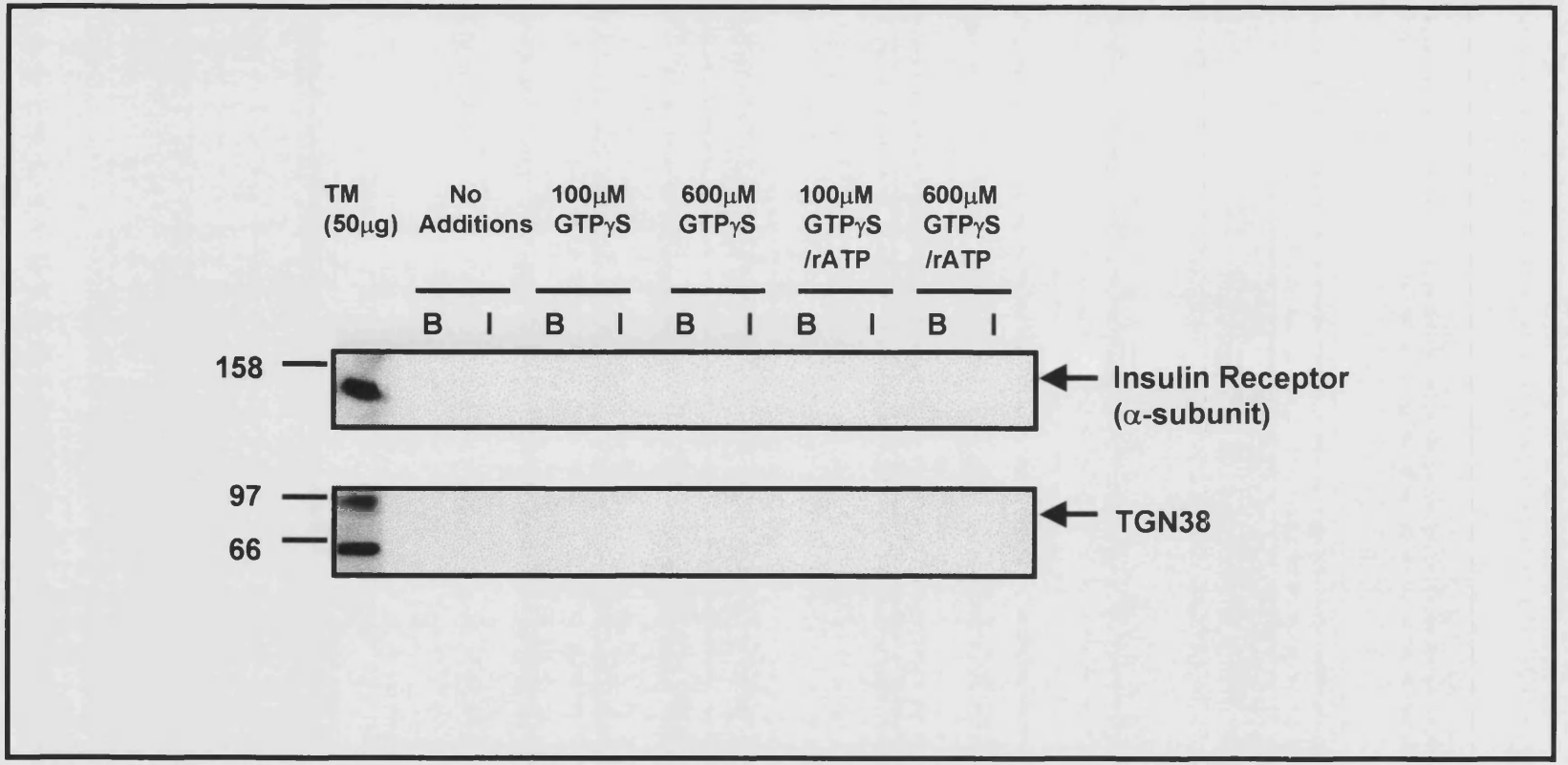

Control experiments confirmed previous studies characterising the GLUT4 vesicle population immunoadsorbed by acrylic beads derivatised with anti-GLUT4 antibodies. These studies showed that neither the insulin receptor, a marker of the plasma membrane, nor TGN38, a marker of the *trans*-Golgi network, are associated with immunoprecipitated GLUT4 (Kandror and Pilch, 1998). Indeed a distinction between the TGN compartment and the GLUT4 compartment has been further demonstrated by morphological studies in 3T3-L1 adipocytes, in which these two proteins were compared (Martin *et al.*, 1994). Furthermore the levels of association of the insulin receptor and TGN38 with GLUT4 vesicles does not increase when these vesicles are prepared from GTPγS treated samples (*Figure 5.11*). This indicates that little non-specific interaction of proteins or membranes with the GLUT4 vesicles occurs, even in the presence of GTPγS.

5.4 The Involvement of ARF in Adaptor Association with GLUT4 Vesicles

5.4.1 The Effect of GTPγS on the Sedimentation of ARF on Nycodenz and Glycerol Gradients

The recruitment of AP1 onto membranes is known to be dependent on the small G-protein ARF1. ARFs are members of the *Ras* family of GTPases. They have been implicated in AP1 recruitment since relocation of AP1 from the cytosol to the TGN membrane is preceded by ARF. Since a GTPγS-enhanced recruitment of AP1 onto GLUT4 vesicles was observed, we next examined whether ARF could be recruited to GLUT4 vesicles under similar conditions. Post-HDM supernatants derived from basal adipocytes, treated with 600 μM GTPγS and an ATP regenerating system or left untreated were centrifuged on Nycodenz gradients at 63, 000 *g* for 2.5 h. Fractions were collected as already described and analysed by SDS-PAGE. The resulting nitrocellulose membranes were probed using a monoclonal antibody to ARF (clone 1D9). This antibody is known to cross-react with ARFs 1, 3, 5 and 6 but has lower affinity for ARF4. ARF was localised to the top of the gradient in the untreated post-HDM supernatant sample, peaking at fractions 37-38. None of the ARF fractionated from the untreated post-HDM supernatant co-localised with GLUT4 from the same sample (*Figure 5.12A*). Treatment of the sample with GTPγS and an ATP regenerating

Figure 5.12 The Effect of GTPγS on the Sedimentation of ARF on Nycodenz and Glycerol Gradients. Post-HDM supernatants from basal cells were left untreated (●) or treated with 600 μM GTPγS and an ATP regenerating system at 37°C for 30 min (●). The supernatants were then returned to ice to arrest the reaction before loading onto either 9-27% Nycodenz gradients (A) or 5-25% glycerol gradients with 50% sucrose cushions (B). The gradients were centrifuged at 63,000*g* for 2.5 hrs or 80,000*g* for 16 hrs respectively. One ml fractions were collected and analysed by SDS-PAGE and Western blotting with a monoclonal pan antibodv to ARF. Densitometric analysis of the Western blotting data is shown in the right hand panels. The positions of the GLUT4 peaks on these gradients are indicated by the bars above the graphs. Neither ARF nor GLUT4 were detected in fractions 1-19 on the Nycodenz gradient and therefore only fractions 20-39 are shown.

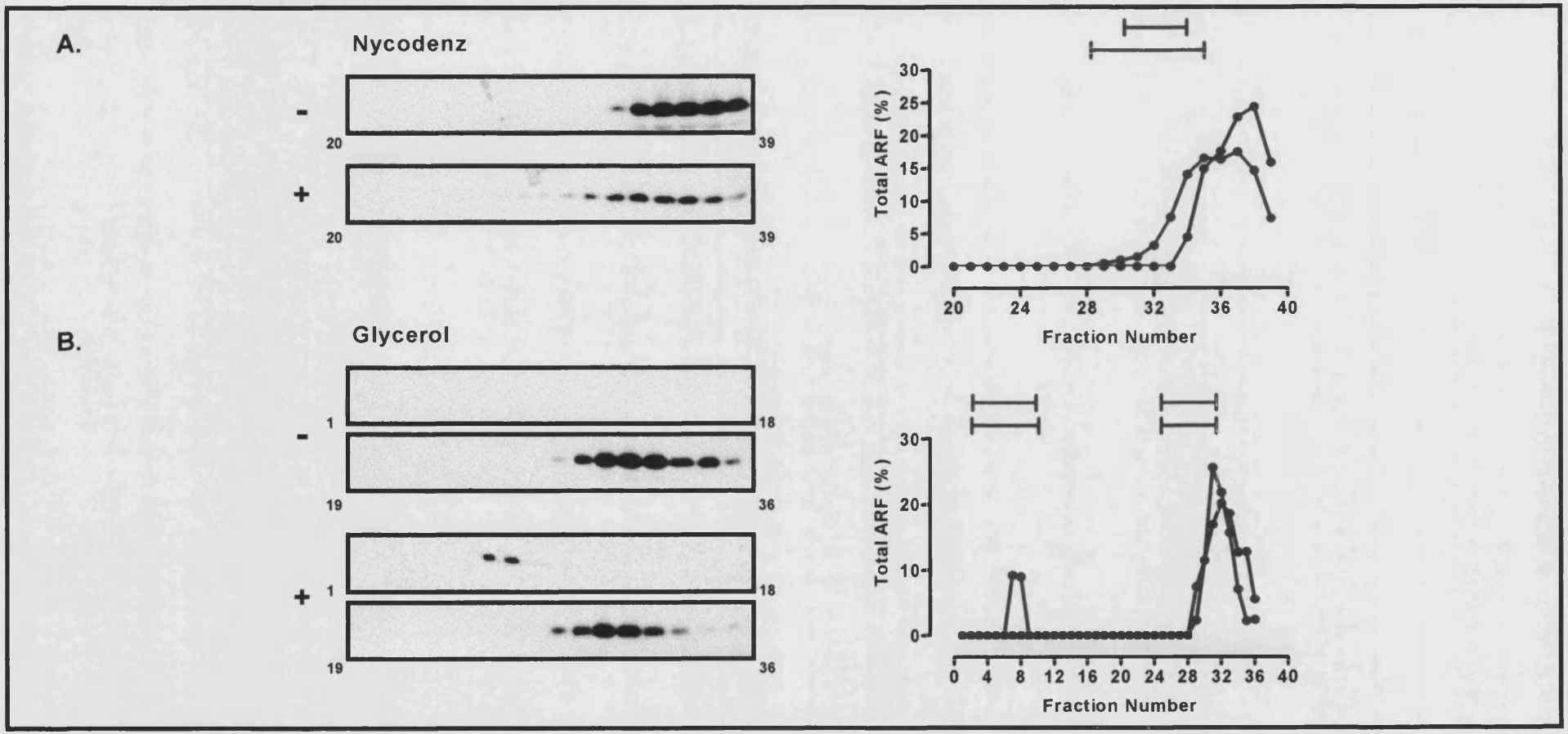

system resulted in a marked shift in immunoreactive ARF to a denser region of the gradient. In this region of the gradient ARF partially co-localised with GLUT4 (*Figure 5.12A*).

These results were confirmed using glycerol gradients. In this case ARF from untreated or GTPγS-treated post-HDM supernatants was fractionated on 5-25% glycerol gradients with a 50% sucrose cushion. The gradients were centrifuged at 80, 000 g for 16 h and fractions were collected as already described (*Section 5.5.2*). The distribution of ARF on the gradient was analysed by SDS-PAGE and Western blotting. In the untreated post-HDM supernatants, ARF migrated at the top of the gradient, in a region that co-localised with Rab4 (*Section 5.2.2*) and presumably represented the cytosol. Treatment of the post-HDM supernatant with GTPγS and an ATP regeneration system for 30 min at 37°C, resulted in a shift in ARF immunoreactivity, such that a small peak of ARF was observed in fractions 4-8. This high density ARF peak completely co-localised with the major pool of GLUT4 (*Figure 5.12B*).

5.4.2 The Association of ARF with GLUT4 Vesicles

To test for a direct interaction of GLUT4 vesicles with ARF, vesicles were immunoprecipitated on acrylic beads coupled to either non-specific rabbit IgG or affinity purified anti-GLUT4 antibodies, and were resolved by SDS-PAGE and Western blotting. In contrast to the association of AP1 with freshly isolated GLUT4 vesicles, significant levels of ARF could not be detected on GLUT4 vesicles in the absence of GTPγS. However *in vitro* recruitment of ARF to GLUT4 vesicles could be driven by GTPγS and an ATP regenerating system, with concentrations as low as 100 μM GTPγS inducing substantial association (*Figure 5.13A*). In these experiments a small amount of non-specific interaction of ARF with the immunoadsorbed precipitates was detected and could not be eliminated by an additional pre-clearing step or by washing with liposomes (*Figure 5.13B*). The latter procedure has been reported to reduce the non-specific ARF-binding effects (Helms *et al.*, 1993). However, the levels of association of ARF detected using the specific GLUT4 acrylic beads were always considerably higher than the non-specific control.

The amounts of ARF recruited reflected the amounts of GLUT4 vesicles recovered from basal and insulin-treated samples. Quantitative comparison with the post-HDM supernatant samples revealed that in the presence of GTPγS and an ATP regeneration system, ≈ 1.5% of the total ARF available was associated with the GLUT4 vesicles. This value takes into account the non-specific association of ARF with the control beads, which has been subtracted. Since the efficiency of the acrylic beads to immunoadsorb GLUT4 vesicles was 67%, the total amount of ARF associated with these vesicles was determined to be ≈ 2.2% (*Figure 5.13B*).

5.4.3 The Effect of the ATP Regeneration System on AP1 and ARF Recruitment

Since both GTPγS alone and GTPγS in conjunction with an ATP regeneration system stimulated recruitment of both AP1 and ARF to GLUT4 vesicles, we next tested whether the ATP regeneration system alone was sufficient to stimulate coat recruitment. Post-HDM supernatants derived from basal adipocytes were either left untreated, treated with the ATP regeneration system, treated with 600 μM GTPγS or treated with both 600 μM GTPγS and the ATP regenerating system for 30 min at 37°C. The post-HDM supernatants were then returned to ice to arrest the coating reaction, before immunoadsorption on acrylic beads. Following a 2 h incubation the immunoprecipitated vesicles were washed and solubilised in a detergent buffer. Vesicle associated proteins were analysed by SDS-PAGE and Western blotting with antibodies against GLUT4, the γ-subunit of AP1 and ARF. GLUT4 was clearly detected in samples precipitated with acrylic beads covalently coupled to anti-GLUT4 antibodies, with little immunoreactivity in the control samples (*Figure 5.14*). AP1 was not detected in control samples, but was detected in all the precipitates derived from the GLUT4-specific acrylic beads. As expected AP1 was associated with vesicles derived from untreated post-HDM supernatants and to a higher level on vesicles immunoadsorbed from post-HDM supernatants treated with GTPγS in the absence or presence of an ATP regenerating system. A small increase in the association of AP1 with GLUT4 vesicles was observed in samples treated with the ATP regenerating system alone, but this probably reflects the slight increase in GLUT4 vesicles immunoprecipitated from this sample. Likewise, the association of ARF with GLUT4 vesicles was only significantly enhanced in samples treated with GTPγS, with little ARF detected on vesicles

Figure 5.13 The Association of ARF with GLUT4 Vesicles. GLUT4 vesicles were immunoadsorbed from post-HDM supernatants of basal (B) and insulin treated (I) adipocytes which had been treated with 100 μM or 600 μM GTPγS and/or an ATP regenerating system (rATP) using acrylic beads covalently coupled to either non-specific rabbit IgG (NS) or affinity purified polyclonal rabbit anti-GLUT4 antibodies (GLUT4). Vesicle associated proteins were eluted by solubilisation in 1% Thesit in HES buffer and resolved by SDS-PAGE. A. Western blotting with antibodies against ARF. B. A standard curve of post-HDM supernatant was constructed and densitometric analysis was used to compare the vesicle associated material with the levels of adaptor subunits found in the post-HDM supernatant. The results shown are representative of 3 separate experiments.

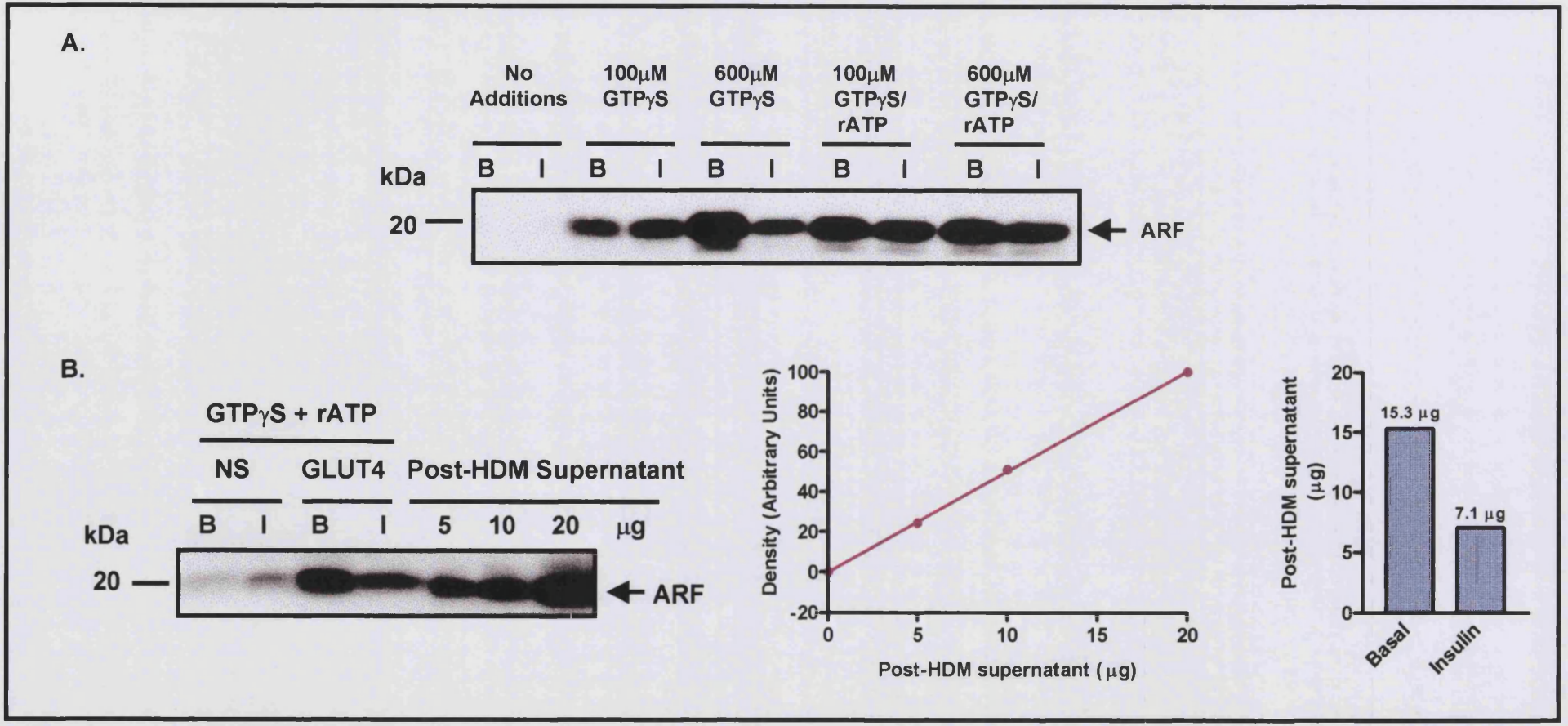

Figure 5.14 The Effect of an ATP Regenerating system on AP1 and ARF Recruitment to GLUT4 Vesicles. Post-HDM supernatants from basal adipocytes were either left untreated (B), treated with an ATP regenerating system (BA), treated with 600 μM GTPγS (BG) or with a combination of both reagents at the same concentrations (BAG). GLUT4 vesicles were immunoadsorbed from the post-HDM supernatants onto acrylic beads coupled to either non-specific IgG (NS) or affinity purified anti-GLUT4 antibodies (GLUT4). Vesicle associated proteins were solubilised in 1% Thesit in HES buffer and resolved by SDS-PAGE. Proteins were characterised by Western blotting with antibodies against GLUT4, the γ-subunit of AP1 and against a panel of ARF proteins.

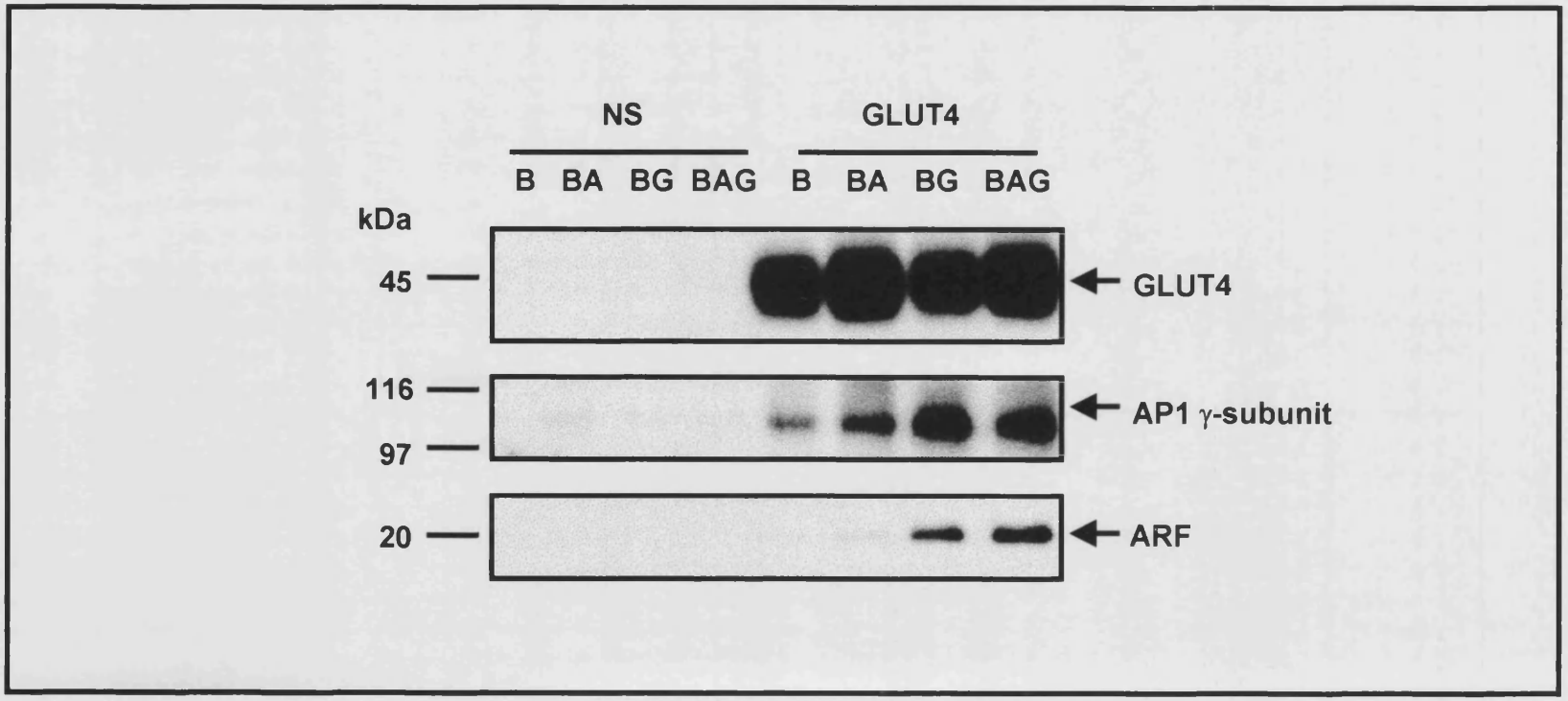

immunoadsorbed from a post-HDM supernatant treated with the ATP regeneration system alone.

5.4.4 Temperature Dependence of AP1 and ARF Recruitment

The *in vitro* recruitment of AP1 in the presence of GTPγS was found to be temperature dependent. In the absence of GTPγS only a small change in amounts of AP1 associated with GLUT4 vesicles was observed when the coating reaction temperature was increased from 4°C to 37°C. However when the recruitment of AP1 was stimulated by the inclusion of GTPγS, the reaction was very temperature dependent (*Figure 5.15A*). AP1 could be detected on vesicles isolated at 4°C. This association was increased markedly by incubating the reaction at 20°C, with maximal recruitment observed at 37°C. The recruitment of AP1 to GLUT4 vesicles observed at 37°C was approximately 5-fold greater than that observed at 4°C (*Figure 5.15A, lower panel*). In addition the temperature dependent *in vitro* recruitment of ARF paralleled the AP1 association, increasing 3-fold over the same temperature range (*Figure 5.15B*).

5.4.5 The Inhibition of AP1 and ARF Recruitment to GLUT4 Vesicles by Brefeldin A

Budding of vesicles from their donor membranes must be accurately organised so that the basic structure of the membrane compartments is not disturbed. The association of AP1 with membranes is finely controlled, being stimulated by GTPγS and inhibited by the fungal heterocyclic lactone, brefeldin A. Brefeldin A inhibits AP1 re-location by blocking GDP.GTP exchange by ARF-GEFs. This prevents ARF association with membranes (Robinson and Kreis, 1992; Wong and Brodsky, 1992; Liang and Kornfeld, 1997). Thus the effect of brefeldin A on AP1 and ARF recruitment to GLUT4 vesicles was examined. Post-HDM supernatants were either left untreated, pre-treated with 100 μg/ml brefeldin A for 10 min at 37°C, followed by incubation with GTPγS and an ATP regenerating system, or treated with GTPγS and an ATP regenerating system alone. All samples were incubated for a total of 45 min at 37°C. The post-HDM supernatants were returned to ice to arrest the coating reaction and GLUT4 vesicles were immunoprecipitated on acrylic beads as already described (*Section 5.3.1*). Vesicular proteins were analysed by SDS-PAGE and Western blotting.

Figure 5.15 The Effects of GTPγS and Temperature on the Recruitment of AP1 and ARF onto GLUT4 Vesicles in a Cell-Free System.
Post-HDM supernatants from basal adipose cells were treated with 600 μM GTPγS for 30 min at either 4, 20 or 37°C. GLUT4 vesicles were then immunoadsorbed on acrylic beads coated with either non-specific rabbit IgG (NS) or polyclonal GLUT4 antibodies (GLUT4). Vesicle associated proteins were eluted and examined by SDS-PAGE and Western blotting with polyclonal antibodies against the γ-subunit of AP1 and monoclonal pan antibodies against ARF. The lower panels are densitometric analyses of the Western blots normalised to the 37°C samples. The results shown are representative of 2 independent experiments.

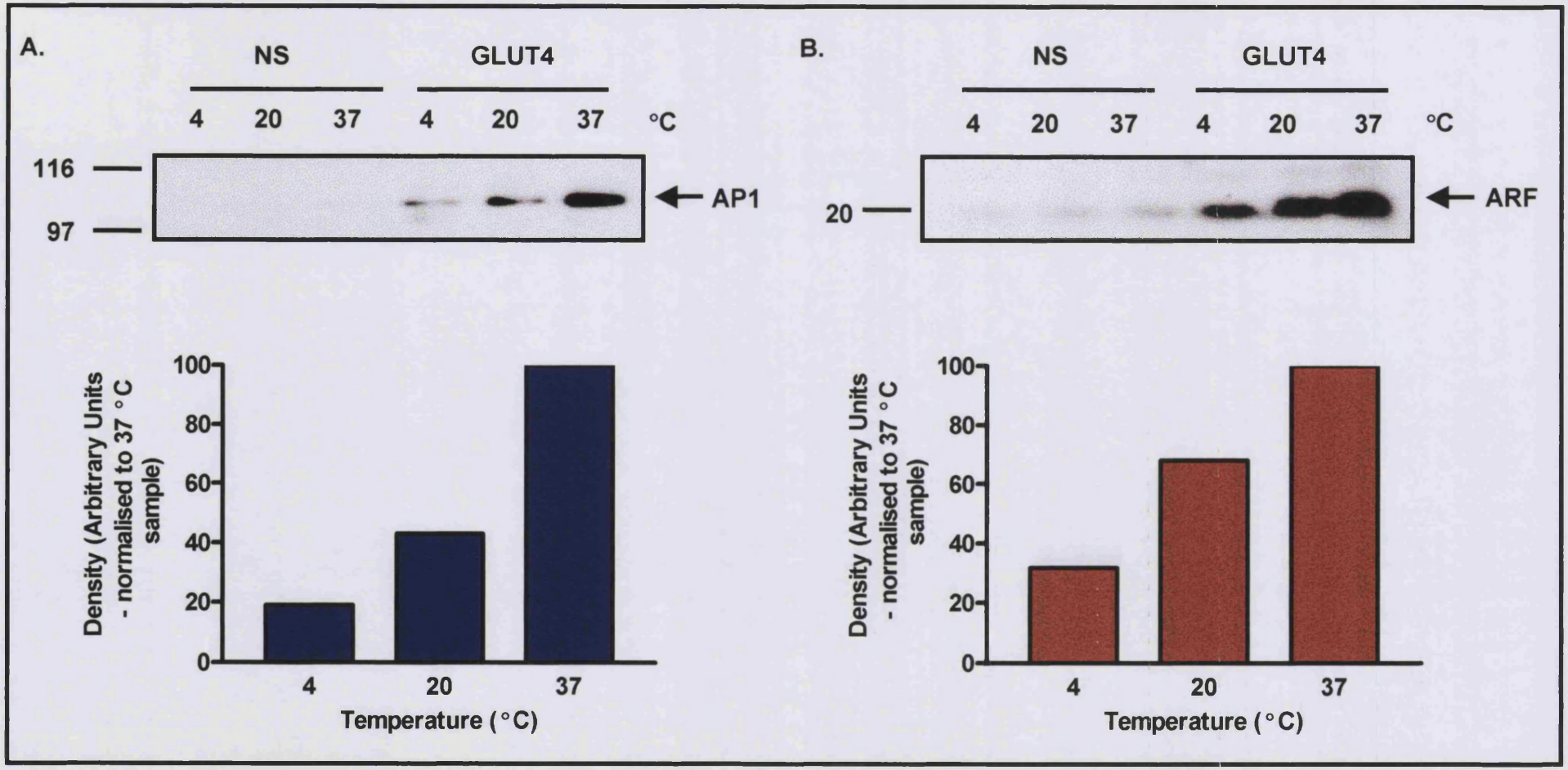

Figure 5.16. The effect of Brefeldin A on the GTPγS driven recruitment of AP1 and ARF onto GLUT4 vesicles. Post-HDM supernatants of basal (B) and insulin treated (I) adipose cells were either left untreated (No Additions), treated with GTPγS and an ATP regenerating system for 30 min at 37°C (GTPγS + rATP) or pre-treated with 100 μg/ml Brefeldin A for 10 min at 37°C, followed by treatment with GTPγS and an ATP regenerating system for 30 min at the same temperature (BFA/GTPγS + rATP). GLUT4 vesicles were then immunoadsorbed on acrylic beads coupled to affinity purified anti-GLUT4 antibodies. Vesicle associated proteins were analysed by SDS-PAGE and Western blotting with a monoclonal antibody to GLUT4 (clone 1F8), a polyclonal antibody to the γ-subunit of AP1 and a monoclonal pan antibody against ARF. The results shown are representative of 2 experiments.

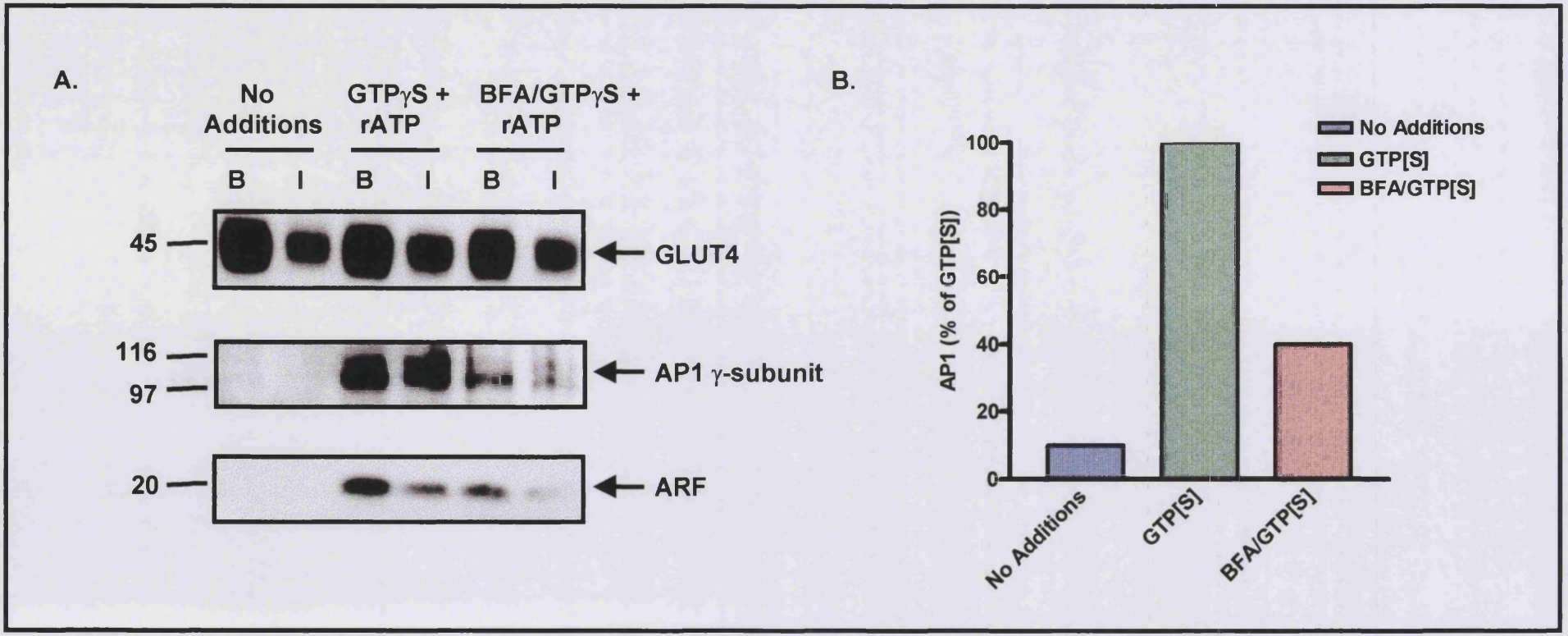

A significant reduction in AP1 recruitment (≈ 60%) to GLUT4 vesicles was observed in the sample pre-treated with brefeldin A before stimulation with GTPγS and an ATP regenerating system. The film shown in *Figure 5.16A* was only exposed long enough to quantitate this difference, however AP1 was also observed in the sample derived from the untreated adipocyte post-HDM supernatant, to a level 10% of the GTPγS/ATP stimulated control sample (*Figure 5.16B*).

The association of ARF with GLUT4 vesicles was also shown to decrease following the brefeldin A incubation, however ARF was not completely dissociated from the membranes. A number of explanations for this observation can be surmised. Firstly the incubation with brefeldin A may not have been sufficiently long to induce a total loss of ARF from the membrane. Secondly the concentration of brefeldin A may not have been stringent enough. To our knowledge no prior study has analysed the effects of brefeldin A on ARF and AP1 recruitment to membranes in a cell-free system. However in permeabilised cells a substantially higher concentration of brefeldin A is required to completely inhibit ARF association with TGN membranes, compared with immunofluorescence studies in intact cells (Wong and Brodsky, 1992). One further, although remote, explanation is that another ARF isoform is associated with GLUT4 vesicles. Since the monoclonal antibody used in this study detects ARFs 1, 3, 5 and 6, this alternative ARF may be ARF6, a brefeldin A-insensitive isoform.

5.4.6 The Effect of Neomycin on Glucose Transport

Phospholipase D (PLD) hydrolyses phospholipids into phosphatidic acid and their respective polar head groups. PLD activity is stimulated by ARF and its activity is required for the formation of certain vesicle populations. Recently it was reported that inhibition of PLD activity using Neomycin, prevents the recruitment of AP2 on to the plasma membrane and the endosomes but has little effect on AP1 (West *et al.*, 1997). However, treatment of cells with ethanol, which diverts the action of PLD from the production of phosphatidic acid to the production of phosphatidylethanol, prevents the formation of coated vesicles at the Golgi membrane, even in the presence of ARF (Ktistakis *et al.*, 1996). Thus there appears to be some controversy over the exact role of PLD in adaptor recruitment, and how it is regulated.

Figure 5.17. The effect of the phospholipase D inhibitor neomycin on glucose transport in rat adipocytes. Rat adipocytes were isolated as described in *Methods 2.2.2.* The cells were pre-treated with the appropriate concentration of neomycin for 30 min at 37°C. During this time the samples were kept in the dark. Following neomycin treatments cells were either left in the basal condition or stimulated for 30 min at 37°C with 20 nM insulin. The uptake of ^{14}C-3-O-methyl-D-glucose was perfomred as described in *Methods 2.4.1.* The results shown represent the mean and s.e.m. of 3 separate experiments.

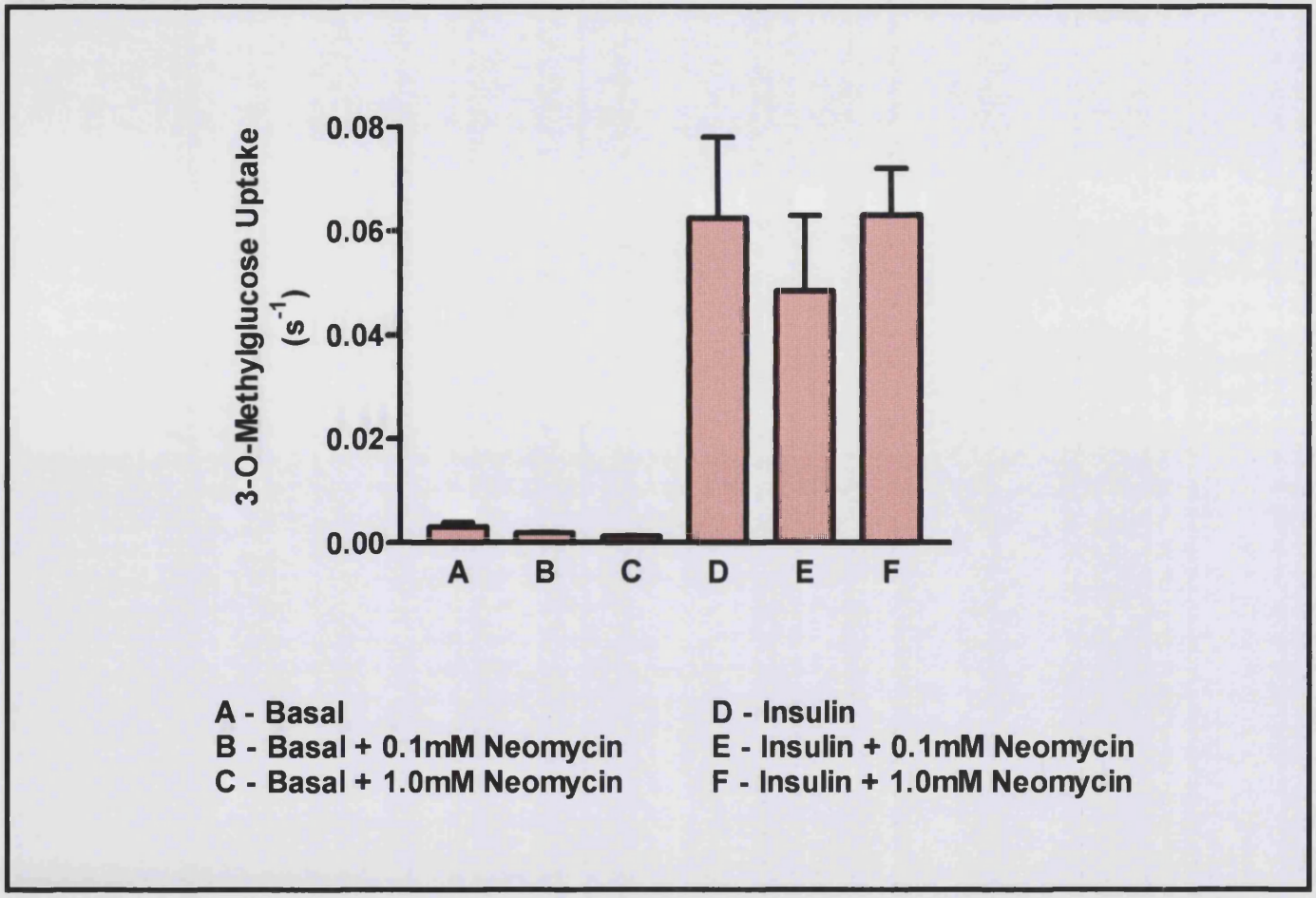

Since GLUT4 vesicles were shown to associate with specific adaptor protein complexes, we decided to test whether inhibition of PLD activity had any effect on glucose transport. Rat adipocytes were therefore incubated for 30 min at 37°C with 0.1 mM or 1.0 mM Neomycin, or were left untreated. Glucose transport was increase 40-fold in insulin-stimulated adipocytes compared with unstimulated basal controls (*Figure 5.17*). However inhibition of PLD activity by Neomycin did not significantly effect glucose transport in either basal or insulin-stimulated rat adipocytes.

5.4.7 Detection of Adaptor Proteins on GLUT4 Vesicles from Other Insulin-Sensitive Tissues

Since the association of adaptor proteins and ARF with GLUT4 vesicles derived from rat adipocytes was clearly established, we next attempted to analyse whether the same adaptor proteins were recruited to GLUT4 vesicles derived from other insulin-sensitive tissues. To this end adaptor protein antibodies were tested on fractions isolated from cardiomyocytes, and compared with adipocyte LDM controls. Myocytes were homogenised, and centrifuged at 541, 000 *g* for 30 min at 4°C to produce a cytosolic fraction and a total membrane fraction. The total membrane fraction was resuspended in 3 ml HES buffer and re-pelleted at the same speed. Samples of adipocyte LDM and cardiomyocyte total membrane and cytosolic fractions were compared by SDS-PAGE and Western blotting with antibodies against AP1, AP3 and ARF (*Figure 5.18A*). Clear signals were obtained for all three antibodies in the cardiomyocyte fractions.

Next, GLUT4 vesicles were prepared from the post-HDM supernatants of cardiomyocytes isolated consecutively from two hearts. The myocytes were homogenised and the plasma membrane and high density microsomes were removed by centrifugation. The post-HDM supernatant was treated with GTPγS and an ATP regenerating system, before the vesicles were immunoprecipitated on acrylic beads covalently coupled to either non-specific rabbit IgG (NS) or affinity purified anti-GLUT4 antibodies (GLUT4). Vesicle associated proteins were analysed by SDS-PAGE and Western blotting. A small number of GLUT4 vesicles could be detected in the GLUT4-specific precipitates, with fewer vesicles isolated from the insulin treated sample, as expected. However significant levels of AP1 γ-subunit could not be detected (*Figure 5.18B*). In addition no association between GLUT4 vesicles and AP3 or ARF was determined (data not shown). Since GLUT4 vesicles comprise only a small

Figure 5.18 The Association of Adaptor Complexes with GLUT4 Vesicles Prepared from Cardiomyocytes. A. Total membranes and cytosol prepared by centrifuging cardiomyocyte homogenates at 541,000*g* for 30 min, were compared with low density microsomes prepared from rat adipocytes (*Methods 2.5.1*) for AP1, AP3 and ARF content. 20 μg of protein from each fraction were resolved by SDS-PAGE and Western blotting. B. GLUT4 vesicles were prepared from post-HDM supernatants of untreated (B) and insulin stimulated (I) cardiomyocytes. The vesicles were immunoadsorbed onto acrylic beads coated with non-specific IgG (NS) or affinity purified anti-GLUT4 antibodies (GLUT4). Vesicle associated proteins were analysed by SDS-PAGE and Western blotting. A total membrane protein standard (50 μg) was run alongside the Thesit solubilised material. The results shown are representative of 2 separate experiments.

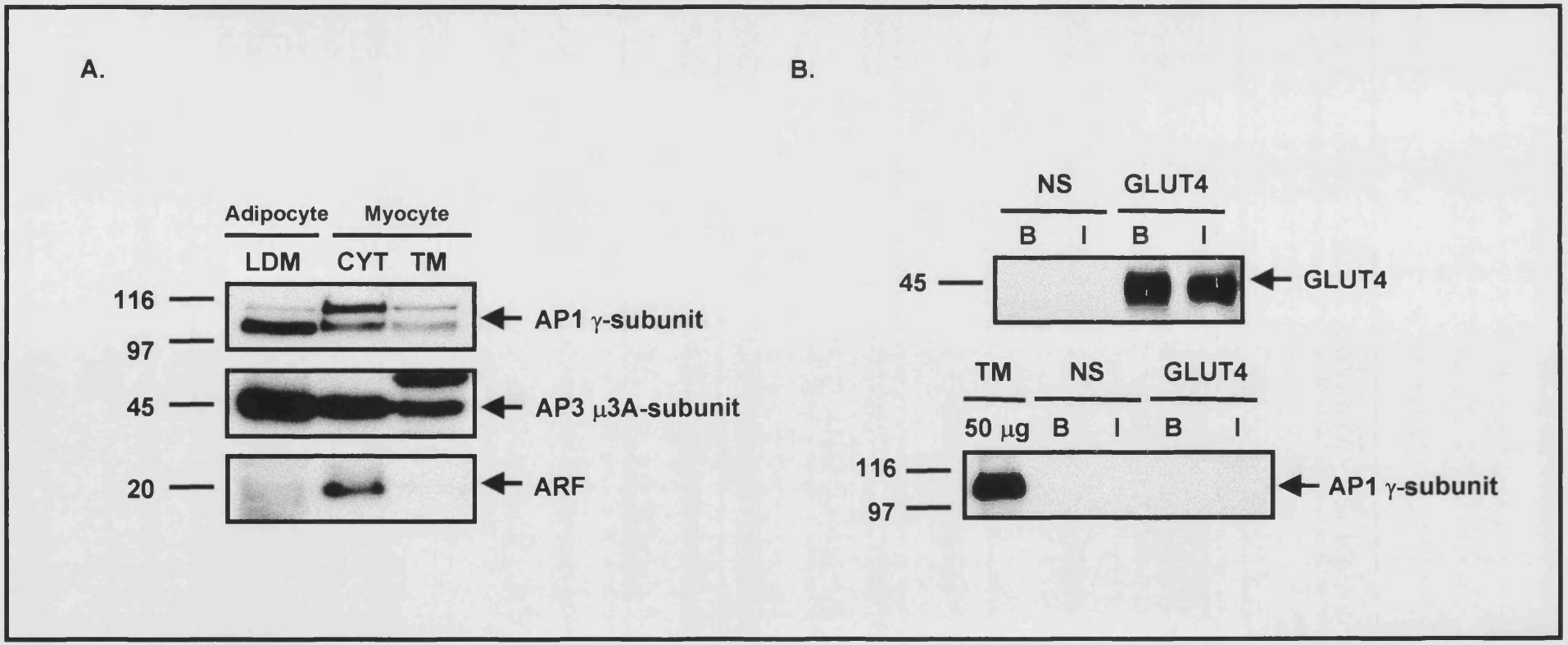

percentage of the post-HDM supernatant protein, it is possible that insufficient vesicles were obtained from two hearts.

5.5 The Effect of Insulin on GLUT4 and Adaptor Proteins

5.5.1 Insulin-induced Redistribution of GLUT4 on Nycodenz Gradients

Recent research suggests that GLUT4 vesicles are spherical, homogeneous particles with a sedimentation co-efficient of 120 *S* in sucrose. Upon insulin stimulation the co-sedimentation co-efficient of the vesicles in sucrose increases by 20 *S* and consequently the buoyant density decreases (Kandror and Pilch, 1998). To examine whether this is the case when vesicles are isolated on other gradients, post-HDM supernatants were prepared from untreated (B) and insulin-stimulated (I) adipocytes, then layered on to the top of linear 9-27% Nycodenz gradients and centrifuged at 63, 000 *g* for 2.5 h. Fractions were collected from the bottom to the top of the gradient and analysed by SDS-PAGE and Western blotting.

As already shown GLUT4 vesicles from the basal adipocyte post-HDM supernatant fractionate as a broad band on Nycodenz gradients (*Section 5.2.1*). Treatment of adipocytes with insulin reduced the concentration of GLUT4 vesicles recovered on the Nycodenz gradient (*Figure 5.19*), although the characteristic broad distribution was retained. The reduction in vesicles is primarily due to the exocytosis of GLUT4 from the intracellular specialised compartment (contained within the post-HDM supernatant) and fusion with the plasma membrane. In addition and although the distribution of GLUT4 on gradients varied slightly between experiments, treatment of cells with insulin before the isolation of vesicles, consistently resulted in a shift of immunoreactive GLUT4 by 1-2 fractions to a less dense region of Nycodenz. These results are in agreement with the shift of GLUT4 vesicles derived from insulin treated adipocytes observed on sucrose gradients (Kandror and Pilch, 1998).

5.5.2 Insulin-induced Redistribution of AP1

The action of insulin on adaptor proteins is of interest since it has been shown that PIP_3 negatively regulates the interaction between adaptor proteins and membrane receptors which contain di-leucine targeting sequences within their cytoplasmic tails (Rapoport *et*

Figure 5.19 The Effect of Insulin on the Distribution of GLUT4 on Nycodenz Gradients. Plasma membrane and high density microsomes were removed by centrifugation of basal (B) (●) and insulin treated (I) (●) rat adipocyte homogenates. The remaining supernatants (the post-HDM supernatants) were layered on to the top of 9-27% Nycodenz gradients and centrifuged for 2.5 hrs at 63,000*g*. One ml fractions were collected from the bottom (most dense) to the top (least dense) of the tube. Fractions were analysed by SDS-PAGE and Western blotting with affinity purified polyclonal rabbit anti-GLUT4 antibodies. Densitometric analysis of the Western blot is shown in the graph on the right. GLUT4 was not detected in fractions 1-19, therefore only fractions 20-39 are shown. The results presented are representative of 5 individual experiments.

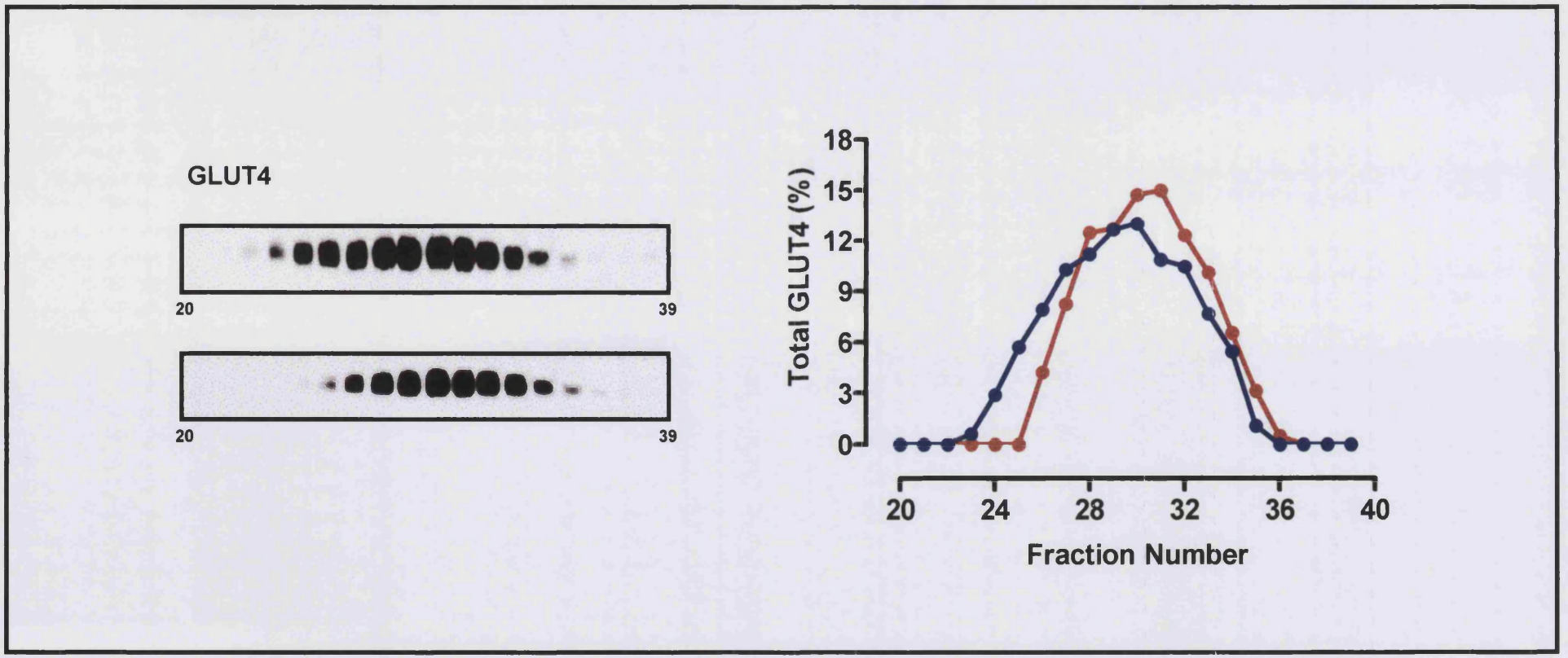

al., 1998). Furthermore the association of a C-terminal peptide and the β1-subunit of AP1 is reduced in the presence of PIP_3 (Rapoport *et al.*, 1998). Thus the association of AP1 with subcellular fractions derived from rat adipose cells in the absence and presence of insulin was examined in more detail (*Figure 5.20A*). Insulin caused a reproducible decrease in the level of association of AP1 with both the plasma membrane and the low density microsomes. The decrease in AP1 recruitment at the plasma membrane was smaller and although consistent, did not reach significance (paired, one tailed t-test, with 95% confidence interval). This is presumably because the AP1 adaptor is TGN-specific, and is probably adhering non-specifically to the plasma membrane. However the decrease in AP1 at the LDM was significant, with a p-value <0.01.

Since insulin appeared to reduce the level of association of AP1 with the LDM fraction, possibly due to the activation of PI 3-kinase and the generation of PIP_3, we next analysed whether incubation of GLUT4 vesicles with an insulin cytosol could reduce adaptor association. GLUT4 vesicles from basal post-HDM supernatants were immunoadsorbed onto acrylic beads covalently coupled to non-specific rabbit IgG or rabbit polyclonal anti-GLUT4 antibodies. The vesicles were washed in HES buffer, then incubated in the presence of cytosol derived from either basal or insulin-stimulated adipocytes. Vesicle associated proteins were eluted in a detergent buffer and analysed by SDS-PAGE and Western blotting. The results are shown in *Figure 5.20B.* Incubation of basal GLUT4 vesicles in the presence of a basal or insulin cytosol had little effect on the levels of immunoreactive GLUT4 detected. A decrease in the AP1 signal was detected which may be due to negative modulation by PIP_3, however no change in the level of AP3 association with GLUT4 vesicles was observed.

5.5.3 The Effect of Wortmannin on the Association of AP1 with GLUT4 Vesicles

Wortmannin is a PI 3-kinase inhibitor. Treatment of mammalian cells with wortmannin results in a massive change in terms of general membrane morphology, indicated by tubulation and vacuolation of the endosomal compartment and by swelling of lysosomes (Shpetner *et al.*, 1996). These wortmannin-induced morphological changes demonstrate the importance of PI 3-kinases in maintaining the integrity of intracellular compartments. However PI 3-kinases also play a fundamental role in both the

Figure 5.20 The Effect of Insulin on Adaptor Protein Complexes. A. Analysis of the effect of insulin on the distribution of AP1 in the plasma membrane (PM) and low density microsomes (LDM). Basal (B) and insulin treated (I) adipocytes were fractionated by centrifugation as described in *Methods 2.5.1.* 20 μg of the plasma membrane and low density microsomal fractions were resolved by SDS-PAGE and Western blotting with an antibody against the γ-subunit of AP1. The results were analysed by densitometry, shown in the graph below. Significance differences following insulin treatment are given by the indicated p values (paired t-test, one tailed). B. The effect of an insulin treated cytosol on AP1 recruitment to GLUT4 vesicles. GLUT4 vesicles were adsorbed from basal post-HDM supernatants using acrylic beads coated with either non-specific rabbit IgG (NS) or with affinity purified anti-GLUT4 antibodies (GLUT4). Following immunoadsorption of the vesicles, the beads were washed in HES buffer and then incubated at 37°C with cytosol derived from either basal or insulin treated adipocytes for 15 min. Following this incubation, the beads were washed and the vesicle associated proteins were eluted and analysed by SDS-PAGE and Western blotting.

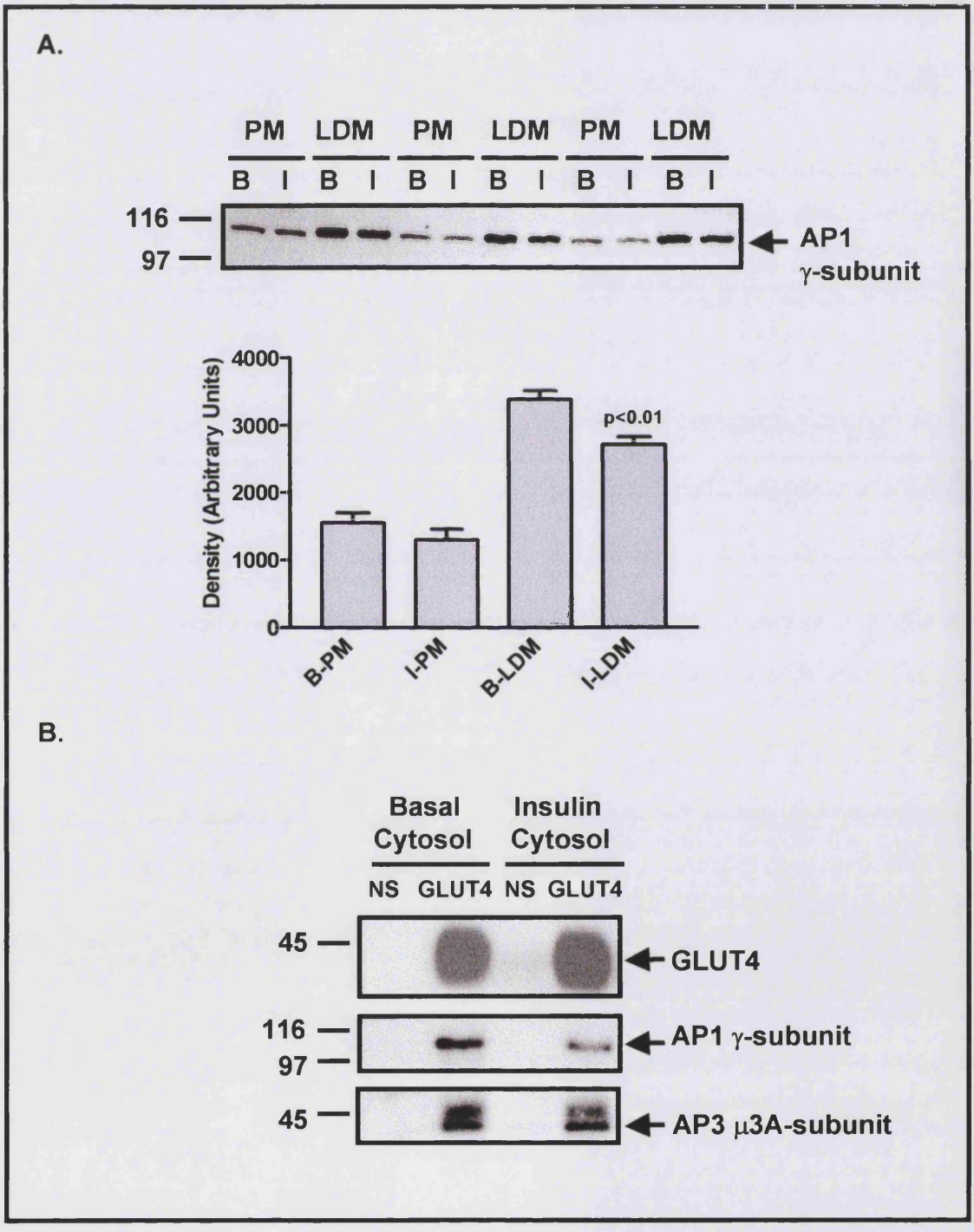

exocytosis and endocytosis of GLUT4 (Malide and Cushman, 1997). Thus in order to establish whether any of these effects are potentiated by changes in adaptor association we analysed coat recruitment to GLUT4 vesicles from wortmannin treated adipocytes. Adipocytes were therefore treated with insulin, with insulin and wortmannin or left untreated. Post-HDM supernatants were prepared, stimulated by GTPγS and an ATP regenerating system and vesicles were immunoadsorbed on acrylic beads as already described (*Section 5.3.1*). Vesicle associated AP1 was analysed by SDS-PAGE and Western blotting. AP1 was found in all the precipitates isolated on GLUT4-specific acrylic beads. Fewer adaptors were detected on vesicles isolated from the insulin treated sample, consistent with the stimulation of GLUT4 vesicles to the plasma membrane. Treatment of cells with wortmannin and insulin together resulted in a level of AP1 association which was intermediate between the basal- and insulin-level of association (*Figure 5.21*).

5.6 How do the GLUT4 Vesicles Associate with Adaptor Proteins?

5.6.1 Immunoprecipitation of GLUT4 Vesicles using an N-terminal Antibody

Adaptor proteins have been shown to bind to membrane receptors and transporters via their tyrosine or di-leucine motifs (Kirchhausen *et al.*, 1997). Furthermore a C-terminal peptide of GLUT4 containing a di-leucine motif has been shown to specifically interact with the β1-subunit of AP1 (Rapoport *et al.*, 1998). Thus if GLUT4 vesicles are immunoadsorbed onto acrylic beads derivatised with an antibody against this very region, how do the adaptor proteins associate with the vesicles? Initially attempts to answer this question centred on the use of an antibody directed against the N-terminal of GLUT4. If vesicles could be isolated with this GLUT4 antibody which was directed against a region of the transporter distant from the di-leucine motif would an enhanced association of adaptors be observed? In these experiments *Staphylococcus aureus* Cowan I cells (Staph cells) were coupled with antibodies raised against the C-terminal of GLUT4, the N-terminal of GLUT4 or a combination of both. Staph cells were used as acrylic beads can not be incubated with azide in which the N-terminal antibody was stored.

Post-HDM supernatants derived from basal adipocytes were either left untreated or treated with GTPγS plus an ATP regenerating system for 30 min at 37°C. The samples were

Figure 5.21 The Effect of Wortmannin on the Association of Adaptor Complexes with GLUT4 Vesicles. GLUT4 vesicles were prepared from post-HDM supernatants derived from unstimulated, basal adipocytes (B), insulin stimulated adipocytes (I) and adipocytes treated with both insulin and wortmannin (1 μM) (IW). Post-HDM supernatants were then incubated with 600μM GTPγS before isolation of vesicles on acrylic beads coated with either non-specific rabbit IgG (NS) or affinity purified anti-GLUT4 antibodies (GLUT4). Vesicle associated proteins were eluted in a detergent buffer and analysed by SDS-PAGE and Western blotting with antibodies against the γ-subunit of AP1. Bound GLUT4 was released by denaturation of the anti-GLUT4 antibodies and probed with a monoclonal 1F8 antibody against GLUT4.

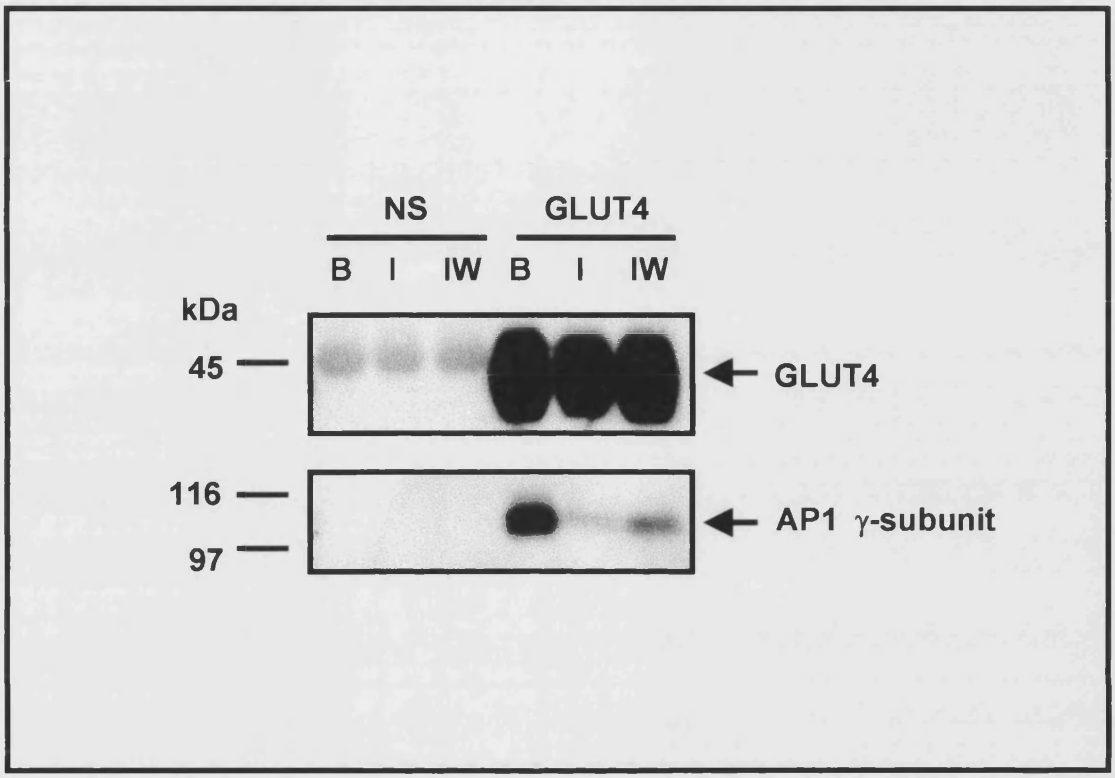

returned to ice before an initial preclearing incubation with Staph cells coupled to non-specific rabbit IgG. Supernatants were then transferred to Staph cells bound with non-specific rabbit IgG or rabbit anti-GLUT4 serum (C-, N-, or a combination of both) and rotated for 2 h at 4°C. Staph cells were subsequently washed once in HES buffer and twice in HES buffer containing 100 mM KCl. Vesicular proteins were solubilised and bound GLUT4 protein was eluted by heating pellets to 95°C in sample buffer. The resulting samples were analysed by SDS-PAGE and Western blotting with monoclonal antibodies against GLUT4 (clone 1F8) and ARF and a polyclonal antibody against the γ-subunit of AP1. The levels of GLUT4 vesicles immunoprecipitated by the different GLUT4 antibodies varied, being greatest for the post-HDM supernatant immunoadsorbed with a combination of N- and C-terminal directed antibodies. The efficiency of the N-terminal GLUT4 antibody was particularly poor, but was increased by incubation with GTPγS and an ATP regenerating system. This may imply that a protein is associated with the N-terminus of GLUT4 blocking the interaction of the N-terminal antibody with this region (*Figure 5.22A*). The actions of a GTPase, an ATPase or a combination of both may release this protein block. The levels of AP1 found in the sample immunoprecipitated on Staph cells bound with N-terminal GLUT4 antibodies were lower than that found in samples immunoadsorbed on Staph cells coupled to the C-terminal GLUT4 antibody. However this presumably reflects the ability of these antibodies to efficiently immunoprecipitate GLUT4 vesicles. Indeed considering the lower efficiency of the N-terminal antibody to immunoprecipitate GLUT4 vesicles, the association of AP1 is relatively high, and may be greater than the levels of AP1 bound to an equivalent population of GLUT4 vesicles immunoadsorbed by the C-terminal GLUT4 antibody.

5.6.2 Detection of GLUT4 in the Thesit-Soluble Eluate

Another approach to analyse the importance of the C-terminus of GLUT4 in adaptor recruitment was to analyse whether any of the GLUT4 in the immunoprecipitated vesicles was freely soluble and therefore available for association with adaptor subunits. Thus both the Thesit-soluble material and the protein eluted by heating the acrylic beads (Thesit-insoluble) was analysed by SDS-PAGE and Western blotting with a GLUT4 antibody. Approximately half of the total GLUT4 was recovered in the soluble material, and half was covalently bound to the beads. This implies that there may be

Figure 5.22 How do GLUT4 Vesicles Associate with the Adaptor Complexes? A. GLUT4 vesicles were isolated from post-HDM supernatants prepared from basal adipose cells. The post-HDM supernatants were either treated with 600 μM GTPγS or left untreated before the immunoadsorption of the vesicles on *Staphylococcus aureus* cells coated either with antibodies against the C-terminus of GLUT4 (C-GT4), or antibodies against the N-terminus of GLUT4 (N-GT4), or a 50:50 mixture of both antibodies (C/N-GT4). Vesicle associated proteins were eluted and resolved by SDS-PAGE and Western blotting. B. GLUT4 vesicles from basal (B) and insulin stimulated (I) adipocytes were isolated on acrylic beads covalently coupled to either non-specific rabbit IgG (NS) or affinity purified polyclonal rabbit anti-GLUT4 antibodies (GLUT4). Vesicle associated proteins were eluted in a Thesit detergent buffer (soluble). Covalently bound GLUT4 was released by denaturing the anti-GLUT4 antibodies (insoluble). Both the soluble and insoluble material was resolved by SDS-PAGE and Western blotting with monoclonal antibodies against GLUT4 (clone 1F8). The results presented are representative of 3 separate experiments.

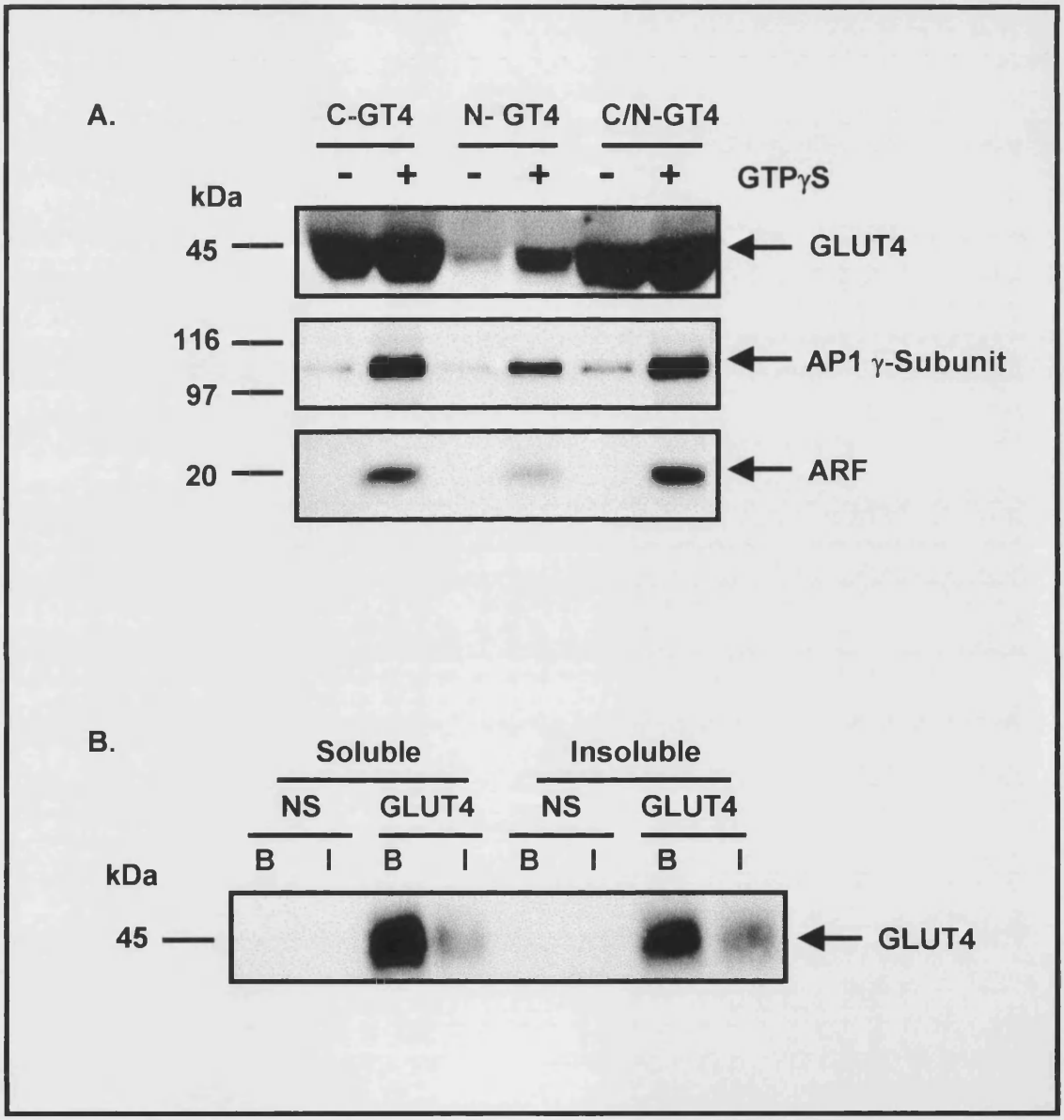

sufficient GLUT4 protein available in the vesicles to interact via its cytoplasmic C-terminal tail with adaptor complexes in the Golgi membrane (*Figure 5.22B*).

5.6.3 Crosslinking Adaptor Proteins and GLUT4

In an attempt to show a direct interaction of GLUT4 with the AP1 adaptor complex, chemical cross-linking studies were performed. Post-HDM supernatants from basal adipocytes were either left untreated or treated with the chemical cross-linkers designated 'ABABA' and 's-ABABA-s' (the structures of which are shown in *Figure 5.23A*). Post-HDM supernatants from basal and insulin treated adipocytes were either left untreated or incubated with one of the cross-linking reagents at a concentration of 1 mM, in the presence of 1 mM WSC (1-(3-Dimethylaminopropyl)-3-Ethylcarboimide Hydrochloride) and 1 mM HAT (1-Hydroxylbenzothiazole) for 1 h at room temperature. The reaction was quenched by the addition of 20 mM Tris-HCl pH 7.4. 20 μg of protein from each condition was analysed on a 7% resolving gel with 4% stacking gel (*Figure 5.23B*). GLUT4, AP1 and AP3 could all be cross-linked using these reagents and formed high molecular weight complexes that did not migrate into the gel. GLUT4 vesicles from cross-linked post-HDM supernatants were immunoprecipitated on acrylic beads covalently coupled to affinity purified GLUT4 antibodies. Cross-linked complexes were cleaved by the addition of 5 mM sodium periodate for 30 min at room temperature. Oxidised proteins were reduced by incubation with 20 mM sodium borohydride for 5 min, then analysed by SDS-PAGE and Western blotting. Neither GLUT4 nor AP1 could be detected in the periodate-cleaved material, the blots being particularly dark (data not shown).

Figure 5.23 The Use of Chemical Cross-linkers to Identify Proteins in Close Proximity to GLUT4 and the Adaptor Complexes. Post-HDM supernatants from basal (B) and insulin stimulated (I) adipocytes were either left untreated (no linker) or cross-linked with 'ababa' or 's-ababa-s', (the structures of which are shown in A). 20 μg of protein from each condition were resolved on a 7% SDS-PAGE gel with a 4% stacker and Western blotted with rabbit polyclonal antibodies against GLUT4 and subunits of the AP1 and AP3 adaptor complexes, shown in B.

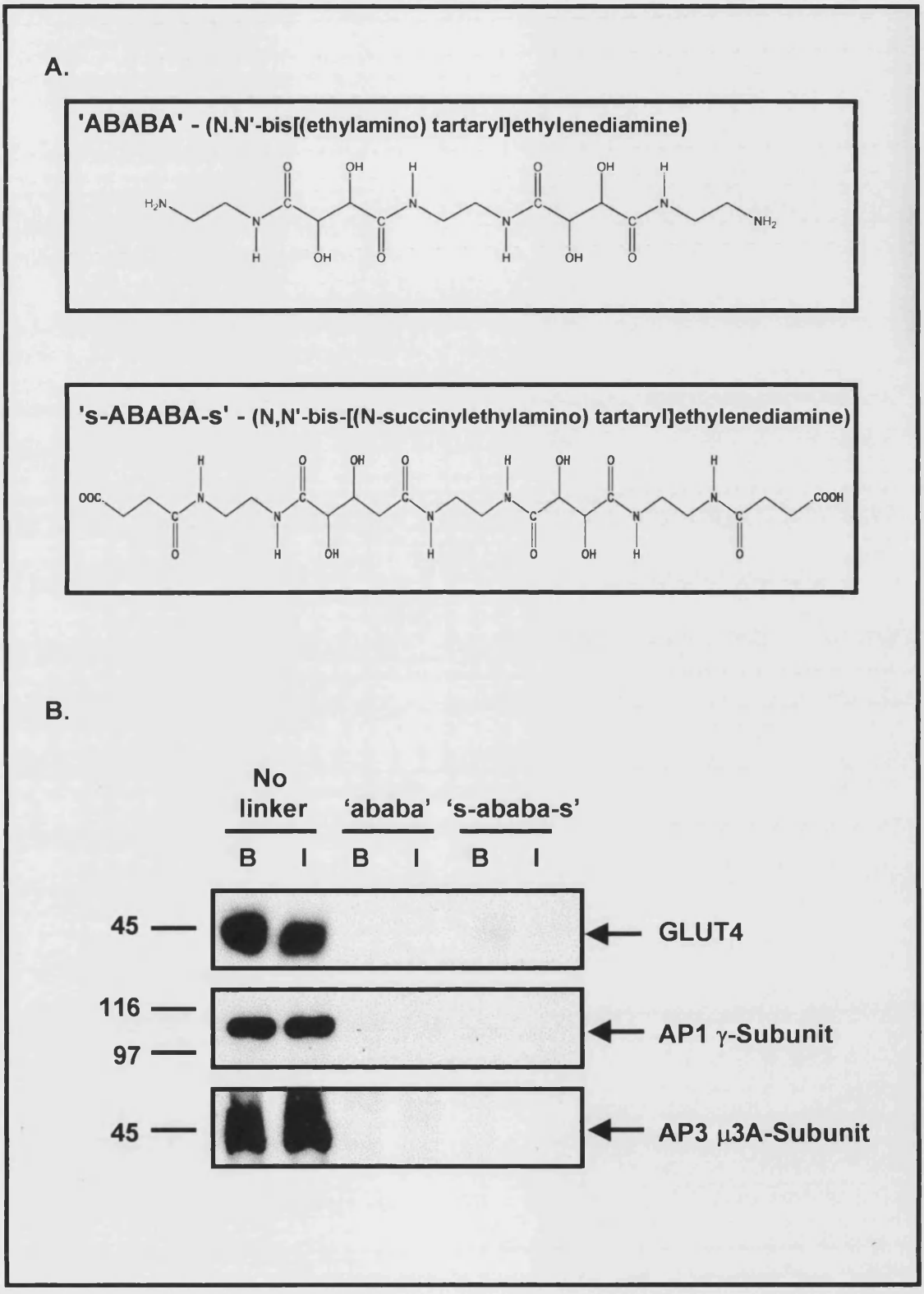

5.7 Discussion

Knowledge of the intracellular itinerary of GLUT4 is fundamental to our understanding of how insulin stimulates a massive increase in GLUT4 levels at the plasma membranes. Trafficking of GLUT4 through the labyrinth of intracellular compartments appears to be important for the generation and maintenance of a GLUT4 reservoir (Holman *et al.*, 1994). Insulin acts upon this reservoir recruiting GLUT4 to the plasma membrane and increasing the levels of the transporter at the cell surface by 10-20 fold. Kinetic analyses using photolabel-tagged GLUT4 have shown that insulin acts primarily on the exocytic limb of the recycling pathway, with little or no effect on the rate of GLUT4 endocytosis (Satoh *et al.*, 1993; Yang and Holman, 1993; Yang *et al.*, 1996). As well as GLUT4, insulin also causes the translocation of a number of other proteins to the plasma membrane, including GLUT1 (Holman *et al.*, 1990; Calderhead *et al.*, 1990) and the TfR (Tanner and Lienhard, 1987). However the stimulatory effect on these proteins is small in comparison with the response of GLUT4. These observations strongly imply that GLUT4 resides in a specialised compartment, which is acted upon by insulin in a unique and selective manner. The discriminatory interaction of GLUT4 with proteins along its recycling pathway may underlie the mechanism for its specialised sorting and sequestration.

GLUT4 contains targeting signals present at both its N- and C-termini. This trafficking information includes a 'tyrosine-like' motif and a di-leucine sequence, which are ideal candidates to interact with adaptor complexes (Piper *et al.*, 1993; Verhey and Birnbaum, 1993; Melvin *et al.*, 1999). Substantial evidence suggests that both these motifs are important for the intracellular sequestration of GLUT4 from the plasma membrane, and for subsequent intracellular trafficking (Corvera *et al.*, 1994; Araki *et al.*, 1996; Garippa *et al.*, 1996). Thus it is likely that GLUT4 interacts with both the plasma membrane adaptor AP2, and other intracellular-specific adaptors including the endosomal adaptor complex, AP3 and the TGN-directed adaptor complex, AP1.

In this study an immunoprecipitation technique was employed to address whether there is any direct association of adaptor proteins with GLUT4 vesicles. Using this procedure approximately 67% of the total GLUT4 population could be absorbed onto acrylic beads derivatised with a C-terminal antibody against GLUT4. This immunoadsorption efficiency is lower than that reported by Kandror and Pilch (Kandror and Pilch, 1994), who recovered 70-80% of the GLUT4 vesicles in the LDM fraction using beads coupled

to monoclonal GLUT4 antibodies (clone 1F8). This difference can be explained in part by the different methods employed; in our study the post-HDM supernatant was rotated for 2 h at 4°C with the acrylic beads compared with an overnight incubation used by Kandror and Pilch (Kandror and Pilch, 1994). This shorter incubation was initially used in an attempt to prevent weakly bound proteins from dissociating during the rotation step. Furthermore in our study the post-HDM supernatant was used rather than the LDM fraction. The cytosol contained within the post-HDM supernatant may include proteins, which interfere with the immunoadsorption procedure, decreasing the association of GLUT4 vesicles with the beads. Finally in our study, an antibody against the C-terminal tail of GLUT4 was used, whereas in the published work an antibody directed against a longer stretch of amino acids in the C-terminus was employed. It is therefore possible that this latter antibody is more efficient at immunoprecipitating GLUT4 vesicles. Indeed the efficiency of GLUT4 antibodies coupled to various inert supports to immunoprecipitate vesicles has been used to reveal distinct populations of GLUT4 vesicles in cardiomyocytes (Fischer *et al.*, 1997).

This work has clearly demonstrated an association of the γ- μ1- and σ1-subunits of AP1 with GLUT4 vesicles from freshly isolated rat adipose cells. These data are consistent with electron micrographs showing that the γ-subunit of AP1 co-localises with GLUT4 vesicles derived from 3T3-L1 adipocytes (Marsh *et al.*, 1998). Furthermore the association of AP1 with GLUT4 observed by microscopy is increased when serine 488 in the C-terminal phosphorylation site is substituted for alanine. Thus phosphorylation may play a role in targeting and sorting of GLUT4 through its interaction with AP1. In addition to the microscopy data, a recent study has shown a direct interaction between a C-terminal peptide of GLUT4 containing the di-leucine motif and the phosphorylation site, and the β1-subunit of AP1 (Rapoport *et al.*, 1998) and this interaction was modulated by PIP_3. Data shown here reveals that the interaction of AP1 with low density microsomes is decreased in adipocytes treated with insulin. Furthermore, GLUT4 vesicles derived from adipocytes treated with insulin and the PI 3-kinase inhibitor, wortmannin, are associated with higher levels of AP1, than those derived from adipocytes treated with insulin alone. Thus it could be hypothesised that in the insulin-stimulated state when PIP_3 is generated by the action of PI 3-kinase, adaptor proteins may be released from GLUT4 vesicles and redistributed to the cytosol. This in turn may allow vesicle fusion with target membranes. The role of PIP_3 could therefore be to evoke uncoating.

Specific kinases present on clathrin coated vesicles regulate adaptor proteins using phosphorylation as a molecular switch (Wilde and Brodsky, 1996). Thus phosphorylation disrupts the interaction of adaptor proteins with clathrin, and results in their dissociation from the membrane. How these kinases are regulated remains to be determined. However it is interesting to speculate that binding of PIP_3 to adaptor subunits results in a conformational or allosteric change, which facilitates phosphorylation on specific residues. Future work could therefore focus on whether adaptor proteins isolated from insulin cell lysates are hyperphosphorylated compared with basal controls.

As well as the high levels of AP1 association, AP3 was also detected at an appreciable concentration on GLUT4 vesicles. In contrast to this, only a minor amount of AP2 was isolated. This data therefore suggests that the steady-state localisation and intracellular sequestration of GLUT4 are more likely to be dependent on AP1 and AP3, than on AP2. However, only the post-HDM supernatant was examined in these experiments, and as such it is not possible to evaluate the extent of association of AP2 with GLUT4 during its sorting and trafficking at the plasma membrane. Indeed vesicles budding at the cell surface are considerably larger than those budding from intracellular structures, which may facilitate their ability to pellet with the plasma membrane fraction. Thus the association of AP2 with GLUT4 vesicles needs to be further examined, perhaps by attempting to immunoprecipitate vesicles from the plasma membrane fraction itself.

Since GTPγS can stimulate AP1 recruitment to the TGN, a number of experiments were performed to examine the effects of GTPγS on recruitment of adaptors to isolated GLUT4 vesicles. Importantly, we have shown for the first time that, in a cell free system, AP1 can be recruited to isolated GLUT4 vesicles. The extent to which AP1 can be recruited to GLUT4 vesicles is large, and is enhanced by the addition of an ATP regenerating system, and by incubation at physiological temperature. Furthermore the recruitment of AP1 to GLUT4 vesicles can be partially blocked by brefeldin A. This implies that an ARF protein is involved in the coating process.

Unlike AP1, ARF could not detected on GLUT4 vesicles from freshly isolated adipocytes, but could be effectively recruited by incubation with GTPγS, with maximum recruitment observed in the presence of an ATP regenerating system. This data implies that an activated ARF is not required to maintain cellular AP1 on vesicles

once the adaptor complex has been recruited. This idea is supported by recent experiments showing that only a small amount of ARF is present in the purified clathrin-coats of vesicles, and that ARF is instead necessary for priming of the vesicle coating process (Zhu *et al.*, 1998).

As in the case of AP1, treatment of the post-HDM supernatant with brefeldin A resulted in a marked loss of ARF from GLUT4 vesicles. However incubation of adipocytes with brefeldin A has no effect on the insulin-stimulated glucose transport and only decreases basal transport moderately (Bao *et al.*, 1995). In addition treatment of cultured skeletal myotubes with brefeldin A causes the fusion of endosomal-TfR with GLUT4-containing compartments *(Section 1.3.3)*, (Ralston and Ploug, 1996). These results suggest that the steady-state recycling of GLUT4 (responsible for maintaining the intracellular location of the transporter) may include a membrane budding step that is brefeldin A-sensitive. Furthermore inhibition of PLD, a downstream effector of ARF, has no effect on insulin-stimulated glucose transport, again suggesting that it is the intracellular trafficking and not the insulin stimulated exocytosis of GLUT4 that contains an ARF-associated step.

In contrast to the recruitment of AP1, GTPγS did not stimulate the association of AP3 with GLUT4 vesicles. This unexpected observation may occur because under the experimental conditions used here, AP1 is preferentially recruited to GLUT4 vesicles and competes with the binding of AP3. Therefore these data do not exclude the possibility that at some sites within the cell, delimited by membranes and where AP1 availability is restricted, recruitment of AP3 may be dependent on ARF. Indeed at least one study has suggested that ARF1 is capable of inducing the re-location of AP3 from the cytosol to the endosomal membranes (Ooi *et al.*, 1998).

The separation of the bulk of GLUT4 from TfR on both Nycodenz and glycerol gradients suggests a specialised compartment exists which is distinct from the recycling system. However these results contradict the findings of Kandror and Pilch, who suggest that up to 60% of GLUT4 co-localises with TfR on sucrose gradients (Kandror and Pilch, 1998). While we are unable to reconcile this difference, our results are in agreement with a number of other studies. Firstly examination of cultured skeletal myotubes by immunogold electron microscopy shows GLUT4 in structures which are close to but distinct from compartments containing TfRs (Ralston and Ploug, 1996).

Secondly glycerol gradients of PC12 cells transfected with GLUT4, show that the vast majority of the TfRs migrate in fractions which are distal from the major GLUT4 pool (Herman *et al.*, 1994). Finally ablation of the endosomal system using internalised transferrin-HRP and diamino benzidine chemistry results in a total loss of TfR but only a 40% reduction in the levels of GLUT4 (Livingstone *et al.*, 1996).

GLUT4 co-localises with AP1 and AP3 on both of the gradients used in this study. Furthermore, the association of AP1 and GLUT4 is increased by GTPγS which is presumably as a result of a vesicle budding or coating reaction. AP1 and AP3 adaptors may therefore act as 'filters' in the GLUT4 trafficking pathway, providing the divergence from the normal endosome-recycling system that is necessary for the generation of a compartment that can respond so markedly to insulin. Thus GLUT4 in the endosomal compartment may be in equilibrium with a TGN recycling system (Melvin *et al.*, 1999).

Since little co-localisation of GLUT4 with the TGN-specific marker TGN38 is observed, large-scale localisation of GLUT4 within this compartment is unlikely (Martin *et al.*, 1994). However GLUT4 has been shown to traffic though this compartment in atrial cardiomyocytes (Slot *et al.*, 1997), and EM studies have localised a sizeable proportion of GLUT4 to this region of the cell (Slot *et al.*, 1991a). Thus it is interesting to speculate that GLUT4 buds from here to form fusion competent vesicles, which constitute the specialised GLUT4 pool. These vesicles may resemble a compartment similar to the TGN-derived pre-secretory compartment (Dittie *et al.*, 1997; Tooze, 1998). This pre-secretory compartment may act as a sorting station at which several proteins may be retrieved back to the TGN or to the endosomal system, resulting in the concentration of proteins such as GLUT4 and vp165. The association of AP1 with GLUT4 vesicles may therefore be part of a mechanism for iterative enrichment of GLUT4 and removal of molecules such as the mannose-6-phosphate receptor that are required elsewhere (Mauxion *et al.*, 1996; Tooze, 1998; Klumperman *et al.*, 1998). In addition it is possible that AP3 acts in an analogous iterative retrieval process that generates GLUT4 enriched vesicles but re-directs associated proteins to other parts of the endosomal system. A general hypothetical scheme for these processes is shown in *Figure 5.24.*

Figure 5.24 The Role of Adaptor Proteins and Internalisation Signals in GLUT4 Trafficking. GLUT4 is internalised from the cell surface, presumably by the interaction of its FQQI and LL motifs with the plasma membrane adaptor complex AP2. GLUT4 vesicles then traffic via the recycling endosomes, where TfRs are removed and recycled back to the plasma membrane, to the *trans*-Golgi network (TGN). The movement of GLUT4 vesicles between the endosomes and the TGN may be mediated by an interaction between AP3 and the FQQI motif of GLUT4. From the TGN, GLUT4 buds to create the GSVs and proteins such as the mannose-6-phosphate receptor are retrieved by the interaction of AP1 with these vesicles. (In this diagram GLUT4 is shown in red, the TfRs in blue, the mannose-6-phosphate receptors in green and the adaptins in purple).

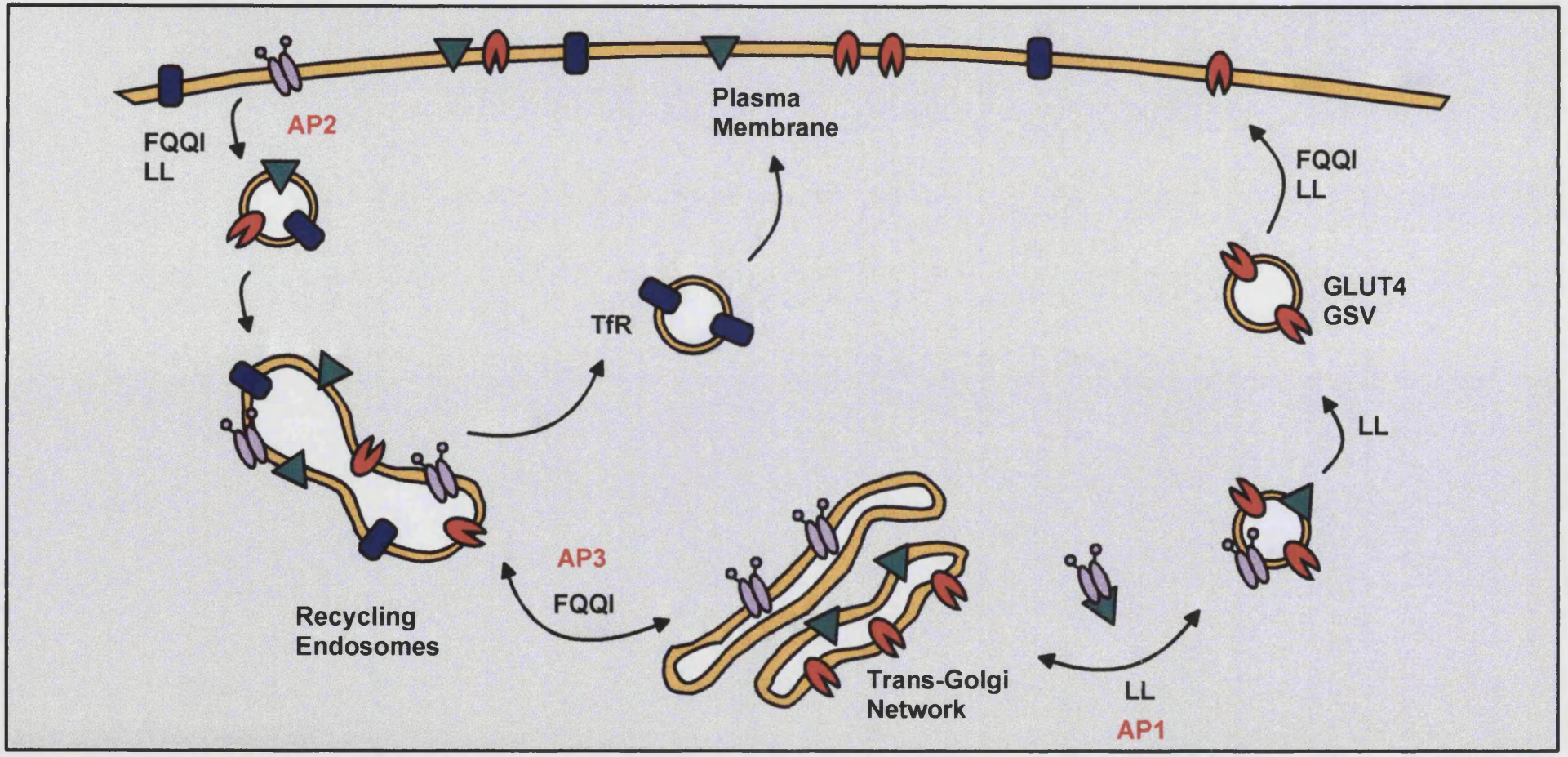

How GLUT4 vesicles specifically interact with adaptor proteins remains to be clarified. Studies presented here suggest that there may be sufficient GLUT4 freely available in vesicles (i.e. not bound to antibodies) to interact with adaptor proteins via their C-terminal targeting sequences. This is supported by the finding that a C-terminal peptide interacts with the β1-subunit of AP1 (Rapoport *et al.*, 1998). However equally plausible is an interaction via the 'tyrosine-like' domain in the N-terminal region of GLUT4. This could be investigated using mutants of GLUT4 in which these two targeting domains are disrupted to analyse whether there are any changes in the levels of adaptor proteins immunoprecipitated with GLUT4 vesicles. A problem with this type of study is that the mutant proteins may not traffic faithfully, and may therefore aggregate in compartments where their association with adaptor proteins would increase, not as a consequence of a change in the interaction of adaptor proteins with the GLUT4 targeting sequence *per se*, but as a consequence of aberrant localisation.

Furthermore a number of other proteins found in varying quantities on GLUT4 vesicles may be responsible for the association of these vesicles with adaptor proteins. These proteins include the mannose-6-phosphate receptor which has been shown to interact directly with AP1 at the level of the Golgi apparatus (Le Borgne *et al.*, 1993; Klumperman *et al.*, 1998), and vp165 which contains two di-leucine motifs (Keller *et al.*, 1995).

In summary, the *in vitro* demonstration of a GTPγS-stimulated increase in AP1 association with GLUT4 vesicles, and an increase in the density of these vesicles on sedimentation gradients, is an important methodological advance. It allows the link between signalling and small G-protein-dependent steps involved in GLUT4 vesicle processing to be studied in a cell-free system.

6.0 Conclusions

The aims of this study were to establish a protocol for the isolation of insulin responsive cardiomyocytes and to investigate the roles of intracellular pH and adaptor protein complexes in GLUT4 trafficking. The isolation of myocytes using a modified procedure has resulted in the preparation of cells with a relatively low level of basal transport, particularly when inosine is added to the preparation. The reason for requiring the addition of inosine during the isolation procedure is unclear at present but would suggest that an alternative energy source is necessary. Inosine is not a particularly efficient metabolite, in that for every inosine molecule absorbed only one molecule of ATP is generated. This suggests that only a small drop in ATP levels occurs in the myocytes during their preparation. Further work is required to determine why the levels of ATP decline during the myocyte isolation and if additional steps can be undertaken to avoid this loss of cellular ATP.

Intracellular pH has been shown to be important for the recycling of a number of proteins including the TfR (Johnson *et al.*, 1993; Presley *et al.*, 1997), TGN38 (Chapman and Munro, 1994) and the cation-independent mannose-6-phosphate receptor (Johnson *et al.*, 1993). Results presented in this thesis show that the maintenance of intracellular pH is also important for the faithful targeting and translocation of GLUT4 in cardiomyocytes and adipocytes. The mechanism by which pH controls targeting is unknown. However some evidence suggests that changes in pH may regulate the interaction of adaptor or adaptin-like proteins with receptor tails carrying internalisation sequences (Johnson *et al.*, 1993). Characterisation of the occluded population of GLUT4 vesicles is therefore required. For example if the internalisation motifs in GLUT4 are disrupted can HOE-642 still induce the formation of fusion-incompetent vesicles? What is the mechanism or 'block' in fusion at the plasma membrane?

Confocal analysis has shown that GLUT4 partially co-localises with the γ-subunit of the adaptor complex AP1 (Malide *et al.*, 1997). Furthermore a direct interaction between the β1-subunit of AP1 and a C-terminal peptide of GLUT4 containing the di-leucine internalisation motif has been demonstrated (Rapoport *et al.*, 1998). In addition work described in this thesis has indicated that GLUT4 vesicles are coated with both AP1 and AP3 complexes. Thus, the role of pH and GLUT4-specific adaptor proteins needs to be investigated with respect to vesicle trafficking. For example, how does the treatment of

adipocytes with HOE-642 or bafilomycin A_1 affect the interactions between GLUT4 vesicles and the adaptor proteins AP1 and AP3? It is conceivable that the block in fusion of GLUT4 vesicles with the plasma membrane and therefore the formation of the 'occluded' vesicles in HOE-642-treated cell is due to a failure of adaptor proteins to dissociate from the vesicles. Since changes in pH may lead to aggregation of receptor tails or result in the failure to cytosolic adaptor-like proteins to transmit information, which may be important for uncoating, GLUT4 vesicles may remain bound to their adaptor proteins. The converse is also true, in that a change in pH could induce a conformational or allosteric change, which does not normally occur, and that this change 'lock's the adaptors onto the GLUT4 vesicles.

Recently a number of coiled coil proteins, for example p230 (also known as Golgin-245) and Giantin, which may act as vesicle tethers, have been shown to contain the 'granin' consensus sequence E(N/S)LX(A/D)X(D/E)XEL (Erlich *et al.*, 1996). In chromatogranin A, a short sequence at the C-terminus containing the granin motif has been shown to be responsible for pH regulated oligomerisation (Yoo and Lewis, 1993) and for pH-dependent association of chromatogranin A with integral membrane proteins of secretory vesicles (Yoo, 1994). The role of the granin motif in vesicle tethering proteins such as giantin is unknown but its presence is suggestive of a role in vesicle sorting or trafficking in response to changes in pH. Thus tethering proteins important for the biogenesis of GLUT4 vesicles need to be isolated and their role with respect to pH regulation needs to be investigated.

Future studies could also focus on the identification of cytosolic interactors for GLUT4/AP1-coated vesicles. Similar studies of M6PR vesicles coated with AP1 have shown that TIP47 is responsible for recognising M6PR tails at the endosome and that this interaction leads to the recycling of M6PRs to the biosynthetic pathway (Diaz and Pfeffer, 1998). Furthermore a novel protein, PACS-1, localises both M6PRs and Furin to the TGN by interacting with their phosphorylated cytoplasmic tails (Wan *et al.*, 1998). Indeed the interaction of PACS-1 with receptor tails is regulated by successive rounds of phosphorylation and dephosphorylation (Molloy *et al.*, 1998). Thus it would be interesting to analyse whether these proteins or similar proteins play a role in AP1 mediated GLUT4 vesicle trafficking.

7.0 References

Ahle, S., Ungewickell, E. (1989). Identification of a clathrin binding subunit in the HA2 adaptor protein complex. J. Biol. Chem. *264*, 20089-20093.

Al Hasani, H., Hinck, C.S., Cushman, S.W. (1998). Endocytosis of the glucose transporter GLUT4 is mediated by the GTPase dynamin. J. Biol. Chem. *273*, 17504-17510.

Alessi, D.R., Kozlowski, M.T., Weng, Q., Morrice, N., Avruch, J. (1998). 3-phosphoinositide-dependent protein kinase 1 (PDK1) phosphorylates and activates the p70 S6 kinase *in vivo* and *in vitro*. Curr. Biol. *8*, 69-81.

Altschuld, R.A., Gibb, L., Ansel, A., Hohl, C., Kruger, F.A., Brierley, G.P. (1980). Calcium tolerance of heart cells. J. Mol. Cell Cardiol. *12*, 1383-1395.

Anant, J.S., Desnoyers, L., Machius, M., Demeler, B., Hansen, J.C., Westover, K.D., Deisenhofer, J., Seabra, M.C. (1998). Mechanism of Rab geranylgeranylation: Formation of the catalytic ternary complex. Biochemistry *37*, 26931-26938.

Anderson, R.G., Brown, M.S., Goldstein, J.L. (1977). Role of the coated endocytic vesicle in the uptake of receptor-bound low density lipoprotein in human fibroblasts. Cell *10*, 351-364.

Ando, A., Yonezawa, K., Gout, I., Nakata, T., Ueda, H., Hara, K., Kitamura, Y., Noda, Y., Takenawa, T., Hirokawa, N., Waterfield, M.D., Kasuga, M. (1994). A complex of Grb2-dynamin binds to tyrosine-phosphorylated insulin receptor substrate-1 after insulin treatment. EMBO J. *13*, 3033-3038.

Aoe, T., Huber, I., Vasudevan, C., Watkins, S.C., Romero, G., Cassel, D., Hsu, V.W. (1999). The KDEL receptor regulates a GTPase-activating protein for ADP-ribosylation factor 1 by interacting with its non-catalytic domain. J. Biol. Chem. *274*, 20545-20549.

Araki, E., Lipes, M.A., Patti, M., Bruning, J.C., Haag, B., Johnson, R.S., Kahn, C.R. (1994). Alternative pathway of insulin signalling in mice with targeted disruption of the IRS-1 gene. Nature *372*, 186-190.

Araki, S., Yang, J., Hashiramoto, M., Tamori, Y., Kasuga, M., Holman, G.D. (1996). Subcellular trafficking kinetics of GLUT4 mutated at the N- and C-termini. Biochem. J. *315*, 153-159.

Aronson, P.S. (1985). Kinetic properties of the plasma membrane Na^+/H^+ exchanger. Annu. Rev. Physiol. *47*, 545-560.

Arsenis, G., Spencer, B.A., Ewert, M.S. (1995). Activation of the Na^+/H^+ exchanger by cellular pH and Na^+ in rat adipocytes; inhibition by isoproterenol. Endocrinology *136*, 3128-3136.

Arsenis, G., Tarvin, J.T. (1986). Isoproterenol reduces insulin stimulation of hexose uptake by rat adipocytes via a post-insulin binding alteration. Endocrinology *119*, 50-57.

Balch, W.E., Glick, B.S., Rothman, J.E. (1984). Sequential intermediates in the pathway of intercompartmental transport in a cell-free system. Cell *39*, 525-536.

Baldini, G., Hohman, R., Charron, M.J., Lodish, H.F. (1991). Insulin and nonhydrolyzable GTP analogues induce translocation of GLUT4 to the plasma membrane in alpha-toxin-permeabilised rat adipose cells. J. Biol. Chem. *266*, 4037-4040.

Baldwin, S.A. (1993). Mammalian passive glucose transporters: Members of a ubiquitous family of active and passive transport proteins. Biochim. Biophys. Acta *1154*, 17-49.

Baldwin, S.A., Baldwin, J.M., Gorga, F.R., Lienhard, G.E. (1979). Purification of the cytochalasin B binding component of the human erythrocyte monosaccharide transport system. Biochim. Biophys. Acta *552*, 183-188.

Ball, C.L., Hunt, S.P., Robinson, M.S. (1995). Expression and localization of α-adaptin isoforms. J. Cell Sci. *108*, 2865-2875.

Bao, S., Smith, R.M., Jarett, L., Garvey, W.T. (1995). The effects of brefeldin A on the glucose transport system in rat adipocytes. Implications regarding the intracellular locus of insulin-sensitive GLUT4. J. Biol. Chem. *270*, 30199-30204.

Barbieri, M.A., Kohn, A.D., Roth, R.A., Stahl, P.D. (1998). Protein kinase B/Akt and Rab5 mediate *ras* activation of endocytosis. J. Biol. Chem. *273*, 19367-19370.

Basu, S.K., Goldstein, J.L., Anderson, R.G., Brown, M.S. (1981). Monesin interrupts the recycling of low density lipoprotein receptors in human fibroblasts. Cell *24*, 493-502.

Beckers, C.J., Block, M.R., Glick, B.S., Rothman, J.E., Balch, W.E. (1989). Vesicular transport between the endoplasmic reticulum and the Golgi stack requires the NEM-sensitive fusion protein. Nature *339*, 397-398.

Bell, G.I., Burant, C.F., Takeda, J., Gould, G.W. (1993). Structure and function of mammalian facilitative sugar transporters. J. Biol. Chem. *268*, 19161-19164.

Beltzer, J.P., Spiess, M. (1991). *In vitro* binding of the asialoglycoprotein receptor to the β-adaptin in plasma membrane coated vesicles. EMBO J. *10*, 3735-3742.

Bihler, I., McNevin, S.R., Sawh, P.C. (1985). Sarcolemmal glucose transport in Ca^{2+}-toletant myocytes from adult rat heart. Calcium dependence of insulin action. Biochim. Biophys. Acta *844*, 9-18.

Birnbaum, M.J. (1989). Identification of a novel gene encoding an insulin-responsive glucose transporter protein. Cell *57*, 305-315.

Birnbaum, M.J. (1992). The insulin-sensitive glucose transporter. Int. Rev. Cytol. *137*, 239-297.

Block, M.R., Glick, B.S., Wilcox, C.A., Wieland, F.T., Rothman, J.E. (1988). Purification of an N-ethylmaleimide-sensitive protein catalysing vesicle transport. Proc. Natl. Acad. Sci. U.S.A *85*, 7852-7856.

Bowman, E.J., Siebers, A., Altendorf, K. (1988). Bafilomycins : A class of inhibitors of membrane ATPases from micro-organisms, animal cells and plant cells. Proc. Natl. Acad. Sci. U.S.A *85*, 7972-7976.

Bucci, C., Parton, R.G., Mather, I.H., Stunnenberg, H., Simons, K., Hoflack, B., Zerial, M. (1992). The small GTPase rab5 functions as a regulatory factor in the early endocytic pathway. Cell *70*, 715-728.

Burgering, B.M.T., Coffer, P.J. (1995). Protein kinase B (c-akt) in phosphatidylinositol-3-OH kinase signal transduction. Nature *376*, 599-602.

Cain, C.C., Trimble, W.S., Lienhard, G.E. (1992). Members of the VAMP family of synaptic vesicle proteins are components of glucose transporter-containing vesicles from rat adipocytes. J. Biol. Chem. *267*, 11681-11684.

Calderhead, D.M., Kitagawa, K., Tanner, L.I., Holman, G.D., Lienhard, G.E. (1990). Insulin regulation of the two glucose transporters in 3T3-L1 adipocytes. J. Biol. Chem. *265*, 13801-13808.

Calera, M.R., Martinez, C., Liu, H., Jack, A.K., Birnbaum, M.J., Pilch, P.F. (1998). Insulin increases the association of Akt-2 with GLUT4-containing vesicles. J. Biol. Chem. *273*, 7201-7204.

Canessa, M., Manriquez, E. (1997). Phosphorylation signals of the insulin receptor in human red cells: Activation of Na^+/H^+ exchange. Nutr. Metab. Cardiovasc. Dis. *7*, 57-62.

Canfield, W.M., Johnson, K.F., Ye, R.D., Gregory, W., Kornfeld, S. (1991). Localisation of the signal for rapid internalisation of the bovine cation-independent mannose-6-phosphate/insulin-like growth factor-II receptor to amino acids 24-29 of the cytoplasmic tail. J. Biol. Chem. *266*, 5682-5688.

Chakrabarti, R., Buxton, J., Joly, M., Corvera, S. (1994). Insulin-sensitive association of GLUT4 with endocytic clathrin-coated vesicles revealed with the use of brefeldin A. J. Biol. Chem. *269*, 7926-7933.

Chapman, R.E., Munro, S. (1994). Retrieval of proteins from the cell surface requires endosomal acidification. EMBO J. *13*, 2305-2312.

Charron, M.J., Brosius III, F.C., Alper, S.L., Lodish, H.F. (1989). A glucose transport protein expressed predominantly in insulin-responsive tissues. Proc. Natl. Acad. Sci. U.S.A *86*, 2535-2539.

Chavrier, P., Goud, B. (1999). The role of ARF and Rab GTPases in membrane transport. Curr. Opin. Cell Biol. *11*, 466-475.

Cheatham, B., Volchuk, A., Kahn, C.R., Wang, L., Rhodes, C.J., Klip, A. (1996). Insulin-stimulated translocation of GLUT4 glucose transporters requires SNARE-complex proteins. Proc. Natl. Acad. Sci. U.S.A *93*, 15169-15173.

Chen, V., McDonough, K.H., Spitzer, J.J. (1985). Effects of insulin on glucose metabolism in isolated heart myocytes from adult rats. Biochim. Biophys. Acta *846*, 398-404.

Cheng, J.Q., Godwin, A.K., Bellacosa, A., Taguchi, T., Franke, T.F., Hamilton, T.C., Tsichlis, P.N., Testa, J.R. (1992). AKT2, a putative oncogene encoding a member of a subfamily of protein-serine/threonine kinases, is amplified in human ovarian carcinomas. Proc. Natl. Acad. Sci. U.S.A *89*, 9267-9271.

Cheung, J.Y., Leaf, A., Bonventre, J.V. (1985). Determination of isolated cell viability: staining methods and functional criteria. Basic Res. Cardiol. *80*, 23-30.

Chinni, S.R., Shisheva, A. (1999). Arrest of endosome acidification by bafilomycin A_1 mimics insulin action on GLUT4 translocation in 3T3-L1 adipocytes. Biochem. J. *339*, 599-606.

Christoforidis, S., McBride, H.M., Burgoyne, R.D., Zerial, M. (1999). The Rab5 effector EEA1 is a core component of endosome docking. Nature *397*, 621-626.

Clague, M.J., Urbe, S., Aniento, F., Gruenberg, J. (1994). Vacuolar ATPase activity is required for endosomal carrier vesicular formation. J. Biol. Chem. *269*, 21-24.

Clark, A.E., Holman, G.D. (1990). Exofacial photolabelling of the human erythrocyte glucose transporter with an azitrifluoroethylbenzoyl-substituted bis-mannose. Biochem. J. *269*, 615-622.

Clark, A.E., Holman, G.D., Kozka, I.J. (1991). Determination of the rates of appearance and loss of glucose transporters at the cell surface of rat adipose cells. Biochem. J. *278*, 235-241.

Clark, S.F., Martin, S., Carozzi, A.J., Hill, M.M., James, D.E. (1998). Intracellular localization of phosphatidylinositide 3-kinase and insulin receptor substrate-1 in adipocytes: Potential involvement of a membrane skeleton. J. Cell Biol. *140*, 1211-1225.

Clarke, J.F., Young, P.W., Yonezawa, K., Kasuga, M., Holman, G.D. (1994). Inhibition of the translocation of GLUT1 and GLUT4 in 3T3-L1 cells by the phosphatidylinositol 3-kinase inhibitor, wortmannin. Biochem. J. *300*, 631-635.

Clary, D.O., Griff, I.C., Rothman, J.E. (1990). SNAPs, a family of NSF attachment proteins involved in intracellular membrane fusion in animals and yeast. Cell *61*, 709-721.

Claude, A., Zhao, B.-P., Yan, J.-P., Armold, A.D., Sullivan, E.M., Melancon, P. (1999). A novel Golgi-associated BFA-resistant guanine nucleotide exchange factor that displays specificity for ADP-ribosylation factor-5. J. Cell Biol. *146*, 71-84.

Clodi, M., Vollenweider, P., Klarlund, J.K., Nakashima, N., Martin, S., Czech, M.P., Olefsky, J.M. (1998). Effects of General Receptor for Phosphoinositides 1 on insulin and insulin-like growth factor 1-induced cytoskeletal arrangement, glucose transporter-4 translocation, and deoxyribonucleic acid synthesis. Endocrinology *139*, 4984-4990.

Coderre, L., Kandror, K.V., Vallega, G., Pilch, P.F. (1995). Identification and characterisation of an exercise-sensitive pool of glucose transporters in skeletal muscle. J. Biol. Chem. *270*, 27584-27588.

Coffer, P.J., Woodgett, J.R. (1991). Molecular cloning and characterisation of a novel putative protein-serine kinase related to the cAMP-dependent and protein kinase C families. Eur. J. Biochem. *201*, 475-481.

Collawn, J.F., Stangel, M., Kuhn, L.A., Esekogwu, V., Jing, S., Trowbridge, I.S., Tainer, J.A. (1990). Transferrin receptor internalisation sequence YXRF implicates a tight turn as the structural recognition motif for endocytosis. Cell *63*, 1061-1072.

Cormont, M., Bortoluzzi, M.N., Gautier, N., Mari, M., Van Obberghen, E., Marchand-Brustel, Y. (1996a). Potential role of Rab4 in the regulation of subcellular localization of GLUT4 in adipocytes. Mol. Cell Biol. *16*, 6879-6886.

Cormont, M., Tanti, J.F., Zahraoui, A., Van Obberghen, E., Le Marchand-Brustel, Y. (1994). Rab4 is phosphorylated by the insulin-activated extracellular-signal-regulated kinase ERK1. Eur. J. Biochem. *219*, 1081-1085.

Cormont, M., Tanti, J.F., Zahraoui, A., Van Obberghen, E., Tavitian, A., Marchand-Brustel, Y. (1993). Insulin and okadaic acid induce Rab4 redistribution in adipocytes. J. Biol. Chem. *268*, 19491-19497.

Cormont, M., Van Obberghen, E., Zerial, M., Marchand-Brustel, Y. (1996b). Insulin induces a change in Rab5 subcellular localization in adipocytes independently of phosphatidylinositol 3-kinase activation. Endocrinology *137*, 3408-3415.

Corvera, S., Capocasale, R.J. (1990). Enhanced phosphorylation of a coated vesicle polypeptide in response to insulin stimulation of rat adipocytes. J. Biol. Chem. *265*, 15963-15969.

Corvera, S., Chawla, A., Chakrabarti, R., Joly, M., Buxton, J., Czech, M.P. (1994). A double leucine within the GLUT4 glucose transporter COOH-terminal domain functions as an endocytosis signal. J. Cell Biol. *126*, 979-989.

Coulombe, A., Leferve, E., Deroubaix, D., Thuringer, D., Caroboeuf, E. (1990). Effect of 2,3-butanedione monoxime on slow inward and transient outward currents in rat ventricular myocytes. J. Mol. Cell Cardiol. *22*, 921-932.

Counillon, L., Franchi, A., Pouyssegur, J. (1993a). A point mutation of the Na^+/H^+ exchanger gene (NHE1) and amplification of the mutated allele confer amiloride resistance upon chronic acidosis. Proc. Natl. Acad. Sci. U.S.A *90*, 4508-4512.

Counillon, L., Scholz, W., Lang, H.J., Pouyssegur, J. (1993b). Pharmacological characterisation of stably transfected Na^+/H^+ antiporter isoforms using amiloride analogues and a new inhibitor exhibiting anti-ischemic properties. Mol. Pharmacol. *44*, 1041-1045.

Cross, D.A.E., Watt, P.W., Shaw, M., van der Kaay, J., Downes, C.P., Holder, J.C., Cohen, P. (1997). Insulin activates Protein Kinase B, inhibits glycogen synthase-3 kinase and activates glycogen synthase by rapamycin-insensitive pathways in skeletal muscle and adipose tissue. FEBS Lett. *406*, 211-215.

Crowther, R.A., Pearse, B.M. (1981). Assembly and packing of clathrin into coats. J. Cell Biol. *91*, 790-797.

Cushman, S. W. and Wardzala, L. J. (1980). Potential mechanism of insulin action on glucose transport in the isolated rat adipose cell. J. Biol. Chem. *355*, 4758-4762.

Czech, M.P., Chawla, A., Woon, C.W., Buxton, J., Armoni, M., Tang, W., Joly, M., Corvera, S. (1993). Exofacial epitope-tagged glucose transporter chimeras reveal COOH-terminal sequences governing cellular localization. J. Cell Biol. *123*, 127-135.

Czech, M.P., Clancy, B.M., Pessino, A., Woon, C.W., Harrison, S.A. (1992). Complex regulation of simple sugar transport in insulin-responsive cells. Trends Biochem. Sci. *17*, 197-201.

D'Souza-Schorey, C., Li, G., Colombo, M.I., Stahl, P.D. (1995). A regulatory role for ARF6 in receptor-mediated endocytosis. Science *267*, 1175-1178.

D'Souza-Schorey, C., van Donselaar, E., Hsu, V.W., Yang, C., Stahl, P.D., Peters, P.J. (1998). ARF6 targets recycling vesicles to the plasma membrane: Insights from an ultrastructural investigation. J. Cell Biol. *140*, 603-616.

Dani, A.M., Cittadini, A., Inesi, G. (1979). Calcium transport and contractile activity in dissociated mammalian heart cells. Am. J. Physiol *237*, C147-C155.

Dell'Angelica, E.C., Mullins, C., Bonifacino, J.S. (1999). AP4, a novel protein complex related to clathrin adaptors. J. Biol. Chem. *274*, 7278-7285.

Dell'Angelica, E.C., Ooi, C.E., Bonifacino, J.S. (1997). Beta3A-adaptin, a subunit of the adaptor-like complex AP-3. J. Biol. Chem. *272*, 15078-15084.

Diaz, M.E., Pfeffer, S.R. (1998). TIP47: A cargo selection device for mannose-6-phosphate receptor trafficking. Cell *93*, 433-443.

Diaz, R., Mayorga, L.S., Weidman, P.J., Rothman, J.E., Stahl, P.D. (1989). Vesicle fusion following receptor-mediated endocytosis requires a protein active in Golgi transport. Nature *339*, 398-400.

Dittie, A.S., Hajibagheri, N., Tooze, S.A. (1996). The AP-1 adaptor complex binds to immature secretory granules from PC12 cells, and is regulated by ADP-ribosylation factor. J. Cell Biol. *132*, 523-536.

Dittie, A.S., Thomas, L., Thomas, G., Tooze, S.A. (1997). Interaction of furin in immature secretory granules from neuroendocrine cells with the AP-1 adaptor complex is modulated by casein kinase II phosphorylation. EMBO J. *16*, 4859-4870.

Domin, J., Dhand, R., Waterfield, M.D. (1996). Binding to the platelet derived growth factor transiently activates the p85α-p100α phosphoinositide 3-kinase complex *in vivo*. J. Biol. Chem. *271*, 21614-21621.

Douen, A.G., Ramlal, T., Klip, A., Young, D.A., Cartee, G.D., Holloszy, J.O. (1989). Exercise-induced increase in glucose transporters in plasma membranes of rat skeletal muscle. Endocrinology *124*, 449-454.

Dow, J.W., Harding, N.G.L., Powell, T. (1981). Isolated cardiac myocytes: I Preparation of adult myocytes and their homology with the intact tissue. Cardiovasc. Res. *15*, 483-514.

Drose, S., Bindseil, K.U., Bowman, E.J., Siebers, A., Zeeck, A., Altendorf, K. (1993). Inhibitory effects of modified bafilomycins and concanamycins on P- and V-type adenosinetriphosphatases. Biochemistry *32*, 3902-3906.

Dschida, W.J., Bowman, B.J. (1992). Structure of the vacuolar ATPase from *Neurospora crassa* as determined by electron microscopy. J. Biol. Chem. *267*, 18783-18789.

Eckel, J. (1989). Einfluss Von Trypsin Auf Die Insulinbindung. In: Molekulare mechanismen der insuliinwirkung am herzmuscle, ed. G.ThiemeStuttgart: Verlag, 40.

Eckel, J., Pandalis, G., Reinauer, H. (1983). Insulin action on the glucose transport system in isolated cardiomyocytes from adult rat. Biochem. J. *212*, 385-392.

Elmendorf, J.S., Chen, D., Pessin, J.E. (1998). Guanosine 5'-O-(3-thiotriphosphate) (GTPγS) stimulation of GLUT4 translocation is tyrosine kinase-dependent. J. Biol. Chem. *273*, 13289-13296.

Emberson, J.W., Muir, A.R. (1969). Changes in the ultrastructure of rat myocardium induced by hypokalemia. J. Exp. Physiol. *54*, 36-40.

Erlich, R., Gleeson, P.A., Campbell, P., Dietzsch, E., Toh, B-H. (1996). Molecular characterisation of *trans*-Golgi p230. J. Biol. Chem. *271*, 8328-8337.

Fidelman, M.L., Seeholzer, S.H., Walsh, K.B., Moore, R.D. (1982). Intracellular pH mediates action of insulin on glycolysis in frog skeletal muscle. Am. J. Physiol *242*, C87-C93.

Fischer, Y., Rose, H., Kammermeier, H. (1991). Highly insulin-responsive isolated rat heart muscle cells yielded by a modified isolation method. Life Sci. *49*, 1679-1688.

Fischer, Y., Thomas, J., Sevilla, L., Munoz, P., Becker, C., Holman, G.D., Kozka, I.J., Palacin, M., Testar, X., Kammermeier, H., Zorzano, A. (1997). Insulin-induced recruitment of glucose transporter 4 (GLUT4) and GLUT1 in isolated rat cardiac myocytes. Evidence of the existence of different intracellular GLUT4 vesicle populations. J. Biol. Chem. *272*, 7085-7092.

Flier, J.S., Mueckler, M., McCall, A.L., Lodish, H.F. (1987). Distribution of glucose transporter messenger RNA transcripts in tissues of rat and man. J. Clin. Invest. *79*, 657-661.

Forgac, M. (1989). Structure and function of vacuolar class of ATP-driven proton pumps. Physiol Rev. *69*, 765-796.

Forgac, M. (1999). Structure and properties of the vacuolar (H^+)-ATPases. J. Biol. Chem. *274*, 12951-12954.

Foster, L.J., Yaworsky, K., Trimble, W. S., Klip, A. (1999). SNAP23 promotes insulin-dependent glucose uptake in 3T3-L1 adipocytes: Possible interaction with cytoskeleton. Am. J. Physiol. *276*, C1108-C1114.

Foster, L.J., Yeung, B., Mohtashami, M., Ross, K., Trimble, W.S., Klip, A. (1998). Binary interactions of the SNARE proteins syntaxin-4, SNAP23, and VAMP-2 and their regulation by phosphorylation. Biochemistry *37*, 11089-11096.

Franke, T.F., Yang, S., Chan, T.O., Datta, K., Kazlauskas, A., Morrison, D.K., Kaplan, D.R., Tsichlis, P.N. (1995). The protein kinase encoded by the akt protooncogene is a target of the PDGF-activated phosphatidylinositol 3-kinase. Cell *81*, 6541-6551.

Fry, D.M., Scales, D., Inesi, G. (1979). The ultrastructure of membrane alterations of enzymatically dissociated cardiac myocytes. J. Mol. Cell Cardiol. *11*, 1151-1164.

Fuchs, R., Schmid, S., Mellman, I. (1989). A possible role for Na^+,K^+-ATPase in regulating ATP-dependent endosome acidification. Proc. Natl. Acad. Sci. U.S.A *86*, 539-543.

Fukumoto, H., Kayano, T., Buse, J.B., Edwards, Y., Pilch, P.F., Bell, G.I., Seino, S. (1989). Cloning and characterisation of the major insulin-responsive glucose transporter expressed in human skeletal muscle and other insulin-responsive tissues. J. Biol. Chem. *264*, 7776-7779.

Gaidarov, I., Chen, Q., Falck, J.R., Reddy, K.K., Keen, J.H. (1996). A functional phosphatidylinositol 3,4,5 trisphosphate binding domain in the clathrin adaptor AP2 α subunit. J. Biol. Chem. *271*, 20922-20929.

Garippa, R.J., Johnson, A., Park, J., Petrush, R.L., McGraw, T.E. (1996). The carboxyl terminus of GLUT4 contains a serine-leucine-leucine sequence that functions as a potent internalisation motif in Chinese hamster ovary cells. J. Biol. Chem. *271*, 20660-20668.

Garippa, R.J., Judge, T.W., James, D.E., McGraw, T.E. (1994). The amino terminus of GLUT4 functions as an internalisation motif but not an intracellular retention signal when substituted for the transferrin receptor cytoplasmic domain. J. Cell Biol. *124*, 705-715.

Geisbuhler, T.P., Sergeant, S., Miramonti, P.L., Kim, H.D., Rovetto, M.J. (1987). Forskolin inhibition of hexose transport in cardiomyocytes. Pflugers Arch. *409*, 158-162.

Gerhardt, B., Kordas, T.J., Thompson, C.M., Patel, P., Vida, T. (1998). The vesicle transport protein Vps33p is an ATP-binding protein that localises to the cytosol in an energy dependent manner. J. Biol. Chem. *273*, 15818-15829.

Gibbs, E.M., Calderhead, D.M., Holman, G.D., Gould, G.W. (1991). Phorbol ester only partially mimics the effects of insulin on glucose transport and glucose-transporter distribution in 3T3-L1 adipocytes. Biochem. J. *275*, 145-150.

Glick, B.S., Rothman, J.E. (1987). Possible role for fatty acyl-coenzyme A in intracellular protein transport. Nature *326*, 309-312.

Goldberg, J. (1998a). Structural basis for activation of ARF-GTPase: Mechanisms of guanine nucleotide exchange and GTP-myristoyl switching. Cell *95*, 237-248.

Goldberg, J. (1998b). Structure of the guanine nucleotide exchange factor sec7 domain of human ARNO and analysis of the interaction with ARF GTPase. Cell *92*, 415-423.

Goldstein, B.J., Basu, S.K., Brown, M.S. (1976). Release of low density lipoprotein from its cell surface receptor by sulphated glycosaminoglycans. Cell *7*, 85-95.

Goto, Y., Kida, K., Kaino, Y., Ito, K., Matsuda, H. (1993). Inhibitory effect of amiloride on glucose transport in isolated rat adipocytes. Diabetes Res. and Clin. Practise *20*, 1-5.

Gould, G.W., Holman, G.D. (1993). The glucose transporter family: Structure, function and tissue-specific expression. Biochem. J. *295*, 329-341.

Griff, I.C., Schekman, R., Rothman, J.E., Kaiser, C.A. (1992). The yeast sec17 gene product is functionally equivalent to mammalian α-SNAP protein. J. Cell Biol. *267*, 12106-12115.

Grinstein, S., Rothstein, A. (1986). Mechanisms of regulation of the Na^+/H^+ exchanger. J. Membr. Biol. *90*, 1-12.

Gustavsson, J., Parpal, S., Stralfors, P. (1996). Insulin-stimulated glucose uptake involves the transition of glucose transporters to a caveolae-rich fraction within the plasma membrane: Implications for type II diabetes. Mol. Med. *2*, 367-372.

Hammonds-Odie, L.P., Jackson, T.R., Profit, A.A., Blader, I.J., Turck, C.W., Prestwich, G.D., Thiebert, A.B. (1996). Identification and cloning of Centaurin-α. A novel phosphatidylinositol 3,4,5-trisphosphate binding protein from rat brain. J. Biol. Chem. *271*, 18859-18868.

Haney, P.M., Slot, J.W., Piper, R.C., James, D.E., Mueckler, M. (1991). Intracellular targeting of the insulin-regulatable glucose transporter (GLUT4) is isoform specific and independent of cell type. J. Cell Biol. *114*, 689-699.

Hansen, P.A., Gulve, E.A., Schluter, J., Mueckler, M., Holloszy, J.O. (1995). Kinetics of 2-deoxyglucose in skeletal muscle; effects of insulin and contraction. Am. J. Physiol *268*, C30-C35.

Hansen, P.A., Wang, W., Adkins Marshall, B., Holloszy, J.O., Mueckler, M. (1998). Dissociation of GLUT4 translocation and insulin-stimulated glucose transport in transgenic mice overexpressing GLUT1 in skeletal muscle. J. Biol. Chem. *273*, 18173-18179.

Hara, K., Yonezawa, K., Sakaue, H., Ando, A., Kotani, K., Kitamura, Y., Ueda, H., Stephens, L., Jackson, T.R., Hawkin, P.T., Dhand, R., Clark, A.E., Holman, G.D., Kasuga, M. (1994). 1-phosphatidylinositol 3-kinase activity is required for insulin-stimulated glucose transport but not Ras activation in CHO cells. Proc. Natl. Acad. Sci. U.S.A *91*, 7415-7419.

Harris, H.W.Jr., Zeidel, M.L., Jo, I., Hammond, T.G. (1994). Characterisation of purified endosomes containing the anti-diuretic hormone-sensitive water channel from rat renal papilla. J. Biol. Chem. *269*, 11993-20000.

Harter, C., Mellman, I. (1992). Transport of the lysosomal membrane glycoprotein to lysosomes does not require appearance on the plasma membrane. J. Cell Biol. *117*, 311-325.

Haworth, R.A., Goknur, A.B., Warner, T.F., Berkoff, H.A. (1989). Some determinants of quality and yield in the isolation of adult heart cells from rat. Cell Calcium *10*, 57-62.

Haworth, R.A., Hunter, D.R., Berkoff, H.A. (1982). Mechanism of Ca^{2+} resistance in adult heart cells isolated with trypsin plus Ca^{2+}. J. Mol. Cell Cardiol. *14*, 523-530.

Haworth, R.A., Hunter, D.R., Berkoff, H.A. (1984). Heterogeneous response of isolate adult rat heart cells to insulin. Arch. Biochem. Biophys. *233*, 106-114.

Hayashi, T., Wojtaszewski, J., Goodyear, L.J. (1997). Exercise regulation of glucose transport in skeletal muscle. Am. J. Physiol *273*, E1039-E1051.

He, W., O'Neill, T.J., Gustafson, T.A. (1995). Distinct modes of action of shc and insulin receptor susbtrate-1 with the insulin receptor NPEY region via non-SH2 domains. J. Biol. Chem. *270*, 23258-23262.

Heller-Harrison, R.A., Morin, M., Czech, M.P. (1995). Insulin regulation of membrane-associated insulin receptor substrate 1. J. Biol. Chem. *270*, 24442-24450.

Heller-Harrison, R.A., Morin, M., Guilherme, A., Czech, M.P. (1996). Insulin-mediated targeting of phosphatidylinositol 3-kinase to GLUT4-containing vesicles. J. Biol. Chem. *271*, 10200-10204.

Helms, J.B., Palmer, D.J., Rothman, J.E. (1993). Two distinct populations of ARF bound to Golgi membranes. J. Cell Biol. *121*, 751-760.

Henkel, J.R., Popovich, J.L., Gibson, G.A., Watkins, S.C., Weisz, O.A. (1999). Selective perturbation of early endosome and/or *trans*-Golgi network pH but not lysosome pH by dose-dependent expression of influenza M2 protein. J. Biol. Chem. *274*, 9854-9860.

Herman, G.A., Bonzelius, F., Cieutat, A.M., Kelly, R.B. (1994). A distinct class of intracellular storage vesicles, identified by expression of the glucose transporter GLUT4. Proc. Natl. Acad. Sci. U.S.A *91*, 12750-12754.

Herskovits, J.S., Shpetner, H.S., Burgess, C.C., Vallee, R.B. (1993). Microtubules and Src homology 3 domains stimulate the dynamin GTPase via its C-terminal domain. Proc. Natl. Acad. Sci. U.S.A *90*, 11468-11472.

Heuser, J.E., Keen, J. (1988). Deep-etch visualisation of proteins involved in clathrin assembly. J. Cell Biol. *107*, 877-886.

Hinshaw, J.E., Schmid, S.L. (1995). Dynamin self assembles into rings suggesting a mechanism for coat vesicle budding. Nature *374*, 190-192.

Hirst, J., Robinson, M.S. (1998). Clathrin and adaptors. Biochim. Biophys. Acta *1404*, 173-193.

Hollenbeck, P.J., Swanson, J.A. (1990). Radial extension of macrophage tubular lysosomes supported by kinesin. Nature *346*, 864-866.

Holloszy, J.O., Narahara, H.T. (1967). Enhanced permeability to sugar associated with muscle contraction. J. Gen. Physiol. *50*, 551-562.

Holman, G.D., Cushman, S.W. (1994). Subcellular localization and trafficking of the GLUT4 glucose transporter isoform in insulin-responsive cells. Bioessays *16*, 753-759.

Holman, G.D., Kasuga, M. (1997). From receptor to transporter: Insulin signalling to glucose transport. Diabetologia *40*, 991-1003.

Holman, G.D., Kozka, I.J., Clark, A.E., Flower, C.J., Saltis, J., Habberfield, A.D., Simpson, I.A., Cushman, S.W. (1990). Cell surface labelling of glucose transporter isoform GLUT4 by bis- mannose photolabel. Correlation with stimulation of glucose transport in rat adipose cells by insulin and phorbol ester. J. Biol. Chem. *265*, 18172-18179.

Holman, G.D., Lo, L.L., Cushman, S.W. (1994). Insulin-stimulated GLUT4 glucose transporter recycling. A problem in membrane protein subcellular trafficking through multiple pools. J. Biol. Chem. *269*, 17516-17524.

Honnor, R.C., Naghshineh, S., Cushman, S.W., Wolff, J., Simpson, I.A., Londos, C. (1992). Cholera and pertussis toxins modify the regulation of glucose transport activity in rat adipose cells: Evidence for mediation of a cAMP-independent process by G-proteins. Cell Signal. *4*, 87-98.

Hooley, R., Yu, C.Y., Symons, M., Barber, D.L. (1996). $G\alpha_{13}$ stimulates Na^+/H^+ exchange through distinct CDC42 dependent and RhoA dependent pathways. J. Biol. Chem. *271*, 6152-6158.

Horiuti, K., Higuchi, H., Umasume, Y., Konishi, M., Okasaki, O., Kurihara, S. (1988). Mechanism of 2,3-butanedione 2-monoxime on contraction of frog skeletal muscle fibres. Muscle Res. Cell Motil. *9*, 156-164.

Hresko, R.C., Heimberg, H., Chi, M.M., Mueckler, M. (1998). Glucosamine-induced insulin resistance in 3T3-L1 adipocytes is caused by depletion of intracellular ATP. J. Biol. Chem. *273*, 20658-20668.

Incerpi, S., Baldini, P., Bellucci, V., Zannetti, A., Luly, P. (1994). Modulation of the Na-H antiport by insulin: Interplay between protein kinase C, tyrosine kinase and protein phosphatases. J. Cell Physiol. *159*, 205-212.

Jacobson, S.L., Piper, H.M. (1986). Cell cultures of adult cardiomyocytes as models for the myocardium. J. Mol. Cell Cardiol. *18* , 661-678.

James, D.E., Brown, R., Navarro, J., Pilch, P.F. (1988). Insulin-regulatable tissues express a unique insulin-sensitive glucose transport protein. Nature *333*, 183-185.

James, D.E., Lederman, L., Pilch, P.F. (1987). Purification of insulin-dependent exocytic vesicles containing the glucose transporter. J. Biol. Chem. *262*, 11817-11824.

James, D.E., Strube, M., Mueckler, M. (1989). Molecular cloning and characterisation of an insulin-regulatable glucose transporter. Nature *338*, 83-87.

Jenkins, A.B., Storlien,L.H., Chisholm, D.J., Kraegen, E.W. (1988). Effects of nonesterified fatty acid availability on tissue specific glucose utilisation in rats *in vivo*. J. Clin. Invest. *82*, 293-299.

Jiang, T., Sweeney, G., Rudolf, M.T., Klip, A., Traynor-Kaplan, A., Tsien, R.Y. (1998). Membrane-permeant esters of phosphatidylinositol 3,4,5-trisphosphate. J. Biol. Chem. *273*, 11017-11024.

Johnson, A.O., Subtil, A., Petrush, R., Kobylarz, K., Keller, S.R., McGraw, T.E. (1998). Identification of an insulin-responsive, slow endocytic recycling mechanism in Chinese hamster ovary cells. J. Biol. Chem. *273*, 17968-17977.

Johnson, K.F., Kornfeld, S. (1992). The cytoplasmic tail of the mannose-6-phosphate/insulin-like growth factor-II receptor has two signals for lysosomal enzyme sorting in the Golgi. J. Cell Biol. *119*, 249-257.

Johnson, L.S., Dunn, K.W., Pytowski, B., McGraw, T.E. (1993). Endosome acidification and receptor trafficking: bafilomycin A_1 slows receptor externalisation by a mechanism involving the receptor's internalisation motif. Mol. Biol. Cell *4*, 1251-1266.

Kaestner, K.H., Christy, R.J., McLenithan, J.C., Braiterman, L.T., Cornelius, P., Pekala, P.H., Lane, M.D. (1989). Sequence, tissue distribution, and differential expression of mRNA for a putative insulin-responsive glucose transporter in mouse 3T3-L1 adipocytes. Proc. Natl. Acad. Sci. U.S.A *86*, 3150-3154.

Kahn, B.B. (1992). Facilitative glucose transporters: regulatory mechanisms and dysregulation in diabetes. J. Clin. Invest *89*, 1367-1374.

Kahn, R.A., Gilman, A.G. (1984). Purification of a protein cofactor required for ADP-ribosylation of the stimulatory regulatory component of adenylate cyclase by cholera toxin. J. Biol. Chem. *259*, 6228-6234.

Kanai, F., Ito, K., Todaka, M., Hayashi, H., Kamohara, S., Ishii, K., Okada, T., Haseki, O., Ui,M., Ebina, Y. (1993a). Insulin-stimulated GLUT4 translocation is relevant to the phosphorylation of IRS-1 and the activity of PI 3-kinase. Biochem. Biophys. Res. Commun. *195*, 762-768.

Kanai, F., Nishioka, Y., Hayashi, H., Kamohara, S., Todaka, M., Ebina, Y. (1993b). Direct demonstration of insulin-induced GLUT4 translocation to the surface of intact cells by insertion of a c-myc epitope into an exofacial GLUT4 domain. J. Biol. Chem. *268*, 14523-14526.

Kandror, K., Pilch, P.F. (1994). Identification and isolation of glycoproteins that translocate to the cell surface from GLUT4-enriched vesicles in an insulin-dependent fashion. J. Biol. Chem. *269*, 138-142.

Kandror, K.V., Coderre, L., Pushkin, A.V., Pilch, P.F. (1995). Comparison of glucose-transporter-containing vesicles from rat fat and muscle tissues: Evidence for a unique endosomal compartment. Biochem. J. *307*, 383-390.

Kandror, K.V., Pilch, P.F. (1996). Compartmentalisation of protein traffic in insulin-sensitive cells. Am. J. Physiol. *271*, E1-14.

Kandror, K.V., Pilch, P.F. (1998). Multiple endosomal recycling pathways in rat adipose cells. Biochem. J. *331*, 829-835.

Kandror, K.V., Yu, L., Pilch, P.F. (1994). The major protein of GLUT4-containing vesicles, gp160, has aminopeptidase activity. J. Biol. Chem. *269*, 30777-30780.

Kaneseki, T., Kadota, K. (1969). The 'vesicle in a basket'. A morphological study of the coated vesicle isolated from the nerve ending of the guinea pig brain, with special reference to the mechanism of membrane movements. J. Cell Biol. *42*, 202-220.

Kao, A.W., Ceresa, B.P., Santeler, S.R., Pessin, J.E. (1998). Expression of a dominant interfering dynamin mutant in 3T3-L1 adipocytes inhibits GLUT4 endocytosis without affecting insulin signalling. J. Biol. Chem. *273*, 25450-25457.

Kao, A.W., Noda, Y., Johnson, J.H., Pessin, J.E., Saltiel, A.R. (1999). Aldolase mediates the association of F-actin with the insulin- responsive glucose transporter GLUT4. J. Biol. Chem. *274*, 17742-17747.

Karmazyn, M., Moffat, M.P. (1998). Role of Na^+/H^+ exchange in cardiac physiology and pathophysiology: Mediation of myocardial reperfusion injury by the pH paradox. Cardiovasc. Res. *27*, 915-924.

Keen, J.H., Willingham, M.C., Pastan, I.H. (1979). Clathrin coated vesicles: Isolation, dissociation and factor dependent reassociation of clathrin baskets. Cell *16*, 303-313.

Keller, S.R., Scott, H.M., Mastick, C.C., Aebersold, R., Lienhard, G.E. (1995). Cloning and characterisation of a novel insulin-regulated membrane aminopeptidase from GLUT4 vesicles. J. Biol. Chem. *270*, 23612-23618.

Keller, S.R., Strube, M., Mueckler, M. (1989). Functional expression of the human HepG2 and rat adipocyte glucose transporters in *Xenopus* oocytes. J. Biol. Chem. *264*, 18884-18889.

Kirchhausen, T., Bonifacino, J.S., Reizman, H. (1997). Linking cargo to vesicle formation: Receptor tail interactions with coat proteins. Curr. Opin. Cell Biol. *9*, 488-495.

Kishi, K., Hayashi, H., Wang, L., Kamohara, S., Tamaoka, K., Shimizu, T., Ushikubi, F., Narumiya, S., Ebina, Y. (1996). G_q-coupled receptors transmit the signal for GLUT4 translocation via an insulin-independent pathway. J. Biol. Chem. *271*, 26561-26568.

Kishi, K., Muromoto, N., Nakaya, Y., Miyata, I., Hagi, A., Hayashi, H., Ebina, Y. (1998). Bradykinin directly triggers GLUT4 translocation via an insulin-independent pathway. Diabetes *47*, 550-558.

Kitagawa, K., Rosen, B.S., Spiegelman, B.M., Lienhard, G.E., Tanner, L.I. (1989). Insulin stimulates the acute release of adipsin from 3T3-L1 adipocytes. Biochim. Biophys. Acta *1014*, 83-89.

Kitamura, T., Ogawa, W., Sakaue, H., Hino, Y., Kuroda, S., Takata, M., Matsumoto, M., Maeda, T., Konishi, H., Kikkawa, U., Kasuga, M. (1998). Requirement for activation of the serine-threonine kinase Akt (protein kinase B) in insulin stimulation of protein synthesis but not of glucose transport. Mol. Cell Biol. *18*, 3708-3717.

Klarlund, J.K., Guilherme, A., Holik, J.J., Virbasius, J.V., Chawla, A., Czech, M.P. (1997). Signalling by phosphoinositide-3,4,5-trisphosphate through proteins containing pleckstrin and Sec7 homology domains. Science *275*, 1927-1930.

Klip, A., Ramlal, T., Cragoe, E.J., Jr. (1986). Insulin-induced cytoplasmic alkalinization and glucose transport in muscle cells. Am. J. Physiol. *250*, C720-C728.

Klip, A., Ramlal, T., Koivisto, U.M. (1988). Stimulation of Na^+/H^+ exchange by insulin and phorbol ester during differentiation of 3T3-L1 cells. Relation to hexose uptake. Endocrinology *123*, 296-304.

Klumperman, J., Kuliawat, R., Griffiths, J.M., Geuze, H.J., Arvan, P. (1998). Mannose-6-phosphate receptors are sorted from immature secretory granules via adaptor protein AP1, clathrin and syntaxin 6-positive vesicles. J. Cell Biol. *137*, 335-345.

Kolter, T., Uphues, I., Wichelhaus, A., Reinauer, H., Eckel, J. (1992). Contraction-induced translocation of the glucose transporter GLUT4 in isolated ventricular cardiomyocytes. Biochem. Biophys. Res. Commun. *189*, 1207-1214.

Konishi, H., Kuroda, S., Tanaka, M., Matsuzaki,H., Ono, Y., Kameyama, K., Haga, T., Kikkawa, U. (1993). Molecular cloning and characterisation of a new member of the RAC protein kinase family: association of the pleckstrin homology domain of three types of RAC protein kinase with protein kinase C subspecies and βγ-subunits of G-proteins. Biochem. Biophys. Res. Commun. *216*, 526-534.

Kotani, K., Ogawa, W., Matsumoto, M., Kitamura, T., Sakaue, H., Hino, Y., Miyake, K., Sano, W., Akimoto, K., Ohno, S., Kasuga, M. (1998). Requirement of atypical protein kinase cλ for insulin stimulation of glucose uptake but not for Akt activation in 3T3-L1 adipocytes. Mol. Cell Biol. *18*, 6971-6982.

Koumanov, F., Yang, J., Jones, A.E., Hatanaka, Y., Holman ,G.D. (1998). Cell-surface biotinylation of GLUT4 using bis-mannose photolabels. Biochem. J. 330, 1209-1215.

Krueger, J. and Wittenberg, B. Sarcomere dynamics and diffracted light intensity changes during uniform contractile activity in isolated cardiac muscle cells. Biophysical J. 25, 113a. 1979.

Ktistakis, N.T., Brown, H.A., Waters, M.G., Sternweis, P.C., Roth, M.G. (1996). Evidence that phospholipase D mediates ADP ribosylation factor-dependent formation of Golgi coated vesicles. J. Cell Biol. *134*, 295-306.

Kurashima, K., Szabo, E., Lukacs, G., Orlowski, J. (1998). Endosomal recycling of the Na^+/H^+ exchanger NHE3 isoform is regulated by the phosphatidylinositol 3-kinase pathway. J. Biol. Chem. *273*, 20823-20836.

Kuroda, M., Honnor, R.C., Cushman, S.W., Londos, C., Simpson, I.A. (1987). Regulation of insulin-stimulated glucose transport in the isolated rat adipocyte: cAMP - independent effects of lipolytic and anti-lipolytic agents. J. Biol. Chem. *262*, 245-253.

Laemmli, U.K. (1970). Cleavage of structural proteins during the assembly of the head of bacteriophage T4. Nature *227*, 680-685.

Langendorff, O. (1895). Untersuchungen am uberlebenden saugertierherzen. Pflugers Arch. *61*, 291-332.

Laurie, S.M., Cain, C.C., Lienhard, G.E., Castle, J.D. (1993). The glucose transporter GLUT4 and secretory carrier membrane proteins (SCAMPs) colocalize in rat adipocytes and partially segregate during insulin stimulation. J. Biol. Chem. *268*, 19110-19117.

Lavan, B.E., Fantin, V.R., Chang, E.T., Lane, W.S., Keller, S.R., Lienhard, G.E. (1997b). A novel 160-kDa phosphotyrosine protein in insulin-treated embryonic kidney cells is a new member of the insulin receptor substrate family. J. Biol. Chem. *272*, 21403-21407.

Lavan, B.E., Lane, W.S., Lienhard, G.E. (1997a). The 60-kDa phosphotyrosine protein in insulin-treated adipocytes is a new member of the insulin receptor substrate family. J. Biol. Chem. *272*, 11439-11443.

Lawrence, J.C., Jr., Hiken, J.F., James, D.E. (1990). Stimulation of glucose transport and glucose transporter phosphorylation by okadaic acid in rat adipocytes. J. Biol. Chem. *265*, 19768-19776.

Le Borgne, R., Schmidt, A., Mauxion, F., Griffiths, G., Hoflack, B. (1993). Binding of AP-1 Golgi adaptors to membranes requires phosphorylated cytoplasmic domains of the mannose-6-phosphate/insulin-like growth factor II receptor. J. Biol. Chem. *268*, 22552-22556.

Lee, W., Jung, C.Y. (1997). A synthetic peptide corresponding to the GLUT4 C-terminal cytoplasmic domain causes insulin-like glucose transport stimulation and GLUT4 recruitment in rat adipocytes. J. Biol. Chem. *272*, 21427-21431.

Liang, J.O., Kornfeld, S. (1997). Comparative activity of ADP-ribosylation factor family members in the early steps of coated vesicle formation on rat liver Golgi membranes. J. Biol. Chem. *272*, 4141-4148.

Lin, B.Z., Pilch, P.F., Kandror, K.V. (1997). Sortilin is a major protein component of GLUT4-containing vesicles. J. Biol. Chem. *272*, 24145-24147.

Lin, X., Barber, D.L. (1996). A calcineurin homologous protein inhibits GTPase-stimulated Na-H exchange. Proc. Natl. Acad. Sci. U.S.A *93*, 12631-12636.

Lindgren, C.A., Paulson, D.J., Shanahan, M.F. (1982). Isolated cardiac myocytes. A new cellular model for studying insulin modulation of monosaccharide transport. Biochim. Biophys. Acta *721*, 385-393.

Liu, M.-L., Gibbs, E.M., McCoid, S.C., Milici, A.J., Stuckenbrok, H.A., McPherson, R.K., Treadway, J.L., Pessin, J.E. (1993). Transgenic mice expressing the human GLUT4/muscle-fat facilitative glucose transporter protein exhibit efficient glycemic control. Proc. Natl. Acad. Sci. U.S.A *90*, 11346-11350.

Livingstone, C., James, D.E., Rice, J.E., Hanpeter, D., Gould, G.W. (1996). Compartment ablation analysis of the insulin-responsive glucose transporter (GLUT4) in 3T3-L1 adipocytes. Biochem. J. *315*, 487-495.

Loh, S.-H., Sun, B., Vaughan-Jones, R.D. (1996). Effect of HOE 694, a novel Na^+/H^+ exchange inhibitor, on intracellular pH regulation in the guinea-pig ventricular myocyte. Br. J. Pharmacol. *118*, 1905-1912.

Lopatin, A.N., Nichols, C.G. (1992). 2,3-butanedione monoxime (BDM) inhibition of delayed rectifier DRK1 (Kv2.1) potassium channels expressed in Xenopus oocytes. J. Pharmacol. Exp. Ther. *265*, 1011-1016.

Lowe, A.G., Walmsley, A.R. (1986). The kinetics of glucose transport in human red blood cells. Biochim. Biophys. Acta *857*, 146-154.

Lund, S., Holman, G.D., Schmitz, O., Pedersen, O. (1995). Contraction stimulates translocation of glucose transporter GLUT4 in skeletal muscle through a mechanism distinct from that of insulin. Proc. Natl. Acad. Sci. U.S.A *92*, 5817-5821.

Lund, S., Pryor, P.R., Ostergaard, S., Schmitz, O., Pedersen, O., Holman, G.D. (1998). Evidence against protein kinase B as a mediator of contraction-induced glucose transport and GLUT4 translocation in rat skeletal muscle. FEBS Lett. *425*, 472-474.

Ma, Y.-H., Reusch, H.P., Wilson, E., Escobedo, J.A., Fantl, W.J., Williams, L.T., Ives, H.E. (1994). Activation of Na^+/H^+ exchange by platelet-derived growth factor involves phosphatidylinositol 3'-kinase and phospholipase C-gamma. J. Biol. Chem. *269*, 30734-30739.

Macaulay, S.L., Hewish, D.R., Gough, K.H., Stoichevska, V., Macpherson, S.F., Jagadish, M., Ward, C.W. (1997). Functional studies in 3T3-L1 cells support a role for SNARE proteins in insulin stimulation of GLUT4 translocation. Biochem. J. *324*, 217-224.

MacDougald, O.A., Hwang, C.-S., Fan, H., Lane, M.D. (1995). Regulated expression of the obese gene product (leptin) in white adipose tissue and 3T3-L1 adipocytes. Proc. Natl. Acad. Sci. U.S.A *92*, 9034-9037.

Malide, D., Cushman, S.W. (1997). Morphological effects of wortmannin on the endosomal system and GLUT4-containing compartments in rat adipose cells. J. Cell Sci. *110*, 2795-2806.

Malide, D., Dwyer, N.K., Blanchette-Mackie, E.J., Cushman, S.W. (1997). Immunocytochemical evidence that GLUT4 resides in a specialised translocation post-endosomal VAMP2-positive compartment in rat adipose cells in the absence of insulin. J. Histochem. Cytochem. *45*, 1083-1096.

Mallet, M.G., Brodsky, F.M. (1996). A membrane-associated protein complex with selective binding to the clathrin coat adaptor AP1. J. Cell Sci. *109*, 3059-3068.

Marette, A., Burdett, E., Douen, A., Vranic, M., Klip, A. (1992). Insulin induces the translocation of GLUT4 from a unique intracellular organelle to transverse tubules in rat skeletal muscle. Diabetes *41*, 1562-1569.

Marjomaki, V., Ritamaki, V., Gruenberg, J. (1994). Isoproterenol-induced redistribution of endosomes in cardiac myocytes. Eur. J. Cell Biol. *65*, 1-13.

Marsh, B.J., Alm, R.A., McIntosh, S.R., James, D.E. (1995). Molecular regulation of GLUT-4 targeting in 3T3-L1 adipocytes. J. Cell Biol. *130*, 1081-1091.

Marsh, B.J., Martin, S., Melvin, D.R., Martin, L.B., Alm, R.A., Gould, G.W., James, D.E. (1998). Mutational analysis of the carboxy-terminal phosphorylation site of GLUT-4 in 3T3-L1 adipocytes. Am. J. Physiol. *275*, E412-E422.

Martin, K.C., Hu, Y.H., Armitage, B.A., Siegelbaum, S.A., Kandel, E.R., Kaang, B.K. (1995). Evidence for synatotagmin as an inhibitory clamp on synaptic vesicle release in aplysia neurons. Proc. Natl. Acad. Sci. U.S.A *92*, 11307-11311.

Martin, L.B., Shewan, A., Millar, C.A., Gould, G.W., James, D.E. (1998). Vesicle-associated membrane protein 2 plays a specific role in the insulin-dependent trafficking of the facilitative glucose transporter GLUT4 in 3T3-L1 adipocytes. J. Biol. Chem. *273*, 1444-1452.

Martin, S., Reaves, B., Banting, G., Gould, G.W. (1994). Analysis of the co-localization of the insulin-responsive glucose transporter (GLUT4) and the *trans*-Golgi network marker TGN38 within 3T3-L1 adipocytes. Biochem. J. *300*, 743-749.

Martin, S., Tellam, J., Livingstone, C., Slot, J.W., Gould, G.W., James, D.E. (1996a). The glucose transporter (GLUT-4) and vesicle-associated membrane protein-2 (VAMP-2) are segregated from recycling endosomes in insulin-sensitive cells. J. Cell Biol. *134*, 625-635.

Martin, S.S., Haruta, T., Morris, A.J., Klippel, A., Williams, L.T., Olefsky, J.M. (1996b). Activated phosphotidylinositol 3-kinase is sufficient to mediate actin rearrangement and GLUT4 translocation in 3T3-L1 adipocytes. J. Biol. Chem. *271*, 17605-17608.

Martincic, I., Peralta, M.E., Ngsee, J.K. (1997). Isolation and characterisation of a dual prenylated Rab and VAMP2 receptor. J. Biol. Chem. *272*, 26991-26998.

Mastick, C.C., Falick, A.L. (1997). Association of N-ethylmaleimide sensitive fusion (NSF) protein and Soluble NSF Attachment Proteins (α and γ) with glucose transporter-4-containing vesicles in primary rat adipocytes. Endocrinology *138*, 2391-2397.

Mattson, J.P., Keeling, D.J. (1999). [^{3}H]Bafilomycin as a probe for the transmembrane proton channel of osteoclast vacuolar H^+-ATPase. Am. J. Physiol. *265*, C1015-C1029.

Mauxion, F., Le Borgne, R., Munier-Lehmann, H., Hoflack, B. (1996). A casein kinase II phosphorylation site in the cytoplasmic domain of the cation-dependent mannose-6-phosphate receptor determines the high affinity interaction of the AP1 Golgi assembly proteins with membranes. J. Biol. Chem. *271*, 2171-2178.

Maxfield, F.R., Yamashiro, D.J. (1991). Acidification of Organelles and the Intracellular Sorting of Proteins During Endocytosis. In: Intracellular trafficking of proteins, ed. C.J.Steer, J.A.HanoverCambridge: Cambridge University Press, 157-182.

Mayer, A., Whickner, W. (1997). Docking of yeast vacuoles is catalysed by the *Ras*-like GTPase Ypt7 after symmetric priming by Sec 18 (NSF). J. Cell Biol. *136*, 307-317.

McGraw, T.E., Pytowski, B., Arzt, J., Ferrone, C. (1991). Mutagenesis of the human transferrin receptor: two cytoplasmic phenylalanines are required for efficient internalisation and a second-site mutation is capable of inverting an internalisation-defective phenotype. J. Cell Biol. *112*, 853-861.

Mellman, I. (1987). Molecular sorting during endocytosis. Kidney Int. Suppl. *23*, S184-S200.

Mellman, I. (1992). The importance of being acid: The role of acidification in intracellular membrane traffic. J. Exp. Biol. *172*, 39-45.

Mellman ,I. (1996). Endocytosis and molecular sorting. Annu. Rev. Cell Dev. Biol. *12*, 575-625.

Mellman, I., Fuchs, R., Helenius, A. (1986). Acidification of the endocytic and exocytic pathways. Annu. Rev. Biochem. *55*, 663-700.

Mellman, I., Plutner, H., Ukkonen, P. (1984). Internalisation and rapid recycling of macrophage Fc receptors tagged with monovalent antireceptor antibodies: Possible role of a prelysosomal compartment. J. Cell Biol. *98*, 1163-1169.

Melvin, D.R., Marsh, B.J., Walmsley, A.R., James, D.E., Gould, G.W. (1999). Analysis of amino and carboxy terminal GLUT-4 targeting motifs in 3T3-L1 adipocytes using an endosomal ablation technique. Biochemistry *38*, 1456-1462.

Metchnikoff, E. (1893). Lectures on the Comparative Pathology of Inflammation. London: Kegan, Paul, Trench, Trubner & Co. Ltd.

Millar, C.A., Campbell, L.C., Cope, D.L., Melvin, D.R., Powell, K.A., Gould, G.W. (1997). Compartment-ablation studies of GLUT4 distribution in adipocytes: Evidence for multiple intracellular pools. Biochem. Soc. Trans. *25*, 974-977.

Millar, C.A., Powell, K.A., Hickson, G.R., Bader, M.F., Gould, G.W. (1999). Evidence for a role for ADP-ribosylation factor 6 in insulin-stimulated glucose transporter-4 (GLUT4) trafficking in 3T3-L1 adipocytes. J. Biol. Chem. *274*, 17619-17625.

Miller, K., Shipman, M., Trowbridge, I.S., Hopkins, C.R. (1991). Transferrin receptors promote the formation of clathrin lattices. Cell *65*, 621-632.

Min, J., Okada, S., Kanzaki, M., Elmendorf, J.S., Coker, K., Ceresa, B.P., Syu, L.-J., Noda, Y., Saltiel, A.R., Pessin, J.E. (1999). Synip: A novel insulin-regulated syntaxin 4-binding protein mediating GLUT4 translocation in adipocytes. Molecular Cell *3*, 751-760.

Molloy, S.S., Thomas, L., Kamibayashi, C., Mumby, M.C., Thomas, G. (1998). Regulation of endosome sorting by a specific PP2A isoform. J. Cell Biol. *142*, 1399-1411.

Moore, M.S., Mahaffey, D.T., Brodsky, F.M., Anderson, R.G. (1987). Assembly of clathrin-coated pits onto purified plasma membranes. Science *236*, 558-563.

Morgan, A., Burgoyne, R.D. (1995). Is NSF a fusion protein? Trends Cell Biol. *5*, 335-339.

Moss, J., Vaughan, M. (1998). Molecules in the ARF orbit. J. Biol. Chem. *273*, 21431-21434.

Moyers, J.S., Bilan, P.J., Reynet, C., Kahn, C.R. (1996). Overexpression of Rad inhibits glucose uptake in cultured muscle and fat cells. J. Biol. Chem. *271*, 23111-23116.

Mueckler, M., Caruso, C., Baldwin, S.A., Panico, M., Blench, I., Morris, H.R., Allard, W.J., Lienhard, G.E., Lodish, H.F. (1985). Sequence and structure of a human glucose transporter. Science *229*, 941-945.

Mukherjee, S.P., Mukherjee, C. (1981). Metabolic activation of adipocytes by insulin accompanied by an early increase in intracellular pH. Ann. N. Y. Acad. Sci. *372*, 347-351.

Mulieri, L.A., Hasenfuss, G., Ittleman, F., Blanchard, E.M., Alpert, N.R. (1989). Protection of human left ventricular myocardium from cutting injury by 2,3-butanedione monoxime. Circ. Res. *65*, 1441-1449.

Nag, A.C., Cheng, M., Fischman, D.A., Zak, R. (1983). Longterm cell culture of adult mammalian cardiac myocytes: Electron and immunofluorescent analysis of myofibrillar structure. J. Mol. Cell Cardiol. *15*, 301-317.

Nass, R., Rao, R. (1998). Novel localisation of a Na^+/H^+ exchanger in a late endosomal compartment of yeast. J. Biol. Chem. *273*, 21054-21060.

Noel, J., Pouyssegur, J. (1995). Hormonal regulation, pharmacology, and membrane sorting of vertebrate Na^+/H^+ exchanger isoforms. Am. J. Physiol. *268*, C283-C296.

Nordeng, T.W., Bakke, O. (1999). Overexpression of proteins containing tyrosine- or leucine-based sorting signals affects transferrin receptor trafficking. J. Biol. Chem. *274*, 21139-21148.

Oatey, P.B., Van Weering, D.H., Dobson, S.P., Gould, G.W., Tavare, J.M. (1997). GLUT4 vesicle dynamics in living 3T3 L1 adipocytes visualised with green-fluorescent protein. Biochem. J. *327*, 637-642.

Ohno, H., Fournier, M.C., Poy, G., Bonifacino, J.S. (1996). Structural determinants of interactions of tyrosine-based sorting signals with the adaptor medium chains. J. Biol. Chem. *271*, 29009-29015.

Ohno, H., Stewart, J., Fournier, M.C., Bosshart, H., Rhee, I., Miyatake, S., Saito, T., Gallusser, A., Kirchhausen, T., Bonifacino, J.S. (1995). Interaction of tyrosine based sorting signals with clathrin associated proteins. Science *269*, 1872-1875.

Okuno, Y., Gliemann, J. (1987). Enhancement of glucose transport by insulin at 37°C in rat adipocytes is accounted for by increased V_{max}. Diabetologia *30*, 426-430.

Omata, W., Shibata, H., Suzuki, Y., Tanaka, S., Suzuki, T., Takata, K., Kojima, I. (1997). Subcellular distribution of GLUT4 in chinese hamster ovary cells overexpressing mutant dynamin: Evidence that dynamin is a regulatory GTPase in GLUT4 endocytosis. Biochem. Biophys. Res. Commun. *241*, 401-406.

Ooi, C.E., Dell'Angelica, E.C., Bonifacino, J.S. (1998). ADP-ribosylation factor 1 (ARF1) regulates recruitment of the AP-3 adaptor complex to membranes. J. Cell Biol. *142*, 391-402.

Orchard, C.H., Kentish, J.C. (1990). Effect of changes of pH on the contractile function of cardiac muscle. Am. J. Physiol. *258*, C967-C981.

Owen, D.J., Evans, P.R. (1998). A structural explanation for the recognition of tyrosine-based endocytotic signals. Science *282*, 1327-1332.

Page, L.J., Robinson, M.S. (1995). Targeting signals and subunit interactions in coated vesicle adaptor complexes. J. Cell Biol. *131*, 619-630.

Palade, G. (1975). Intracellular aspects of the process of protein synthesis. Science *189*, 347-358.

Pallanck, L., Ordway, R.W., Ganetzky, B. (1995). A drosphila NSF mutant. Nature *376*, 25.

Palmer, R.H., Dekker, L.V., Woscholski, R., LeGood, J.A., Giggs, R., Parker, P.J. (1995). Activation of PRK1 by phosphatidylinositol 4,5-bisphosphate and phosphatidylinositol 3,4,5-trisphosphate - a comparison with protein kinase C isoforms. J. Biol. Chem. *270*, 22412-22416.

Paris, S., Beraud-Dufour, S., Robineau, S., Bigay, J., Antonny, B., Chabre, M., Chardin, P. (1997). Role of protein-phospholipid interactions in the activation of ARF1 by the guanine nucleotide exchange factor ARNO. J. Biol. Chem. *272*, 22221-22226.

Patki, V., Lawe, D.C., Corvera, S., Virbasius, J., Chawla, A. (1998). A functional PI-3-P-binding motif. Nature *394*, 433-434.

Patki, V., Virbasius, J., Lane, W.S., Toh, B.H., Shpetner, H.S., Corvera, S. (1997). Identification of an early endosomal protein regulated by phosphatidylinositol 3-kinase. Proc. Natl. Acad. Sci. U.S.A *94*, 7326-7330.

Pearse, B.M. (1975). Coated vesicles from pig brain: Purification and biochemical characterisation. J. Mol. Biol. *97*, 93-98.

Pearse, B.M. (1985). Assembly of the mannose-6-phosphate receptor into reconstituted clathrin coats. EMBO J. *4*, 2457-2460.

Pearse, B.M., Robinson, M.S. (1990). Clathrin, adaptors, and sorting. Annu. Rev. Cell Biol. *6*, 151-171.

Peyroche, A., Antonny, B., Robineau, S., Acker, J., Cherfilis, J., Jackson, C.L. (1999). Brefeldin A acts to stabilise an abortive ARF-GDP-Sec7 domain protein complex: Involvement of specific residues of the Sec7 domain. Mol. Cell *3*, 275-285.

Pfeffer, S.R. (1994). Rab GTPases: Master regulators of membrane trafficking. Curr. Opin. Cell Biol. *6*, 522-526.

Piper, H.M., Volz, A., Schwartz, P. (1990). Adult Ventricular Rat Heart Muscle Cells. In: Cell culture techniques in heart and vessel research, ed. H.M.Piper 36-60.

Piper, R.C., Tai, C., Kulesza, P., Pang, S., Warnock,D., Baenziger, J., Slot, J.W., Geuze, H.J., Puri, C., James, D.E. (1993). GLUT-4 NH2 terminus contains a phenylalanine-based targeting motif that regulates intracellular sequestration. J. Cell Biol. *121*, 1221-1232.

Piper, R.C., Tai, C., Slot, J.W., Hahn, C.S., Rice, C.M., Huang, H., James, D.E. (1992). The efficient intracellular sequestration of the insulin-regulatable glucose transporter (GLUT-4) is conferred by the NH2 terminus. J. Cell Biol. *117*, 729-743.

Ploug, T., Galbo, H., Vinten, J., Jorgensen, M., Richter, E.A. (1987). Kinetics of glucose transport in rat muscle: Effects of insulin and contractions. Am. J. Physiol *253*, E12-E20.

Ploug, T., van Deurs, B., Ai, H., Cushman, S.W., Ralston, E. (1998). Analysis of GLUT4 distribution in whole skeletal muscle fibres: Identification of distinct storage

compartments that are recruited by insulin and muscle contractions. J. Cell Biol. *142*, 1429-1446.

Presley, J.F., Mayor, S., McGraw, T.E., Dunn, K.W., Maxfield, F.R. (1997). Bafilomycin A_1 treatment retards transferrin receptor recycling more than bulk membrane recycling. J. Biol. Chem. *272*, 13929-13936.

Radhakrishna, H., Donaldson, J.G. (1997). ADP-ribosylation factor 6 regulates a novel plasma membrane recycling pathway. J. Cell Biol. *139*, 49-61.

Ralston, E., Ploug, T. (1996). GLUT4 in cultured skeletal myotubes is segregated from the transferrin receptor and stored in vesicles associated with TGN. J. Cell Sci. *109*, 2967-2978.

Rameh, L.E., Arvidsson, A., Carraway, K.L., III, Couvillon, A.D., Rathbun, G., Crompton, A., VanRenterghem, B., Czech, M.P., Ravichandran, K.S., Burakoff, S.J., Wang, D.S., Chen, C.S., Cantley, L.C. (1997). A comparative analysis of the phosphoinositide binding specificity of pleckstrin homology domains. J. Biol. Chem. *272*, 22059-22066.

Rameh, L.E., Cantley, L.C. (1999). The role of phosphoinositide 3-kinase lipid products in cell function. J. Biol. Chem. *274*, 8347-8350.

Rapoport, I., Chen, Y.C., Cupers, P., Shoelson, S.E., Kirchhausen, T. (1998). Dileucine-based sorting signals bind to the β chain of AP-1 at a site distinct and regulated differently from the tyrosine-based motif binding site. EMBO J. *17*, 2148-2155.

Rapoport, I., Miyazaki, M., Boll, W., Duckworth, B., Cantley, L.C., Shoelson, S., Kirchhausen, T. (1997). Regulatory interactions in the recognition of endocytic sorting signals by AP-2 complexes. EMBO J. *16*, 2240-2250.

Rea, S., James, D.E. (1997). Moving GLUT4: The biogenesis and trafficking of GLUT4 storage vesicles. Diabetes *46*, 1667-1677.

Rea, S., Martin, L.B., McIntosh, S., Macaulay, S.L., Ramsdale, T., Baldini, G., James, D.E. (1998). Syndet, an adipocyte target SNARE involved in the insulin-induced translocation of GLUT4 to the cell surface. J. Biol. Chem. *273*, 18784-18792.

Reaves, B., Banting, G. (1994). Overexpression of TGN38/41 leads to mislocalisation of γ-adaptin. FEBS Lett. *351*, 448-456.

Reiser, G., Sabbadini, R., Paolini, R.P., Fry, M., Inesi, G. (1979). Sarcomere motion in isolated cardiac cells. Am. J. Physiol. *236*, C70-C77.

Resh, M.D., Nemenoff, R.A., Guidotti, G. (1980). Insulin stimulation of (Na^+,K^+)-adenosine triphosphatase-dependent ^{86}Rb uptake in rat adipocytes. J. Biol. Chem. *255*, 10938-10945.

Robinson, L.J., Pang, S., Harris, D.S., Heuser, J., James, D.E. (1992). Translocation of the glucose transporter (GLUT4) to the cell surface in permeabilised 3T3-L1 adipocytes: Effects of ATP, insulin and GTPγS and localization of GLUT4 to clathrin lattices. J. Cell Biol. *117*, 1181-1196.

Robinson, M.S., Kreis, T.E. (1992). Recruitment of coat proteins onto Golgi membranes in intact and permeabilised cells: Effects of brefeldin A and G protein activators. Cell *69*, 129-138.

Robinson, M.S., Watts, C., Zerial, M. (1996). Membrane dynamics in endocytosis. Cell *84*, 13-21.

Rodionov, D.G., Bakke, O. (1998). Medium chains of adaptor complexes recognise leucine-based sorting signals from the invariant chain. J. Biol. Chem. *273*, 6005-6008.

Romanek, R., Sargeant, R., Paquet, M.R., Gluck, S., Klip, A., Grinstein, S. (1993). Chloroquine inhibits glucose-transporter recruitment induced by insulin in rat adipocytes independently of its action on endomembrane pH. Biochem. J. *296*, 321-327.

Rosic, N.K., Standaert, M.L., Pollet, R.J. (1985). The mechanisms of insulin stimulation of (Na^+,K^+)-ATPase transport activity in muscle. J. Biol. Chem. *260*, 6206-6212.

Ross, S.A., Herbst, J.J., Keller, S.R., Lienhard, G.E. (1997). Trafficking kinetics of the insulin-regulated membrane aminopeptidase in 3T3-L1 adipocytes. Biochem. Biophys. Res. Commun. *239*, 247-251.

Roth, M.G. (1999). Snapshots of ARF1: Implications for mechanisms of activation and inactivation. Cell *97*, 149-152.

Roth, R.A., Liu, F., Chin, J.E. (1994). Biochemical mechanisms of insulin resistance. Hormone Res. *41*, 51-55.

Roth, T.F., Porter, K.R. (1964). Yolk protein uptake in the oocyte of the mosquito *Aedes aegypti*. J. Cell Biol. *20*, 313-332.

Rothman, J.E. (1996). The protein machinery of vesicle budding and fusion. Protein Sci. *5*, 185-194.

Rothman, J.E., Warren, G. (1994). Implications of the SNARE hypothesis for intracellular membrane topology and dynamics. Curr. Biol. *4*, 220-233.

Rothman, J.E., Wieland, F.T. (1996). Protein sorting by transport vesicles. Science *272*, 227-234.

Russ, U., Balser, C., Scholz, W., Albus, U., Lang, H.J., Weichert, A., Scholkens, B.A., Gogelein, H. (1996). Effects of the Na^+/H^+-exchange inhibitor HOE 642 on intracellular pH, calcium and sodium in isolated rat ventricular myocytes. Pflugers Arch. *433*, 26-34.

Sada, H., Sada, S., Sperelakis, N. (1985). Effects of diacetylmonoxime (DAM) on slow and fast action potentials of young and embryonic chick hearts and rabbit hearts. Eur. J. Pharmacol. *112*, 145-152.

Sardet, C., Franchi, A., Pouyssegur, J. (1989). Molecular cloning, primary structure and expression of the human growth factor activatable Na^+/H^+ antiporter. Cell *56*, 271-280.

Sata, M., Moss, J., Vaughan, M. (1999). Structural basis for the inhibitory effect of brefeldin A on guanine nucleotide-exchange proteins for ADP-ribosylation factors. Proc. Natl. Acad. Sci. U.S.A *96*, 2752-2757.

Satoh, S., Nishimura, H., Clark, A.E., Kozka, I.J., Vannucci, S.J., Simpson, I.A., Quon, M.J., Cushman, S.W., Holman, G.D. (1993). Use of bis-mannose photolabel to elucidate insulin-regulated GLUT4 subcellular trafficking kinetics in rat adipose cells. Evidence that exocytosis is a critical site of hormone action. J. Biol. Chem. *268*, 17820-17829.

Schaffer, J.E., Lodish, H.F. (1994). Expression, cloning and characterisation of a novel adipocyte long chain fatty acid transport protein. Cell *79*, 427-436.

Schimmoller, F., Simon, I., Pfeffer, S.R. (1998). Rab GTPases, directors of vesicle docking. J. Biol. Chem. *273*, 22161-22164.

Schlossman, D.M., Schmid, S.L., Braell, W.A., Rothman, J.E. (1984). An enzyme that removes clathrin coats: Purification of an uncoating ATPase. J. Cell Biol. *99*, 723-733.

Schmid, S.L. (1997). Clathrin-coated vesicle formation and protein sorting: An integrated process. Annu. Rev. Biochem. *66*, 511-548.

Schmidt, A., Hannah, M.J., Huttner, W.B. (1997). Synaptic-like microvesicles of neuroendocrine cells originate from a novel compartment that is continuous with the plasma membrane and devoid of transferrin receptor. J. Cell Biol. *137*, 445-458.

Scholz, W., Albus, U., Counillon, L., Gogelein, H., Lang, H.J., Linz, W., Weichert, A., Scholkens, B.A. (1995). Protective effects of HOE642, a selective sodium-hydrogen exchange subtype 1 inhibitor, on cardiac ischemia and reperfusion. Cardiovasc. Res. *29*, 260-268.

Scholz, W., Albus, U., Lang, W., Martorana, P.A., Englert, H.C., Scholkens, B.A. (1993). HOE-694 a new Na^+/H^+ exchange inhibitor and its effects in cardiac ischemia. Br. J. Pharmacol. *109*, 562-568.

Schu, P.V., Takegawa, K., Fry, M.J., Stack, J.H., Waterfield, M.D., Emr, S.D. (1993). Phosphatidyl 3-kinase encoded by the yeast vps34 gene is essential for protein sorting. Science *260*, 88-91.

Seaman, M.N.J., Sowerby, P.J., Robinson, M.S. (1996). Cytosolic and membrane-associated proteins involved in the recruitment of AP-1 adaptors onto the *trans*-Golgi network. J. Biol. Chem. *271*, 25446-25451.

Semenza, J.C., Hardwick, K.G., Dean, N., Pelham, H.R.B. (1990). ERD2, a yeast gene required for the receptor-mediated retrieval of luminal ER proteins from the secretory pathway. Cell *61*, 1349-1357.

Semplicini, A., Mozzato, M.G., Sama', B., Nosadini, R., Fioretto, P., Trevisan, R., Pessina, A.C., Crepaldi G., Dal Palu', C. (1989). Na^+/H^+ and Li^+/Na^+ exchange in red blood cells of normotensive and hypertensive patients with insulin-dependent diabetes mellitus (IDDM). Am. J. Hypertens. *2*, 174-177.

Serafin, W.E., Guidry, U.A., Dayton, E.T., Kamada, M.M., Stevens, R.L., Austin, K.F. (1991). Identification of aminopeptidase activity in the secretory granules of mouse mast cells. Proc. Natl. Acad. Sci. U.S.A *88*, 5984-5988.

Sevilla, L., Tomas, E., Munoz, P., Guma, A., Fischer, Y., Thomas, J., Ruiz-Montasell, B., Testar, X., Palacin, M., Blasi, J., Zorzano, A. (1997). Characterisation of two distinct intracellular GLUT4 membrane populations in muscle fibre. Differential protein composition and sensitivity to insulin. Endocrinology *138*, 3006-3015.

Shanahan, M.F., Edwards, B.M., Ruoho, A.E. (1986). Interactions of insulin, catecholamines and adenosine in the regulation of glucose transport in isolated rat cardiac myocytes. Biochim. Biophys. Acta *887*, 121-129.

Shepherd, P.R., Nave, B.T., O'Rahilly, S. (1996). The role of phosphoinositide 3-kinase in insulin signalling. J. Mol. Endocrinol. *17*, 175-184.

Shepherd, P.R., Siddle, K., Nave, B.T. (1997). Is stimulation of class-1 phosphatidylinositol 3-kinase activity by insulin sufficient to activate pathways involved in glucose metabolism. Biochem. Soc. Trans. *25*, 978-981.

Shepherd, P.R., Withers, D.J., Siddle, K. (1998). Phosphoinositide 3-kinase: The key switch mechanism in insulin signalling. Biochem. J. *333*, 471-490.

Sherman, L.A., Hirshman, M.F., Cormont, M., Marchand-Brustel, Y., Goodyear, L.J. (1996). Differential effects of insulin and exercise on Rab4 distribution in rat skeletal muscle. Endocrinology *137*, 266-273.

Shibata, H., Omata, W., Kojima, I. (1997). Insulin stimulates guanine nucleotide exchange on rab4 via a wortmannin-sensitive signalling pathway in rat adipocytes. J. Biol. Chem. *272*, 14542-14546.

Shibata, H., Omata, W., Suzuki, Y., Tanaka, S., Kojima, I. (1996). A synthetic peptide corresponding to the Rab4 hypervariable carboxyl-terminal domain inhibits insulin action on glucose transport in rat adipocytes. J. Biol. Chem. *271*, 9704-9709.

Shibata, H., Suzuki, Y., Omata, W., Tanaka, S., Kojima, I. (1995). Dissection of GLUT4 recycling pathway into exocytosis and endocytosis in rat adipocytes. Evidence that GTP-binding proteins are involved in both processes. J. Biol. Chem. *270*, 11489-11495.

Shoelson, S.E., Chatterjee, S., Chaudhuri, M., White, M.F. (1992). YMXM motifs of IRS-1 define substrate specificity of the insulin receptor kinase. Proc. Natl. Acad. Sci. U.S.A *89*, 2027-2031.

Shpetner, H., Joly, M., Hartley, D., Corvera, S. (1996). Potential sites of PI-3 kinase function in the endocytic pathway revealed by the PI-3 kinase inhibitor, wortmannin. J. Cell Biol. *132*, 595-605.

Shpetner, H., Vallee, R.B. (1992). Dynamin is a GTPase stimulated to high levels of activity by microtubules. Nature *355*, 733-735.

Shpetner, H.S., Vallee, R.B. (1989). Identification of dynamin a novel mechanochemical enzyme that mediates interactions between microtubules. Cell *59*, 421-432.

Simons, K., Zerial, M. (1993). Rab proteins and the road maps for intracellular transport. Neuron *11*, 789-799.

Simpson, F., Peden, A.A., Christopoulou, L., Robinson, M.S. (1997). Characterisation of the adaptor-related protein complex, AP-3. J. Cell Biol. *137*, 835-845.

Simpson, I.A., Yver, D.R., Hissin, P.J., Wardzala, L.J., Karnieli, E., Salans, L.B., Cushman, S.W. (1983). Insulin-stimulated translocation of glucose transporters in the isolated rat adipose cell: Characterisation of subcellular fractions. Biochim. Biophys. Acta *763*, 393-407.

Sleeman, M.W., Donegan, N.P., Heller-Harrison, R., Lane, W.S., Czech, M.P. (1998). Association of acyl-CoA synthetase-1 with GLUT4-containing vesicles. J. Biol. Chem. *273*, 3132-3135.

Slot, J.W., Garruti, G., Martin, S., Oorschot, V., Posthuma, G., Kraegen, E.W., Laybutt, R., Thibault, G., James, D.E. (1997). Glucose transporter (GLUT-4) is targeted to secretory granules in rat atrial cardiomyocytes. J. Cell Biol. *137*, 1243-1254.

Slot, J.W., Geuze, H.J., Gigengack, S., James, D.E., Lienhard, G.E. (1991b). Translocation of the glucose transporter GLUT4 in cardiac myocytes of the rat. Proc. Natl. Acad. Sci. U.S.A *88*, 7815-7819.

Slot, J.W., Geuze, H.J., Gigengack, S., Lienhard, G.E., James, D.E. (1991a). Immuno-localization of the insulin regulatable glucose transporter in brown adipose tissue of the rat. J. Cell Biol. *113*, 123-135.

Smith-Hall, J., Pons, S., Patti, M.E., Burks, D.J., Yenush, L., Sun, X.J., Kahn, C.R. (1997). The 60 kDa insulin receptor substrate functions like an IRS protein (pp60 (IRS3)) in adipose cells. Biochemistry *36*, 8304-8320.

Smith, U., Kuroda, M., Simpson, I.A. (1984). Counter-regulation of insulin-stimulated glucose transport by catecholamines in the isolated rat adipose cell. J. Biol. Chem. *259*, 8758-8763.

Sollner, T., Whiteheart, S.W., Brunner, M., Erdjument-Bromage, H., Geromanos, S., Tempst, P., Rothman, J.E. (1993). SNAP receptors implicated in vesicle targeting and fusion. Nature *362*, 318-324.

St Denis, J.F., Cushman, S.W. (1998). Role of SNARE's in the GLUT4 translocation response to insulin in adipose cells and muscle. J. Basic Clin. Physiol. Pharmacol. *9*, 153-165.

Stamnes, M.A., Rothman, J.E. (1993). The binding of AP-1 clathrin adaptor particles to Golgi membranes requires ADP-ribosylation factor, a small GTP-binding protein. Cell *73*, 999-1005.

Standaert, M.L., Galloway, L., Karnam, P., Bandyopadhyay, G., Moscat, J., Farese, R.V. (1997). Protein kinase Cζ as a downstream effector of phosphatidyl 3-kinase during insulin stimulation in rat adipocytes - potential role in glucose transport. J. Biol. Chem. *272*, 30075-30082.

Stephens, L., Hughes, K.T., Irvine, R.F. (1991). Pathway of phosphotidyl (3,4,5) trisphosphate synthesis in activated neutrophils. Nature *351*, 33-39.

Stephens, L., Jackson, T.R., Hawkin, P.T. (1993). Agonist stimulated synthesis of phosphatidylinositol (3,4,5) trisphosphate: a new signalling system? Biochim. Biophys. Acta *1179*, 27-75.

Stoorvogel, W., Geuze, H.J., Strous, G.J. (1987). Sorting of endocytosed transferrin and asialoglycoprotein occurs immediately after internalisation in HepG2 cells. J. Cell Biol. *104*, 1261-1268.

Subtil, A., Gaidarov, I., Kobylarz, K., Lampson, M.A., Keen, J.H., McGraw, T.E. (1999). Acute cholesterol depletion inhibits clathrin-coated pit budding. Proc. Natl. Acad. Sci. U.S.A *96*, 6775-6780.

Sun, X.J., Rothenberg, P., Kahn, C.R., Backer, J.M., Araki, E., Wilden, P.A., Cahill, D.A., Goldstein, B.J., White, M.F. (1991). Structure of the insulin-receptor substrate IRS1 defines a unique signal transduction protein. Nature *352*, 73-77.

Sun, X.J., Weng, L., Zhang, Y., Yenush, L., Myers, M.G., Galsheen, E., Lane, W.S., Pierce, J.H., White, M.F. (1995). Role of IRS-2 in insulin and cytokine signalling. Nature *377*, 173-177.

Suzuki, K. (1988). Reassessment of the translocation hypothesis by kinetic studies on hexose transport in isolated rat adipocytes. J. Biol. Chem. *263*, 12247-12252.

Suzuki, K., Kono, T. (1980). Evidence that insulin causes translocation of glucose transport activity to the plasma membrane from an intracellular storage compartment. Proc. Natl. Acad. Sci. U.S.A *77*, 2542-2545.

Tamori, Y., Hashiramoto, M., Araki, S., Kamata, Y., Takahashi, M., Kozaki, S., Kasuga, M. (1996). Cleavage of vesicle-associated membrane protein (VAMP)-2 and cellubrevin on GLUT4-containing vesicles inhibits the translocation of GLUT4 in 3T3-L1 adipocytes. Biochem. Biophys. Res. Commun. *220*, 740-745.

Tamori, Y., Kawanishi, M., Niki, T., Shinoda, H., Araki, S., Okazawa, H., Kasuga, M. (1998). Inhibition of insulin-induced GLUT4 translocation by Munc18c through interaction with syntaxin4 in 3T3-L1 adipocytes. J. Biol. Chem. *273*, 19740-19746.

Tanner, L.I., Lienhard, G.E. (1987). Insulin elicits a redistribution of transferrin receptors in 3T3-L1 adipocytes through an increase in the rate constant for receptor externalisation. J. Biol. Chem. *262*, 8975-8980.

Taylor, L.P., Holman, G.D. (1981). Symmetrical kinetic parameters for 3-*O*-methyl-D-glucose transport in adipocytes in the presence and in the absence of insulin. Biochim. Biophys. Acta *642*, 325-335.

Tellam, J.T., Macaulay, S.L., McIntosh, S., Hewish, D.R., Ward, C.W., James, D.E. (1997). Characterisation of Munc-18c and syntaxin-4 in 3T3-L1 adipocytes. Putative role in insulin-dependent movement of GLUT-4. J. Biol. Chem. *272*, 6179-6186.

Tellam, J.T., McIntosh, S., James, D.E. (1995). Molecular identification of two novel Munc-18 isoforms expressed in non- neuronal tissues. J. Biol. Chem. *270*, 5857-5863.

Thurmond, D.C., Ceresa, B.P., Okada, S., Elmendorf, J.S., Coker, K., Pessin, J.E. (1998). Regulation of insulin-stimulated GLUT4 translocation by Munc18c in 3T3-L1 adipocytes. J. Biol. Chem. *273*, 33876-33883.

Till, M., Kolter, T., Eckel, J. (1997). Molecular mechanisms of contraction-induced translocation of GLUT4 in isolated cardiomyocytes. Am. J. Cardiol. *80*, 85A-89A.

Timmers, K.I., Clark, A.E., Omatsu-Kanbe, M., Whiteheart, S.W., Bennett, M.K., Holman, G.D., Cushman, S.W. (1996). Identification of SNAP receptors in rat adipose cell membrane fractions and in SNARE complexes co-immunoprecipitated with epitope-tagged N- ethylmaleimide-sensitive fusion protein. Biochem. J. *320*, 429-436.

Todaka, M., Hayashi, H., Imanaka, T., Mitani, Y., Kamohara, S., Kishi, K., Tamaoka, K., Kanai, F., Shichiri, M., Morii, N., Narumiya, S., Ebina, Y. (1996). Roles of insulin, guanosine 5'-[gamma-thio]triphosphate and phorbol 12-myristate 13-acetate in signalling pathways of GLUT4 translocation. Biochem. J. *315*, 875-882.

Toker, A., Cantley, L.C. (1997). Signalling through the lipid products of phosphoinositide-3-OH kinase. Nature *387*, 673-676.

Tooze, S.A. (1998). Biogenesis of secretory granules in the *trans*-Golgi network of neuroendocrine and endocrine cells. Biochim. Biophys. Acta *1404*, 231-244.

Traub, L.M., Ostrom, J.A., Kornfeld, S. (1993). Biochemical dissection of AP-1 recruitment onto Golgi membranes. J. Cell Biol. *123*, 561-573.

Trowbridge, I.S., Collawn, J.F., Hopkins, C.R. (1993). Signal-dependent membrane protein trafficking in the endocytic pathway. Annu. Rev. Cell Biol. *9*, 129-161.

Tsakiridis, T., Vranic, M., Klip, A. (1994). Disassembly of the actin network inhibits insulin-dependent stimulation of glucose transport and prevents recruitment of glucose transporters to the plasma membrane. J. Biol. Chem. *269*, 29934-29942.

Turkewitz, A.P., Schwartz, A.L., Harrison, S.C. (1988). A pH-dependent reversible conformational transition of the human transferrin receptor leads to self association. J. Biol. Chem. *263*, 16309-16315.

Urrutia, R., Henley, J.R., Cook, T., McNiven, M.A. (1997). The dynamins: Redundant or distinct functions for an expanding family of related GTPases. Proc. Natl. Acad. Sci. U.S.A *94*, 377-384.

van der Sluijs, P., Hull, M., Webster, P., Male, P., Goud, B., Mellman, I. (1992). The small GTP-binding protein rab4 controls an early sorting event on the endocytic pathway. Cell *70*, 729-740.

Vanhaesebroeck, B., Leevers, S.J., Panayotou, G., Waterfield, M.D. (1997). Phosphoinositide 3-kinase: A conserved family of signal transducers. Trends Biochem. Sci. *22*, 267-272.

Vannucci, S.J., Nishimura, H., Satoh, S., Cushman, S.W., Holman, G.D., Simpson, I.A. (1992). Cell surface accessibility of GLUT4 glucose transporters in insulin- stimulated rat adipose cells. Modulation by isoprenaline and adenosine. Biochem. J. *288*, 325-330.

VanRenterghem, B., Morin, M., Czech, M.P., Heller-Harrison, R.A. (1998). Interaction of insulin receptor substrate-1 with the σ3A subunit of the adaptor protein complex-3 in cultured adipocytes. J. Biol. Chem. *273*, 29942-29949.

Venkateswarlu, K., Oatey, P.B., Tavare, J.M, Jackson, T.R., Cullen, P.J. (1999). Identification of centaurin-α1 as a potential *in vivo* phosphatidylinositol 3,4,5-trisphosphate-binding protein that is functionally homologous to the yeast ADP-ribosylation factor (ARF) GTPase-activating protein, Gcs1. Biochem. J. *340*, 359-363.

Venkateswarlu, K., Oatey ,P.B., Tavare, J.M., Cullen, P.J. (1998). Insulin-dependent translocation of ARNO to the plasma membrane of adipocytes requires phosphatidylinositol 3-kinase. Curr. Biol. *8*, 463-466.

Verhey, K.J., Birnbaum, M.J. (1994). A Leu-Leu sequence is essential for COOH-terminal targeting signal of GLUT4 glucose transporter in fibroblasts. J. Biol. Chem. *269*, 2353-2356.

Verhey, K.J., Hausdorff, S.F., Birnbaum, M.J. (1993). Identification of the carboxy terminus as important for the isoform-specific subcellular targeting of glucose transporter proteins. J. Cell Biol. *123*, 137-147.

Verrecchia, F., Herve, J.C. (1997). Reversible blockade of gap junctional communication by 2,3-butandione monoxime in rat cardiac myocytes. Am. J. Physiol *272*, C875-C885.

Vigers, G.P.A., Crowther, R.A., Pearse, B.M. (1986). Location of the 100 kDa accessory proteins in clathrin coats. EMBO J. *5*, 2079-2085.

Vik, S.B., Antonio, B.J. (1994). A mechanism of proton translocation by F_1F_0 ATP synthases suggested by double mutants of the a subunit. J. Biol. Chem. *269*, 30364-30369.

Virbasius, J., Guilherme, A., Czech, M.P. (1996). Mouse p170 is a novel phosphatidylinositol 3-kinase containing a C2 domain. J. Biol. Chem. *271*, 13304-13307.

Virshup, D.M., Bennett, V. (1988). Clathrin-coated vesicle assembly polypeptides: physical properties and reconstitution studies with brain membranes. J. Cell Biol. *106*, 39-50.

Volchuk, A., Narine, S., Foster, L.J., Grabs, D., De Camilli, P., Klip, A. (1998). Perturbation of dynamin II with an amphiphysin SH3 domain increases GLUT4 glucose transporters at the plasma membrane in 3T3-L1 adipocytes. Dynamin II participates in GLUT4 endocytosis. J. Biol. Chem. *273*, 8169-8176.

Volchuk, A., Sargeant, R., Sumitani, S., Liu, Z., He, L., Klip, A. (1995). Cellubrevin is a resident protein of insulin-sensitive GLUT4 glucose transporter vesicles in 3T3-L1 adipocytes. J. Biol. Chem. *270*, 8233-8240.

Vollenweider, P., Martin, S.S., Haruta, T., Morris, A.J., Nelson, J.G., Cormont, M., Marchand-Brustel, Y., Rose, D.W., Olefsky, J.M. (1997). The small guanosine triphosphate-binding protein Rab4 is involved in insulin-induced GLUT4 translocation and actin filament rearrangement in 3T3-L1 cells. Endocrinology *138*, 4941-4949.

Wakabayashi, S., Shigekawa, M., Pouyssegur, J. (1997). Molecular physiology of vertebrate Na^+/H^+ exchangers. Physiol. Rev. *77*, 51-74.

Walker, K.S., Deak, M., Paterson, A., Hudson, K., Cohen, P., Alessi, D.R. (1998). Activation of protein kinase B β and γ isoforms by insulin *in vivo* and by 3-phosphoinositide-dependent protein kinase-1 *in vitro*. Biochem. J. *331*, 299-308.

Wallberg-Henriksson, H., Holloszy, J.O. (1985). Activation of glucose transport in diabetic muscle: Responses to contraction and insulin. Am. J. Physiol. *249*, C233-C237.

Wan, L., Molloy, S.S., Thomas, L., Liu, G., Xiang, Y., Rybak, S.L., Thomas, G. (1998). PACS-1 defines a novel gene family of cytosolic sorting proteins required for *trans*-Golgi network localization. Cell *94*, 205-216.

Wang, G., Witkin, J.W., Hao, G., Bankiatis, V.A., Scherer, P.E., Baldini, G. (1997). Syndet is a novel SNAP-25 related protein expressed in many tissues. J. Cell Sci. *110*, 505-513.

Wang, Q., Bilan, P.J., Tsakiridis, T., Hinek, A., Klip, A. (1998). Actin filaments participate in the relocalisation of phosphatidylinositol 3-kinase to glucose transporter-containing compartments and in the stimulation of glucose uptake in 3T3-L1 adipocytes. Biochem. J. *331*, 917-928.

Wang, Q., Somwar, R., Bilan, P.J., Liu, Z., Jin, J., Woodgett, J.R., Klip, A. (1999). Protein kinase B/Akt participates in GLUT4 translocation by insulin in L6 myoblasts. Mol. Cell Biol. *19*, 4008-4018.

Warnock, D.E., Schmid, S.L. (1996). Dynamin GTPase, a force-generating molecular switch. Bioessays *18*, 885-893.

Waters, M.G., Pfeffer, S.R. (1999). Membrane tethering in intracellular transport. Curr. Opin. Cell Biol. *11*, 453-459.

Weber, T., Joost, H.G., Simpson, I.A., Cushman, S.W. (1988). Methods of Assessment of Glucose Transport Activity and the Number of Glucose Transporter in Isolated Rat Adipose Cells and Membrane Fractions. In: Insulin Receptors., ed. R. Alan Liss Inc., 171-187.

Wei, M.L., Bonzelius, F., Scully, R.M., Kelly, R.B., Herman, G.A. (1998). GLUT4 and transferrin receptor are differentially sorted along the endocytic pathway in CHO cells. J. Cell Biol. *140*, 565-575.

Werner, G., Hagenmaier, H., Drautz, H., Baumgartner, A., Zahner, H. (1984). Metabolic products of micro-organisms. Bafilomycins, a new group of macrolide antibiotics. Production, isolation, chemical structure and biological activity. J. Antibiot. *37*, 110-117.

West, M.A., Bright, N.A., Robinson, M.S. (1997). The role of ADP-ribosylation factor and phospholipase D in adaptor recruitment. J. Cell Biol. *138*, 1239-1254.

Whiteheart, S.W., Griff, I.C., Brunner, M., Clary, D.O., Mayer, T., Buhrow, S.A., Rothman, J.E. (1993). SNAP family of NSF attachment proteins includes a brain-specific isoform. Nature *362*, 353-355.

Whitesell, R.R., Abumrad, N.A. (1985). Increased affinity predominates in insulin stimulation of glucose transport in the adipocyte. J. Biol. Chem. *260*, 2894-2899.

Whitesell, R.R., Gliemann, J. (1979). Kinetics and parameters of transport of 3-*O*-methylglucose and glucose in adipocytes. J. Biol. Chem. *254*, 5276-5283.

Wilde, A., Brodsky, F.M. (1996). *In vivo* phosphorylation of adaptors regulates their interaction with clathrin. J. Cell Biol. *135*, 635-645.

Wilson, D.W., Whiteheart, S.W., Orci, L., Rothman, J.E. (1991). Intracellular membrane fusion. Trends Biochem. Sci. *16*, 334-337.

Wong, D.H., Brodsky, F.M. (1992). 100-kDa proteins of Golgi- and *trans*-Golgi network-associated coated vesicles have related but distinct membrane binding properties. J. Cell Biol. *117*, 1171-1179.

Wong, P.P., Daneman, N., Volchuk, A., Lassam, N., Wilson, M.C., Klip, A., Trimble, W.S. (1997). Tissue distribution of SNAP-23 and its subcellular localization in 3T3- L1 cells. Biochem. Biophys. Res. Commun. *230*, 64-68.

Yang, J., Clark, A.E., Harrison, R., Kozka, I.J., Holman, G.D. (1992). Trafficking of glucose transporters in 3T3-L1 cells. Inhibition of trafficking by phenylarsine oxide implicates a slow dissociation of transporters from trafficking proteins. Biochem. J. *281*, 809-817.

Yang, J., Clarke, J.F., Ester, C.J., Young, P.W., Kasuga, M., Holman, G.D. (1996). Phosphatidylinositol 3-kinase acts at an intracellular membrane site to enhance GLUT4 exocytosis in 3T3-L1 cells. Biochem. J. *313*, 125-131.

Yang, J., Holman, G.D. (1993). Comparison of GLUT4 and GLUT1 subcellular trafficking in basal and insulin-stimulated 3T3-L1 cells. J. Biol. Chem. *268*, 4600-4603.

Yeh, J.I., Gulve, E.A., Rameh, L., Birnbaum, M.J. (1995). T he effects of wortmannin on rat skeletal muscle. J. Biol. Chem. *270*, 2107-2111.

Yin, Y., Terauchi, Y., Solomon, G.S., Aizawa, S., Rangarajan, P.N., Yazaki, Y., Kadowaki, T., Barrett, J.C. (1998). Involvement of p85 in p53-dependent apoptotic response to oxidative stress. Nature *391*, 707-710.

Yoo, S.H. (1994). PH-dependent interaction of chromatogranin A with integral membrane proteins of secretory vesicles including 260 kDa protein reactive to inositol 1,4,5-triphosphate receptor antibody. J. Biol. Chem. *269*, 12001-12006.

Yoo, S.H. and Lewis, M.S. (1993). Dimerisation and tetramerisation properties of the C-terminal region of chromatogranin A: A thermodynamic analysis. Biochemistry *32*, 8816-8822.

Yoshimori, T., Yamamoto, A., Moriyama, Y., Futai, M., Tashiro, Y. (1991). Bafilomycin A_1, a specific inhibitor of vacuolar-type H^+-ATPase, inhibits acidification and protein degradation in lysosomes in cultured cells. J. Biol. Chem. *266*, 17707-17712.

Zaninetti, D., Greco-Perotto, R., Assimacopoulos-Jeannet, F., Jeanrenaud, B. (1988). Effects of insulin on glucose transport and glucose transporters in rat heart. Biochem. J *250*, 277-283.

Zaremba, S., Keen, J.H. (1983). Assembly polypeptides from coated vesicles mediate reassembly of unique clathrin coats. J. Cell Biol. *97*, 1339-1347.

Zerial, M., Stenmark, H. (1993). Rab GTPases in vesicular transport. Curr. Opin. Cell Biol. *5*, 613-620.

Zeuzem, S., Feick, P., Zimmermann, P., Haase, W., Kahn, R.A. (1992). Intravesicular acidification correlates with binding of ADP-ribosylation factor to microsomal membranes. Proc. Natl. Acad. Sci. U.S.A *89*, 6619-6623.

Zhang, J., Feng, Y., Forgac, M. (1994b) . Proton conduction and bafilomycin binding by the V_0 domain of the coated vesicle V-ATPase. J. Biol. Chem. *269*, 23518-23523.

Zhang, J.Z., Davletov, T.C., Sudhof, T.C., Anderson, R.G. (1994a). Synaptotagmin I is a high affinity receptor for clathrin AP-2: Implications for membrane recycling. Cell *78*, 751-760.

Zhu, Y., Traub, L.M., Kornfeld, S. (1998). ADP-ribosylation factor 1 transiently activates high-affinity adaptor protein complex AP-1 binding sites on Golgi membranes. Mol. Biol. Cell *9*, 1323-1337.

Zorzano, A., Balon, T.W., Goodman, M.N., Ruderman, N.B. (1986). Glycogen depletion and increased insulin sensitivity and responsiveness in muscle after exercise. Am. J. Physiol. *251*, E664-E669.

Zorzano, A., Wilkinson, W., Kotliar, N., Thoidis, G., Wadzinkski, B.E., Ruoho, A.E., Pilch, P.F. (1989). Insulin-regulated glucose uptake in rat adipocytes is mediated by two transporter isoforms present in at least two vesicle populations. J. Biol. Chem. *264*, 12358-12363.